NITROGEN ISOTOPE CHARACTERISTICS OF OROGENIC LODE GOLD DEPOSITS AND TERRESTRIAL RESERVOIRS

A thesis
submitted to the College of Graduate Studies and Research
in partial fulfillment of the requirements
for the degree of
Doctor of Philosophy
in the Department of Geological Sciences
University of Saskatchewan

by

Yiefei Jia

Spring 2002

In presenting this thesis in partial fulfillment of the requirements for a Postgraduate degree from the University of Saskatchewan, I agree that the Libraries of this University may make it freely available for inspection. I further agree that permission for copying of this thesis in any manner, in whole or in part, for scholarly purposes may be granted by the professor who supervised my thesis work or, in their absence, by the Head of the Department or the Dean of the College in which my thesis work was done. It is understood that any copying or publication or use of this thesis or parts thereof for financial gain shall not be allowed without my written permission. It is also understood that due recognition shall be given to me and to the University of Saskatchewan in any scholarly use which may be made of any material in my thesis.

Requests for permission to copy or to make other use of material in this thesis in whole or part should be addressed to:

Head of the Department of Geological Sciences
University of Saskatchewan
Saskatoon, Saskatchewan S7N 5E2

ABSTRACT

This doctoral research reports the first N-isotope characteristics of micas from orogenic gold deposits utilizing continuous flow isotope ratio mass spectrometer (CF-IRMS), and the first systematic study of Se/S ratios in pyrite from these deposits using high precision Hexapole ICP-MS. The aim is to better constrain the ore-forming fluid and rock source reservoirs for this class of deposit. Orogenic gold quartz vein systems constitute a class of epigenetic precious metal deposit; they formed syntectonically and near peak metamorphism of subduction-accretion complex's of Archean to Cenozoic age, spanning over 3 billion years of Earth's history. This class of gold deposits is characteristically associated with deformed and metamorphosed mid-crustal blocks, particularly in spatial association with major crustal structures. However, after many decades of research their origin remains controversial: several contrasting genetic models have been proposed including mantle, granitoid, meteoric water, and metamorphic-derived ore-forming fluids.

Nitrogen, as structurally bound NH_4^+, substitutes for K in potassium-bearing silicates such as mica, K-feldspar, or its N-endmember buddingtonite; it also occurs as N_2 in fluid inclusions. The content and isotope composition of nitrogen has large variations in geological reservoirs, which makes this isotope system a potentially important tracer for the origin of terrestrial silicates and fluids: The $\delta^{15}N$ of mantle is –8.6‰ to –1.7‰, and of granitoids is 5‰ to 10‰, both with generally low N contents of less 1-2 ppm and average 21-27 ppm respectively; meteoric water is 4.4 ± 2.0‰ with low N contents of 2μmole; kerogen and Phanerozoic sedimentary rocks are 3 to 5‰, with high N contents of 100's to 1000's ppm; and metamorphic rocks are +1.0‰ to more than 17‰ for $\delta^{15}N$, and tens to >1000 ppm N content. Accordingly, nitrogen isotope systematics of hydrothermal micas from lode gold deposits might provide a less ambiguous signature of the ore-forming fluid source reservoir(s) than other isotope systems.

The studied orogenic gold deposits were selected from a number of geological environments: ultramafic, turbidite, granitoid hosted in the late Archean gold provinces in the Superior Province of Canada and the Norseman terrane in Western Australia; Paleozoic turbidite-hosted gold province in the central Victoria, Australia; and the Mesozoic-Cenozoic western North American Cordillera from the Mother Lode gold in southern California, through counterparts in British Columbia and the Yukon, to the Juneau district in Alaska, providing ca 40° latitude. The latter sampling design is to test for latitudinal variations of δD in a subset of robust hydrothermal micas. Also, given sparse data on $\delta^{15}N$ in Archean silicate reservoirs, new N-isotope data on granites, sedimentary rocks, and organic-rich material were obtained.

New data on N-isotopic compositions of robust hydrothermal K-silicates in orogenic gold deposits and other rock types show: (1) Archean micas in orogenic gold deposits have enriched $\delta^{15}N$ values of 10 to 24‰, and N contents of 20 to 200 ppm. Sedimentary rocks also have $\delta^{15}N$ of 12 to 17‰, and 15 to 50 ppm N contents. In contrast, granites have $\delta^{15}N$ values of –5 to 5‰, and N contents of 20 to 50 ppm. (2) Proterozoic micas in orogenic gold deposits have intermediate $\delta^{15}N$ values of 8.0 to 16.1‰, and N contents of

30 to 240 ppm. Sedimentary rocks have $\delta^{15}N$ of 9.1 to 11.6‰, and N contents of 150 to 450 ppm. (3) Phanerozoic micas in orogenic gold deposits have relatively low $\delta^{15}N$ values of 1.6 to 6.1‰, and high N contents of 130 to 3500 ppm. Sedimentary rocks are also low $\delta^{15}N$ of 3.5 ± 1.0‰, and high N contents of hundreds to thousands ppm. On the basis of these results, N in the micas from orogenic gold deposits rules out magmatic, mantle, or meteoric water ore fluids. Nor do δD values of micas from gold vein locations in the western North American Cordillera show any covariation over 30° latitude; the calculated δD and $\delta^{18}O$ values of ore fluid range from -10 to –65‰, and 8 to 16‰, respectively, ruling out the meteoric water model based on fluid inclusions (secondary).

Selenium contents and Se/S ratios in sulfide minerals have been used to constrain the genesis of sulfide mineralization given large differences in $S/Se \times 10^6$ ratios of most mantle-derived magmas (230 to 350) and crustal rocks of <10's. Hydrothermal pyrites have Se abundances from 0.9 to 15.2 ppm (n = 28), corresponding to $Se/S \times 10^6$ ratios of 2 to 34, hence Se/S systematics of hydrothermal pyrite indicate crustal not mantle sources. A metamorphic fluid origin is further endorsed by $\delta^{13}C$ values of hydrothermal carbonates, coexisting with micas, decreasing with increasing metamorphic grade, consistent with progressive loss of ^{12}C-enriched fluids during decarbonation reactions. Independent lines of geological and geochemical evidence such as restriction of these deposits to metamorphic terranes; lithostatic vein-forming fluid pressures; and consistently low aqueous salinity; demonstrate that metamorphic ore fluids were involved in this class of deposit.

Given that these gold-bearing quartz vein systems formed by metamorphic dehydration they may proxy for bulk crust $\delta^{15}N$. The new data of N contents and $\delta^{15}N$ values from crustal hydrothermal systems and limited sedimentary rocks both show systematic trends over 2.7 billion years from the Archean ($\delta^{15}N$ = 16.5 ± 3.3‰; 15.4 ± 1.9‰); through the Paleoproterozoic ($\delta^{15}N$ = 9.5 ± 2.4‰; 9.7 ± 1.0‰); to the Phanerozoic ($\delta^{15}N$ = 3.0 ± 1.2‰; 3.5 ± 1.0‰). Crustal N content has increased in parallel from 84 ± 67 ppm, through 103 ± 91 ppm, to 810 ± 1106 ppm. If the initial mantle acquired a $\delta^{15}N$ of –25‰ corresponding to enstatite chondrites as found in some diamonds, whereas the final atmosphere from late accretion of volatile-rich C1 carbonaceous chondrites was +30 to +42‰, the results may provide a specific mechanism for shifting $\delta^{15}N$ in these reservoirs to their present-day values of –5‰ in the upper mantle and 0‰ for the atmosphere by early growth of the continents, sequestering of atmospheric N_2 into sediments, and recycling into the mantle.

ACKNOWLEDGMENTS

First and foremost, I owe my deepest thanks to my supervisor Rob Kerrich for his guidance, friendship and never-ending interest. He continually challenged and expanded my scientific boundaries, and allowed my Ph.D. experience to be an intellectual cornerstone for my future career. I also acknowledge that, during the course of my studies, I received the University of Saskatchewan Graduate Scholarships and the Hugh E. McKinstry Grant from the Society of Economic Geologists Foundation Inc. USA.

This study would not have been possible without the support of abundant technical assistance in acquiring geochemical data for this thesis, for which the following people are duly acknowledged: N-isotopes – G. Parry and M. Stocki; C and O-isotopes – D. Pezderic and T. Prokopiuk; H-isotopes – E. Hoffman; ICP-MS – Q. Xie and G. Yip; Microprobe – T. Bonli; and Thin Sections – B. Novakovski. The thesis has been benefited greatly from the critical helpful discussions and comments of Drs. K.M. Ansdell, Y. Pan, B. Pratt, G.R. Davis, J. F. Basinger (Univ. of Saskatchewan); R.J. Goldfarb (U.S.G.S); and A. Delsemme (Univ. of Toledo, Ohio).

Special thanks to L. Caron, L. Hunt, and C. Hart for field assistance in southern British Columbia, northern British Columbia, and Yukon respectively. I am also grateful to Drs. R.J. Goldfarb and C. Ash for supplying samples from the Fern and Christina in Alaska and the Bralorne, Snowbird in British Columbia. I wish to thank all of my fellow graduate students, namely A. Abeleira, P. Dong, S. Ivanov, J. King, J. Muise, T. Birkham, and K. Fanton, for their provocative discussions.

Finally, I whole-heartedly thank my wife Xia, and my daughters Lingsa and Lilyan, for their support and encouragement throughout the years of my study.

TABLE OF CONTENTS

LIST OF TABLES

LIST OF FIGURES

Chapter One

INTRODUCTION AND SCOPE

1.1 Background

Nitrogen comprises 78% of the Earth's atmosphere (Cox, 1995), is a principal element of living organisms (Jacobson et al., 2000), and is present in the hydrosphere (Heaton, 1986) and hydrothermal fluids (Bottrell et al., 1988; Casquet, C., 1986; Ortega et al., 1991). Nitrogen as NH_4^+ may substitute for potassium in many common rock-forming minerals in the crust, such as K-micas and K-feldspar (Yamamoto and Nakahira, 1966; Honma and Itihara, 1981; Bos et al., 1988; Guidotti and Sassi, 1998), and is present as a trace element in the mantle and mantle fluids (Javoy et al., 1984; Boyd et al., 1987; Navon et al., 1988; Ozima, 1989; Marty, 1995).

The origin and evolution of N in the Earth's major reservoirs (atmosphere, biosphere, crust, and mantle) through time have been a subject of debate for over fifty years (Brown, 1952). The mantle may have acquired an initial $\delta^{15}N$ of –25‰, as observed in rare diamonds, corresponding to enstatite chondrite (Kung and Clayton, 1978; Javoy et al., 1984), or some value intermediate between –25‰ and +30 to +43‰ of C1 carbonaceous chondrites. The final atmosphere from late accretion of volatile-rich C1 carbonaceous chondrites was likely +30 to +43‰ (Kung and Clayton, 1978; Javoy and Pineau, 1983; Kerridge, 1982, 1985). However, it is not clear how the mantle acquired its present value of –5‰ recorded in the majority of diamonds and mid-ocean ridge basalts (MORB), the crust a value of +6‰, or the atmosphere 0‰ from these pre-accretion reservoirs (Javoy et al., 1984; Boyd et al., 1987; Javoy, 1997; Marty and Humbert, 1997; Cartigny et al., 1998).

Nitrogen in kerogen, sequestered from the atmosphere and hydrosphere by microorganisms, presently has $\delta^{15}N$ of +4.1 ± 0.8‰ (Ader et al., 1998). During diagenesis and burial, N in kerogen is either lost as part of volatiles, or incorporated into authigenic K-silicates such as illite, to give present sedimentary $\delta^{15}N$ of +4‰ (Williams et al., 1995; Kao and Liu, 2000). If N was incorporated into Archean sedimentary rocks by microorganisms by the same processes as at present, then Archean crust might proxy for the contemporaneous atmosphere - hydrosphere system. Given sparse N and N-isotope data for Archean and Proterozoic crustal rocks a principal objective of this study is to establish if secular trends exist in these parameters. The $\delta^{15}N$ of Precambrian crust bears on the origin of the rich Precambrian orogenic gold deposits.

Over half of the world's gold production of 129,000 tonnes has been from orogenic lode gold deposits, also termed 'mesothermal' gold deposits (Hodgson et al., 1993; Sutton-Pratt, 1996). These orogenic gold deposits have formed sporadically over more than ca. 3 billion years of Earth's history, especially during the Neoarchean to Paleoproterozoic, and in many Phanerozoic orogenic belts. This class of gold deposit is characteristically associated with deformed and metamorphosed mid-crustal blocks, in particular spatially related to major crustal structures. Archean lode gold provinces are predominantly located in volcanic-plutonic (greenstone) terranes, whereas Phanerozoic examples are in siliciclastic sedimentary-plutonic terranes, such as the Ordovician Bendigo-Ballarat belt of Victoria, Australia (Groves and Phillips, 1987; McCuaig and Kerrich, 1998). Figures 1.1-3 show the distribution of selected orogenic lode gold deposits, worldwide, hosted within crust of a given age.

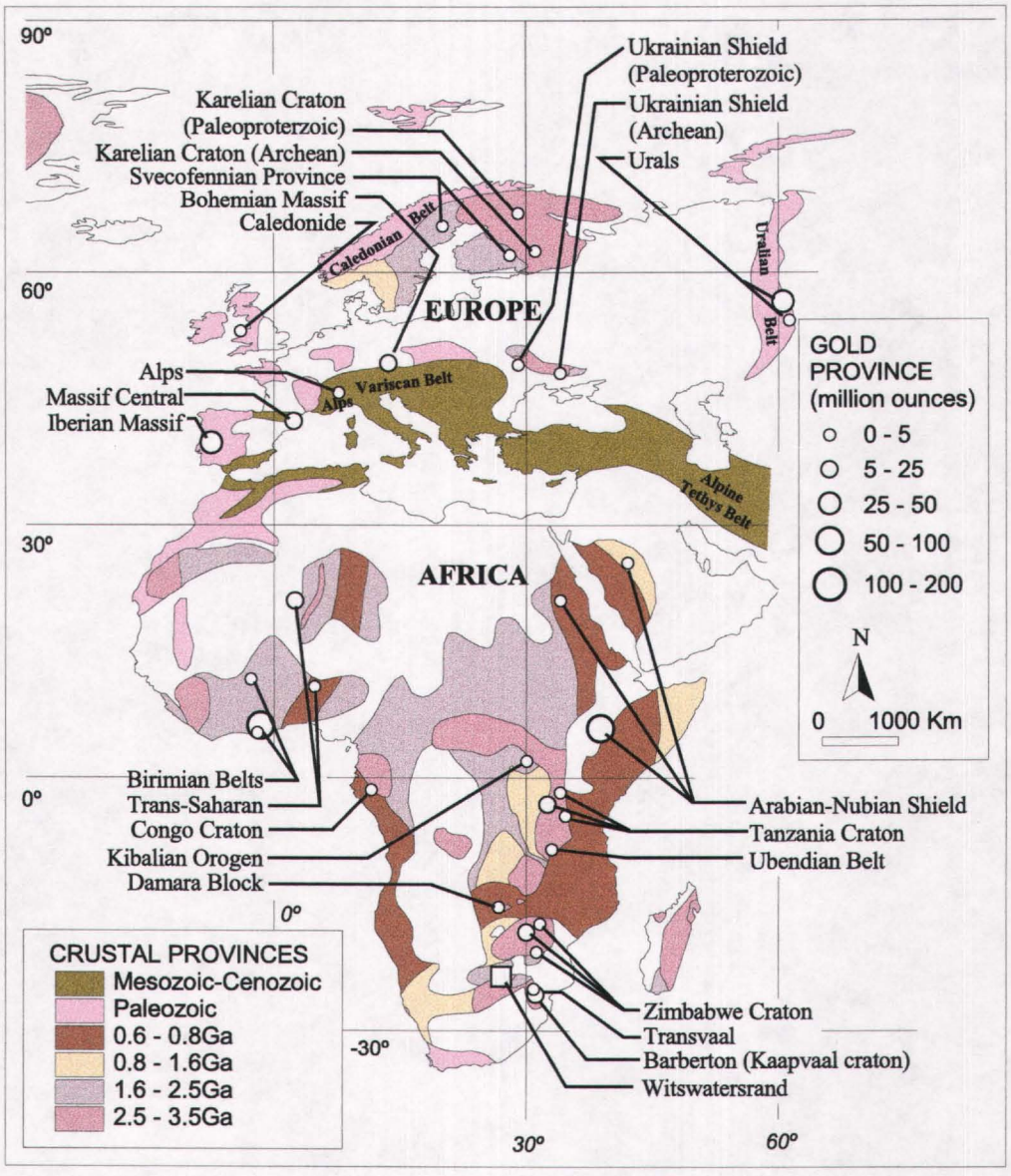

Fig. 1.1. Map showing the distribution of selected orogenic lode gold deposits hosted within crust of specified age (after Goldfarb et al., 2001). Europe and Africa.

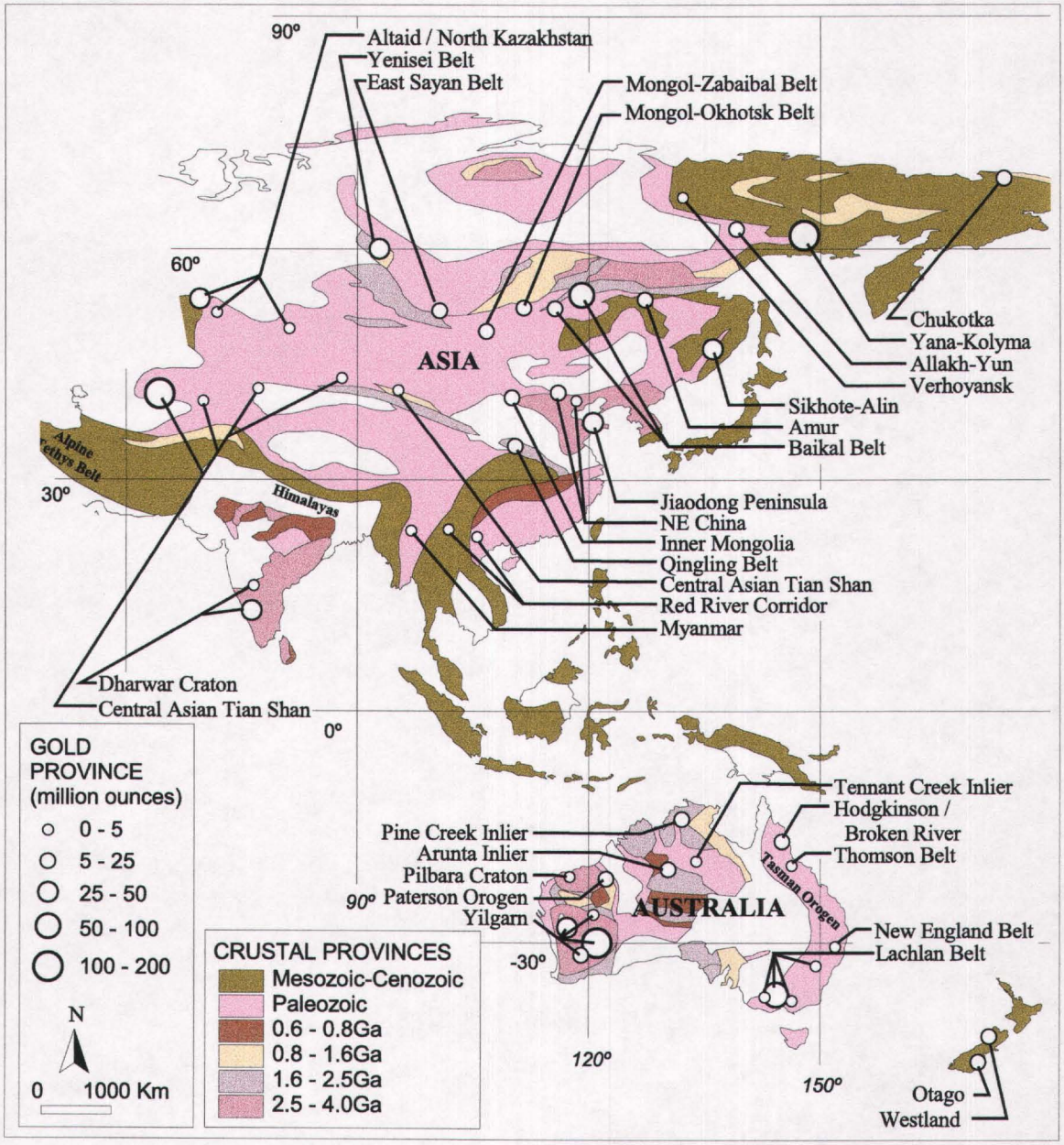

Fig. 1.2. Map showing the distribution of selected orogenic lode gold deposits hosted within crust of specified age (after Goldfarb et al., 2001). Asia, Australia, and New Zealand.

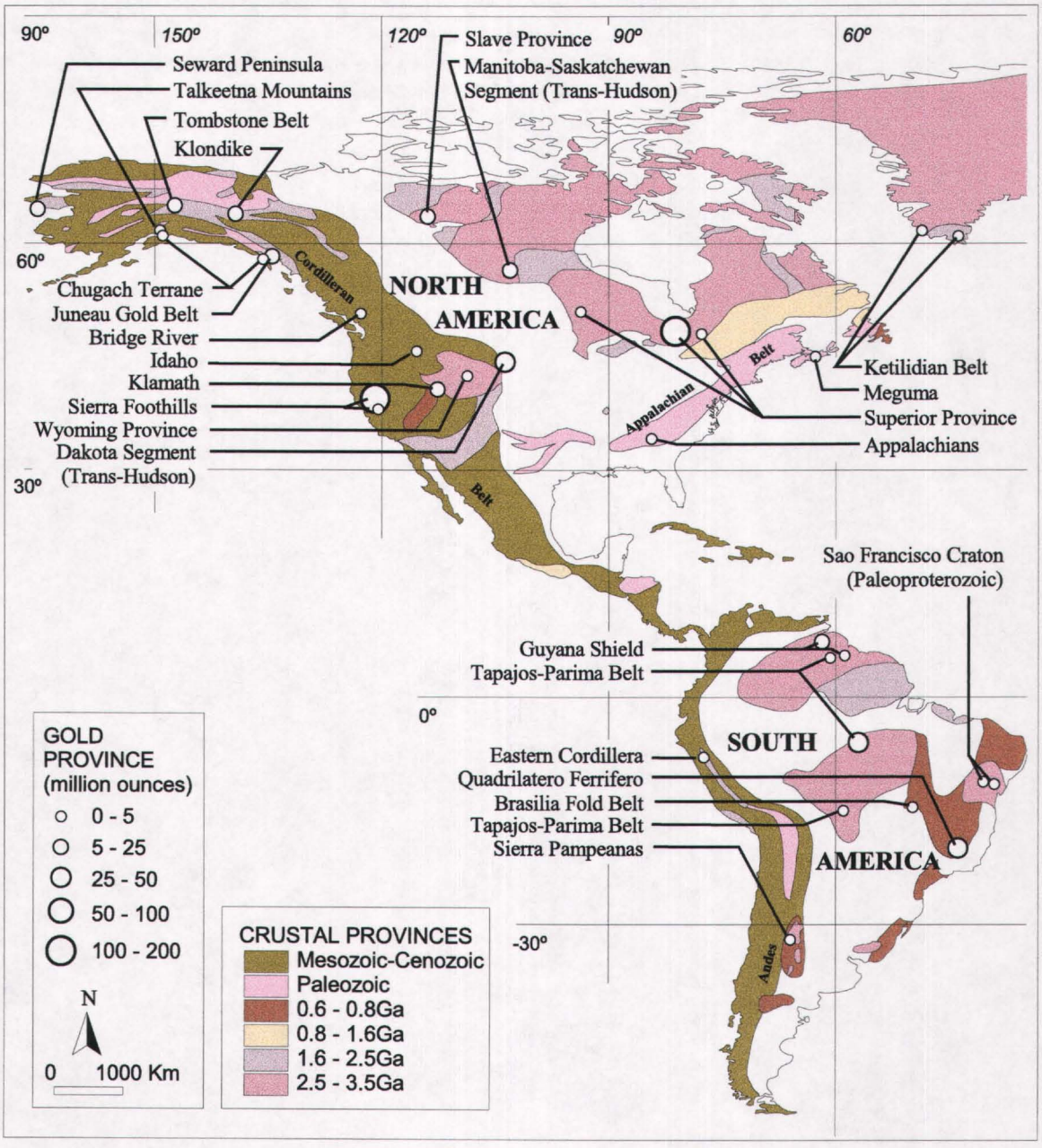

Fig. 1.3. Map showing the distribution of selected orogenic lode gold deposits hosted within crust of specified age (after Goldfarb et al., 2001). North and South America.

The genesis of these orogenic lode-gold deposits remains controversial, although a general consensus for an epigenetic origin has arisen during the past twenty years of intensive research (Kerrich and Cassidy, 1994; McCuaig and Kerrich, 1988; Ridley and Diamond, 2000), as against the syngenetic model of the 1970's and 80's (Hutchinson, 1975, 1987). The principal models are: (1) granitoid-related magmatic hydrothermal fluids (Burrows and Spooner, 1985; Burrows et al., 1986), (2) mantle derived fluids (Colvine et al., 1984; Fyon et al., 1984), (3) convecting meteoric waters (Nesbitt, 1988; Nesbitt and Muehlenbachs, 1991), and (4) fluids generated by metamorphic devolatilization reactions of ocean crust and sediments in subduction-accretion complexes (Kerrich and Wyman, 1990; Goldfarb et al., 1991a).

1.2 Aims and objectives

The first aim of this thesis is to conduct new measurements of N and $\delta^{15}N$ on metasedimentary rocks, and separated organic materials, from Archean black shales in the Hoyle Pond area of the Abitibi belt, Canada; and carbonaceous schist in the Paleoproterozoic Ashanti belt of Ghana, West Africa. Together with a compilation of data from previous studies most on Phanerozoic rocks, these results will better constrain the N content and $\delta^{15}N$ of Precambrian crustal rocks and test for secular trends to the well-established values for Phanerozoic and Recent sedimentary rocks.

Nitrogen contents and N-isotope compositions of the present atmosphere and hydrosphere, and Phanerozoic crust and mantle, are distinctive (Javoy, 1997; Marty and Humbert, 1997; Cartigny et al., 1998). Consequently, analysis of N content and $\delta^{15}N$ of hydrothermal K-silicates in orogenic gold deposits, in the framework of new data for Precambrian crust, may provide new constraints on the source reservoir of the ore-

forming hydrothermal fluids. To date, stable (H, O, C, and S) and radiogenic (Sr and Pb) isotopes have not provided unambiguous tests of the four models for orogenic gold deposits.

Specifically, the meteoric water model is based on δD compositions of bulk decrepitated fluid inclusions that apparently covary with latitudinal variation of δD in meteoric water. However, these could include multiple populations, primary and secondary (McCuaig and Kerrich, 1998). Accordingly, one of the sample designs was to collect K-mica bearing quartz-gold veins along the Mesozoic-Cenozoic western North American Cordillera from the Mother lode gold in Southern California, through Bralorne, and Cassiar in British Columbia, to the Juneau district in Alaska, providing 30° of latitude. The latter sampling is specifically designed to test for latitudinal variations of δD in robust silicates.

In this thesis the new technology of Hexapole ICP-MS was also employed to study trace element distribution in ore minerals, specifically to determine selenium contents of hydrothermal pyrite, hence utilizing Se/S ratios to constrain the ore-forming fluid reservoirs of crustal versus mantle given distinctive Se/S ratios between the two sources.

1.3 Structure of the thesis

This thesis is divided into eight chapters, which include this chapter on introduction and scope. Chapter two first briefly introduces the characteristics of orogenic lode gold deposits from Neoarchean to Cenozoic age including the tectonic setting, chemistry of fluids, alteration association, metal budget, and the timing of mineralization and magmatism, and then summarizes recent developments of

understanding their origin and remaining problems. Chapter three describes in detail the geochemistry of nitrogen, nitrogen contents and N-isotopic compositions in various geological reservoirs, and N-isotope fractionations. Collectively, these chemical and isotopic properties are compared with published N-isotopic data from other environments in an attempt to gain insight on the origin of N-bearing ore-forming fluids from orogenic lode gold deposits. As a consequence, Chapters four to six of this thesis documented N-isotope systematics of Archean, Paleozoic, and Mesozoic to Cenozoic orogenic lode gold deposits, respectively. In Chapter six Se/S systematics of hydrothermal pyrite of these gold deposits are also documented.

In Chapter seven, N cycling in the atmosphere-crust-mantle system through geological time from Archean to the Recent is modeled, based on secular variations of N-isotope data from crustal hydrothermal vein systems and sedimentary rocks established in this study, combined with a database for Phanerozoic crustal rocks, The final Chapter eight summarizes the major contributions of this study, and the implications of the results obtained to the understanding of the genesis of orogenic lode gold deposits and nitrogen cycling in Earth's major reservoirs.

Four of the chapters in this thesis are based largely on published papers or papers submitted, with Jia as first author. Chapter four is from Jia and Kerrich (1999, 2000); the sample suites were provided by Kerrich, Jia conducted all of the analyses and the majority of writing. Additional samples collected and analyzed by Jia are included. Chapter five is based on Jia et al. (2001). Samples for this paper were jointly collected by Jia and Li; H and S isotope analyses are from the Ph.D. thesis of Li. Jia conducted the C, O, and N isotope analyses at the University of Saskatchewan, and headed up the writing. Chapter six is based on a paper submitted to Economic Geology in November

2001 by Jia, Kerrich, and Goldfarb. Jia and Kerrich collected the samples together, excepting suites from the Fern and Christina mines in Alaska (R. Goldfarb), and the Bralorne, and Snowbird mines in British Columbia (C. Ash). Jia conducted all of the analytical work and did the majority of the writing and interpretation. Chapter seven is based on a paper by Jia and Kerrich submitted to Geology in September 2001. Jia did all of the analytical work and headed up the writing and interpretation.

Chapter Two

CHARACTERISTICS OF OROGENIC GOLD DEPOSITS AND RECENT DEVELOPMENTS IN UNDERSTANDING THEIR ORIGIN

2.1 Introduction

Structurally hosted lode gold vein systems in metamorphic terranes of all ages constitute a coherent class of epigenetic precious-metal deposit; they are associated in space and time with accretionary tectonics, and are here termed orogenic gold deposits (Kerrich and Wyman, 1990; Barley and Groves, 1992; Groves et al., 1998; Goldfarb et al., 2001a). Observations from throughout the world's preserved Archean accretionary volcanic-plutonic (greenstone) belts, and most Phanerozoic accretionary siliciclastic sedimentary-plutonic metamorphic belts, indicate a strong association of gold and greenschist facies terranes.

2.2 Characteristics

Studies of orogenic gold deposits of all ages have revealed a number of common characteristics in terms of paragenesis, alteration association, metal budget, ore-forming fluid geochemistry, structural style, and geodynamic setting (also see Tables 2.1-4 and references therein).

1. They are structurally hosted in metamorphosed volcanic-plutonic or sedimentary terranes, within accretionary orogenic belts. Normally, a spatial association with large-scale compressional to transpressional structures.
2. Mineralization occurs synaccretion, near peak metamorphism, in brittle to ductile shear zones.

Table 2.1. Summary of the characteristics of selected Archean orogenic gold deposits. Resource estimates are combined from numerous sources to give the most reliable numbers as of the year 2000.

Host terrane Gold province	Districts (main deposits)	Dominant host-rock lithology	Tectonic association/ Associated structures	Au production (reserve) Moz	Deformation age (Ma)	Granitoid ages (Ma)	Age of veining (Ma)	References
Archean orogenic gold metallogenic provinces								
Kaapvaal craton Barberton greenstone belt	Sheba, New Consort, Fairview, Agnes	Volcanic-plutonic rocks with minor sedimentary rocks	Saddleback-Inyoka	>10 placer present	3230-3080	3490-3450, 3230, 3105, 2690	3126-3084	Anhaeusser (1986), deRonde al. (1991), de Ronde and deWitt (1994), Poujol and Anhaeusser (2001)
Pilbara craton Northern Pilbara	Mount York, Bamboo Creek, Marble Bar, Blue Spec	Banded iron formation, mafic, ultramfic rocks with minor sedimentary rocks		2.2 (0.8)	3340, 3200, 3000-2900	3520-3400, 3315-3270, 3000-2900 3100,	3430-3300, 3200, 3000-2900	Neumayr et al. (1995, 1998) Witt et al. (1998)
Yilgarn craton Eastern Goldfields	Golden Mile, Norseman, Kambalda, Bronzewing, Sunrise Dam, Jundee	Volcanic-plutonic rocks with minor sedimentary rocks	Boulder-Lefroy, Boorara-Menzies	90 (75)	2660-2640	2900-2630	2670-2660 2640-2620, 2600	Kent et al. (1996), Witt et al. (1998) Yeats et al. (1999) Qiu and McNaughton (1999)
Yilgarn craton Southern Cross	Transvaal, Marvel Loch	same as above		8 (8)	2660-2650	2700-2620	2650-2620	same as above
Yilgarn craton West Yilgarn	Big Bell, Hill 50	same as above		18 (20)	2900, 2660-2640	2900-2630	2640-2620	same as above
Canadian shield Superior Province	McIntyre-Hollinger, Sigma-Lamaque, Hemlo, Dome, Kerr-Addison	same as above	Larder Lake-Cadillac, Destor-Porcupine	180 (200?)	2710-2670	2720-2670	2720-2660, 2600	Robert (1990, 1996), Kerrich and Cassidy (1994), Polat and Kerrich (1999)
Canadian shield Slave Province	Yellowknife (Con, Giant), (Lupin), Gordon Lake	Siliciclastic sedimentary-plutonic (turbidite)	Campbell-Giant	16 (10)	>2800, 2700-2600	2800, 2700-2580	2670-2656, 2585	Abraham et al. (1994) King and Helmstaedt (1997)
Indian shield E. Dharwar block	Kolar (Champion, Mysore, Nandydroog, Oorgaum), Hutti, Ramagiri, Gadag	Volcanic-plutonic rocks (Dharwar Schist)		27.6 (17) placer >30	2630-2520	2750-2510	≥2550	Hamilton and Hodgson (1986) Balakrishnan et al. (1999) Radhakrishna and Curtis (1999) Vasudev et al. (2000)
Zimbabwe craton Harare-Bindure-Shamva and Odzi-Mutare	Kwekwe (Globe/Phoenix), Kadoma (Cam/Motor, Freda-Rebecca, Shamva, Rezende, Redwing)	Metavolcanic and meta-sedimentary rocks and granodiorite	Kadoma, Lilly, Munyati, Shamva	17 (5)	2710-2620	2680-2580	2670-2650, 2618-2604, 2413(?)	Blenkinsop and Frey (1996), Darbyshire et al. (1996), Schmidt-Mumm et al. (1994), Vinyu et al. (1996) Oberthur et al. (2000)
Between Kaapvaal and Zimbabwe Limpopo belt	(Renco)	Plutonic rocks and charnoenderbitic rocks	Tuli Sabi	0.5	2700-2600, 2550-2530	2720-2550, 2400	2570	Kisters et al. (1998), Blenkinsop and Frei (1996), Kolb et al. (2000)
Tanzania craton Lake Victoria	Geita, (Bulyanhulu, Buhemba, Macalder)	Bimodal volcanic-sedimentary rocks	Suguti shear zone	3 (20)	2750-2530	2680, 2580-2570, 2530,	<2644, 2568-2534	Borg (1994), Walraven et al. (1994) Chamberlain et al. (2000)
S. Sao Francisco Rio das Velhas	Quadrilatero Ferrifero (Cuiaba, Morro Velho, Raposos, Sao Bento, Santana)	Volcanic-plutonic rocks with sedimentary rocks		30 (>10) placers at Moeda	2780-2770, 2150-1800, ca. 600	2780-2770, 2720-2700, 2600	2710-2580, 1830, ca. 600	Chauvet et al. (1994) Olivio et al. (1996) Lobato et al. (1999)

Note: The sited mineralization ages are from what are viewed as the most reliable published isotopic dates.
Sources: Hodgson et al. (1993), Kerrich and Cassidy (1994), McCuaig and Kerrich (1998), Goldfarb et al. (1998, 2000), and Jia et al. (2000).

Table 2.2. Summary characteristics of selected Proterozoic orogenic gold deposits. Resource estimates are combined from numerous sources to give the most reliable numbers as of the year 2000.

Host terrane Gold province	Districts (main deposits)	Dominant host-rock lithology	Tectonic association/ Associated structures	Au production (reserve) Moz	Deformation age (Ma)	Granitoid ages (Ma)	Age of veining (Ma)	References
Proterozoic orogenic gold metallogenic provinces								
West Africa Birimian greenstone	Obuasi (Ashanti), Prestea, Bogosu, Konongo, (Sadiola Hill, Damang)	Paleoproterozoic volcanic-sedimentary Birimian Group and clastic sedimentary Tarkwaian Group	Regional foliation and subparallel shear zone	50 (30) placer 0.7 at Tarkwa	2190-2080	2180-2145, 2110-2090, 2000	>2132-2116, 2105-2080	Oberthur et al. (1998)
SW Tanzanian Ubendian belt	Mpanda, Lupa (Ntumbi Reef, New Saza)		Saza shear zone; Magamba	6.3 (10.5) most from placers	2100-2025, 1860, 1725, 750	2025, 1900-1800, 725	Paleo-proterozoic(?)	Lenoir et al. (1994), Kuehn et al. (1990), Chamberlain et al. (2000)
NE Sao Francisco Rio Itapicuru	Fazenda Brasileiro, Fazenda, Maria Preta, Ambrosio	Paleoprterozoic volcanic-sedimentary sequence	Back-arc environment relative to plate collision/ shear zone controlled	minor (>3)	2127, 2100-2070	2130, 2100-2070, 2025	2083-2031	Xavier and Foster (1999) Vasconcelos and Becker (1992)
N Amazonian Guyana	El Callao, Las Cristinas, Omai, Gross Rosebel, Camp Cayman, Paul Isnard, Vila Nova	Paleoproterozoic volcanic-sedimentary rocks	Makapa-Kuribrong, Issano-Appaparu	> 4 Moz (>20)	2250-2000	2120-2090, 1790	2000	Sidder and Mendoza (1995) Norcross (1998), Santos (1999) Voicu et al. (1999, 2000)
W. Amazonian Tapajos-Parima	Alta Floresta, Tapajos, Parima			uncertain placer 35	2100-1850	2030-1980, 1920-1890, 1870-1850	1850	Santos (1999)
Trans-Hudson orogen Flin Flon and La Range	Rio, Tartan Lake, Star Lake, Snow Lake	Mafic volcanics, siltstone, sandstone, shale, diorite, graywacke	Shear zone controlled	1.25 (5)	1860-1790	1860-1834	1815	Ibrahim and Kyser (1991) Ansdell and Kyser (1992)
Trans-Hudson orogen Dakota segment	Homestake	Grunerite-siderite iron formation, graphitic shale and basaltic schist	Thrust faulting	37 (4)	1770-1715	1720-1715	<1840, >1720	Caddey et al. (1991) Dahl et al. (1999)
Baltic shield Svecofennian, N. Sweden	Tampere, Rantasalmi (Osikonmaki),Seinajoki (Kalliosalo), Haapavesi (Kiimala), Skellefte	Proterozoic plutonic and volcanosedimentary rocks	Raahe-Ladoga deformation zone	0.3 (0.5)	1850, 1820-180	2000-1860	1840-1820	Eilu (1999) Billstrom and Weihed (1996)
Kaapvaal craton Transvaal basin	Sabie-Pilgrim's Rest	Paleoproterozoic (Malmani Subgroup) sediments		6 (9)	2100-2050	2100, 2050	ca. 2050	Boer et al. (1995)
North Australian Northern Territory and central Australia	Arunta (Callie, Granites, Tanami, Tennant Creek), Pine Creek (Cosmo Howley)	metasediments, iron-formation, mafic rocks; iron-rich mudstone	Shear zone controlled; thrust faulting	9 (12)	1880-1840	1835-1810	1835-1820	Cooper and Ding (1997), Campbell et al. (1998), Matthai et al. (1995)
Paterson orogen Paterson, N.W. Australia	Telfer	Yeneena Group includes calcareous and carbonaceous siltstone	Telfer lineament	>4 (6)	620-540	633-617	ca. 620	Myers et al. (1996) Rowins et al. (1997)
Arabian shield Pan-African orogen	Sukhaybarat East, Al Wajh (Umm al Qurayyat)	Neoproterozoic volcanic and sedimentary rocks	Najd, Yanbu	0.5 (2.5)	700-660, <620	620-615, 585-565	700-660, ca. 620	LeAnderson et al. (1995) Albino et al. (1995)
Hoggar (or Tuareg) shield (Pan-African orogen)	(Amesmessa, Tirek), Bin Yauri	Neoproterozoic sedimentary rocks	East Ouzzal, Anka	minor (6)	650-613, 566-535	620	611-575, ca. 500	Ferkous and Monie (1997) Garba (1996)
South American platform Brasilia fold belt	Luziania, Morro do Ouro, Bossoroca, Mina III	Neoproterozoic sedimentary and volcanic rocks		0.5 (3)	790-600	590-563, 503-492	500	Fortes et al. (1997) Valeriano et al. (1995)

Table 2.3. Summary of characteristics of selected Paleozoic orogenic gold deposits. Resource estimates are combined from numerous sources to give the most reliable numbers as of the year 2000.

Host terrane Gold province	Districts (main deposits)	Dominant host-rock lithology	Tectonic association/ Associated structures	Au production (reserve) Moz	Deformation age (Ma)	Granitoid ages (Ma)	Age of veining (Ma)	References
Paleozoic orogenic gold metallogenic provinces								
Tasman orogen Lachlan fold belt	Ballarat, Bendigo, Stawell, Hill End	Cambro-Ordovian (west) to Siluro-Devonain (east) turbidite	Accretion of terrane(s) to Pacific margin of Gondwana	34 placer 46	460-250	420-390, 370-360, 320	460-370, 357, 343	Arne et al. (1998), Lu etal. (1996), Bierlein et al. (1999)
Tasman orogen Westland, South Island, New Zealand	Reefton (Blackwater, Globe-Progress)	Cambro-Devonian turbidites and granites	Accretion of micro-plate to Gondwana/ Globe-Progress shear	2.1 (>12) placer 8	420-260	380-370	500(?) 370(?)	Cooper and Tulloch (1992) Muir et al. (1996)
Tasman orogen Thomson fold belt	Charters Towers, Etheridge, Croyden			8	490-250	490-407, 330-270	415-398, 320	Perkins and Kennedy (1998) Bain et al. (1998)
Tasman orogen Hodgkinson-Broken River	Hodgkinson	Siluro-Devonian turbidites	Major fault controlled	0.15	490-250	330-270	300	Peters et al. (1993)
Angara craton East Sayan fold belt	Urik-Kitoi (Zun-Kholba, Zun-Ospa, Tain, Vodorazdel'noe)		Okino-Kitoi, Kholbin	minor (>3)	500-450	510-430	450	Neimark et al. (1995), Mironov and Zhmodik (1999), Vladimirov et al. (1999)
Angara craton Baikal fold belt	Sukhoi Log, Irokindinskoe, Kedrovskoe, Vysochaishee		Karakonsk, Tompudo-Nerpinsk, Tochersk	minor (40) placer 70	L. Pt-Pz	354, 330-290	380-365, 280-250	Larin et al. (1997), Yarmolyuk et al. (1997), Bulgatov and Gordienko (1999), Rytsk et al. (1998
Caledonian orogen Kazakhstan and Irtysh-Zaisanskaya provinces	Vasil'kovsk, Zholymbet, Bestyube, Stepnyak, Bakyrchik	Volcanic and sedimentary rocks		(>30)	E-M Paleozoic	455-440	L. Ordovician?	Sengor and Natal'in (1996a, b) Spiridonov (1995)
Central Asia Variscan orogen Southern Tian Shan	Muruntau, Daugyztau, Charmitan, Jilau, Kumtor, Axi	Carboniferous turbidites Upper Proterozoic pelites	Hercynian coninental collision/Tian Shan suture zone, Sangruntau-Tamdytau shear zone	40 (120)	M-L Paleozoic	Permian-E. Triassic	Permian-E. Triassic	Ansdell et al. (1999), Bortnikov et al. (1996), Cole et al. (2000) Drew et al. (1996, 1998) Shayakubov et al. (1999)
Northern Appalachian Meguma, Nova Scotia	Goldenville, Caribou, Beaver Dam,Cochrane Hill, Forest Hill	Cambro-Ordovician turbidites	Docking of suspect terrane with continen-tal platform; obduction	1.4	415-360	380-370	380-362	Kontak et al. (1990), Gibbons et al. (1998), Ryan and Smith (1998)
Paleozoic Andes Eastern Cordillera	Pataz, La Rinconada, Yani		Maranon lineament		374-360	329	313	Fornari and Herail (1991) Haeberlin et al. (1999)
Caledonian orogen Caledonides, Wales, UK	Dolgellau gold belt (Gwyn-fynydd, Clogua), Dolaucothi, Tyndrum, Clontibret	Ordovician turbidites	Tyndrum fault, Orlock Bridge fault	0.2 (0.6) placer minor	520-480, 460-440, 420-400	425-390	410-380 368(?), 345(?)	Ineson and Mitchell (1975) McArdle (1989), Curtis et al. (1993) Steed and Morris (1986)
European Variscan Massif Central, France	Saint Yrieix (Le Bourneix), Salsigne, Brioude-Massiac, La Marche (Le Chatelet)	Ordovician-Silurian turbidites and granites	Laurussia & Gondwana Collision belt. Marche-Combrailles shear zone	25 (mainly by Romans)	440-280	360-290	320-285	Bouchot et al. (1989), Guen et al. (1992), Marignac and Cuney (1999)
European Variscan Bohemian Massif, Ceech Republic	Celina-Mokrsko, Kasperske Hory, Jilove	Cambro-Ordovician volcano-sediementary rocks	Laurussia & Gond-wana Collision belt.	5 (13)	440-280	360-290	349-342	Stein et al. (1997) Moravek (1996a, b)
Uralian orogen East-central Ural, Russia	Berezovsk, Kochkar	Granite-gneiss complexes; mafic dikes	European platform & Asian microplates collision belt Main Uralian fault	>28 placer >60	370-250	360-320	L. Carbonifer-ous to Permian	Bortnikov et al. (1997) Puchkov (1997) Kistlers et al. (1999, 2000)

Table 2.4. Summary of characteristics of selected Mesozoic-Tertiary orogenic gold deposits. Resource estimates are combined from numerous sources to give the most reliable numbers as of the year 2000.

Host terrane Gold province	Districts (main deposits)	Dominant host-rock lithology	Tectonic association/ Associated structures	Au production (reserve) Moz	Deformation age (Ma)	Granitoid ages (Ma)	Age of veining (Ma)	References
Mesozoic orogenic gold metallogenic provinces								
Mongol-Okhotsk orogen Trans-Baikal belt, Mongolia	Darasun, Mogocha (Klyuchevsk),Selemdzha, Niman, Kerbi, Tokur, Malomyr, Unglichikan	mid-Paleozoic to early Mesozoic marine sequences	Mongolia-Okhotsk suture	2 (7) placer 35	190-140	280-260, 164-145	L. Jurassic-E. Cretaceous	Krivolutskaya (1997), Stepanov (1998), Yakubchuk and Edwards (1999), Zorin (1999)
Tasman orogen New England fold belt	Hillgrove, Gympie, Timbarra Great Serpentinite Belt	Carboniferous-Permain turbidites and granites	Peel fault system	4 (minor) placer 0.25	320-230	310-300, 285 270-240,	E-M Triassic	Ashley (1997), Cranfield et al. (1997)
Tasman orogen(?) Otago Schist, New Zealand	Macraes, Carrick	Permain-Late Triassic turbidites	Hyde-Macraes shear zone	>1 (3) placer 8	200-140	no granitoids	E. Jurassic-E. Cretaceous	Paterson (1986), McKeag and Craw (1989), Adams et al. (1998)
Cordilleran orogen East-cenreal Alaska	Fairbanks (Ft. Knox, Ryan Lode, True North), Goodpastor (Pogo),	Early Paleozoic turbidites	Tintina and Denali fault systems	1.5 (12) placer 12	Jurassic	105-90	105, 92-87, 77(?)	McCoy et al. (1997), Goldfarb et al. (2000), Newberry (2000)
Cordilleran orogen Klondike, Yukon,	(Sheba, Mitchell, Hunker)	mid Paleo zoic-early Mesozoic sedimentary and ignous rocks	Regional-scale thrust faults in Klondike	<0.1 placer 15	Jurassic	no granitoids	175	Rushton et al. (1993) Goldfarb et al. (1998)
Cordilleran orogen Interior British Columbia	Atlin, Cassiar, Cariboo, Stuart Lake, Greenwood	Late Paleozoic-early Mesozoic sedimentary mafic/ultramafic rocks		>1? (1) placer 1	Jurassic	E.- M. Jurassic	170-140	Ash et al. (1996)
Cordilleran orogen Southern Alaska	Chichagof (Chichagof, Hirst-Chichagof), Port Valdez, Moose Pass, Nuka Bay	Late Cretaceous turbidites	Subduction of accretionary prism under N. American continent/ Border Ranges	0.9 placer 0.1	L. Cretaceous to Eocene	66-50	57-49	Goldfarb et al. (1986) Haeussler et al. (1995)
Cordilleran orogen Southeast Alaska	(Juneau, Berner's Bay, Windham Bay, Snettisham)	Permain-mid Cretaceous turbidites	Fanshaw, Sumdum	6.8 (5)	mid-Cretaceous 70-60	mid-Cretaceous, 70-48	57-53	Goldfarb et al. (1991) Miller et al. (1994)
Cordilleran orogen South-central Alaska	Willow Creek	Cretaceous arc rocks; Paleozoic-mid Cretaceous turbidites	Subduction of Chugach terrane; oroclinal bending of Alaska/Border Ranges	0.6	Jurassic	74-66	66	Madden-McGuire et al. (1989)
Cordilleran orogen Bridge River, British Columbia	(Pioneer, Bralorne)	Late Paleozoic-early Mesozoic of Bridge River and Cadwallader terranes	Yalakom	4.3 (0.6)	Jura-Cretaceous	270, 91-43	70	Leitch et al. (1991) Goldfarb et al. (2000)
Cordilleran orogen Sierra Foothills and Klamath Mountains	Alleghany, Grass Valley, Mother Lode French Gulch, Deadwood	Carboniferous-Jurassic turbidites and volcano-genic rocks	Accretion of complex terranes and volcanic arcs to N. American crston	35 (15) placer 65 3.5 placer 3.5	Jurassic to E. Cretaceous Jurassic to E. Cretaceous	150-80 177-135	144-141, 127-108 ≥147, ≤136	Bohlke and Kistler (1986) Landefeld (1988) Elder and Cashman (1992)
Russian Far East Yana-Kolyma Allakh-Yun fold belt	Omchak, Kumroch, Maldyak Yur-Duet (Nezdaninskoye) (Kartalveem, Maiskoe, Palyangai)	Paleozoic-mid Mesozoic turbidites	Tenka fault Kiderikinsk deep fault, Tyrynsk fault	15 (46) placer 125	L. Jurassic-Cretaceous	170-110 154-94	147-131, 125-115, 105-95 170-130, 124-110, 115-100	Parfenov (1995), Abzalov (1999), Bortnikov et al. (1998) Goryachev and Edwards (1999) Nokleberg et al. (1996)
Alpine-Carpathian orogen European Alps	W. Alps (Brusson, Vogogna) Swiss Alps (Mont Chemin), E. Alps (Rotgulden)	Paleozoic gneiss, schist and Mesozoic ophiolites and associated Calc-schist	Subduction and underplating of oceanic and European continental plate convergence	1	90-60, 44-19	43-20	32-10	Pettke et al. (1999) Marshall et al. (1998)

3. Orogenic gold deposits are distributed in belts of great geological complexity, with gradients of lithology, strain, and metamorphic grade, reflecting an orogenic environment.
4. Gold precipitation is syn-kinematic, typically in structures with high-angle oblique displacement, commonly with reverse slip, but with some examples in transcurrent fault regimes.
5. The alteration mineral association is dominated by quartz, carbonate, muscovite-paragonite (± albite greenschist facies deposit), biotite (higher temperature deposits), chlorite, and pyrite (± scheelite, tourmaline).
6. Metal budget is characterized by enrichment in the rare elements Au, Ag (± As, Sb, Te, W, Mo, Bi, and B), with low enrichments of the abundant base metals Cu, Pb, and Zn relative to background abundances.
7. Ore forming hydrothermal fluids are dilute aqueous carbonic fluids, with uniformly low fluid salinities (typically $\leq$ 6 wt% NaCl equivalent), and CO_2+CH_4 contents of 5-30 mole%, with up to 55 mole% of N_2. Typical $\delta^{18}O$ values of ore fluids are about 6 to 12‰ and δD about –15 to –80‰.
8. The orogenic gold deposits normally consist of abundant quartz-carbonate veins and show evidence for formation from fluids at pressures from supra-lithostatic to sub-lithostatic within the brittle-ductile shear zones.
9. The mineralized lodes formed over a uniquely broad range of upper to mid-crustal pressures and temperatures, between 100-500MPa and 200-650°C.

10. In most of these deposits, vein systems may have vertical extents of more than 2 km, with a lack of zoning or weak zoning, albeit with some zoning of metal content at the scale of an entire mining district.

Most of these deposits occur in terranes that experienced greenschist facies metamorphism, and the deposits feature greenschist-facies alteration assemblages. Recently, it has been recognized that Archean lode gold deposits in sub-greenschist, amphibolite, and even granulite facies terranes share numerous characteristics, such as structural setting, metal inventory, element association, and ore fluid properties and likely source, in common with greenschist hosted mesothermal counterparts (Colvine et al., 1988; Kerrich, 1989; Ho et al., 1992; Groves et al., 1992; Groves, 1993; McCuaig and Kerrich, 1998). Accordingly, this class of structurally hosted orogenic gold vein deposits may be viewed as forming over a crustal depth range, or 'crustal continuum', extending from granulite to sub-greenschist facies environments (Groves et al., 1992; Groves, 1993). All gold deposits of this orogenic class are hosted in metamorphosed terranes, and this feature is arguably one of the most significant unifying characteristics. There is debate as to whether some of the Archean Superior Proince deposits, for example, Hemlo and MacIntyre, belong to the orogenic class.

The orogenic gold deposits discussed in this thesis are different in characteristics and origin from other types of precious metal deposits such as epithermal/hot spring Au-Ag veins, gold-rich porphyry and skarn deposits, Carlin type Au, or Au-rich volcanogenic massive sulfide mineralization. The last five deposit types are formed at different geodynamic settings than lode gold deposits, even if some are associated with convergent margin orogens (Fig. 2.1; Groves et al., 1998; Kerrich et al., 2000; Goldfarb et al., 2001b).

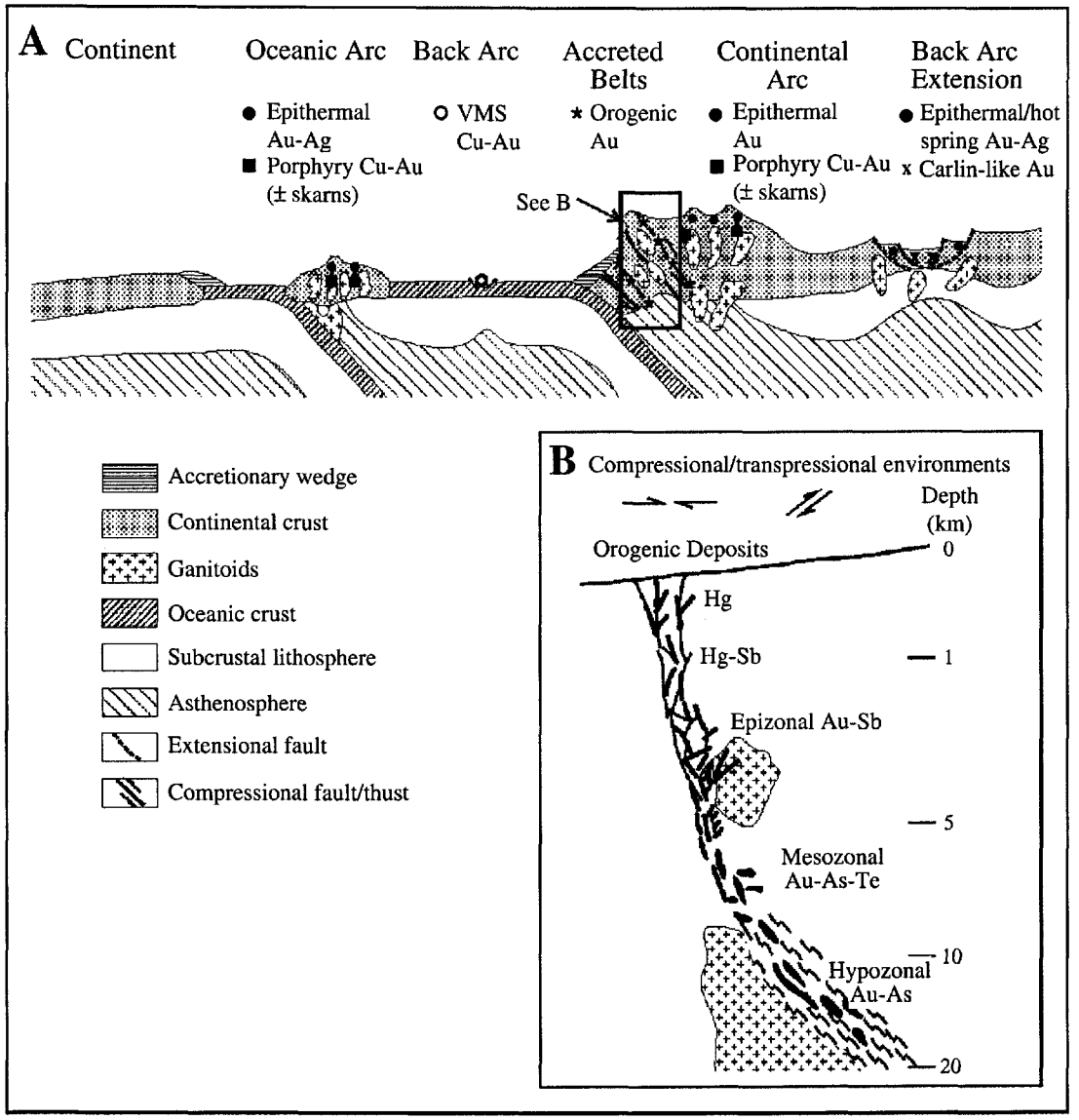

Fig. 2.1. A. Schematic section showing the tectonic settings of orogenic gold deposits and other gold deposit types. For orogenic gold deposits, they are emplaced in the accretionarty belts during collisional events throughout much of the middle to upper crust. In contrast, epithermal veins, gold-rich porphyry and skarn deposits, and massive volcanogenic sulfide deposits form in the shallow (< 5km) parts of both island and conintental arcs in compressional through extensional settings. The epithermal veins, as well as the sedimentary rock-hosted Carlin-like ores, are also emplaced in the shallow regions of back-arc crustal thinning and extension (after Groves et al., 1998).

2.3 Review of Genetic Models

Orogenic, or mesothermal, lode gold-bearing quartz vein systems constitute a coherent group of epigenetic precious metal deposits; they occur in accretionary orogenic belts of Mesoarchean to Cenozoic age. The chemistry of the ore-forming fluids, alteration association, metal budget, and the late orogenic timing of the deposits are remarkably similar through time and space (Kerrich and Cassidy, 1994; McCuaig and Kerrich, 1998; Ridley and Diamond, 2000). Their origin, however, has been long debated in terms both of the source of the solvent and its solutes and the timing of ore formation. Several contrasting genetic models have been proposed in the literature (Table 2.5).

2.3.1 Magmatic hydrothermal fluid models

Magmatic models view the auriferous fluids as the aqueous fractionation products of crystallizing felsic intrusions (Burrows et al., 1986; Wood et al., 1986; Hattori, 1987; Burrows and Spooner, 1989) or as genetically linked to lamprophyres (Rock and Groves, 1988; Rock et al., 1989). In the felsic magmatic model, fluids and gold are derived from felsic intrusions based in large part on the spatial association of some gold deposits with felsic stocks (Hattori, 1987; Cameron and Hattori, 1987). According to Hattori (1987), some of these stocks are analogs of I-type granites, and the gold is likely orthomagmatic in origin. Burrows and Spooner (1985) described alteration zones in the Archean Cu-Mo-Au 'magmatic' Mink Lake deposit, that are closely associated with igneous intrusions. Alteration zones have carbonate $\delta^{13}C = -3.3 \pm 0.4‰$ ($n = 23$), and involve enrichment of sodium and potassium. Burrows et al. (1986) and Burrows and Spooner (1987) interpreted $\delta^{13}C$ values for carbonate in Au mineralizing veins from

Table 2.5. Hypothesis testing for orogenic gold deposits - summary of genetic models

Characteristics	Magmatic	Mantle	Meteoric	Metamorphic
Lithological Associations				
	Pro: Spatially associated with intrusions **Con**: But intrusions often older and many deposits not spatially related			**Pro**: Majority of deposits not spatially associated with granitiods
Stable Isotopes				
	Pro: $\delta^{13}C$ values of carbonates in igneous range (-6 to -2‰) **Con**: But $\delta^{13}C$ of many deposits extend outside this range (-11 to -2‰)	**Pro**: $\delta^{13}C$ values of mantle range (-5 to -7 ‰) **Con**: But $\delta^{13}C$ from granulite fluids range from -5 to -22‰.		**Pro**: Extended range of $\delta^{13}C$ reflects mixed low and high $\delta^{13}C$ sources **Con**: $\delta^{13}C$ values (ca. -3‰) in largest deposits are within magmatic or mantle range
	Pro: Calculated $\delta^{18}O$ (+6 to +11‰) and δD (-20 to -80‰) of ore-forming fluids in some deposits overlap the magmatic field **Con**: But most $\delta^{18}O$ values greater than +8‰; cannot be magmatic fluids alone		**Pro**: δD of ore fluid is very depleted within meteoric water range **Con**: Shouldn't be at low water/rock ratios. δD may be from secondary fluid inclusions. Low δD refects exchange with organic matter in some deposits.	**Pro**: δD of robust silicates not depleted. **Con**: δD of fluid inclusions from some deposits depleted
N and Nitrogen Isotope				
	Con: Lower nitrogen contents and $\delta^{15}N$ (5 to 10‰)	**Con**: Nitrogen contents very low <1-2 ppm, and depleted $\delta^{15}N$ (-10 to 0‰, with a mean of -5‰)		**Pro**: N content from lode gold deposit fluids is relatively high and variable $\delta^{15}N$ in metamorphic range (+1 to >+17‰)
Gold Source Content				
	Pro: high Au content in lamprophyres **Con**: Fresh lamprophyres Au content within the continental average			
Fluid Pressure				
			Con: Pressure of convecting meteoric water hydrostatic	**Pro**: Superlithostatic fluid pressures, as expected from metamorphic dehydration
Radiogenic Isotopes				
		Pro: Initial $^{87}Sr/^{86}Sr$ of some ore deposits within mantle range **Con**: Only in some deposits		**Pro**: Initial $^{87}Sr/^{86}Sr$ in lode gold deposits are variable
Fluid Composition				
	Pro: Ore fluid compositions H_2O-CO_2 magmatic-like **Con**: Only alkaline magmas with CO_2-rich saline fluids $\delta^{18}O_{H2O}$ is too variable. Fluids non-saline			**Pro**: Dilute, aqueous carbonic fluids ± CH_4 ± N_2, and low salinities (≤ 6 wt% NaCl equiv.) expected from metamorphic dehydration
Halogens				
			Pro: I/Cl, Br/Cl ratios from ore fluids similar to meteoric water **Con**: Maybe from secondary inclusions	No database of halogen systematics to rule out metamorphic source or other fluids
Model Proponents				
	Burrows et al. (1986) Burrows and Spooner (1987) Rock et al. (1988)	Fyon et al. (1984) Colvine et al. (1984, 1988) Cameron (1988)	Nesbitt et al. (1986, 1989) Nesbitt (1988) Yardley et al. (1993)	Kerrich and Fryer (1979) Phillips and Groves (1983) Groves et al. (1987) Goldfarb et al. (1991a) Jia and Kerrich (1999)

Hollinger-McIntyre (Superior Province, Canada) and Golden Mile (Western Australia) orogenic gold deposits, which were -3.1 ± 1.3‰ (n = 275) and -3.4 ± 0.4‰ (n=19), respectively, as close to magmatic values of –6 to –2‰. From this comparison of $\delta^{13}C$ in orogenic gold deposits to the Mink Lake 'magmatic' deposits and the magmatic $\delta^{13}C$ range, they suggested that the H_2O-CO_2 fluid which deposited this type of Archean Au mineralization was also magmatically derived.

However, precise age determinations of felsic intrusions and gold deposits have shown that the latter significantly post-date synkinematic magmatism, such that a direct orthomagmatic relationship of gold to the stocks can be ruled out (e.g., Colvine et al., 1988). According to Phillips (1999), most orogenic gold deposits in Archean greenstone belts are not spatially associated with granitic intrusions. In fact, gold mineralization is most closely related in space and time to minor post-kinematic alkaline magmatism (Wyman and Kerrich, 1988; Kerrich and Cassidy, 1994). Collectively, the $\delta^{13}C$ values of these gold deposits span –11 to +2‰ and hence cannot uniquely be orthomagmatic in origin.

In another orthomagmatic model, Rock et al. (1988) thought that the ore fluids were derived from lamprophyre magmas based on the temporal and spatial association of lamprophyres with gold deposits. In support they cited an average gold abundance in lamprophyres 100-1,000 times higher than common igneous rocks, and lamprophyre volatile and incompatible element compositions (high H_2O, CO_2, F, K, Rb and Ba but moderate S contents) interpreted as similar to ore fluids for gold veins. However, by analyzing Au and PGE, Wyman and Kerrich (1988) showed that fresh lamprophyres are not intrinsically rich in gold (mean Au ~ 3.8 ppb), or Ag, B, and W that are typically

associated with gold in the deposits. Rather, elevated gold contents reported by Rock et al. (1988) resulted from analyzing altered lamprophyres. Wyman and Kerrich (1988) interpreted the common spatial and temporal association as reflecting a shared geodynamic setting, not a common origin.

2.3.2 Mantle-derived ore fluid models

Mantle degassing models invoke mantle-derived CO_2-rich fluids interacting with the lower crust, inducing granulite metamorphism with dehydration and accompanied loss of Au and incompatible elements to the mid-crust (Fyon et al., 1983; Colvine et al., 1984; Cameron, 1988). Fyon et al. (1983) and Colvine et al. (1984) first suggested a possible link between the mantle CO_2 streaming hypothesis of Newton et al. (1980) for granulitization and gold mineralization. They considered that the CO_2-rich inclusions in granulites are comparable with the CO_2-rich fluids recognized in gold deposits, and are juvenile CO_2 from the mantle given $\delta^{13}C$ values of -5 to -7 ‰ from inclusions in granulites. This model was rejected on the basis that (1) $\delta^{13}C_{CO_2}$ values in granulite fluids range from -5 to -22 ‰ and so are unlike those of carbonate in gold quartz veins (Burrows et al., 1986); (2) granulite fluids are extremely CO_2-rich, whereas those in the deposits are dominantly aqueous; (3) $\delta^{13}C$ values of -11 to +2‰ are not uniquely diagnostic of any one carbon source, but cannot reflect mantle C or magmatic C alone (Table 2.5; Kerrich, 1989, 1990); and (4) robust Sr-isotope compositions of tourmaline in the Superior Province gold deposits are too radiogenic to be mantle derived (King and Kerrich, 1989).

2.3.3 Meteoric water circulation model

The meteoric water model invokes ground waters that circulated deep into the crust (Nesbitt, 1988; Nesbitt et al., 1986, 1989; So and Yun, 1997). Nesbitt et al. (1986) proposed a meteoric water model for Cordilleran lode gold deposits involving deep circulation of meteoric water along transcurrent faults under conditions of low water/rock ratios. The model was based on the observation that the δD values of H_2O, obtained by decrepitating fluid inclusions from some vein quartz were very depleted (-120‰). They extended this model to Archean lode gold deposits (Nesbitt, 1988; Nesbitt and Muehlenbachs, 1989). Uncertainties about this model are as follows: (1) in several areas, adjacent gold deposits have widely differing fluid inclusion δD values, inconsistent with latitudinally controlled δD of meteoric waters (Fig. 2.2; Zhang et al., 1989; Peters et al., 1991; McCuaig and Kerrich, 1998); (2) low δD of ore fluids could result from isotopic exchange with δD-depleted organic bearing sedimentary rocks in the crust (Peters et al., 1991); or (3) the bulk extracted fluid inclusions were dominated by secondary inclusions formed in the presence of meteoric water during uplift of the deposits, rather than being primary ore fluids (Goldfarb et al., 1991b; McCuaig and Kerrich, 1998).

As well, for surface meteoric waters convecting deep into the crust, $P_{fluid} \approx 1/3P_{lithostatic}$. However, in the gold deposits there is clear field evidence, in the form of horizontal veins dilated vertically, for lithostatic to super-lithostatic fluid pressures ruling out hydrostatic convection (Kerrich and Allison, 1978; Sibson et al., 1988). Further, there is a common problem with the meteoric model for deposits in the Cordillera and Korea, as discussed by Kerrich (1989) and Goldfarb et al. (1989). Given

palaeometeoric water with values of $\delta D \approx -140‰$, $\delta^{18}O$ would have been -19 ‰ (Zhang et al., 1989). Consequently, $\delta^{18}O$ in the meteoric ore-fluid would have shifted by +27‰ from –19‰ by fluid/rock interaction at low water/rock ratios to the observed values of about +8‰, and δD values shifted to the magmatic or metamorphic range (McCuaig and Kerrich, 1998). Accordingly, the primary meteoric water signatures would be lost (see Fig. 2.2). Also, the magnitude of the dispersion in δD_{H_2O} values cannot be attributed to mixing of depleted and enriched fluid reservoirs; any such would be reflected in shifts of both δD and $\delta^{18}O$ fluid, but the characteristic uniformity of quartz $\delta^{18}O$ values of individual deposits rules out this possibility.

An additional complexity in the meteoric water model for Cordilleran deposits is constraining the latitude at the time the deposits formed, and distance from the paleo-Pacific ocean, given the allochthonous character of the host terranes. Latitude and distance from oceans are the two factors that primarily control the present day δD and $\delta^{18}O$ of meteoric water on the North American continent (Taylor, 1997). These Cordilleran deposits from the Mother lode gold in southern California, through deposits in the Canadian Cordillera, to Juneau Alaska are of Jurassic to Cenozoic age (147 Ma-53Ma). From paleomagnetic and geologic data allochthonous terranes such as western Mexico, southern California, and terranes of the Canadian Cordillera have translated northward along the western paleo-margin of North America before or after the deposits formed. At 100 to 90 Ma, the Interior domain comprising much of interior British Columbia, central Yukon, and eastern and central Alaska was situated at the latitude of northern California. The Coast domain including southeastern Alaska, much of the Coast Ranges and islands of British Columbia, and the Cascade Mountains of

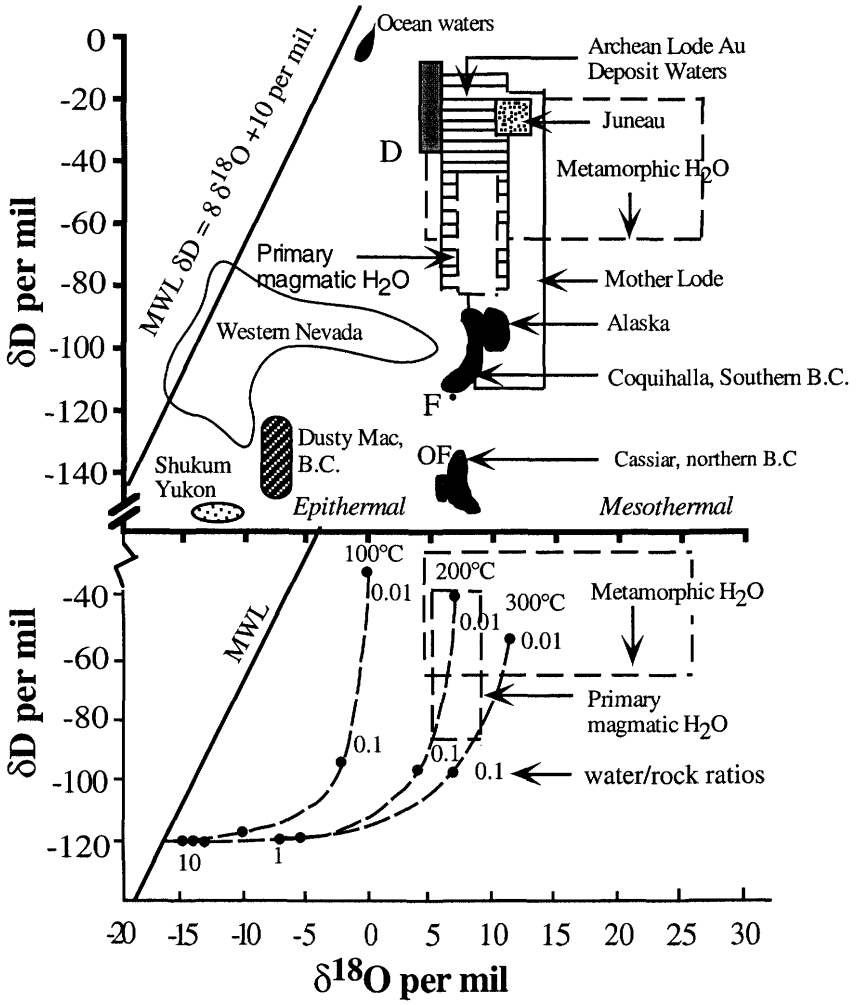

Fig. 2.2. Calculated isotopic compositions (δD and $\delta^{18}O$) of ore-forming fluids associated with Archean to Phanerozoic lode gold deposits (after McCuaig and Kerrich, 1998).

Note that δD-depleted values from the Cordilleran mesothermal deposits are exclusively based on bulk extraction of fluid inclusions. F and OF are the adajcent Fairview and Oro Fino deposits in southern British Columbia (after Zhang et al., 1989).

Washington were situated at a latitude similar to northern Mexico. Subsequently, both superterranes moved northward about 3000 km, reaching their present locations before 45 Ma (Fig. 2.3; Irving et al., 1995, 1996; Wynne et al., 1995; Ward et al., 1997).

2.3.4 Metamorphic dehydration model

In the metamorphic hypothesis, it is suggested that the ore fluids were generated by deep devolatilization of large rock volumes at the greenschist-amphibolite facies transition. Subsequent mineral deposition occurred at shallower levels (Fyfe and Henly, 1976; Kerrich and Fryer, 1979; Kerrich and Fyfe, 1981; Phillips and Groves, 1983; Groves and Phillips, 1987; Phillips, 1993), or following a period of fluid ponding at depth (Goldfarb et al., 1991a). The metamorphic fluid hypothesis for lode gold deposits rests on a number of observations: (1) restriction of this class of precious metal deposits to metamorphic terranes, specifically synaccretion near-peak metamorphic timing; (2) lithostatic ore-fluid pressures; (3) calculated δD and $\delta^{18}O$ of the ore fluids in the metamorphic field; and (4) variability of H, C, O, Sr, and Pb isotopes of the deposits consistent with lithologically heterogeneous crust.

The compositions of fluids in metamorphic rocks in general are comparable in several respects with the ore-forming fluids. These are low-salinity (i.e., 0~ 10 wt% NaCl equiv.), high-temperature (T>200°-500°C), reducing fluids, with variable CO_2, CH_4 and N_2, at lithostatic pressure. Such fluids have been implicated in the formation of many large gold provinces regardless of age or the relative proportions of supracrustal rock types. From these observations, Kerrich and Fryer (1979), Phillips and Groves (1983), Groves and Phillips (1984) and Phillips (1993) suggested that metamorphic

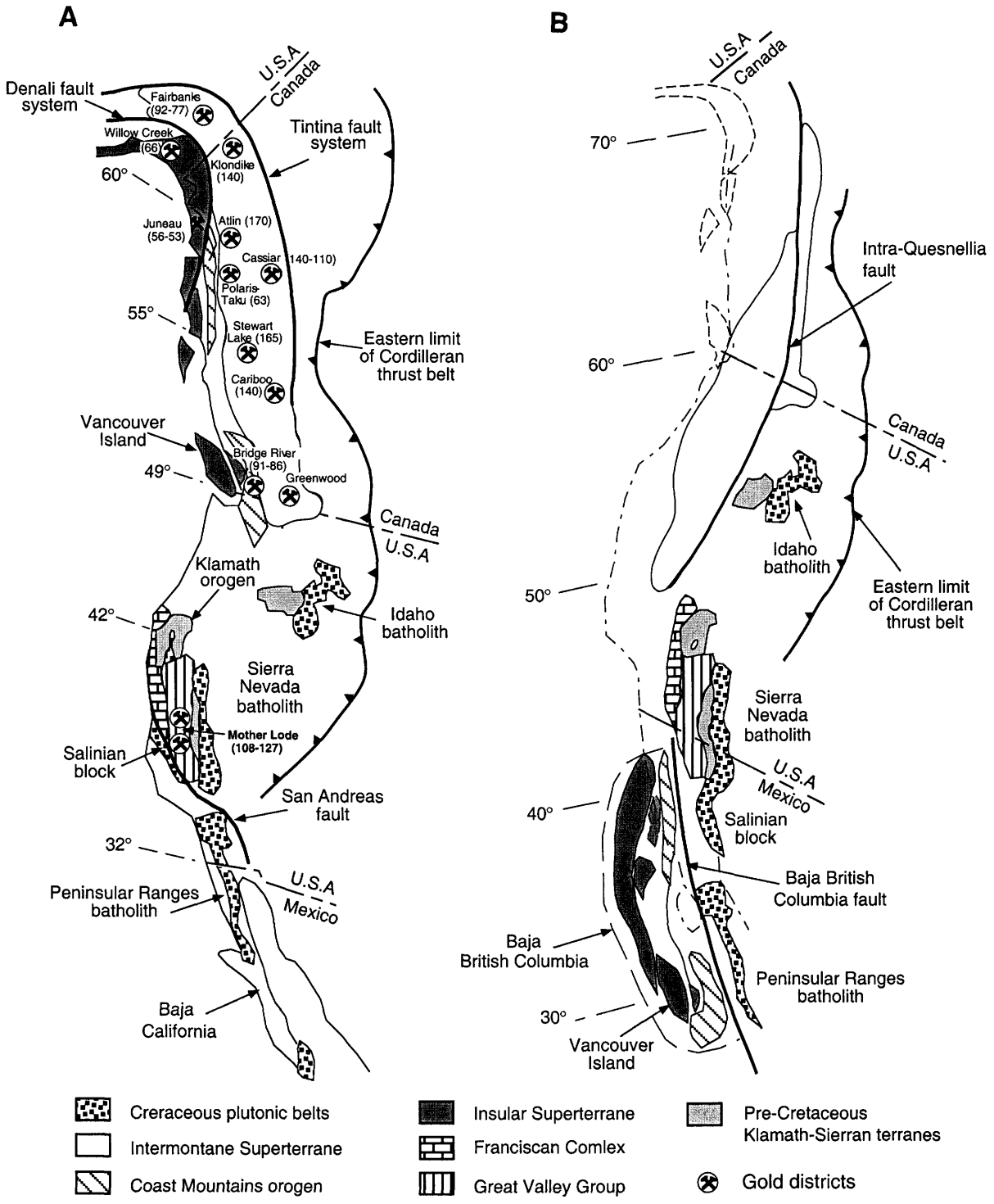

Fig. 2.3. A. Present geographic positions of major crustal and tectonic elements of the western North American Cordillera, including the Insular and Intermontane superterranes and the distribution and forming ages of gold districts. Present-day latitudes are indicated. Superterrnes modified from Cowan et al. (1996) and Ward et a. (1997). B. Paleographic reconstruction for late-Cretaceous time (75-85 Ma). The Paleo-latitudes for North American Cordillera at this time is also shown from Ward et al. (1997).

devolatilization associated with the greenschist-amphibolite facies transition is a major source of the ore fluid.

The involvement of metamorphic fluids in orogenic gold deposits has also received considerable support recently with the experimental demonstration that devolatization of chlorite-calcite-albite-quartz (e.g., mafic-graywacke; Will et al., 1990) at the greenschist to amphibolite transition produces large volumes of fluids with H_2O/CO_2 ratios about 75:25, at 4-5 kbar, comparable with fluid inclusion compositions in gold deposits (Ho et al., 1990). Further similarities between observed characteristics and calculations occur in the inferred temperature range and the reducing nature of fluids that transported the gold (Phillips et al., 1987). According to Phillips (1993) and Phillips and Powell (1993), the generation of fluids by devolatilization accompanying thermal events is inevitable in high heat flow environments. Evidence that mafic sequences lose volatiles (H_2O, CO_2) during metamorphism is easily deduced by comparing the volatile contents of typical greenschist and amphibolite facies (H_2O: chlorite 9-13%, actinolite 1.5-2.5%, epidote 1-1.8%; CO_2: calcite 44%, dolomite 48%, S: pyrite 53%, pyrrhotite 36-38%) assemblages. This facies transition equates to a significant loss of H_2O-CO_2-H_2S-N_2 at temperatures of 400° to 500°C (Will et al., 1990)

Yardley et al. (1993) examined the detailed composition of H_2O-CO_2 fluid inclusions associated with post-metamorphic lode gold-quartz veins from part of the Italian Alps. They determined that fluids were compositionally uniform, with 5wt% NaCl equivalent, dominated by NaCl, with lesser $CaCO_3$ (aq), KCl, and Na_2CO_3 (aq). There are substantial H_2S contents of $> 10^{-3}$ molal, and minor CH_4 (< 0.002-0.003 mole %). Trace element concentrations in ppm are as follows: Al (300-1000), Mg (10-135),

Fe (20-170), B (100's), Li, Zn, and As (10's-100's), and Rb, Sr, Ba, 10's ppm. Bromine/Cl and I/Cl ratios are consistent with deeply circulating surface waters that underwent extensive exchange with crustal rocks. However, there is no sufficient database or knowledge of halogen systematics to rule out a metamorphic source or other fluids, and this meteoric water model has the same difficulty of other meteoric models explaining lithostatic fluid pressures.

2.4 Summary

Orogenic vein-type gold deposits in greenstone and turbidite belts are an important class of gold deposit; however, their mode of formation is still not fully constrained. Among all the models mentioned above, each has difficulty in explaining some of the characteristics of the deposits, and giving an integrated and satisfactory interpretation for the sum of their characteristics. None of the models can uniquely define the source of mineralizing fluids for lode gold deposits from the presently available data. These proposed genetic models are based on various lines of geological and geochemical evidence (mainly H, O, C, and S isotope studies) from different deposits. However, much of the isotopic data cannot be interpreted uniquely: (1) some of the H and O isotope compositions of fluids plot where metamorphic and magmatic fields overlap, and where meteoric waters would evolve to at low water/rock ratios and temperatures of 300° to 500°C; (2) many of the $\delta^{13}C$ of carbonate data have values consistent with mantle fluids, crustal magmas, or crustal dehydration; and (3) the same is true of the majority of S-isotope data on sulfides. Collectively, Sr and Pb isotope data permit mixing of fluids derived from crustal and mantle reservoirs. Clearly, new, less ambiguous, approaches are required to distinguish between these hypotheses.

Chapter Three

REVIEW OF PREVIOUS STUDIES OF NITROGEN AND N-ISOTOPES

3.1 Introduction

Research on the isotope geochemistry of nitrogen in geological systems began with the work of Hoering (1950), who measured nitrogen isotope ratios in silicate minerals. There was some early reconnaissance study of the isotope composition, concentration, and chemical state of nitrogen in rocks (Mayne, 1957; Scalan, 1958; Wlotzka, 1961, 1972; Stevenson, 1962; Vinogradov et al., 1962; Miloskiy and Volynets, 1966), but few reliable results were reported before the 1970's. The main reason was experimental, since nitrogen concentrations in minerals and rocks are low, generally < 1000 ppm and commonly <100 ppm, and extraction techniques were complicated (Boyd et al., 1993). Particularly it is difficult to check the completeness of the extraction, and resolve isobaric interferences from more abundant species including CO, CH_4 and H_2 giving rise to C_2H_5 and N_2H^+, respectively (Javoy, et al., 1986). Also it is important to decompose completely condensable and non-condensable nitrogen oxides (Javoy, et al., 1984). These difficulties of silicate N-isotope analysis have limited applications of N isotopes in the geochemistry of rocks and minerals. The situation has changed rapidly since the end of 1970's with the development of high temperature techniques for decomposition, and more sensitive mass spectrometers.

3.2 Nitrogen geochemistry

Nitrogen has two stable isotopes $^{14}_{7}N$ and $^{15}_{7}N$, where $^{14}_{7}N$ is the 'magic' nuclide making up more than 99 % of total N in the present atmosphere. Nitrogen has valence

states between +5 and -3 in different forms, such as nitric acid, nitrogen dioxide, nitric oxide, nitrous oxide, dinitrogen molecule, ammonia, amines, and amides. Table 3.1 lists the most common nitrogen compounds that exist in the natural world, by oxidation state. In minerals nitrogen as the ammonium ion (NH_4^+), may substitute for potassium in K-silicates because of its similar ionic radius and charge. For example, buddingtonite is the NH_4^+ counterpart to K-feldspar (Table 3.2; Erd et al., 1964; Vedder, 1965; Yamamoto and Nakahia, 1966; Whittaker and Muntus, 1970; Khan and Baur, 1972; Higashi, 1978,1982; Itihara and Honma, 1979; Honma and Itihara, 1981; Shigorova et al., 1981; Bos et al., 1988; Williams et al., 1989, 1992; Willaims and Ferrel, 1991; Sucha et al., 1998; Guidotti and Sassi, 1998).

3.3 Nitrogen content in various geological reservoirs

3.3.1 Introduction

Nitrogen comprises 78% of the Earth's atmosphere (Cox, 1995), and is a principal element of living biomass (2.5‰) and sedimentary hydrocarbons (Mayewski et al., 1986; Stahl, 1977; Quinn et al., 1988; Galloway et al., 1995; Jacobson et al., 2000). Nitrogen is a trace to major element in potassium silicate minerals in sedimentary, igneous, and metamorphic rocks (Itihara and Honma, 1979; Honma and Itihara, 1981; Bebout and Fogel, 1992; Boyd et al., 1993); is a significant component of crustal metamorphic fluids (Bottrell et al., 1988; Ortega et al., 1991); and also is present in trace quantities of 2-36 ppm in mantle volatiles, and at variable level diamonds (Javoy et al., 1986; Marty, 1995; Javoy, 1997, 1998; Cartigny et al., 1998).

Table 3.1. The most common nitrogen oxidation states, compounds in the natural world (from Cox, 1995; Jaffe, 2000)

Oxidation state	Name of compounds	Formula	Comments
+5	Nitrate ion	NO_3^-	(1) Man-made nitric acid (HNO_3 for industrial purposes) (2) Natural photochemical reaction produces nitric acid (acid rain). (3) Nitrate (KNO_3, $NaNO_3$ for fertilizers and explosives)
+4	Nitrogen dioxide	NO_2 (N_2O_4)	Produced by the oxidation of NO (a significant source of photochemical smog).
+3	Nitrite ion	NO_2^-	
+2	Nitric oxide	NO	Produced by the oxidation of NH_3 (a significant source of photochemical smog).
+1	Nitrous oxide	N_2O	A "greenhouse" gas, plays a significan role in stratospheric ozone chemistry.
0	dinitrogen molecule	N_2	(1) Predominant atmospheric gas (78%) (2) A trace component in mantle volatiles (3) A significant component in crustal metamorphic fluids
-3	Ammonia	NH_3	Man-made by the Haber process, principally for nitric acid production, then used for fertilizers and explosives
-3	Ammonium ion	NH_4^+	A trace component in potassium-silicates (illite, micas and K-feldspar).
-3	Amines	$R\text{-}NH_2$	An organic derivative of ammonia (biological nitrogen)
-3	Amides	$NH_2\text{-}CO\text{-}NH_2$	An component in urea and proteins (biological nitrogen)

Table 3.2. Ionic radii of ammonium and other cations (Å) (from Whittaker and Muntus, 1970; Khan and Baur,1972)

Coordination	K^+	NH_4^+	Rb^+	Cs^+
[6]	1.46	1.61	1.57	1.78
[8]	1.59	1.66	1.68	1.82
[9]	1.63	1.69	-	1.86
[12]	1.68	-	1.81	1.96

Å = 10^{-4} micrometer

3.3.2 Sediments and low-grade metasedimentary rocks

Ammoniacal nitrogen (NH_4^+) occurs widely in sedimentary rocks and low-grade metasedimentary rocks, where it is believed to be derived from the decomposition of nitrogen-bearing organic material (kerogen) during diagenesis. This is confirmed by the nitrogen isotopic composition of sediments, which is indistinguishable from that of coexisting kerogen (Williams et al., 1995).

A generalized model for the nitrogen cycle in a modern marine environment involved in biological processes and diagenesis and metamorphism, with accompanying isotopic fractionations is shown in Figure 3.1. For biological processes, atmospheric N_2 enters the biosphere via the process of biological nitrogen fixation (pathway 1) by a variety of bacteria and algae, to form N-bearing organic compounds, and ammonia (NH_3) or NH_4^+. Ammonia or NH_4^+ is also taken up by organisms to form N-bearing organic compounds, a process called ammonia assimilation (pathway 2), or can be further transformed into NO_3^- (or NO_2^-) during nitrification (pathway 3). The nitrate ions can undergo either assimilatory nitrate reduction (pathway 4) by organisms to form organic nitrogen compounds, or denitrification (pathway 5) to release N_2 into the atmosphere (Berner, 1971; Ehrlich, 1996; Hopkins et al., 1998; Owens and Watts, 1998; Beaumont and Robert, 1999; Boyd, 2001; Jaffe, 2001).

During diagenesis, organic nitrogen compounds decompose and are stored in sediments as kerogen (pathway 6). During progressive diagenesis and metamorphism, part of the N in kerogen is incorporated into potassium silicate minerals. The ammonium ion can first occupy interlayer sites of clay minerals such as smecitite or illite (pathway 7), and then be incorporated into the crystal structure of silicates, such as K-feldspar or K-micas (pathway 8). Organic N compounds can be also denitrified to

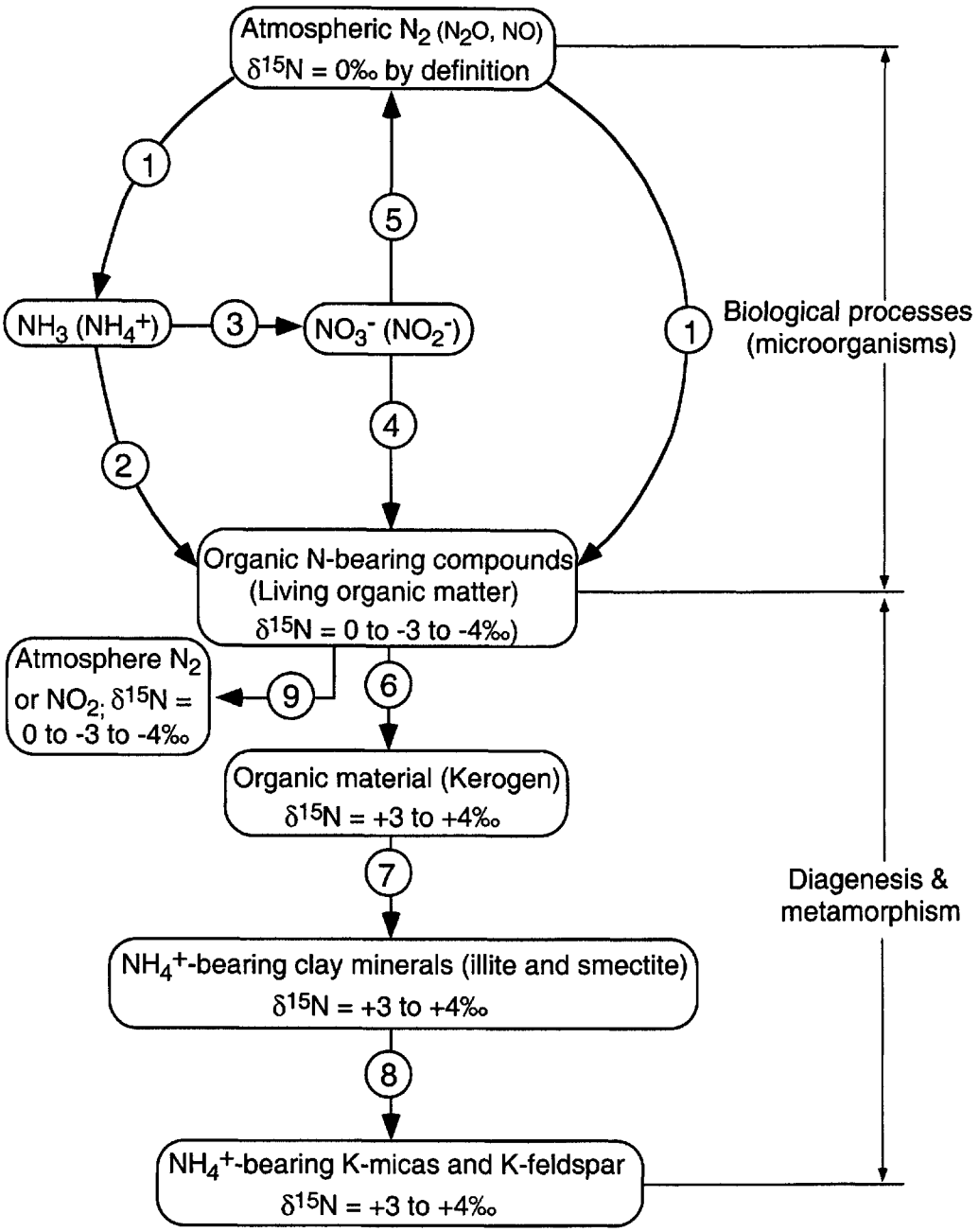

Fig. 3.1. A simplified model for the nitrogen cycle in a modern marine environment. Note: The numbers refer to precosses. Biological processes include 1, biological nitrogen fixation; 2, ammonia assimilation; 3, nitrification; 4, assimilatory nitrate reduction; 5, denitrification. Diagenesis and metamorphism include 6, diagenesis; 7 and 8, diagenesis and metamorphism (see tex for references).

denitrogen into the atmosphere (pathway 9; Milovskiy and Volynets, 1966; Berner, 1971; Honma and Itihara, 1981; Boyd and Philippot, 1998; Guidotti and Sassi, 1998; Hall, 1999; Boyd, 2001). As a result of these changes, most of the NH_4^+ in sediments eventually resides either in micas and/or K-feldspar. Therefore, the N concentrations of Phanerozoic sedimentary rocks and low-grade metasedimentary rocks will depend on their original organic content, and generally have wide ranges from a few hundred up to several thousand ppm (Table 3.3, and references therein). Precambrian metasedimentary rocks show relatively lower N concentrations, clustering within the range 6 to 575 ppm with a mean of 20 to 315 ppm (Table 3.3).

3.3.3 Metamorphic rocks

Nitrogen concentrations of metamorphic rocks depend both on their precursor and metamorphic grade. Milorskiy and Volynets (1966), Haendel et al. (1986) and Bebout and Fogel (1992) reported that N contents range from more than one thousand ppm N in sub-greenschist or greenschist facies rocks, to tens ppm in high grade metamorphic rocks (see Table 3.4). Nitrogen is also a common component of crustal metamorphic fluids as determined from fluid inclusions (Casquet, 1986; Bottrell et al., 1988; Darimont et al., 1988; Ortega et al., 1991).

3.3.4 Igneous rocks

There have been numerous studies concerning the nitrogen contents of igneous rocks, especially, of granites (Wlotzka, 1961, 1972; Itihara and Honma, 1979; Hall, 1987, 1988; 1999; Tainosho and Itihara, 1988; Cooper and Bradley, 1990; Hall and Neiva, 1990; Hall et al., 1991; Hall and Liverton, 1992). Igneous rocks, on the whole, have much lower nitrogen contents than sedimentary or metasedimentary rocks;

Table 3.3. Summary of Nitrogen contents of sedimentary and low-grade metasedimentary rocks

Sample location	N (ppm)			Nos. of samples	Metamorphic grade	References
	range	Median ± 1σ	mean			
Phanerozoic						
Cenozoic sandstone, Louisiana		1600 ± 100	1600	64		Williams et al. (1989)
Cenozoic shale, California	100 - 2800	1500 ± 760	1420	31		Compton et al. (1992)
Cretaceous Catalina subduction-complex zone, California	100 - 1100	540 ± 284	500	31	Low to greenschist facies	Bebout and Fogel (1992), Bebout (1997)
Devonian-Carbonniferous slates, Cornwall			1130			Hall (1988)
Ordovinian mudstone, N. England	750 - 1400					Cooper and Bradley (1990)
Ordovician phyllites, Germany	223 - 650	531 ± 147	726	14	Low to greenschist facies	Haendel et al. (1986)
Cambrian shale, Wales	322 - 1467	673 ± 483	780	5		Bottrell and Miller (1990)
Precambrian						
2.4 - 1.9 Ga Svecokarelic metasedimentary rocks, Finland	81 - 530	225 ± 195	266	6	Low to greenschist facies	Itihara and Suwa (1985)
2.1 Ga metasedimentary rocks, Ashanti belt, Ghana	140 - 575	300 ± 147	315	11	Low to greenschist facies	Jia and Kerrich (2001)
2.7 Ga metasedimentary rocks Superior Province, Canada	14 - 54	32 ± 15	33	14	Low to greenschist facies	Honma (1996) Jia and Kerrich (2000)
2.7 Ga metasedimentary rocks Hoyle Pond area, Canada	100 - 230	102 ± 15	110	7		Jia and Kerrich (2001)
2.5 - 2.8 Ga Kavirondian metasedimentary rocks, Kenya	25 - 61	54 ± 19	46	3	Low to greenschist facies	Itihara et al. (1986)
3.8 Ga Isua metasedimentary rocks, central Western, Greenland	6 - 86	31 ± 30	39	8	Low to greenschist facies	Honma (1996)
3.8 Ga Isua metasedimentary rocks, central Western, Greenland	7 - 30	18 ± 7	19	12	Greenschist facies	Jia and Kerrich (2001)

Table 3.4. Nitrogen content in metamorphic rocks

Rock type Location	Sample description	N (ppm) mean	N (ppm) range	No. of samples	Metamorphic grade	Refs.
Metamorphic rocks, Mugodzhar, Russia	Phyellite, shale and quartz-sericite schist	326	149 - 440	5	greenschist facies and lower	1
	Two micas and muscovite schist	114	73 - 162	5	lower amphibolite facies	1
	Plago, amphibolite gneiss	36	9 - 58	5	upper amphibolite facies	1
Metamorphic rocks, Russia and Austria	Orthogneisses	20	9 - 40	8	amphibilite facies	1, 2
	paragneisses	47	7 - 106	23	amphibilite facies	1, 2
Metasedimentary rocks, Germany	Phyllites	476	223 - 650	14	greenschist facies or lower	3
	Mica schists	203	40 -502	19	lower amphibolite facies	3
	Gneisses	35	25 - 82	7	high amphibolite facies	3
Metasedimentary rocks, (biotite separate), Japan		279	68 - 346	6	greenschist facies	4
Catalina Schist, California	Subduction complex	476	100 - 1100	32	greenschist facies or lower	5, 6
	Subduction complex	148	30 - 250	14	amphibolite facies	5, 6

Refs: 1 = Milorskiy and Volynets (1960); 2 = Wlotzka (1961); 3 = Haendel et al. (1986); 4 = Itihara and Honma (1979); 5 = Bebout and Fogel (1992); 6 = Bebout (1997).

average N contents are 23 ppm (n = 217; this study) for intrusive rocks, and 37 ppm (n = 53; Wlotzka, 1972) for volcanic rocks (Table 3.5, and references herein).

Nitrogen content increases from mafic to felsic igneous rocks: 11 ppm (n = 24; Wlotzka, 1972) for gabbro and diorites (Table 3.5), whereas 21 ppm (n =52; Wlotzka, 1972), or 27 ppm for worldwide Phanerozoic granitoids (Hall, 1987, 1988, 1989, 1999), and 24 to 27 ppm for Archean granitoids (Jia and Kerrich, 1999, 2000). Nitrogen contents tend to be higher in peraluminous granites, which are believed to have had a significant input of melted sedimentary rocks (so called S-type granite), whereas N contents are lower for granites formed from an igneous reservoir (e.g., I-type granite).

3.3.5 Mantle nitrogen

Nitrogen is a trace component of volatiles in the mantle; however, the content of nitrogen and the level to which this element is compatible or incompatible are uncertain. For example, Marty and coworkers inferred an upper mantle nitrogen abundance between 1 and 2 ppm from covariations of $N_2/^{36}Ar$ with $^{40}Ar/^{39}Ar$ and $^{3}He/^{4}He$ in MORB (here computed with an upper mantle $^{40}Ar/^{39}Ar$ ratio of 44,000; Moreira et al., 1998), and assumed that nitrogen, like He and CO_2, behaves as an incompatible element during melting (Table 3.6; Marty, 1995; Marty and Humbert, 1997). Assuming that nitrogen behaves as an incompatible element, a mantle carbon concentration of 400 ppm (Javoy et al., 1982; Javoy and Pineau, 1991), and the initial C/N ratios of mantle melts (i.e., the diamond growth medium) from which diamonds crystallize of between 200 and 500 (Cartigny et al., 2001), then a mantle nitrogen concentration between ~1 and 2 ppm can be calculated. This value is in agreement with Marty's estimate for MORB (Cartigny et al., 2001), and other previous measurements

Table 3.5. Nitrogen content in igneous rocks

Rock type Location	No. of samples	N (ppm) mean	N (ppm) range	References
Intrusive rocks				
Granites, U.S.A	6	6	1.4 - 12.5	Scalan (1959)
Granites, U.S.A	7	30	17 - 57	Stevenson (1962)
Granites, Russia, Japan	8	25	7 - 51	Vinogradov et al. (1963)
Granites, Worldwide	28	22	4 - 66	Wlotzka (1961)
Granodiorites, Worldwide	5	16	6 - 30	Wlotzka (1961)
All granites and granodiorites	**54**	**21**		Wlotzka (1972)
Gabbro, U.S.A	7	5	1.8 - 13.4	Scalan (1959)
Doirites and gabbro, worldwide	14	13	11 - 26	Wlotzka (1961)
All gabbro and diorites	24	11		Wlotzka (1961)
All intrusive rocks	**103**	**16**		Wlotzka (1972)
Granites, Japan	11	22	5 - 53	Itihara and Honma (1979)
Granites, British Isles	35	33	0 - 167	Hall (1987)
Granites, Finland	13	38	10 - 91	Itihara and Suwa (1985)
Granites, Germany		29	10 - 55	Junge et al. (1989)
Granites, English Lake district	28	< 30	1 - 150	Cooper and Bradley (1990)
Granites, Italy		17	0 - 50	Hall et al. (1991)
Granites, SW England	27	36	3 - 179	Hall (1988), Boyd et al. (1993)
All granites and granodiorites		27		Hall (1987)
All granites and granodiorites	**114**	**31**		This study (compilation)
All intrusive rocks	**217**	**23**		This study (compilation)
Volcanic rocks				
Rhyolites, obsidian	10	28	5 - 119	Wlotzka (1972)
Phonolites	27	37		Wlotzka (1972)
Trachytes	5	30	6 - 102	Wlotzka (1972)
Alkali olivine basalts	7	22	9 - 68	Wlotzka (1972)
All basalts	8	33	14 - 64	Wlotzka (1972)
Alkali olivine basalts	22	30	9 - 68	Wlotzka (1972)
Volcanic rocks	6	24	8 - 37	Scalaan (1959)
Volcanic rocks, worldwide	7	46	7 - 105	Vinogradov et al. (1963)
All volcanic rocks	**53**	**37**		Wlotzka (1972)

Table 3.6. Nitrogen content in the mantle

Rock type	No. of samples	N (ppm) mean	N (ppm) range	References
Fresh Ocean-floor basalts	7	1.4	0.3 - 2.8	Sakai et al. (1984)
MORB glasses	14		0.2 - 0.8	Zhang and Clayton (1988)
Ocean basalts	38		n.d. - 1.3	Marty (1995), Marty and Humber (1997)
Estimated from deep sea basalts			1 - 2	Norris and Schaeffer (1980), Sakai et al. (1984), Javoy and Pineau (1991)
Calculated from mass balance		35		Javoy (1997)
Estimated from $\delta^{13}C$-N relationship in diamonds		2 - 40		Cartigny et al. (2001)

Table 3.7. Summary of classification for chondritic meteorites(1)

	Group	Fe/SiO_2(2)	Fe0/Fe(2, 3)	FeO/(FeO +MgO)(4)	SiO_2/MgO(2)
Enstatite chondrites	E	0.77	0.8	0	1.9
		± 0.30	± 0.10		± 0.15
Carbonaceous chondrites	C	0.77			1.42
		± 0.07			± 0.05
Ordinary chondrites	H	0.77	0.63	18	1.55
		± 0.07	± 0.07	± 2	± 0.05
	L	0.55	0.33	24	1.59
		± 0.05	± 0.07	± 2	± 0.05
	LL	0.49	0.08	29	1.58
		± 0.05	± 0.07	± 2	± 0.05

Sources: (1), Data from Schmus and Wood (1967), ± ranges are not totally inclusive but represent approximate probable errors; (2), weight ratios; (3), metallic Fe/total Fe; (4), mole% FeO/(FeO+MgO) in olivine (=mole% fayalite)

(Table 3.6; Sakai et al., 1984; Zhang and Clayton, 1988). Alternatively, Javoy (1997,1998) deduced a mantle nitrogen abundance of about 36 ppm based on his formation model of the Earth. He concluded that terrestrial nitrogen is mostly stored in the mantle, and that nitrogen behaves as a compatible element (see Table 3.6). Nitrogen in the mantle is discussed further in Chapter seven.

3.3.6 Meteorites

Based on chemical properties and petrologic characteristics, chondritic meteorites are divided into three groups: (1) C group, carbonaceous chondrites, such as C1, C2, C3, and CM; (2) E group of enstatite chondrites, such as E4, E6; and (3) ordinary chondrites, the H, L, and LL groups (Table 3.7; Mason, 1963; Ahrens, 1964; Schmus and Wood, 1967). The Tagish Lake meteorite that fell in January 2000 is a carbonaceous chondrite (C group) of uncertain further classification (Brown et al., 2000; Pizzarello et al., 2001). Nitrogen abundances of these meteorites vary ranging from a few to tens ppm for ordinary involatile chondrites, through tens to a hundred ppm in C3 carbonaceous chondrites, a few hundreds ppm in enstatite chondrites, to several hundreds to 1500 ppm in the volatile rich C1, C2, and Tagish Lake carbonaceous chondrites (Table 3.8 and references therein).

3.4 N-isotope compositions in various geological reservoirs

3.4.1 Organic compounds and sediments

Nitrogen isotope compositions of different geological reservoirs are distinctive. It has been suggested that atmospheric N_2 ($\delta^{15}N = 0‰$, by definition) is the initial source for organic matter (Boyd and Philippot, 1998; Jaffe, 2000; Boyd, 2001). Biological nitrogen fixation is the enzyme-catalyzed reduction of N_2 or dissolved species (mainly

Table 3.8. Abundances and isotopic compositions of nitrogen in chondritic meteorites

Meteorite	Group*	Extraction method**	N (ppm)	$\delta^{15}N$ (‰)	reference
Alais	C1		1250	+31	1
Ivuna	C1		1855	+52	1
Orgueil	C1		1476	+46	2
			1360	+39	3
Banten	C2		780	+43	1
Bells	C2		685	+47	1
Boriskino	C2		520	+16	1
Cochabamba	C2		670	+35	1
Cold Bokkeveld	C2	P	560	+22	4
			850	+35	1
			1060	+20	1
Erakote	C2		700	+43	1
Mighei	C2		810	+26	2
		P	690	+27	4
Murchison	C2		760	+39	3
			845	+43	2
		P	830	+44	4
			360	+39	5
Murray	C2		990	+39	3
			1020	+46	2
Ngooya	C2		550	+13	1
Pollen	C2		1150	+39	1
Allende	C3	P	18	-43	4
			19	+6	2
			21	-26	6
			20	-34	6
			17	-36	5
			18	+20	1
Leoville	C3	P	88	-24	4
			102	-24	1
Ornans	C3	P	12	-13	7
Grosnaja	C3	P	54	-25	4
Abee	E4	P	277	-29	4
		BK	344	-30	4
Indarch	E4	P	544	-26	4
			204	-20	2
Hvitis	E6	P	785	-43	4
Pillistfer	E6	P	310	-36	4
Daniel's Kuil	E6	P	167	-24	4
Parnallae	LL3	P	10	-3.5	4
Hamlet	LL3,4	P	11	+8	4
Soko-Banja	LL4	P	75	+6	4
Olivenza	LL5	P	5	+20	4
Ttysnes Island	H4 (dark)	P	11	+22	4
	H4 (light)	P	12	+36	4
Weston	H4 (dark)	P	7	+14	4
	H4 (light)	P	10	+19	4
Richardton	H5	P	6	+14	4
Bjurbole	L4	P	13	+7	4

* C = carbonaceous chondrite; E = enstatite chondrite; H, L, LL = ordinary chondrite

** P = vacuum pyrolsis; BK = bomb kjeldahl

References: 1 = Kerridge (1985); 2 = Injerd and Kaplan (1974); 3 = Robert and Epstein (1982); 4 = Kung and Clayton (1978); 5 = Lewis et al. (1983); 6 = Thiemens and Clayton (1981); 7 = Smith and Kaplan (1970).

nitrate formed from N_2) to NH_3 or NH_4^+, which is taken up by an organism to become part of its biomass in the form of nitrogen-bearing organic compounds. Organic materials, such as plants, leaf letter, sapropels, and living phytoplankton, all have negative $\delta^{15}N$ values of about <0 to –4‰, but typically between –3 to -4‰ (Fig. 3.1; Table 3.9; Kao and Liu, 2000; Nadelhoffer and Fry, 1998; Sachs and Repeta, 1999), due to the kinetically preferred use of ^{14}N relative to ^{15}N by organisms.

The $\delta^{15}N$ value of organic matter in sediments is controlled by its degree of maturation. Studies of early diagenesis commonly report whole rock $\delta^{15}N$ values close to that of organic matter (Rau et al., 1987). With progressive diagenesis, thermal decomposition of nitrogen-bearing organic compounds is a major process, causing preferentially release of ^{14}N given lower energy to break ^{14}N-^{12}C bonds than ^{15}N-^{12}C bonds. Residual organic nitrogen compounds are stored in sedimentary rocks as kerogen having $\delta^{15}N$ values of 3.6 ± 0.55‰ (n = 22) according to Ader et al. (1998) and Williams et al. (1995), which is indistinguishable from the value of 3.9 ± 0.1‰ (n = 5) reported by Kao and Liu (2000). Modern sedimentary rocks and bulk crust having $\delta^{15}N$ values of +3.0 to +3.5‰ are virtually indistinguishable from the isotopic composition of kerogen, which implies that NH_4^+ is incorporated from kerogen into authigenic K-silicates (Table 3.9; Ader et al., 1998; Kao and Liu, 2000; Williams et al., 1995; Sachs et al., 1999). This conclusion is consistent with insignificant nitrogen isotope fractionation between kerogen and nitrogen fixed as NH_4^+ in minerals (Delwiche and Steyn, 1970; Heaton, 1986; Shearer and Kohl, 1993). In detail, changes in the $\delta^{15}N$ of organic matter in sediments during diagenesis and burial are complex

Table 3.9. Summary of nitrogen isotope compositions in various rocks

Rock type	No. of samples	$\delta^{15}N$ (‰) range	$\delta^{15}N$ (‰) mean ± 1σ	References
Organic materials				
Terrestrial and aquatic plants	14		-4.4 ± 1.2	Kao and Liu (2000)
Terrestrial leaf litter			-3.8 ± 0.2	Nadelhoffer and Fry (1988)
Chlorin in sapropels	7		-5.0 ± 0.4	Sachs and Repeta (1999)
Living phytoplankton	3		-6.4 ± 1.4	Sachs and Repeta (1999)
Sediments				
Marine sediments	60	+2.4 to +9.9		Pters et al. (1978)
Marine sediments	34	-2.6 to +5.7		Rau et al. (1987)
Marine sediments	4		5.4 ± 0.7	Sachs et al. (1999)
Marine sediments	4		3.1 ± 0.3	Williams et al. (1995)
Terrestral sediments	3		3.9 ± 0.1	Kao and Liu (2000)
Terrestral sediments	18	+2.7 to +5.1	4.1 ± 0.8	Ader et al. (1998)
Coal and crude oil	29	-0.5 to +3.7		Rigby and Batts (1986)
Igneous rocks				
S-type granites	11	+5.1 to +10.2	+8.7	Boyd et al. (1993)
Metamorphic rocks				
Metasedimentary rocks	43	+2.5 to +17.0		Haendel et al. (1986)
Catalina Schist	46	+1.0 to +6.4		Bebout and Fogel (1992), Bebout (1997)
Mantle derived materials				
Nitrogen in MORB		-2.4 to -5.9	-5.0	Javoy and Pineau (1991)
Nitrogen in MORB		-1.0 to -6.4	-5.0	Marty (1995), Marty and Humbert (1997)
Nitrogen in diamonds				
1. Fibrous diamond	55	-11.2 to +6.0	-5.0	Javoy et al. (1984, 1986)
		-8.7 to -1.7	-6 to -5	Boyd et al. (1987, 1992, 1994)
2. P-type diamond	40	-26.0 to 0	-4.5	Cartigny et al. (1997)
3. E-type diamond	39	-10.1 to -1.1	-5.5	Cartigny et al. (1998)
Chondritic meteorites				
C1 & C2 carbonaceous	22	+20 to +50		Kung and Clayton (1978)
chondrites				Kerridge (1985), Javoy and Pineau (1983)
Enstatite chondrites	7	-20 to -43		Kung and Clayton (1978)
				Javoy and Pineau (1983)
C3 carbonaceous chondrites	6	-43 to +20		Kung and Clayton (1978), Kerridge (1982)
H, L, LL ordinary chondrites	10	-10 to +20		Kung and Clayton (1978)

due to variable mixtures of a range of organic compounds that decompose under different thermal conditions (Stiehl and Lehmann, 1980).

3.4.2 Metasedimentary rocks

During metamorphism of N-bearing sedimentary rocks, ammonium becomes incorporated into the crystal lattices of common rock-forming K-silicate minerals. The N-isotopic composition and content in metasedimentary rocks has been investigated by Haendel et al. (1986) for regional metamorphism of intra-continental rocks, whereas Bebout and Fogel (1992) and Bebout (1997) studied metamorphism in subduction zones. Similar behavior was observed in both cases: the $\delta^{15}N$ values obtained by Haendel et al. (1986) of between +3.3 and +7.8‰ were typical of modern sediments (Table 3.9, and references therein), whereas those of Bebout and Fogel (1992) overlapped the range of modern sediments, but were towards the low end at +1.1 to +2.7‰. Thus it is possible that nitrogen in low-grade metasedimentary rocks may preserve the original $\delta^{15}N$ value of the precursor organic matter.

With increasing metamorphic grade, ammonium starts to break down due to devolatilization reactions (Haendel et al., 1986; Bebout and Fogel, 1992), the nitrogen being released as N_2, which represents a common component in crustal metamorphic fluids (Table 3.10; Casquet, 1986; Bottrell et al., 1988; Ortega et al., 1991). According to Haendel et al. (1986), concentrations and isotopic compositions of nitrogen in metamorphic rocks show systematic changes: the nitrogen content decreases whereas $\delta^{15}N$ increases with increasing metamorphic grade, due to progressive loss of $\delta^{15}N$-depleted metamorphic fluids, and $\delta^{15}N$ values may acquire a wide range from +3 to +17 ‰. However, a number of studies show that N concentrations decrease, but

Table 3.10. Evidence for N_2 as a common component in crustal metamorphic fluids

Location	Vein composition	Host rock	Fluid inclusion composition	N_2 content* mol%	Reference
Berzosa Shear Zone Spain	quartz	garnet-staurolite schist	CH_4-CO_2-H_2O-N_2	trace to 71.4	Casqet (1986)
Bastogne Belgium	quartz	meta-arkoses and sandstone	CH_4-CO_2-N_2	0.6 to 99.0	Darimont et al. (1988)
Llanbedr Formation North Wales	quartz ± albite ± pyrite ± mica ± Au	slates	CH_4-CO_2-H_2O-N_2	1.52 to 55.36	Bottrell et al. (1988)
Mari Rosa, Cacers Spain	quartz ± chlorite ± albite ± mica ± Au	schist-greywacke	CH_4-CO_2-N_2	9.6 to 77.4	Ortega et al. (1991)
Monte Rosa district Italy	quartz ± carbonate ± mica ± Au	gneiss and schist	CH_4-CO_2-H_2O-N_2	0.2 to 0.32	Yardley et al. (1993)
Dome de Montredon France	quartz ± albite ± chlorite ± mica	black shale	CH_4-CO_2-H_2O-N_2		Moine et al. (1994)

* N_2 results from laser-Raman analyses

nitrogen isotopic compositions do not change significantly with increasing metamorphic grade (Wada et al., 1975; Delwiche and Steyn, 1970; Heaton, 1986; Williams et al., 1995, Ader et al., 1998).

3.4.3 Granitic rocks

There are few studies of nitrogen isotopic composition on igneous rocks. Boyd et al. (1993) found that $\delta^{15}N$ of all peraluminous Hercynian S-type granites in SW England were low between 5 and 10 ‰ (Table 3.9), with low N contents averaging 21 ppm. These results are consistent with the result of Wlotzka (1972) and Hall (1987). New data from this study show that peraluminous granites in the Archean Abitibi subprovince, and tonalites in the Uchi subprovince (Red Lake areas) of the Superior Province have $\delta^{15}N$ values of 1.3 to 5.3‰ and –5.3‰ to +5.1‰, respectively, and also lower N contents of 24-27 ppm (Jia and Kerrich, 1999, 2000).

3.4.4 Mantle-derived materials

Mantle nitrogen isotope composition has been determined from mid-ocean ridge basalts, and initially on fibrous diamonds in Zaire by Javoy et al. (1984), Javoy and Pineau (1991), Marty (1995) and Marty and Humbert (1997). Data for diamonds were expanded on a worldwide sampling basis by Boyd et al. (1987, 1992). Their results show that $\delta^{15}N$-values are negative (-8.7 up to –1.7‰) with a mean of –6 to –5‰. Independently, Cartigny et al. (1997, 1998) and Marty and Zimmerann (1999) suggested that mantle $\delta^{15}N$ values were between –5 and –8‰ from a survey of nitrogen isotopes in diamonds (Table 3.9).

3.4.5 Meteorites

Nitrogen isotopic compositions of chondritic meteorites have been studied since the nineteen seventies (Injerd and Kaplan, 1974; Kung and Clayton, 1978; Robert and Epstein; 1982; Kerridge, 1982, 1985; Javoy and Pineau, 1983). A review of the published literature shows that nitrogen isotopic compositions of two carbonaceous chondrites (C1 and C2) have enriched $\delta^{15}N$ values of +13 to +52‰, with most values lying within +30 to +42‰ (Table 3.9; Kung and Clayton, 1978; Javoy and Pineau, 1983; Kerridge, 1985), whereas enstatite chondrites have depleted $\delta^{15}N$ ranging from –20 to –43‰, with most between –25 and –30‰ (Table 3.9; Injerd and Kaplan, 1974; Kung and Clayton, 1978). C3 carbonaceous chondrites have large internal variations of $\delta^{15}N$ between –43 to +20‰ (Smith and Kaplan, 1970; Kung and Clayton, 1978; Kerridge, 1985). For ordinary chondrites, their $\delta^{15}N$ values range from –10 to +20‰ (Table 3.9; Kung and Clayton, 1978). The variability of $\delta^{15}N$ in meteorites collectively has been interpreted to result from non-uniform injection of material having distinctive nucleosynthetic pathways, from a neighboring supernova, into the presolar system accretion disc (Schramm and Clayton, 1978; A. Delsemme, 2001; personal communication).

3.5 N-isotope fractionation

Variations in the isotopic composition of nitrogen in samples (spl) relative to the standard (std) are expressed as:

$$\delta^{15}N = [(^{15}N/^{14}N)_{spl}/(^{15}N/^{14}N)_{std} - 1] \times 1000 \qquad (3.1)$$

where the standard is atmospheric N_2, defined to be zero per mil (Hoering, 1955).

Two studies have published N-isotope fractionation factors calculated based on spectroscopic data (Hanschmann, 1981; Richet et al., 1977). Experimental data of mineral-fluid fractionations are conspicuously absent. Of the two theoretical studies, only Hanschmann (1981) calculated fractionations involving NH_4^+ in solid and fluid phases; the results of those calculations for temperatures of 327° to 927°C are tabulated in Haendel et al. (1986). According to an interpolation of the data in Hanschmann (1981), the calculated $\Delta^{15}N_{fluid\text{-}rock}$ ($\Delta^{15}N = \delta^{15}N_{fluid} - \delta^{15}N_{rock}$) would range from approximately –3.4 to –2.25‰ at temperatures of 350° to 600°C for the isotope exchange reaction (after Scalan, 1958):

$$^{15}N^{14}N + {}^{14}NH_4^+ = {}^{14}N_2 + {}^{15}NH_4^+ \qquad (3.2)$$

Bebout and Fogel (1992) evaluated fluid-rock isotope fractionation of N during devolatilization of metasedimentary rocks of the Catalina Schist Belt using a Rayleigh distillation model based on direct measurement of nitrogen isotope ratios of whole rock powder. They obtained $\delta^{15}N$ of 1.9 ± 0.6‰ (632 ± 185 ppm N) in lowest grade rocks and 4.3 ± 0.9‰ (138 ± 76 ppm N) for high grade rocks. The calculated $\Delta^{15}N_{fluid\text{-}rock}$ of –1.5 ± 1‰ is similar to, but somewhat smaller than, the calculated N_2-NH_4^+ fractionations of Hanschmann (1981) for the appropriate temperature range (350° to 600°C) of the Catalina Schist. Other studies on the N-isotopic fractionations during metamorphism by both measurement and experiment also show that the N content decreases relatively from low to high metamorphism, whereas the N-isotopic composition does not increase significantly with metamorphic ranks (Williams et al., 1995; Ader et al., 1998). Jia and Kerrich (1999, 2000) further confirmed minor fractionation of nitrogen isotopes between fluid and rock (see Chapters 4 to 6).

3.6 Summary

The occurrence of nitrogen, its content and isotopic composition in minerals and rocks has been studied over the last three decades. Nitrogen, primarily as structurally bound NH_4^+, may substitute for K in potassium-bearing silicates such as muscovite, biotite, or K-feldspar, because of its similar ionic radius and charge. The isotopic composition of nitrogen has large variations in geological reservoirs, which makes this isotope system a potentially important tracer for the origin of terrestrial silicates and volatiles:

(1) Mid-oceanic ridge basalt (MORB, $\delta^{15}N$ = -8.7 to –1.7‰) and diamonds ($\delta^{15}N$ = -10 to 0‰) reflect mantle N and collectively have a mean $\delta^{15}N$ value about –5‰ and low N contents of 1 to 2 ppm or 36 ppm.

(2) Organic nitrogen compounds have a mean $\delta^{15}N$ value of about <0 to -3 to -4‰. Sediments show relative enrichments in ^{15}N, with mean $\delta^{15}N$ values of +3 to +4‰ for organic N (kerogen) in marine sediments, and N content of ten's to 3000 ppm.

(3) Sedimentary rocks have N in organic matter and authigenic K-silicates with $\delta^{15}N$ of about +4‰, inherited from kerogen.

(4) Peraluminous S-type granites have $\delta^{15}N$ between +5‰ to < +10‰ with low N content, averaging 21 ppm.

(5) Metamorphic rocks range from +1‰ to > +17‰, with ten's to > 1000 ppm N contents.

(6) Meteorites have been grouped into four classes based on composition: C1 and C2 carbonaceous chondrites have $\delta^{15}N$ of +20 to +50‰ (mostly within +30 to +40‰), with higher N contents of a few hundreds to 1500 ppm; enstatite chondrites have

depleted $\delta^{15}N$ of –20 to –43‰ (mostly within –25 to -30‰), with a few hundreds ppm N; C3 carbonaceous chondrites have large internal variations of $\delta^{15}N$ of –43 to +20‰, with lower N contents of tens ppm; Ordinary chondrites (H, L, LL) have $\delta^{15}N$ of –10 to +20‰, with lower N contents of few to tens ppm.

(7) The fractionation of nitrogen isotopes between fluid and rock is small, ca. –1.5 ± 1‰ at temperatures of 350 to 600°C.

Chapter Four

N AND $\delta^{15}N$ SYSTEMATICS OF SELECTED ARCHEAN OROGENIC GOLD QUARTZ VEIN SYSTEMS

4.1 Introduction

The Superior Province of Canada is the largest exposed craton of Archean age, and more than 5,000 tonnes of gold has been produced from orogenic gold deposits (Colvine et al., 1989; Hodgson et al., 1993). Most of this gold has been recovered from deposits within 2.9 to 2.7 Ga volcanic-plutonic greenstone belts (Fig. 4.1). Within the Superior Province, the Abitibi greenstone belt is the most prolific Au-producing greenstone terrane and is endowed with a relatively large number of unusually rich vein gold deposits, such as the Hollinger, Dome, and Kerr Addison mines, which account for more than 60 percent of the production.

Virtually all gold deposits in the Superior Province occur within and immediately adjacent to greenstone belts in rocks which range in metamorphic grade from low-greenschist to amphibolite faceis (Hodgson and MacGeehan, 1982; Colvine, 1989). All greenstone belts are composed predominately of mafic and ultramafic rocks, with relatively subordinate quantities of felsic volcanic rocks, and variable volumes of clastic sedimentary rocks (Fig. 4.1).

Gold deposits in the Norseman terrane, Western Australia, are part of the richly mineralized 2.7 Ga Norseman-Wiluna greenstone belt. They are hosted in mafic rocks of greenschist – amphibolite facies transitional metamorphic grade (McCuaig et al., 1993). Collectively, the deposits occur in the entire spectrum of greenstone belt lithologies. It is beyond the scope of this thesis to go into details of the geology of

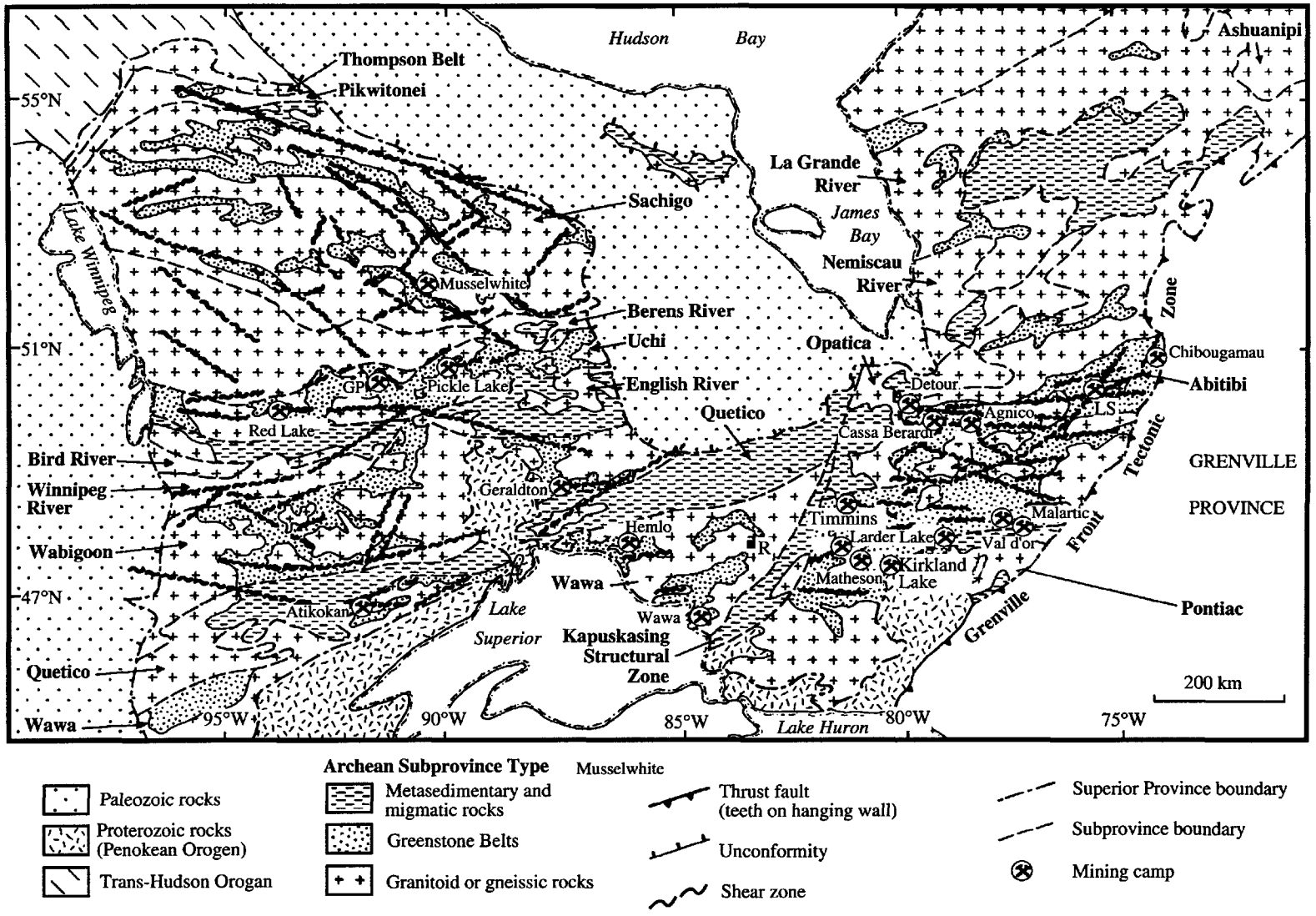

Fig. 4.1. Geological map of the Superior Province of Canada showing the distribution and location of gold camps (Modified from Hodgson and MacGeehan, 1982; Colvine, 1989)

deposits within the Superior Province and Norseman terrane. This topic has been comprehensively discussed by numerous authors (Table 4.1).

The purpose of this chapter is to report new data for nitrogen contents and N-isotopes on hydrothermal micas from Archean orogenic lode gold deposits of the Superior Province, Canada, and the Norseman terrane, Western Australia, to constrain their genesis. There are few N-isotope studies of major hydrothermal vein systems (Jia and Kerrich, 1999, 2000). Accordingly, a study was warrented given the intense potassic alteration associated with such systems; the substitution of NH_4^+ for K^+ in K-silicates; known presence of N_2 in fluids inclusions in the quartz veins (Table 3.10 in Chapter 3; Kreulen and Schuling, 1982; Kreulen et al., 1986; Casquet, 1986; Ortega et al., 1991); and the distinct N-isotope compositions of different crustal and mantle reservoirs (Chapter 3). N-isotope data for hydrothermal K-silicates might preserve a less ambiguous signature of the fluid source reservoirs than other stable or radiogenic isotopes.

There is no systematic study of the N content and $\delta^{15}N$ of K- silicates, and $\delta^{13}C$ and $\delta^{18}O$ of carbonates, versus metamorphic grade for these quartz vein systems, which formed in lower greenschist to upper amphibolite facies metamorphic environments (Groves, 1993; McCuaig et al., 1993). According to Haendel et al. (1986), N content is expected to decrease and $\delta^{15}N$ increase during progressive loss of $\delta^{15}N$-depleted metamorphic fluids with increasing metamorphic grade. $\delta^{13}C$ may also decrease, with increasing metamorphic grade, due to progressive loss of ^{13}C depleted carbonic metamorphic fluids during decarbonation reactions. $\delta^{18}O$ should also decrease as

Table 4.1. Brief summary of the geology of deposits in the Superior Province and Norseman terrane

Craton Mining district	Deposits	Age (Ma)	Metamorphic grade	Source
Superior Province, Canada				
Timmins	Dome, Hollinger, Goldhawk, Beaumont	2720-2660	Mid- to upper greenschist facies	Ferguson et al. (1968), Kerrich and Fryer (1979), Pyke (1982), Hodgson (1983), Moritz and Crocket (1991), Burrow et al. (1993)
Kirkland Lake	Kerr-Addison	2700	Low greenschist facies	Jensen (1980), Kishida and Kerrich (1987)
Red Lake	Cochenour, Dickenson	2720	Greenschist-amphibolite transition	Andrews and Wallace (1983), Durocher and Hugon (1983), Lavigne and Crocket (1983)
Hemlo	Williams, David Bell	2672-2670	Greenschist-amphibolite transition	Heather and Arias (1987), Pan and Fleet (1995)
Geraldton	MacLeod, Hardrock	2700	Greenschist-amphibolite transition	Lavigne (1983), MacDonald (1983)
Pickle Lake	Pickle Crow	2700	Greenschist-amphibolite transition	Thompson (1939)
Norseman terrane, Western Australia				
Norseman		2670-2660	Low amphibolite facies	McCuaig et al. (1993)

mineral-water fractionations become smaller at higher temperatures (Lattanzi et al., 1980; Rumble, 1982; Bebout and Carlson, 1986).

Consequently, sample selection was designed to cover a range of metamorphic grade of the host terranes, inasmuch as the metamorphic grade of alteration associated with the veins typically matches that of the host terrane; i.e. quartz vein systems in higher grade terranes precipitated at higher temperatures, and are not metamorphosed equivalents of pre-existing veins formed at lower temperature (McCuaig et al., 1993).

4.2 Characteristics of quartz-carbonate-mica vein systems

Quartz-carbonate-mica vein systems in these orogenic gold deposits are characterized by intense and extensive wall-rock alteration including development of hydrothermal quartz, carbonate, sulfides (primarily pyrite), and K or Na silicates. Mica, as a common hydrothermal mineral in the veins, or their altered wallrocks, is compositionally variable with metamorphic grade: greenschist facies deposits are characterized by K or more rarely Na mica, or intermediate compositions. Other elements in micas that display variations include FeO (0.44 – 1.04 wt%); MgO (1.26 – 1.95 wt%); TiO_2 (0.15 – 0.45 wt%); and Cr_2O_3 (0.00 – 3.16 wt%). The ratios of FeO/(FeO + MgO) and $Al_2O_3/(CaO + Na_2O + K_2O)$ extends from 0.22 to 0.40 and 2.60 to 3.30, respectively. MnO contents of muscovite are generally low, from below detection limit to 0.06 wt% (see Appendix II).

Biotite is prevalent in the higher temperature deposits that formed in upper greenschist to granulite facies terranes (McCuaig et al., 1993). Abundances of FeO and MgO are higher, ranging from 10.43 to 21.06 wt% and 9.01 to 17.25 wt%, respectively. Ratios of FeO/(FeO + MgO) and $Al_2O_3/(CaO + Na_2O + K_2O)$ vary from 0.38 to 0.70 and 1.71 to 1.93, respectively. MnO and TiO_2 contents are also relatively higher between

0.10 and 0.20 and 1.00 and 2.11, respectively. Generally, as K_2O contents in micas go down, FeO, MgO, and TiO_2 contents go up (Appendix II).

Carbonate is also an abundant hydrothermal mineral in the giant quartz vein systems: in general, ankerite to ferroan-dolomite is prevalent in sub- to greenschist facies deposits, whereas calcite is dominant in upper-greenschist to amphibolite facies deposits (McCuaig et al., 1993). Therefore, hydrothermal micas and carbonates in these vein systems are ideal minerals for analyzing N and C isotopic compositions to constrain the $\delta^{15}N$ and $\delta^{13}C$ of the vein-forming fluids.

4.3 Sample population

In this study samples analyzed were selected from the collection of R. Kerrich and C. McCuaig. Y. Pan donated samples from Hemlo. They include six regions in the Superior Province of Canada and the Norseman terrane in the Yilgarn craton, Western Australia (Table 4.1). Samples were obtained from mines that provide access to unweathered samples in a vein geometry constrained in three dimensions. These vein systems are hosted in different grade metamorphic terranes based on geological and geochemical studies, and hydrothermal alteration mineral assemblages (Table 4.2).

Samples were processed for mineral separation to obtain pure mica and pyrite separates, and a carbonate concentrate from quartz veins. Analytical methods for N contents and N-isotopes are reported in Appendix I. Electron microprobe analyses were conducted on grain mounts of micas, and C and O isotope data for coexisting carbonate, are also reported.

Table 4.2. Summary table of hydrothermal alteration assemblages of giant gold-bearing quartz vein systems from the Neoarchean Superior Province of Canada and the Norseman terrane of western Australia (Modified from Jia and Kerrich, 2000)

Metamorphic grade	Deposit Location	Host rocks	Hydrothermal alteration mineral assemblage[a]	Ore-fluid[b] (T°C; MPa)
Superior Province of canada				
Low-greenschist facies	Kerr-Addison Kirkland Lake	ultramafic-mafic rocks syenites	q + ab + mus + cab + sul	270-300°C 100-200 MPa
Mid-to upper-greenschist facies	Dome, Hollinger, goldhawk Porcupine	mafic volcanic and felsic intrusive rocks	q + mus +ab + chl + cab + sul	340-450°C; 100-300 MPa
Greenschist-amphibolite transition	Macleod-Cockshutt Geraldton	malfic volcanic and felsic intrusive rocks	q + chl + mus + tour + cab + sul	400-500°C; 200-400 MPa
	Williams, Davis Bell Hemlo	ultramafic-mafic rocks	q + Ca-amp + mus + chl +cab + sul	400-500°C; 200-400 MPa
Western Australia				
Lower amphibolite facies	Norseman Norseman terrane	ultramafic-mafic rocks	cal + q +chl + bi + sch +tour + pl	420-500°C; 200-400 MPa

[a] Abbreviations: q = quartz, ab = albite. mus = muscovite, chl = chlorite, tour = tourmaline, Ca-amp = Ca-amphibole, bi = biotite, sch = scheelite, pl = plagioclase, cab = carbonate, sul = sulfide.

[b] Vein systems in the Superior Province of Canada from Hodgson and MacGeehan (1982), Kerrich and Fryer (1979). Kishida and Kerrich (1987), and Pan and Fleet (1995). Vein systems in the Norseman terrane of Western Australia from McCuaig et al. (1993).

For comparison, nine metasedimentary host rock samples from the Abitibi greenstone belt and 14 K-feldspars and micas from granites of the Abitibi and the Red Lake greenstone belts were analyzed.

4.4 Results

N and N-isotope, and C-isotope data are reported in Tables 4.3 – 4.5 and Figs. 4.2 – 4.5. The hydrothermal micas from quartz vein systems in lower to upper greenschist facies terranes have relatively high N abundances that covary with high K_2O contents. For muscovites in lower greenschist facies quartz veins (Kerr-Addison), the N abundances are between 193 and 205 ppm (average 198 ppm), with corresponding K_2O contents of 11.80-11.30%, and $\delta^{15}N$ values range from 18.2 to 20.3‰. The C-isotope compositions of hydrothermal ferroan dolomite and calcite are tightly clustered with similar mean values of –2.8 ± 0.1‰ (1σ) and –2.8 ± 0.2‰ (1σ) respectively. However, O-isotope compositions of calcite (13.8 ± 0.6‰; n = 8) are systematically ^{18}O- enriched compared with ferroan dolomite (12.4 ± 0.1‰; n = 8).

In mid- to upper greenschist facies vein systems (Hollinger, Dome and Goldhawk), the N concentrations range from 30 to 191 ppm (average 111 ppm), with K_2O contents of 10.59-11.29%, and $\delta^{15}N$ has a larger range from 14.6 and 21.0‰. Calcite has $\delta^{13}C$ and $\delta^{18}O$ values (-3.7 ± 0.4‰ and 12.60 ± 0.7‰, n = 16) close to those of ferroan dolomite (-3.3 ± 0.4‰ and 12.3 ± 0.9‰, n =16), but both appear relatively depleted in ^{13}C and ^{18}O relative to counterparts in lower greenschist facies terranes (Table 4.3 and Figs. 4.2 - 4.5).

For quartz vein systems hosted in higher metamorphic grade terranes, the N concentrations of micas are relatively low and correlate with relatively low K_2O

Table 4.3. Nitrogen, carbon and oxygen isotope data for Neoarchean giant quartz vein systems (Modified from Jia and Kerrich, 1999, 2000)

Mining district	Sample	Nitrogen		Carbon		Oxygen		K_2O (mica)
		N (mica)	$\delta^{15}N$ (mica)	$\delta^{13}C$ (dolomite)	$\delta^{13}C$ (calcite)	$\delta^{18}O$ (dolomite)	$\delta^{18}O$ (calcite)	
Deposit	No.	(ppm)	(‰)	(‰)	(‰)	(‰)	(‰)	(%)
Superior Province								
Kirkland Lake (hosted in low-greenschist facies terrane; mean ± 1σ)				-2.7 ± 0.1	-2.8 ± 0.1	12.6 ± 0.4	13.8 ± 0.8	
Kerr-Addson I	KA II-1	195	19.4	-2.7	-2.7	12.5	14.2	11.28
	KA II-2	203	18.9	-2.8	-2.7	12.5	14.5	
	KA II-3	198	19.2	-2.6	-3.1	12.4	13.1	
	KA II-3*			-2.9	-2.9	12.3	13.6	
Kerr-Addson II	KA I-1	202	20.3	-2.8	-2.7	12.8	13.7	11.30
	KA I-2	205	19.4	-2.7	-2.7	13.5	15.0	
	KA I-3	194	18.2	-2.6	-2.7	12.4	12.6	
	KA I-4	193	19.9					
Porcupine (hosted in mid-to upper greenschist facies terrane; mean ± 1σ)				-3.3 ± 0.4	-3.7 ± 0.4	12.3 ± 0.9	12.6 ± 0.7	
Dome	B4	186	16.8	-3.3	-3.9	12.5	13.1	11.20
	B4-1*	191	17.2	-3.3	-3.3	11.8	13.0	11.25
	B5	170	16.7	-2.8	-4.4	12.9	12.9	11.14
	D-1	160	15.6	-3.3	-3.3	12.1	12.7	11.05
Goldhawk	GH IA	150	18.2	-3.6	-3.2	13.4	12.7	10.87
	GH IB	170	19.8	-3.2	-3.0	12.1	13.6	11.04
	GH IC	140	16.9	-3.3	-3.3	12.6	13.5	10.79
Beaumont	NMT170	110	11.8					11.04
	NMT230	114	13.5					
Hollinger 1	GH I-B	100	15.1	-3.2	-3.2	12.2	12.6	11.14
	GH I-C*	120	14.6	-3.0	-3.5	12.1	13.0	11.28
	GH I-D*	111	17.8	-3.0	-3.7	12.0	12.8	11.17
	GH I-E	113	15.6	-3.5	-3.6	12.8	12.9	11.26
	GH I-F	128	16.0	-4.0	-4.3	11.9	10.7	11.29
Hollinger 2	GH II-1	30	14.7	-3.5	-4.3	13.7	10.7	10.59
	GH II-2	40	17.1	-4.1	-3.8	10.9	13.0	10.66
	GH II-3	38	20.9	-2.7	-4.1	12.1	11.2	9.77
	GH II-4	42	21.0	-2.9	-3.8	11.4	11.6	
	GH II-5	42	17.0					
Geraldton (hosted in greenschist-amphibolite transition; mean ± 1σ)				-5.9 ± 0.6	-6.1 ± 0.3	11.4 ± 0.9	12.8 ± 0.3	
Macleod	MAC	57	17.0	-5.8	-6.1	11.7	12.7	9.39
	MAC-1	53	14.0	-5.6	-5.6	12.0	13.1	9.80
	MAC*			-4.5	-5.3	12.4	12.4	
	MAC-1*			-5.9	-6.3	11.6	13.0	

Table 4.3. (continued)

Mining district	Sample	Nitrogen		Carbon		Oxygen		K_2O (mica)
		N (mica)	$\delta^{15}N$ (mica)	$\delta^{13}C$ (dolomite)	$\delta^{13}C$ (calcite)	$\delta^{18}O$ (dolomite)	$\delta^{18}O$ (calcite)	
Deposit	No.	(ppm)	(‰)	(‰)	(‰)	(‰)	(‰)	(%)
Hardrock	HD-1	23	13.6	-6.1	-6.2	11.2	13.2	9.69
	HD-2	19	10.4	-6.1	-6.1	12.0	13.2	9.50
	HD-3			-6.1	-6.2	10.4	12.6	
	HD-1*			-6.5	-6.1	9.6	12.5	
	HD-2*			-6.2	-6.3	9.9	12.8	
Hemlo (hosted in greenschist-amphibolite transition; mean ± 1σ)								
Williams	WL170	19	12.8					9.81
	WL230	19	14.8					
	WL100	19	20.7					
	WL230*	20	16.6					
David Bell	DVB100	40	10.1					
	DVB170	35	11.4					
	DVB230	35	11.1					
Pickle Lake (hosted in greenschist-amphibolite transition; mean ± 1σ)								
Pickle Crow	PL	28	14.3					9.48
	PL-1	30	13.9					9.72
Red Lake (hosted in greenschist-amphibolite transition; mean ± 1σ)								
Cochenour	CHR-A	30	12.9					9.13
	CHR-B	31	14.6					10.17
Norseman, Western Australia								
Norseman (hosted in Lower amphibolite facies terrane; mean ± 1σ)				-6.5 ± 0.9	-6.6 ± 0.9	9.8 ± 1.0	10.1 ± 0.7	
	NR7-1	70	22.6	-6.5	-5.9	10.1	10.2	9.87
	NR7-1*	70	22.2	-6.3	-5.4	12.1	9.7	
	NR10	20	8.7	-4.7	-5.2	10.2	9.7	9.43
	NR10*			-5.2	-5.6	9.6	10.9	
	MRAI-1	20	13.0	-8.1	-7.3	10.8	10.8	9.60
	MRA I-2	20	19.0	-7.5	-7.5	10.0	10.2	9.83
	MRA II-1	20	14.0					9.88
	VHW-1	10	12.6	-6.3	-7.2	9.7	10.7	9.40
	VHW-1*			-7.1	-6.7	10.4	10.3	
	NNM-1	30	10.9	-7.6	-6.6	9.1	11.3	9.26
	NNM-2	30	20.6	-7.1	-8.0	8.4	9.1	9.44
	NNM-a	50	16.1					9.68
	NNM-b	40	16.4					9.60
	RT-1	20	15.9	-5.5	-7.2	8.8	9.1	9.78
	RT-2	20	23.7	-6.1	-6.7	9.0	9.3	

* Duplicates

Table 4.4. Nitrogen content and $\delta^{15}N$ for host rocks (metasedimentary rocks) in the Abitibi greenstone belt of the Superior Province (from Jia and Kerrich, 2000)

Sample location	Sample number	$\delta^{15}N$ (‰)	N (ppm)
Larder Lake Group			
	S4-2	13.8	37
	S4-4	17.3	20
	S4-5	12.3	16
Dome Formation			
	813-14	11.8	27
	813-13	15.4	51
	813-14	13.9	39
Matachewan Sediments			
	723-17	8.7	14
	723-20	15.5	16
	723-14	14.6	15

Table 4.5. Nitrogen content and $\delta^{15}N$ for K-silicates in granites from the Abitibi and Red Lake greenstone belts (from Jia and Kerrich, 1999, 2000)

Location Granite	Sample no.	Mineral	$\delta^{15}N$ (‰)	N (ppm)
Abitibi subprovince				
Peraluminous	4	K-feldspar	5.3	20
granite	MO#7	K-feldspar	5.0	20
	86-1	K-feldspar	2.6	20
	86-1-1	Lepidolite	1.3	20
	NS-85-49	Muscovite	1.6	20
Uchi subprovince				
Tonalites	#39	Biotite	-1.6	50
	#21	Biotite	-3.0	20
	23	Biotite	0.3	30
	90A	Biotite	-1.2	30
	#13	Biotite	-5.3	20
	34	Biotite	-3.8	20
	37	Biotite	2.3	20
	#76	Biotite	5.1	20
	#68	Biotite	-0.9	20

contents. In the Geraldton and Hemlo vein systems, N contents range from 19 to 57 ppm (average 29 ppm), with K_2O contents of 9.39-9.81%, and $\delta^{15}N$ spans 10.4 to 20.7‰. The $\delta^{13}C$ and $\delta^{18}O$ values of both ferroan dolomite and calcite show greater depletion compared with lower greenschist facies veins: mean values (n = 8) are –5.9 ± 0.6‰ and 11.4 ± 0.9‰ for dolomite, and –6.1 ± 0.4‰ and 12.8 ± 0.3‰ for calcite, respectively.

Micas in Norseman quartz veins have low N contents between 10 and 70 ppm (average 32 ppm), and low K_2O contents of 9.40-9.87%, and $\delta^{15}N$ ranges from 10.9 to 23.7‰ (two outliers). Compared with lower greenschist facies quartz vein systems, the C- and O-isotope compositions are even more depleted, with an average $\delta^{13}C$ = –6.5 ± 0.9‰ in ferroan dolomite and –6.6 ± 0.9‰ for calcite, and $\delta^{18}O$ = 9.8 ± 1.0‰ in ferroan dolomite and 10.1 ± 0.7‰ for calcite (see Table 4.3 and Figs. 4.2 – 4.5).

For metasedimentary host rocks in the Abitibi greenstone belt, N contents are relatively low between 15 and 51 ppm, but nitrogen isotopic compositions are relatively higher ranging from 11.8 to 17.3‰ (one outlier; Table 4.4). These values are similar to those of micas in the gold deposits (Table 4.3). In contrast, micas and K-feldspars from granitoids in the Abitibi and Red Lake greenstone belts are characterized by both systematically lower $\delta^{15}N$ of +1.6 to +5.3‰ and –5.3 to 5.1‰, and generally lower N contents averaging 27 and 24 ppm, respectively. The results are consistent with other studies of N content and N-isotope in granitiods, which have an average nitrogen of 21 ppm (n = 54) according to Wlotzka (1972), or 27 ppm from the survey of Hall (1987), and $\delta^{15}N$ of –5 to 10‰ (Boyd et al., 1993; Jia and Kerrich, 1999; Table 4.5 and Fig. 4.3).

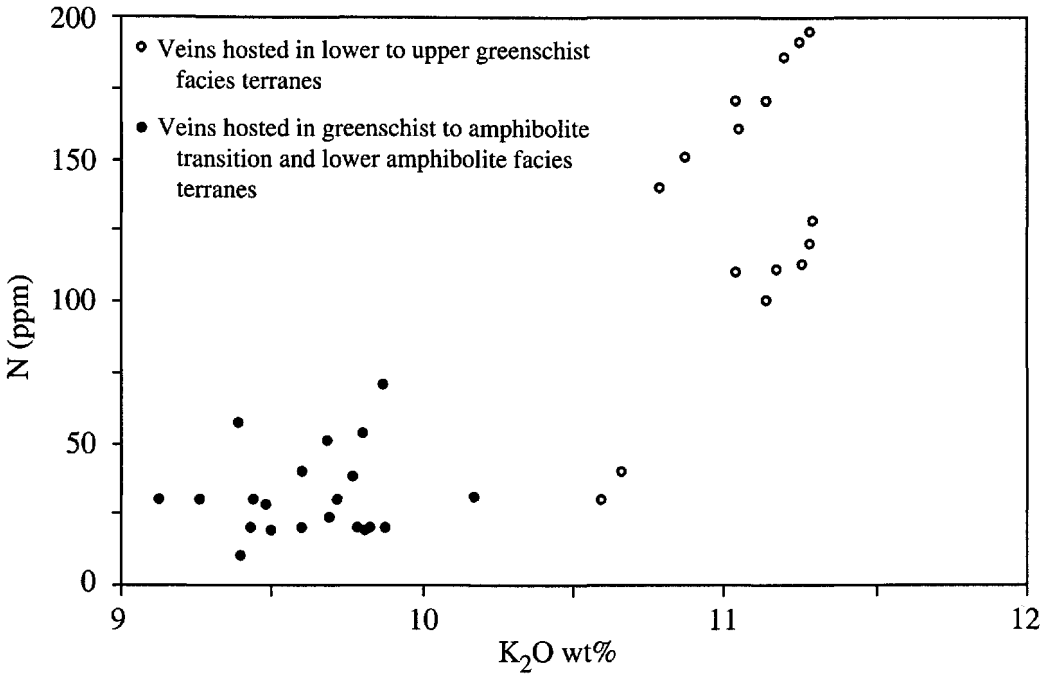

Fig. 4.2. Covariation of K_2O and N contents of micas from Archean orogenic gold quartz-carbonate-mica vein systems of the Superior Province of Canada and the Norseman district, Western Australia (modified from Jia and Kerrich, 2000). Uncertainty for N content is omitted because it is smaller than the plot symbol.

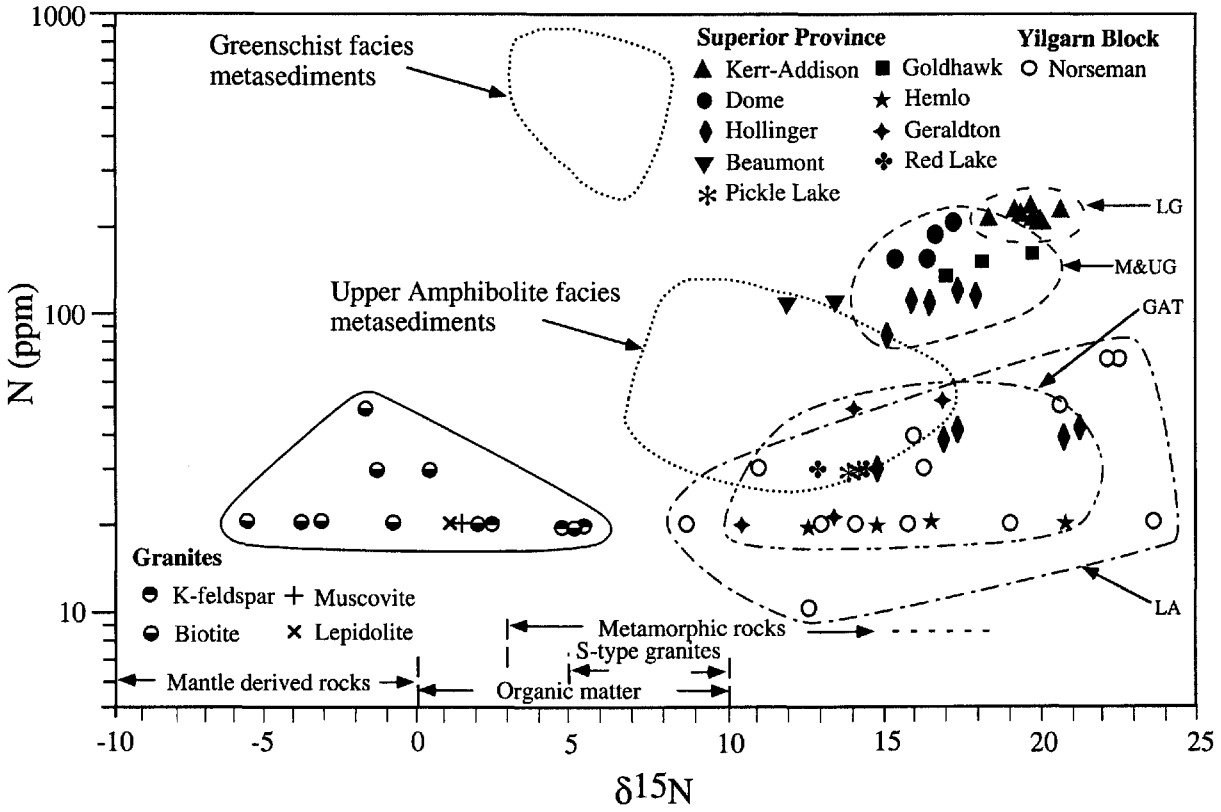

Fig. 4.3. Distribution of $\delta^{15}N$ values and nitrogen contents of mica separates from Au-bearing quartz veins compared to results for K-silicates from granites. Data in Tables 4.4 and 4.6. Note: LG = lower greeschist facies terranes; M&UG = mid- to upper greenschist facies terranes; GAT = greenschist to amphibolite transition terranes; LA = lower amphibolite facies terranes. Fields for rock reservoirs are from Peters et al. (1978), Haendel et al. (1986), Boyd et al. (1993), Boyd and Pillinger (1994), and Cartigny et al. (1998). Modified from Jia and Kerrich (1999, 2000).

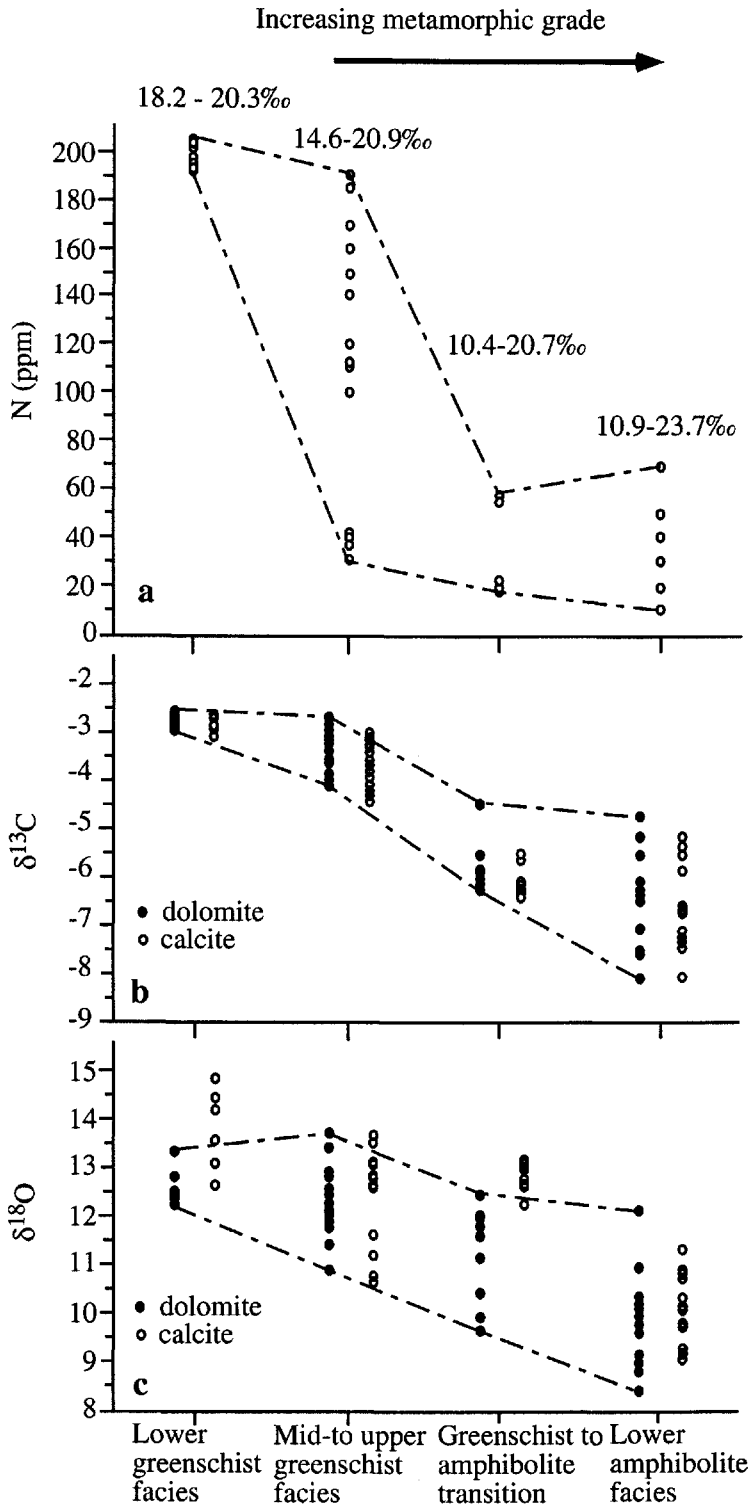

Fig. 4.4. N content in micas and $\delta^{13}C$ and $\delta^{18}O$ data in carbonates of gold-bearing quartz veins from the Superior Province of Canada and the Norseman of Western Australia: a. N versus metamorphic grade, and showing $\delta^{15}N$ ranges in different metamorphic grade; b. $\delta^{13}C$ versus metamorphic grade; c. $\delta^{18}O$ versus metamorphic grade. Note: data in Table 4.4 (after Jia and Kerrich, 2000).

4.5 Discussion

The data presented in Tables 4.3 – 4.5, and Figs. 4.2-4.5, allow some conclusions to be made regarding N, C, and O isotope compositions of the gold quartz vein systems, the source of the hydrothermal fluids, and trends with increasing metamorphic grade.

4.5.1 N and N-isotope characteristics

The N and N-isotope results for hydrothermal micas from these Neoarchean gold vein systems are not consistent with either mantle-derived fluids, or magmatic hydrothermal fluids evolved from crystallizing granitoids. Mantle nitrogen concentration and isotope composition have been determined previously from mid-ocean ridge basalts and from fibrous diamonds in Zaire. Their results show that nitrogen contents are very low (<1-2 ppm), and that δ^{15}N-values are negative (-8.7 up to –1.7‰) with a mean of –6 to –5‰ (Chapter 3; Javoy et al., 1984; Boyd et al., 1987, 1992; Javoy and Pineau, 1991; Marty, 1995). These values are distinct from micas of 10.4 to 23.7‰ in the quartz vein systems (Table 4.3 and Figs. 4.3 and 4.5).

The N-isotope composition of granitoids from both the Abitibi and Red Lake greenstone belts are also depleted in ^{15}N (δ^{15}N= -5.3 to +5.1‰), consistent with other granitoids. According to Boyd et al. (1993), peraluminous, or S-type, granites have nitrogen isotope compositions restricted to 5 to 10‰. Micas in quartz veins are all enriched in ^{15}N compared to granitoids (Table 4.5 and Figs. 4.3 and 4.5). The characteristics and timing of granitoids and gold mineralization in the two giant gold quartz vein systems of the Superior Province and the Yilgarn craton are well constrained by crosscutting relationships with precisely dated igneous rocks. Formation of the giant quartz vein systems in general, and associated lode gold deposits, immediately post-dates

termination of the main pulse of tonalitic granitoid emplacement at ca. 2685 Ma, and closely follows peak metamorphism within these accretionary orogenic belts, whereas rare peraluminous S-type granites at 2660 to 2635 Ma are all post quartz vein formations (Kerrich and Cassidy, 1994; Kent et al., 1996; Cassidy et al., 1998).

Most Archean granitoids belong to the high Al, high La/Yb tonalite-trondhjemite-granodiorite (TTG) series generated from melting of subducted ocean lithosphere or ocean plateau basalt (Tarney and Jones, 1994; Drummond et al., 1996). These sources are expected to have low mantle-like N-isotope compositions.

It is also unlikely that N in the hydrothermal micas of the giant quartz vein systems is meteoric surface water. Global mean nitrogen isotopic values of meteoric water are 4.4 ± 2.0‰ (n= 263; Owens, 1987). Meteoric water could evolve to more positive $\delta^{15}N$ values by exchange with N in rocks during convective circulation in the crust. However, they cannot generate observed values of 10 to 24‰ in micas of veins under small rock – fluid N-isotope fractionations (Bebout and Fogel, 1992). Furthermore, vein geometry requires hydraulic fracturing given conditions:

$$P_{fluid} > P_{lithostatic} + T \qquad 4.1$$

And metamorphic fluids are generated under conditions:

$$P_{fluid} \geq P_{lithostatic} \qquad 4.2$$

Where T is the tensile strength (Fyfe et al., 1978; Jia et al, 2000).

Accordingly deeply convecting meteoric water under hydrostatic conditions can be ruled out. Other geological and geochemical evidence such as the δD of micas and other isotope systems (O, Sr, and Pb) of these quartz vein systems are also inconsistent with

the meteoric water model (see Fig. 2.2 in Chapter 2; McCuaig and Kerrich, 1998; Jia and Kerrich, 1999).

The N concentrations and nitrogen isotope compositions of hydrothermal micas from these giant gold quartz vein systems are consistent with those of Archean metasedimentary rocks (12 to 17‰; Table 4.4), and also overlap the previously measured range of $\delta^{15}N$ for metamorphic rocks, but extend to higher values than reported by Haendel et al. (1986). Hence the results are consistent with fluids evolved by dehydration of crustal rocks during metamorphism.

Nitrogen contents of micas in these gold quartz covary well with K_2O contents; both decrease with increasing metamorphic grade (Table 4.3; Fig. 4.2). These results confirm that N appears to reside predominantly in the hydrothermal micas as NH_4^+, as concluded in earlier studies of the N concentrations of coexisting minerals in igneous and metamorphic rocks (see Honma and Itihara, 1981; Guidotti and Sassi, 1998; Sucha et al., 1998). The results are also consistent with previous studies in which the nitrogen contents were found to decrease with increasing metamorphic grade (Milovsky and Volynets, 1966; Rösler et al., 1977; Haendel et al., 1986).

Collectively, the N-isotopic compositions of hydrothermal micas for these gold quartz veins systems are restricted to the metamorphic rock field (see Figs. 4.3 and 4.5; with two outliers), in keeping with the vein-forming fluids of these giant gold quartz vein systems having been derived from metamorphic dehydration. The data do not show a clear trend of increasing $\delta^{15}N$ from lower greenschist facies quartz veins to lower amphibolite facies quartz veins as has been reported for a composite set of metamorphic rocks by Haendel et al. (1986) (Table 4.3; Fig. 4.3).

4.5.2 $\delta^{13}C$ and $\delta^{18}O$ characteristics

Carbon isotope composition of carbonates from quartz vein systems have been extensively studied over the last two decades (for a review see Groves et al., 1988; Kerrich, 1990; McCuaig and Kerrich, 1998). Various genetic hypotheses have been proposed based on the C-isotope compositions from different gold quartz vein systems. A mantle CO_2-lower crustal process for quartz vein systems was suggested from $\delta^{13}C$ values of about –4‰, and the observation that the vein emplacement was coeval with 'cratonization' of these shield areas, driven by mantle CO_2-induced granulite formation in the lower crust (Fyon et al., 1984; Colvine et al., 1988). The mean of the present set of data for MORB $\delta^{13}C$ is –5.2 ± 0.7‰ (Marty and Zimmermann, 1999), and diamond data (2700 analyses) show mean values of –5 ± 1‰ (Cartigny et al., 1997, 1998). Thus, the similarity of MORB and diamonds in terms of $\delta^{13}C$ confirms a first-order homogeneity for mantle carbon isotope composition (Deines et al., 1991; Javoy and Pineau, 1991; Marty and Zimmermann, 1999). Hence a component of carbon in the aqueous carbonic ore fluids could be of mantle origin (Fig. 4.5), but mantle C cannot account for the total range of $\delta^{13}C$ from –11 to +2‰ in this class of Au deposits collectively (Kerrich, 1990).

Based on a comparison of $\delta^{13}C$ values for the granodiorite-related Mink Lake quartz-Mo vein deposits and carbonates from the two largest gold-bearing quartz vein systems (Hollinger-McIntyre, -3.1 ± 1.3‰; Golden Mile, -3.4 ± 0.4‰) which have statistically indistinguishable $\delta^{13}C$ distributions, Burrows et al. (1986) and Burrows and Spooner (1987) suggested that all three are magmatic origin (Chapter 2). However, $\delta^{13}C$ values of –6 to -2‰ are also difficult to interpret uniquely with regard to the carbon source, precisely because magmatic, sedimentary, metamorphic rocks, and average crust

are all characterized by average $\delta^{13}C$ values in this range (Ohmoto and Rye, 1979; Boyd et al., 1987; Javoy et al., 1986; Marty and Zimmermann, 1999). The total range of $\delta^{13}C$ carbonate in all gold quartz veins of this type is –11 to +2‰ (Kerrich, 1990). Consequently, a magmatic model fails to account for those gold quartz veins where $\delta^{13}C$ carbonate is beyond the magmatic range (Tables 4.3 and 4.6).

The $\delta^{13}C$ values of hydrothermal carbonates are dependent on temperature, fO_2, and pH during mineral precipitation, as well as the $\delta^{13}C_{\Sigma c}$ of the hydrothermal fluids (see Ohmoto and Rye, 1979). The fluid depositing hydrothermal carbonates in these gold quartz veins are generally considered to be characterized by conditions of fO_2 close to the QFM buffer and above CO_2-CH_4, pH near neutral to slightly acid, and T > 270°C (Mikucki and Ridley, 1993). At these conditions, carbon isotope fractionation attributable to redox effects is minor ($\delta^{13}C_{Carbonate} \approx \delta^{13}C_{\Sigma Cfluid}$; Ohmoto and Rye, 1979). The general trend of decreasing $\delta^{13}C$ of carbonate in veins from lower greenschist (-2.7‰; Kerr-Addison), through mid- to upper greenschist (-3.3‰; Porcupine), greenschist-amphibolite transition (-5.9‰; Geraldton), to lower amphibolite facies (-6.5‰; Norseman) is therefore consistent with progressive loss of ^{13}C-depleted aqueous carbonic fluid as metamorphic grade increases (Fig. 4.4b; Valley, 1986).

The oxygen isotope composition of dolomite in these gold vein systems is more robust than in calcite, where the latter may be reset during uplift and reactivation by retrograde exchange with surface fluids (Kerrich, 1990). The trend to lower $\delta^{18}O$ values of dolomite at higher metamorphic grade is compatible with decreasing mineral-water fractionations at greater temperatures (Ohmoto, 1986; see Fig. 4.4c]. Together, the coupled $\delta^{13}C$ and $\delta^{18}O$ depletion trends with increasing metamorphic grade in these giant

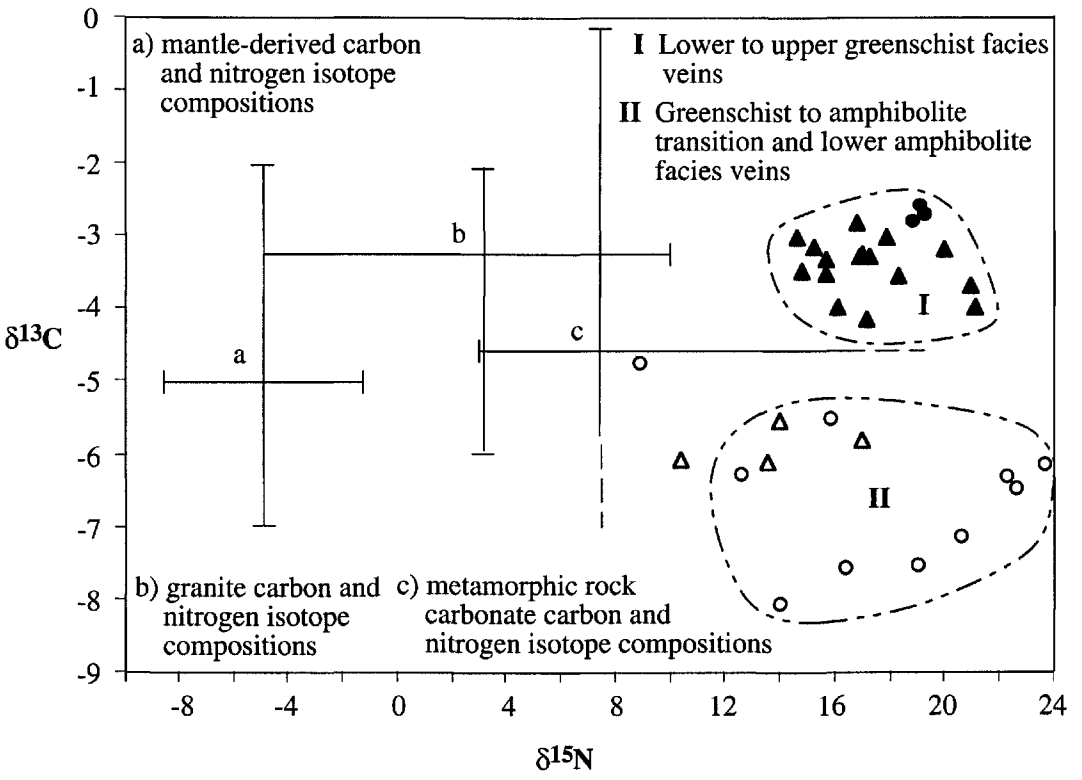

Fig. 4.5. $\delta^{15}N$ and $\delta^{13}C$ variations of Neoarchean gold-bearing quartz veins of the Superior Province of Canada and the Norseman in Western Australia. Note: data in Table 4.3. Symbols: ● Kirkland Lake; ▲ Porcupine; Δ Geraldton; ○ Norseman (after Jia and Kerrich, 2000).

Table 4.6. Summary statistics for C and O isotope compositions of hydrothermal carbonate from Neoarchen giant quartz vein systems (from Jia and Kerrich, 2000)

District	Metamorphic grade	Estimated ore	$\delta^{13}C$ (‰PDB)			$\delta^{18}O$ (‰SMOW)			Source
Deposit		fluid (T°C, P)	range	n	mean ± st.dev.	range	n	mean ± st.dev.	
Superior Province of Canada									
Kirkland-Lake									
Kerr-Addison	Low-G	270-300, low P	-3.1 to -2.6	7	-2.8 ± 0.2	12.3 to 14.4	7	13.2 ± 0.9	1
			-3.0 to -1.6	11	-2.2 ± 0.45	12.0 to 13.8	11	12.8 ± 0.5	2
Timmins									
Dome, Goldhawk,	Mid-to upper-G	340-450, 1-3 kb	-4.4 to -2.0	27	-3.4 ± 0.6	10.7 to 14.0	27	12.4 ± 0.9	1
and Hollinger				275	-3.1 ± 1.3				3
Geraldton									
Macleod-Cockshutt,	G-A transition	400-500, 2-4 kb	-6.3 to -4.5	16	-5.9 ± 0.5	9.9 to 13.2	16	12.1 ± 1.0	1
Hardrock									
Yilgarn Block, Western Australia									
Norseman-Wiluna belt									
Golden Mile No.4 lode	Mid-G	350-400, low P	-4.1 to -1.5	21	-3.4 ± 0.4		3	13.3 ± 0.7	4
Golden Mile main lode			-3.8 to -3.1	16	-3.35 ± 0.2				
Victory Defiance	G-A transition	340-430, 2kb	-8.7 to -4.6	22	-7.1 ± 1.3		5	10.7 ± 1.8	4
Northern Noresman	Low-A	420-475, 3kb	-6.5 to -4.7	8	-5.6 ± 0.6	9.6 to 10.9	8	10.9 ± 1.9	1
Central Norseman	Low-A	475-500, 3kb	-8.1 to -5.5	14	-7.1 ± 0.9	8.8 to 10.8	14	9.9 ± 0.9	1

Note: G = Greenschist facies; A = Amphibolite facies; n = number of analyses; st.dev. = standard deviation. 1 = this study; 2 = Kishida and Kerrich (1987); 3 = Burrow et al. (1986); 4 = Groves et al. (1988).

Neoarchean quartz vein systems suggests that CO_2 contribution to the vein-forming fluids was via decarbonation processes during regional metamorphism (Lattanzi et al., 1980; Rumble et al., 1982; Valley, 1986; Bebout and Carlson, 1986).

4.6 Implications and conclusions

From geological observations the sites of these giant shear zone hosted gold quartz vein systems of Neoarchean to Cenozoic age are in convergent margin subdution-accretion orogenic belts (Kerrich and Wyman, 1990; Goldfarb et al., 1991; Kerrich and Cassidy, 1994; Kent et al., 1996). The temporal and spatial relationship of the vein systems to subduction-accretion, and the characteristics of the hydrothermal fluids, are consistent with metamorphic-related dehydration of hydrated oceanic crust and sediments within the accretionary complexes. The Sr and Pb isotope characteristics of quartz veins systems are also consistent with lithological complexity in the source-plumbing conduit-sink system (McCuaig and Kerrich, 1998).

The nitrogen isotope composition of hydrothermal micas is consistent with fluids derived from progressive metamorphism in a lithologically complex and ^{15}N enriched crust. The coupled $\delta^{15}N$ and $\delta^{13}C$ values in these quartz vein systems strongly support the metamorphic fluid hypothesis for the origin of the vein-forming fluids. Numerous independent lines of geological and geochemical evidence are consistent with a metamorphic fluid origin: restriction of these quartz vein systems to metamorphic terranes; lithostatic vein-forming fluid pressures; the consistently low aqueous salinity; and local uniformity but regional variations of other isotope systems (H, O, S, Sr, and Pb) consistent with lateral variability of crustal lithologies. A dilute, aqueous carbonic and N-bearing composition (C-O-H-N) is common to metamorphic fluids (Table 3.10 of

chapter 3; Krenlen et al., 1986; Casquet, 1986; Bottrell et al., 1988; Ortega et al., 1991) generated at the greenschist to amphibolite transition (Kerrich and Fryer, 1979; Powell et al., 1991). Phillips (1993) independently concluded that the hydrothermal fluids specific to the giant quartz vein systems were also derived from a $\delta^{15}N$-enriched source of volcanic and siliciclastic sedimentary rocks at the greenschist to amphibolite transition within a subduction-accretion complex, where fluids advect on regional scale structures into the supracrustal sequences where the giant gold quartz vein systems form.

4.7 Summary

(1) N and K_2O contents of hydrothermal micas covary which reflects that N appears to reside in micas as NH_4^+; both decrease with increasing metamorphic grade.

(2) For lower to upper greenschist facies gold quartz veins, N contents and $\delta^{15}N$ values of micas are between 40 and 200 ppm and 15 and 21‰ respectively, whereas in gold quartz vein formed at the greenschist to amphibolite transition and lower amphibolite facies, micas have N contents of 20 – 70 ppm and $\delta^{15}N$ of 11 – 24‰.

(3) Metasedimenary host rocks in the Superior Province have N contents of 15 to 51 ppm and $\delta^{15}N$ values of 12 to 17‰.

(4) In contrast, micas and K-feldspar from granitoids are characterized by systematically lower $\delta^{15}N$ of –5 to +5‰ and generally lower N contents of 20 to 50 ppm, comparable to other granitoids.

(5) Carbon and oxygen isotopic compositions of hydrothermal ferroan dolomite and calcite show systematic depletions with increasing metamorphic grade. The mean values range from –2.7 to –3.3‰ for $\delta^{13}C$ and 12.6 to 12.3‰ for $\delta^{18}O$ in veins

formed at lower to upper greenschist facies, but from –5.9 to –6.6‰ for $\delta^{13}C$ and 11.4 to 9.8‰ for $\delta^{18}O$ at higher metamorphic grade.

(6) The N contents and N-isotope values of 20 to 200 ppm and 10 to 24‰ for hydrothermal micas from these gold vein systems of the Neoarchean Superior Province and Norseman of Western Australia are not consistent with either mantle-derived fluids, magmatic hydrothermal fluids evolved from crystallizing granitoids, or convecting meteoric water, but are consistent with metamorphic dehydration.

(7) The coupled ^{13}C and ^{18}O depletion trends with increasing metamorphic grade in these giant Neoarchean quartz vein systems also suggests that CO_2 contribution to the vein-forming fluids was via decarbonation processes during regional metamorphism.

Chapter Five

H, C, N, O, AND S ISOTOPE SYSTEMATICS OF THE PALEOZOIC DEBORAH DEPOSITS, BENDIGO GOLD PROVINCE, AUSTRALIA

5.1 Introduction

The majority of giant Archean orogenic gold metallogenic provinces occur in volcanic-plutonic (greenstone) terranes, whereas Paleoproterozoic examples are in volcanic-sedimentary accretionary orogenic belts, and Phanerozoic deposits in siliciclastic dominated accretionary terranes (Groves and Phillips, 1987; Kerrich, 1987; Groves et al., 1989; Ho et al., 1992; McCuaig and Kerrich, 1998). Phanerozoic examples of these vein systems are listed in Tables 2.3 and 2.4 of chapter two. There is no consensus on the origin of these turbidite-hosted gold vein systems; they have been classified separately (Robert et al., 1997), or together with greenstone hosted gold deposits (Kerrich et al., 2000).

The Bendigo-Ballarat goldfield is a world-class gold metallogenic province with a cumulative production of 2500 tonnes of gold, hosted in metaturbidites of the Paleozoic succession of central Victoria, that is part of large metallogenic provinces in the Tasman Orogenic Belt of eastern Australia. In the Bendigo-Ballarat goldfield, about 1100 tonnes of gold production has been from quartz veins and the rest from derivative placer deposits (Whiting and Bowen, 1976; Sandiford and Keays, 1986; Phillips and Hughes, 1996; Jia et al., 2000). This chapter addresses two representative deposits, the Central and North Deborah deposits, in order to provide further constraints on the origin of the "Bendigo type" turbidite-hosted gold deposits.

The Central and North Deborah gold deposits both contain a set of six systematically developed and sequential quartz-carbonate-mica-sulfide veins, and therefore provide an excellent opportunity for isotope studies. The present work comprises the first detailed stable isotope study (C, N, and O) on quartz vein systems from the Central and North Deborah gold deposits. These data, together with a compilation of data for other deposits in the Bendigo goldfield, are used to infer potential source reservoirs for the vein-forming fluids. In the discussion, the results are considered in the context of metaturbidite-hosted and other orogenic gold deposits worldwide.

5.2 Regional and Local Geological Setting

The regional and local geological setting and characteristics of gold deposits in the Bendigo goldfield have been described previously (Gray, 1988; Cox et al., 1991a, b; Gao and Kwak, 1995; Phillips and Hughes, 1996; Ramsay et al., 1998; Jia et al., 2000) and only a summary is presented here. The Bendigo goldfield is located 152 km NNW of Melbourne (36° 45′ S longitude, 144° 15′ E latitude), within a belt of Ordovician quartz-rich turbidites that is part of the Lachlan fold belt, and forms a structural entity known as the Bendigo-Ballarat Zone (BBZ; Gray, 1988; Fig. 5.1). Its eastern boundary is marked by a narrow domain of intensely faulted rocks known as the Heathcote Fault Belt that includes the Cambrian Heathcote greenstones (Crawford, 1988), which separates it from Siluro-Devonian sedimentary rocks of the Melbourne Zone. Major displacement in the Heathcote Belt has resulted in the BBZ overthrusting the Melbourne Zone (Cox et al., 1983; Fergusson et al., 1986; Gray, 1988; Cox et al., 1991a). To the west, the Avoca Fault Zone, with a discontinuous belt of Cambrian greenstones, forms the boundary between the Stawell and Bendigo-Ballarat Zones (Cas and Vandenberg, 1988; Morand et

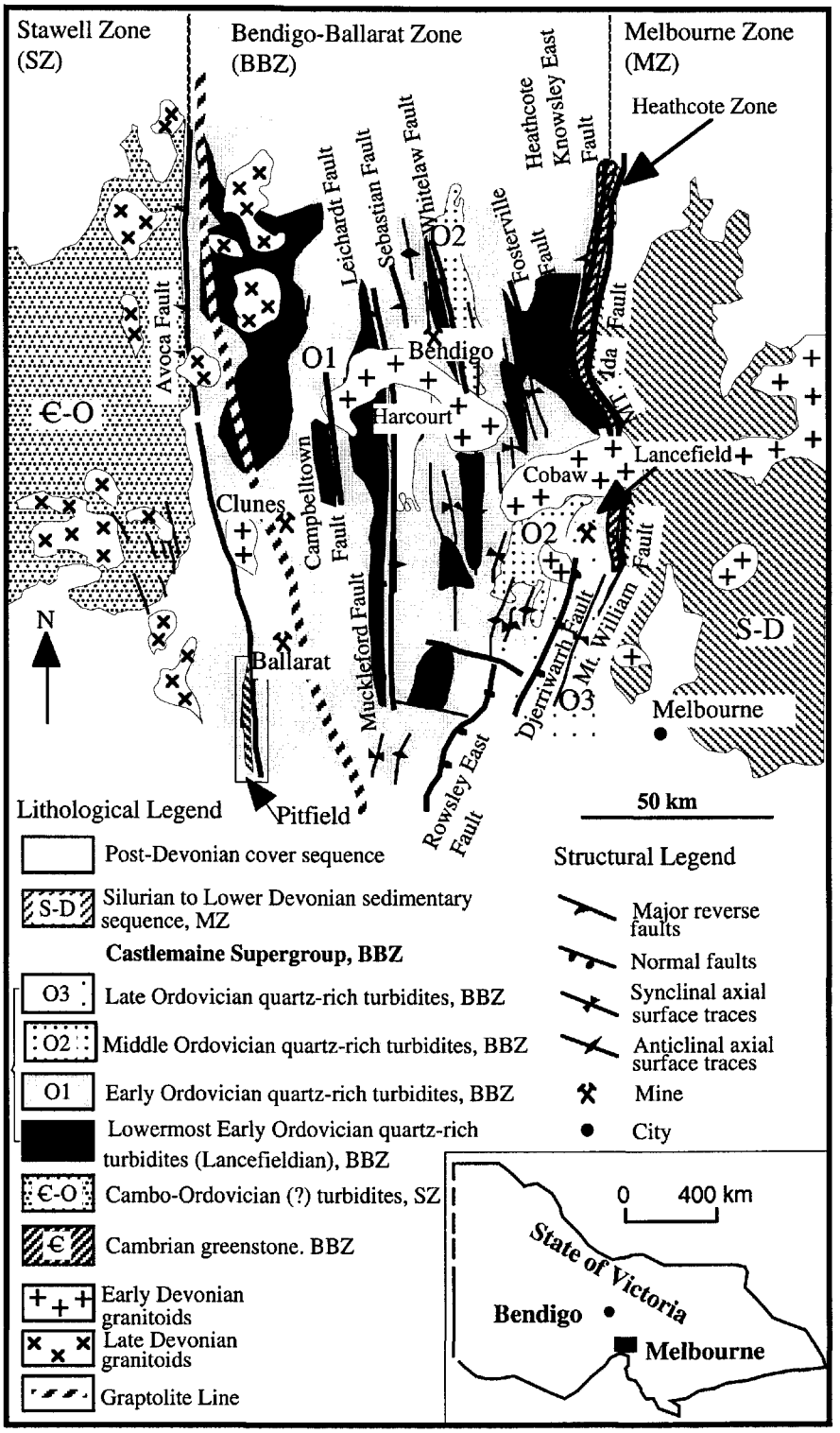

Fig. 5.1. General Geology of the Stawell, Bendigo-Ballarat, and Melbourne Zones (after Gray, 1988; Cas & Vandenberg, 1988; Gray & Willman, 1991a; Cox et al., 1991a, 1995; Morand et al., 1995).

al., 1995). Along the Avoca Fault Zone turbidites of presumed Cambrian age, and apparently devoid of fossils, were thrust over Ordovician graptolite-bearing sedimentary rocks of the BBZ (Cas and Vandenberg, 1988; Cox et al., 1991a).

The Bendigo-Ballarat Zone encompasses all Ordovician outcrops between the graptolite line to the west and the Mount William-Mount Ida Fault Zones in the east (Fig. 5.1). This zone consists of a 110 km wide belt of folded, cleaved, metamorphosed and faulted Ordovician quartz-rich turbidites, known as the Castlemaine Supergroup that has a total thickness of around 2,000 m (Cas and Vandenberg, 1988). The major structural trace of the BBZ is approximately north-south, reflecting a major episode of crustal shortening along the active continental margin that produced regular, upright, NS-trending folds, with associated cleavage and reverse faults (Cox et al., 1991a,b; Gray and Willman, 1991; Fig. 5.1).

The presence of late Devonian post-tectonic granites, and conformity between the Castlemaine Supergroup and the Silurian to lower Devonian succession immediately northwest of Melbourne (VandenBerg et al., 1976; VandenBerg, 1978; Richards and Singleton, 1981; Arne et al., 1998) indicates that regional deformation, in the eastern part of the Bendigo-Ballarat zone at least, did not occur until the middle Devonian. Emplacement of the late Devonian Harcourt granodiorite postdates gold quartz vein mineralization at Maldon, 15 km north of Castlemaine (Thomas, 1953).

Regional anticlinoria and synclinoria have wavelengths of 10-15 km, and amplitudes in the order of 1-2 km. N-S trending dome-like anticlinoria and basin-like synclinoria are marked by changes of plunge and stratigraphic succession. The cores of these domes are N to NNW trending, with oval-shaped interference outcrop patterns of

lowermost Ordovician turbidites. These regional folds are truncated by west-dipping, N-NNW-striking, high angle reverse faults.

The Bendigo goldfield is hosted by the Lower to Middle Ordovician Castlemaine Supergroup, 2 to 3 km west of the major Whitelaw Fault, and 10 km NNE of the Middle Devonian Harcourt Batholith, which is part of the BBZ (Cas and Vandenberg, 1988; Fig. 5.1). The dominant lithologies are sandstone, siltstone, slate, and graphitic slate; they have all undergone zeolite to greenschist facies metamorphism (Phillips and Hughes, 1996; Bierlein et al., 2000). Wallrock alteration around vein mineralization is generally extensive, and includes development of hydrothermal carbonate, quartz, muscovite, chlorite, albite, and sulfide minerals (Li et al., 1998; Bierlein et al., 1998, 2000).

The absolute timing of mid-Paleozoic gold-forming episodes across the productive Victorian part of the Lachlan fold belt is still poorly constrained. Most data suggest some overlap of gold veining with diachronous Late Ordovician to Early Devonian deformation, but mineralization generally developed eastward younging from latest Ordovician (455-440 Ma) in the west to late Silurian-early Devonian (410-385 Ma) in the east, with a phase of reactivation in the west at ca. 420 Ma (Gray and Foster, 1997; Arne et al., 1998; Foster et al., 1998; Bierlein et al., 1999). The majority of the gold veining in the Bendigo goldfield is considered to have been coeval with regional metamorphism and thrusting between 450 and 420 Ma, although a second period of veining occurred at about 410-370 Ma (Arne et al., 1998; Foster et al., 1998; Bierlein et al., 1999).

5.3 Gold Quartz Vein Systems in the Central and North Deborah Deposits

Mineralization occurs as saddle reefs and as discordant veins, predominantly in the apical areas of domes. At least fifteen major anticlinal domes, termed the "Goldfield Structural Domain" contain mineralization of variable gold grades and tonnages in the Bendigo goldfield, including the Central and North Deborah gold deposits. Gold mineralization is predominantly hosted by quartz vein systems, with minor disseminated gold in host rocks. These veins have been classified on the basis of their morphology and structure (Sharpe and MacGeehan, 1990; Cox et al., 1991a).

Figure 5.2 is a cross-section of the Central and North Deborah deposits illustrating the different vein types and the distribution of samples collected. Six main stages of quartz veins can be distinguished in the Deborah deposits on the basis of mineral paragenesis, metal association, geometry, veining events and their crosscutting relationships; these characteristics have previously been described in detail by Jia et al. (2000). From oldest to youngest the stages are:

(1) laminated veins having a mineral parageneses of quartz + albite + sericite + chlorite + ankerite + boulangerite + arsenopyrite + pyrite + other sulfides, with a metal budget of Au-As-Sb-Pb-Zn-Ni;

(2) spur veins of quartz + sericite + ankerite + arsenopyrite (minor) + pyrite, with a metal budget of Au;

(3) massive barren veins containing quartz + ankerite + sericite + chlorite;

(4) brecciated veins comprising sericite + ankerite + arsenopyrite + pyrite + other sulfides, with a metal budget of Au-As;

(5) quartz-ankerite veinlets; and

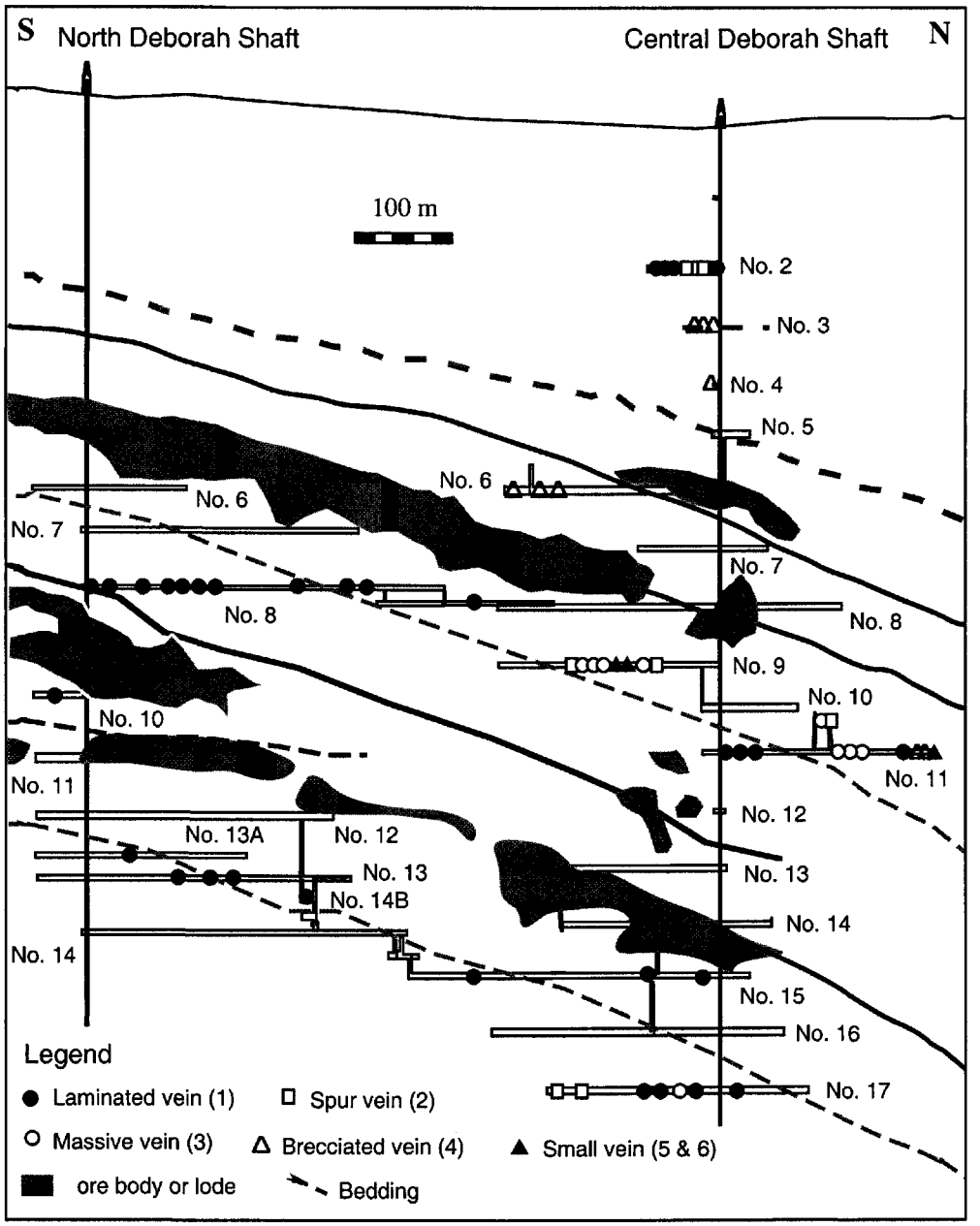

Fig. 5.2. Cross-section of the Central and North Deborah deposits, illustrating the distribution of samples collected, with different vein types. Vertical and Horizontal scales are equal. Viewed looking west (after Hinde, 1988).

(6) late pure quartz or calcite veinlets.

Of the three mineralized vein stages (1, 2, and 4), only stage 1 predated or was synkinematic with the main folding event, whereas stages 2 and 4 postdated deformation.

5.4 Sample populations

Samples used in this investigation were collected from different quartz veins at different levels in the Central and North Deborah mines (Fig. 5.2). Among these samples, 20 muscovite separates were used for N contents and N-isotopic compositions; 20 quartz separates for oxygen isotope analyses; and 10 whole rock powder samples for carbon and oxygen isotope analyses from carbonate. Analytical methods are given in Appendix I. Hydrogen isotope data on muscovite and sulfur isotope data for sulfide separates from both veins and adjacent wall rocks are from Li (1998). Mineral separates prepared in this study are from the same sample suite as H and S isotope analyses reported by Li (1998).

5.5 Results

5.5.1 Nitrogen and N-isotope compositions of muscovite

The results for N contents and nitrogen isotope compositions of hydrothermal muscovites from the Central and North Deborah mines are reported in Table 5.1. For the gold-bearing quartz vein stages 1, 2, and 4, nitrogen concentrations are between 652 and 895 ppm and $\delta^{15}N$ values range from 3.3 to 4.5‰, with a mean of 3.7‰. In the barren stage 5 and 6 quartz veins, the N concentrations range from 858 to 888 ppm and $\delta^{15}N$ has slightly lower values of 2.8 to 3.0‰.

Table 5.1. Nitrogen contents and nitrogen isotope compositions of muscovites, and carbon and oxygen isotope compositions of carbonates from veins in the Central and North Deborah gold deposits (from Jia et al., 2001)

Sample no.	Vein stage	Vein morphology paragenesis	Muscovite		Dolomite		Calcite	
			N (ppm)	$\delta^{15}N$ (‰)	$\delta^{13}C$ (‰)	$\delta^{18}O$ (‰)	$\delta^{13}C$ (‰)	$\delta^{18}O$ (‰)
CD11-21-1	(1)	asp-sph-gold-rich	893	3.4	-5.9	14.0	-5.6	15.3
CD11-21-2	(1)	asp-sph-gold-rich	895	3.3				
CD11-21-3	(1)	asp-sph-gold-rich	892	3.3				
CD11-13-I	(1)	asp-gold -rich	662	3.9	-6.3	12.4	-7.2	14.3
CD11-13-II	(1)	asp-gold -rich	679	4.0	-6.8	15.7	-5.9	15.2
CD11-13-III	(1)	asp-gold -rich	660	3.8				
CD11-13-IV	(1)	asp-gold -rich	667	3.9				
ND8-2A	(1)	asp-rich	680	3.7	-6.8	13.5	-6.5	13.7
ND8-2B	(1)	asp-rich	692	3.6				
ND8-2C	(1)	asp-rich	682	3.8				
ND8-2D	(1)	asp-rich	685	4.0				
ND13-3	(1)	asp-gold-rich			-6.6	14.9	-6.2	14.4
ND13-1	(1)	py-gold-rich			-5.7	17.4	-5.6	15.8
CD2-18A	(2)	chl-py-rich	852	3.4				
CD2-18B	(2)	chl-py-rich	861	3.3				
CD2-18C	(2)	chl-py-rich	860	3.3				
CD1-18D	(2)	chl-py-rich	845	3.0				
CD2-8	(2)	py-rich			-5.5	14.5	-6.1	14.9
CD11-3-A	(4)	asp-sph-rich	679	3.9	-6.7	13.4	-6.4	15.4
CD11-3B	(4)	asp-sph-rich	652	4.5				
CD9-18	(4)	asp-py-rich			-8.3	15.7	-9.0	15.2
CD9-6a	(5)	qtz-carb	858	2.9	-5.3	15.2	-5.1	17.1
CD9-6b	(5)	qtz-carb	888	2.9				
CD9-6c	(5)	qtz-carb	880	2.8				

$\delta^{15}N$ relative to atmospheric N_2; $\delta^{13}C$ relative to PBD; $\delta^{18}O$ relative to V-SMOW

Vein stages: (1), laminated auriferous quartz-carbonate veins; (2), spur auriferous quartz-carbonate veins; (4), brecciated auriferous quartz-carbonate veins; (5), barren quartz-carbonate veins.

Abbreviations: asp = arsenopyrite, carb = carbonate, chl = chalcopyrite, py = pyrite, qtz = quartz, sph = sphalerite

5.5.2 Oxygen and hydrogen isotope compositions of silicates

The total range of $\delta^{18}O$ values for vein quartz from the Central and North Deborah deposits is between 14.4 and 17.2‰ (Table 5.2). There are no systematic differences in the $\delta^{18}O$ values of quartz from a given auriferous vein stage at different mining levels, or between different vein stages 1, 2, and 4; the range is from 15.9 to 17.2‰, with mean values of 16.2‰, 16.8‰, and 16.7‰ respectively (Fig. 5.3A; Table 5.2). Barren vein stages 3, 5, and 6 have a total range of 14.4 to 16.8‰, overlapping with auriferous veins but tending to lower overall values, where mean values are 15.7‰ (stage 3) and 15.4‰ (stages 5 and 6) respectively (see Fig. 5.3A; Table 5. 2).

Assuming mineral-water equilibrium, quartz-muscovite fractionations of 3.7 to 4.8 per mil correspond to temperatures of 375° to 250°C based on the mineral-water equations of Matsuhisa et al. (1979) and O'Neil and Taylor (1969). The mean $\Delta^{18}O_{quartz\text{-}muscovite}$ value of 3.9‰ yields a temperature of 340 ± 40°C. These temperatures overlap the PT conditions of ore-deposition determined from fluid inclusion studies of 350° ± 25°C and 200 to 300 MPa, with CO_2 immiscibility (Jia et al., 2000). Quartz-muscovite fractionations are relatively small at the calculated temperatures and hence have commensurately larger errors. Accordingly, measured $\delta^{18}O_{quartz}$ values are used with temperatures determined from fluid inclusions to calculate $\delta^{18}O_{water}$ values for the hydrothermal fluids of 8.3‰ at 325°C to 11.4‰ at 375°C.

Similarly, $\delta^{18}O$ values of hydrothermal muscovite are uniform ranging from 11.6 to 12.8‰ (mean 12.4‰; Table 5.2; Li, 1998). The δD values of the muscovites vary between –55 and –68‰ (Table 5.2; Li, 1998). Calculated δD values of ore fluids from muscovite δD values (Suzuoki and Epstein, 1976) range from –17 to –37‰.

Table 5.2. Oxygen and hydrogen isotope data for silicatesfrom quartz vein systems in the Central and North Deborah deposits, and other deposits elsewhere in the Bendigo gold province (from Jia et al., 2001)

Sample no.	Vein stage	Vein morphology paragenesis	$\delta^{18}O$ (‰) quartz	$\delta^{18}O$ (‰) muscovite	δD (‰) muscovite	$\delta^{18}O$ (‰) quartz, median	Sources
Central and North Deborah mines							1
CD11-21	(1)	asp-sph-gold-rich	16.0	12.1	-64	16.2; n = 6	
ND13-1	(1)	py-gold-rich	16.6				
CD11-13	(1)	asp-gold-rich	15.9				
ND8-12	(1)	asp-rich	15.9	12.2	-68		
ND13-3	(1)	asp-gold-rich	16.3	12.0			
CD5-1	(1)	asp-sph-gold-rich	16.2	12.3			
CD2-9	(2)	py-rich	16.7			16.8; n = 4	
CD9-11	(2)	chl-py-rich	16.9				
CD9-2	(2)	py-rich	16.6	12.7			
CD2-18	(2)	chl-py-rich	17.2	12.8	-67		
CD11-8	(3)	milky quartz	15.7			15.7; n = 4	
CD11-10a	(3)	milky quartz	14.7				
CD11-10b	(3)	milky quartz	16.8				
CD9-15	(3)	musovite-milky quartz	15.6	11.7			
CD11-1	(4)	asp-py-rich	16.7			16.7; n = 3	
CD11-3	(4)	asp-sph-rich	16.3	12.5			
CD9-18	(4)	asp-py-rich	17.1	12.8	-55		
CD9-6a	(5)	qtz-carb	15.4			15.4; n = 3	
CD9-6b	(5)	qtz-carb	14.4				
CD9-5	(6)	qtz-carb	16.4	11.6	-62		
Other deposits in the Bendigo goldfield							
Wattle Gully mine		vein quartz	15.6 to 18.0			16.5; n = 19	2
Maxwells mine		vein quartz	17.2 to 17.9			17.5; n = 7	3
New Cambrian mine		vein quartz	16.7 to 17.5			17.0; n = 5	3
Castlemaine region		vein quartz	14.3 to 17.0			16.2; n = 10	2
Bendigo-Ballarat Zone		vein quartz	15.2 to 17.8			16.8; n = 71	4

$\delta^{18}O$ and δD relative to V-SMOW; In parentheses, number denotes vein stages; n denotes the number of analyses
Vein stages: (1), Laminated auriferous quartz-carbonate veins; (2) Spur auriferous quartz-carbonate veins; (3), Massive veins; (4), Brecciated auriferous quartz-carbonate veins; (5) and (6), quartz-carbonate veinlets.

References: 1 = this study; 2 = Cox et al. (1995); 3 = Gao and Kwak (1995); 4 = Gregory et al. (1988)

Abbreviations: as same as in Table 1

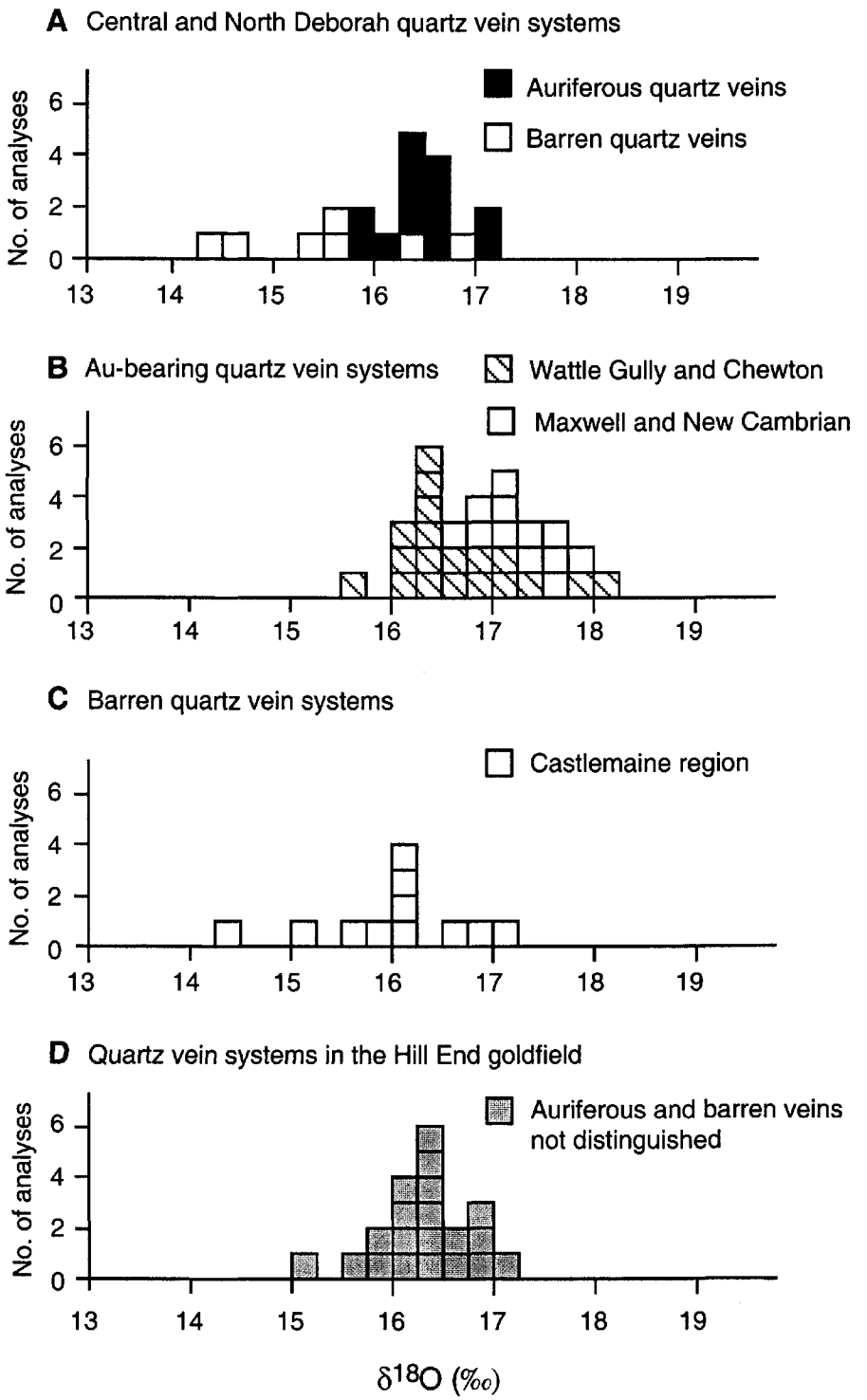

Fig. 5.3. Oxygen isotope compositions of vein quartz from turbidite-hosted gold deposits. A. Vein quartz from the Central and North Deborah deposits. B. Gold-bearing vein quartz from other specified deposits (data from Gao and Kwak, 1995; Cox et al., 1995). C. Barren vein quartz (data from Cox et al., 1995). D. Vein quartz from Hill End, NSW, Australia (data from Lu et al., 1996).

5.5.3 Carbon and oxygen isotope compositions of carbonates

Coexisting ferroan dolomite and calcite in auriferous quartz veins (stages 1, 2, and 4) from the Central and North Deborah mines have a total range of $\delta^{13}C$ values from –5.5 to –9.0‰, with the majority in a restricted range of –5.5 to –7.2‰ (Fig. 5.4A; Table 5.1). One sample from late stage 5, post-mineralization, also has a $\delta^{13}C$ value in this range. These results are similar to those from other gold deposits in the Bendigo goldfield, such as the Wattle Gully –5.2 to –6.8‰ (Cox et al., 1995), and the New Cambrian and Maxwells –3 to –8‰ (Gao and Kwak, 1995).

Carbonates in the gold-bearing veins have $\delta^{18}O$ values in the range 12.4 to 17.4‰, with a mean of 14.8‰ (Fig. 5.4B; Table 5.1). One sample from a barren vein of stage 5 has an $\delta^{18}O$ value of 17.1‰. Carbonates have more dispersed $\delta^{18}O$ values compared to the restricted range for quartz. Coexisting quartz-carbonate pairs have $\Delta^{18}O$ values of –0.8 to 3.5‰, signifying variable retrograde oxygen isotope exchange of carbonate.

5.6 Discussion

The new stable isotope (O, C, and N) data, together with existing data (H and S isotopes) of Li (1998) can be used to place a number of constraints on the source of the vein-forming fluids and to estimate the conditions of vein formation (Ohmoto and Rye, 1979; O'Neil, 1986; Kerrich, 1987; Ohmoto and Goldhaber, 1997; Jia and Kerrich, 1999).

5.6.1 Ore-forming fluid and temperature

The narrow range of 14 to 17‰ for vein quartz from the Central and North Deborah deposits is typical for vein quartz from orogenic lode gold deposits of all ages

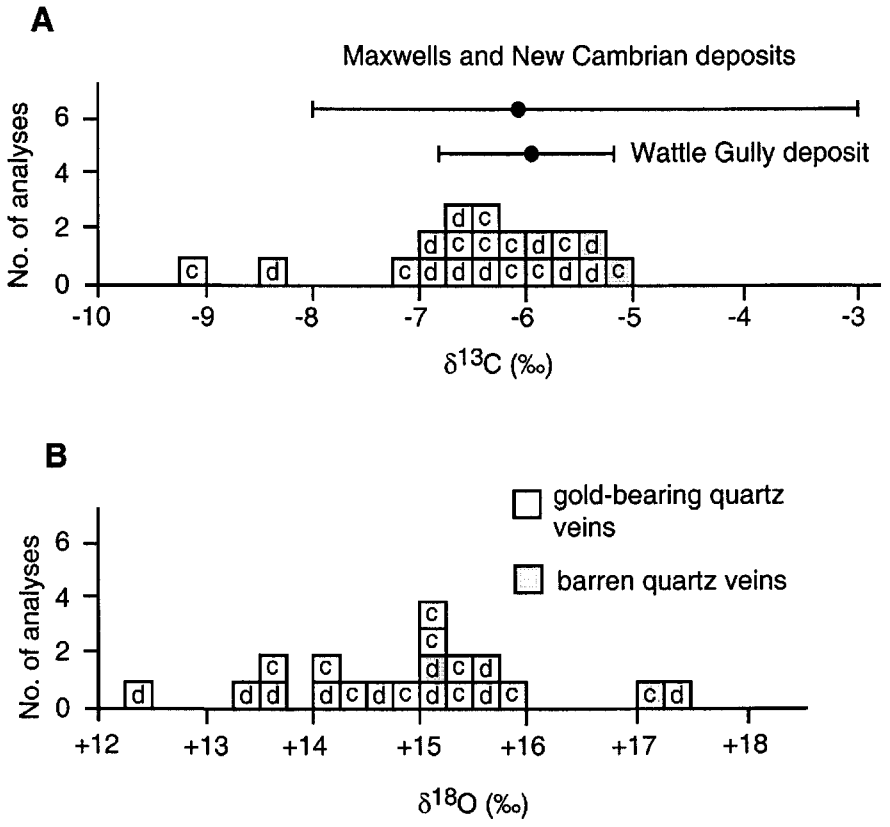

Fig. 5.4. Carbon (A) and oxygen (B) isotope compositions of carbonates in gold-bearing veins and barren veins in the Central and North Deborah deposits. Note: c = calcite; d = dolomite; solid circle = median values.

from Neoarchean to Cenozoic ($\delta^{18}O$ = 12 to 18‰; Böhlke and Kistler, 1986; Curti, 1987; Kerrich, 1987; Golding et al., 1989; Goldfarb et al., 1991, 1997; de Ronde et al., 1992; Oberthür et al., 1996; McCuaig and Kerrich, 1998). This distinct uniformity of $\delta^{18}O$ values of quartz for individual orogenic gold deposits has been interpreted as a corresponding isotopic homogeneity of the hydrothermal ore fluids, and uniform ambient temperatures of ore formation. In contrast, epithermal gold deposits are characterized by variable $\delta^{18}O$ quartz values (Taylor, 1997).

The isotopic composition of the ore-forming fluid is 8 to 11‰ $\delta^{18}O$, and –17 to –37‰ δD, with vein precipitation at 350° ± 25°C. The calculated $\delta^{18}O_{H2O}$ range is consistent with estimates for other gold-bearing vein systems elsewhere within the Bendigo goldfield, other orogenic gold deposits in the Lachlan fold belt of southeastern Australia (Tables 5.2 and 5.3), and is similar to $\delta^{18}O_{H2O}$ values of 7 to 14‰ for other turbidite-hosted gold deposits, worldwide (Table 5.3; Böhlke and Kistler, 1986; Goldfarb et al., 1991, 1997; Kontak and Kerrich, 1995; Oberthür et al., 1996; and Ivanov et al., 2000). This range overlaps with, but tends to be higher overall fluid $\delta^{18}O$ values of 6 to 11‰ obtained for Neoarchean orogenic gold deposits (Table 5.3; Kerrich, 1987; Golding et al., 1989; de Ronde et al., 1992; McCuaig and Kerrich, 1998).

Together, the calculated $\delta^{18}O$ and δD values are consistent with fluids derived from metamorphic dehydration reactions, or exchanged meteoric water, but do not plot in the field of magmatic fluids. Vein geometry requires hydraulic fracturing under conditions:

$$P_{fluid} > P_{lithostatic} + T \qquad 5.1$$

And metamorphic fluids are generated under conditions:

$$P_{fluid} \geq P_{lithostatic} \qquad 5.2$$

Table 5.3. Comparison of oxygen and hydrogen isotope compositions of ore-forming fluid in the Central and North Deborah mines, Bendigo goldfield with other turbidite-hosted lode gold deposits and late Archean lode gold deposits

Era District	Mine	$\delta^{18}O$ (‰) quartz	T(°C)	$\delta^{18}O$ (‰) Ore fluid	δD(‰) Ore fluid	Sources
Phanerozoic						
Victorian slate belt, Australia[1]	Central and North Deborah	14.4 to17.2	350° ± 25°C	8 to 11	-17 to -37	1
	Wattle Gully, Maxwells, and New Cambrian	15.6 to 18.0	320° ± 25°C	ca. 10		2, 3, 4
	Bendigo-Ballarat Zone	15.2 to 17.8				5
Hill End goldfield, N.S.W., Australia[2]	Hill End goldfield	15.1 to 15.6	420°C	8 to 12	-36 to -49	6
Southeastern Alaska[1]	Juneau gold belt	15.2 to 20 .8	225°~ 375°C	7 to 12	-15 to -35	7
Meguma, Nova Scotia, Canada[2]	Beaver Dam and others	13.0 to15.0	400° ± 50°C	6 to 12	-34 to -46	8
Mother Lode, California, USA[1]	Mother lode belt	16.0 to 21.7	250°~400°C	8 to 14	-10 to -50	9
Yukon Territory, Canada[2]	Klondike district	13.1 to 19.3	325° ± 25°C	7 to 10	-100 to -170	11
Proterozoic						
Ashanti, West Africa[2]	Ashanti gold belt	12.8 to 15.6	400° ± 50°C	9 to 12	-37 to -53	10
Archean						
Superior Province, Canada and Yilgarn craton, Western Australia[1]	Hollinger-McIntype and Dome, Kalgoorlie and Norseman	10.0 to 15.2	220° ~ 500°C	6 to 11	-20 to -80	12, 13, 14

$\delta^{18}O$ and δD relative to the V-SMOW

[1] δD values from mineral-water fractionation factors (Suzuoki and Epstein, 1976)

[2] δD values from fluid inclusions

Sources: 1 = this study; 2 = Cox et al. (1995); 3 = Gao and Kwak (1995); 4 = Phillps and Hughes (1996); 5 = Gregory et al. (1988); 6 = Lu et al. (1996); 7 = Goldfarb et al. (1989, 1991, 1997); 8 = Kontak and Kerrich (1995); 9 = Böhlke and Kistler (1986); 10 = Oberthür et al. (1996); 11 = Rushton et al. (1993); 12 = Kerrich (1987); 13 = Golding et al. (1989); 14 = McCuaig and Kerrich (1998)

Where T is the tensile strength (Fyfe et al., 1978; Jia et al, 2000).

In contrast, meteoric water convects through the crust under hydrostatic conditions, and the dispersed $\delta^{18}O_{quartz}$ values of epithermal gold deposits are distinct from the uniform $\delta^{18}O$ values for individual orogenic gold deposits.

According to de Ronde et al. (2000), the ore fluid for the Round Hill shear zone-hosted gold deposit, New Zealand, was a mixture of early stage (ore-bearing stockwork veins) meteoric water and late stage (Hanging-wall shear veins) magmatic fluid, based mainly on a low range in fluid inclusion δD values of –43 to –77‰. However, the uniform quartz vein $\delta^{18}O$ values of 15.6 to 16.7‰ of this deposit are similar to other individual orogenic lode gold deposits, signifying that mixing of different fluid reservoirs is unlikely. A spread of δD values may reflect secondary fluid inclusions that contain low-δD meteoric water. Alternatively deep sourced non-meteoric ore fluids may react with δD-depleted organic matter (Goldfarb et al., 1989; McCuaig and Kerrich, 1998), which is consistent with relatively low $\delta^{13}C$ values of carbonate (-9.5 to –12.9‰; de Ronde et al., 2000; see McCuaig and Kerrich, 1998 for a review). The calculated $\delta^{18}O$ values of ore fluid were between 8.5 and 9.3‰; they plot in the metamorphic field.

Given an original meteoric water with δD –80‰, $\delta^{18}O$ would have been –12‰ (de Ronde et al., 2000). Consequently, the ore fluid would have shifted in $\delta^{18}O$ by +21 per mil from –12‰ to the calculated value of about +9‰ into the magmatic and metamorphic fields by fluid/rock interaction at low water/rock ratios; hence it would of necessity lose the initial meteoric water δD signature. Furthermore, based on studies of fluid inclusion, stable isotopes, and hydrothermal systems in the southern Alps, New Zealand, McKeag and Craw (1989) and Craw (2000) suggest that mineralizing fluids

were produced by metamorphic dehydration, which were chemically distinct from meteoric water.

5.6.2 Sulfur isotopes

Sulfur isotope compositions were determined by Li (1998) on 59 mineral separates including pyrite, sphalerite, pyrrhotite, and galena from the three auriferous vein stages 1, 2, and 4, and from adjacent wall rocks (Table 5.4). The $\delta^{34}S$ values of vein pyrite span –5.3 to +8.1‰, with a mean ca. +2.5 ‰ (Fig. 5.5A; Table 5.4). In contrast, the few sulfur isotope compositions of coexisting sphalerite, pyrrhotite, and galena are more variable and depleted in ^{34}S, ranging from –1.4 to –7.4‰. The pyrite data display a relatively tight normal distribution (Fig. 5.5A). Pyrite of synsedimentary-diagenetic origin displays a wide scatter of sulfur isotope compositions, from +12 to –23.5‰; in black slate pyrite has $\delta^{34}S$ values of –8.0 to –23.5‰, whereas in sandstone it is –0.1 to 12‰ (Fig. 5.5; Table 5.4).

The sulfur isotope compositions of coexisting sphalerite and galena (-1.8 and –3.7‰, respectively) from a gold-bearing quartz vein indicate a temperature of about 350°C for vein formation, based on the data of Ohmoto and Rye (1979). This result is consistent with temperatures estimated from fluid inclusion studies (Jia et al., 2000), and is also compatible with those inferred from sulfur isotope data in the neighbouring Wattle Gully mine (314° ± 25°C; Cox et al., 1995).

Sulfur isotope compositions of sulfides in hydrothermal ore deposits are controlled by the isotopic compositions of the fluids, as well as temperature, Eh, and pH at the site of mineralization; the first parameter is characteristic of the source of sulfur and other three relate to the conditions of deposition (Ohmoto, 1986; Ohmoto and Goldhaber,

1997). Constraints on ambient temperature, Eh, and pH can be obtained from alteration mineral assemblages and fluid inclusion studies. Mikucki and Ridley (1993) concluded from investigation of ore and alteration mineral parageneses in Neoarchean gold deposits that the pH of the ore fluids was near neutral to slightly acidic, and never far from equilibrium with sericite-albite at temperatures corresponding to low to mid-greenschist facies conditions. Furthermore, the fluid inclusion characteristics and ore parageneses indicate that most deposits form from relatively reduced hydrothermal ore fluids, the fluid redox state generally being below SO_2/H_2S boundary and above the CO_2/CH_4 buffer (Phillips and Groves, 1983; Kerrich, 1987; Mikucki and Ridley, 1993). McCuaig and Kerrich (1998) and Kerrich et al. (2000) conclude that the majority of orogenic gold deposits from Neoarchean to Phanerozoic have similar conditions of ore deposition.

The S isotope composition of vein pyrite is relatively uniform, indicating a commensurately large isotopically uniform sulfur source, in contrast to the dispersed range of $\delta^{34}S$ values in the turbidites (Fig. 5.5; Table 5.4). Sulfur of this isotopic composition may originate directly from magmatic fluids, or indirectly from leaching or desulfidation of primary magmatic sulfide minerals, or average crustal sulfur (Lambert et al., 1984; Kerrich, 1987). Equilibrium isotope fractionation between H_2S and most sulfides is small ($\leq \pm 2‰$) at temperatures above 250°C (Ohmoto and Rye, 1979).

Sulfur isotope compositions of sulfides (mainly pyrite, pyrrhotite, and arsenopyrite) in most Neoarchean gold deposits display a relatively tight cluster, ranging from +8 to –1‰ (Lambert et al., 1984; Kerrich, 1987; de Ronde et al., 1992; Ho et al., 1992). This characteristic range of $\delta^{34}S$ values is interpreted to indicate that the fluid redox state was

Table 5.4. Sulfur isotope compositions of sulfide minerals from the Central and North Deborah mines

Sample No.	Vein morphology/ stage	Minerals and description	$\delta^{34}S$ (‰)	mean ± 1σ
Veins	Laminated veins (1)			2.7 ± 4.7
CD2-1	"	py	8.1	
CD2-2	"	py	3.9	
CD2-20(I)	"	py (visible gold)	3.1	
CD2-20(1I)	"	py (visible gold)	7.1	
CD2-21(I)	"	py	4.3	
CD2-21(II)	"	py	5.6	
CD11-23(a)	"	py	2.5	
CD11-23(b)	"	py	1.6	
ND13-lG(I)	"	py in the Kingsley Reef	5.5	
ND13-3(I)	"	py in the Kingsley Reef	5.6	
ND13-3(II)	"	py in the Kingsley Reef	2.8	
ND13-3(III)	"	py in the Kingsley Reef	-4.1	
ND13-4	"	py in the Kingsley Reef	3.3	
CD17-25L(a)	"	py	-2.6	
CD17-25L(b)	"	py	-2.6	
CD17-25(I)	"	py	6.0	
CD17-27(I)	"	py	1.4	
CD17-27(II)	"	py	0.3	
ND10-T(a)	"	py (-chl-Au)	6.5	
ND 10-T(b)	"	py (Au-rich)	-3.8	
ND10-T(c)	"	py	-5.3	
NDT-l0(I)-pl	"	sph (-po)	-6.9	
NDT-l0(II)-pl	"	po (-sph)	-7.1	
NDT-l0(III)	"	py	2.2	
NDT- l0(IV)	"	py as inclusion in po	2.9	
NDT- l0(V)	"	po (-py)	-5.4	
	Spur veins (2)			2.1 ± 2.3
CDl l-5(I)	"	py	2.7	
CDl l-5(II)	"	py	-3.2	
CDl l-5(III)	"	py	1.7	
CDl l-l lS(a)	"	py	-0.1	
CD11-l lS(b)	"	py	2.7	
CDl l-l lS(c)	"	py	2.5	
	Brecciated veins (4)			0.4 ± 3.6
CD9-18(I)	"	py	4.0	
CD9-18(1I)	"	py	4.7	
CD3(1)	"	py	-1.6	
CD3(II)	"	sph	-7.4	
CD3(III)	"	gal (-sph)	-1.8	
CD3(IV)	"	sph (-gal)	-3.7	
CD3-1(V)	"	py (-sph-gal)	0.4	
CD3-1(II)	"	py (-sph-gal)	1.9	
CD11-3(a)	"	py	3.3	
CD11-3(b)	"	py	1.6	
CD11-3(c)	"	py	-1.4	
Host rocks				
BD2006	black slate	frambiodal py	-23.5	-15.5 ± 6.4
SGD001-1	"	py cluster	-8.0	
SGD001-2	"	py cluster	-14.3	
SGD001-3	"	py cluster	-16.7	
BD3001-10	sandstone	py	4.9	4.5 ± 3.6
SGD001-1a	"	py	3.3	
SGD001-1b	"	py	3.8	
SGD001-2	"	py	-0.1	
SGD001-3	"	py	2.0	
SGD001-5	"	py	6.2	
SGD001-6	"	py	6.9	
BD2011-13	"	py	5.7	
BD2014-12a	"	py	0.9	
BD2014-12b	"	py	4.0	
BD2012-3	"	py	11.1	
BD2014-4	"	py	11.9	

$\delta^{34}S$ relative to CDT

Abbreviations: py = pyrite; po = pyrrhotite; sph = sphalerite; chl = chalcopyrite; gal = galena

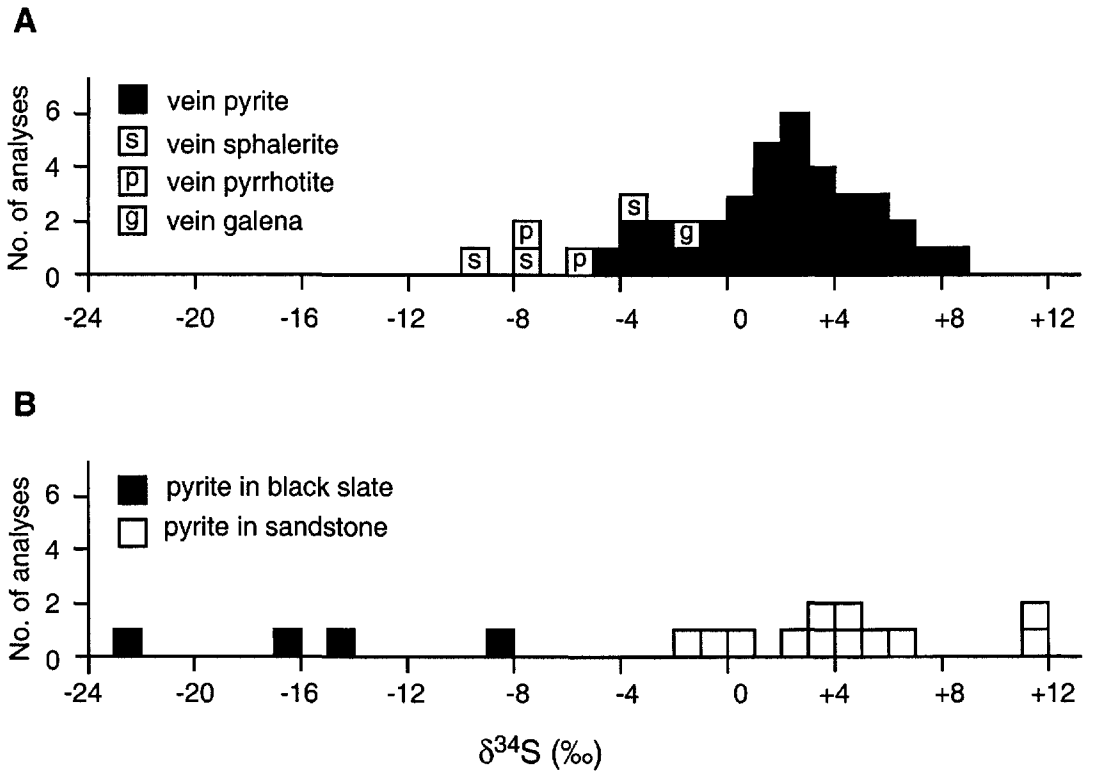

Fig. 5.5. Sulfur isotope compositions of sulfide minerals. A. Sulfides from vein systems. B. Pyrite from adjacent wall rocks. Data sources in Table 5.3.

below the SO_2/H_2S boundary and that the sulfur source was isotopically uniform (Kerrich, 1987; McCuaig and Kerrich, 1998).

In the Central and North Deborah mines, the $\delta^{34}S$ values of hydrothermal sulfides range from –7 to +8‰, and most are between –4 and +7‰ (mean +2.5‰; Fig. 5.5A; Table 5.4). These values overlap with, but overall are isotopically depleted compared to Neoarchean counterparts where $\delta^{34}S$ = +8 to –1‰. However, mineralogical, geochemical, and fluid inclusion studies of the Central and North Deborah mineralization (Li, 1998; Jia et al., 2000) suggest generally similar conditions to late Archean gold deposits. The ore deposition was largely synmetamorphic and took place under greenschist facies conditions at temperature of 325° ± 25°C, with fluid oxygen fugacity of 10^{-25} to 10^{-37} bars, and conditions generally above the CO_2/CH_4 but below the SO_2/H_2S boundary throughout gold mineralization. The paragenesis is pyrite-arsenopyrite-pyrrhotite assemblage; magnetite or sulfate is absent from the host rocks and ores (Li, 1998; Jia et al., 2000).

Therefore, the relatively depleted sulfur isotope compositions of sulfides in the Central and North Deborah mines do not result from oxidized fluids, but rather matches synsedimentary-diagenetic sulfides in sandstones (Fig. 5.5B). Shifts to lower values than the sandstones may reflect exchange with ^{34}S depleted sulfides in black slate during transport of ore fluid to the site of deposition. The same pattern is observed for other turbidite-hosted gold deposits in the Bendigo-Ballarat goldfields, such as the Maxwells, New Cambrian, and Wattle Gully (Cox et al., 1995; Gao and Kwak, 1995); Paleoproterozoic Birimian deposits (Oberthür et al., 1996); and the Cenozoic Juneau Gold Belt (Goldfarb et al., 1991), but is rare for counterparts in volcanic-plutonic

terranes where black sulphidic shales are rare (Kerrich, 1987; McCuaig and Kerrich, 1998).

5.6.3 Carbon isotopes

The $\delta^{13}C$ values of hydrothermal carbonates are dependent on temperature, fo_2, and pH during mineral precipitation, as well as the $\delta^{13}C_{\Sigma C}$ of the fluid (Ohmoto and Rye, 1979; Ohmoto and Goldhaber, 1997). The fluids depositing hydrothermal carbonates in mesothermal lode gold deposits are generally considered to be characterized by conditions of fo_2 close to the QFM buffer and above CO_2/CH_4, pH near neutral to slightly acid, and T > 270°C (Kerrich, 1990). At these conditions, carbon isotope fractionations attributable to redox effects or temperature differences are minor ($\delta^{13}C_{Carbonate} \approx \delta^{13}C_{\Sigma Cfluid}$; Ohmoto and Rye, 1979). These conditions also hold true for the Central and North Deborah gold mineralization, as indicated by: (1) the mineral assemblages of pyrite + arsenopyrite ± boulangerite at low temperatures, and pyrite + arsenopyrite ± pyrrhotite at higher temperatures; (2) absence of magnetite or sulfate; and (3) the characteristics of the ore fluids, H_2O-CO_2-CH_4-NaCl system, ≤ 8 wt% NaCl equiv. (Li, 1998; Li et al., 1998; Jia et al., 2000).

The range of $\delta^{13}C$ values of hydrothermal carbonates of –9.0 to –5.5‰, with a mean of about –6.5‰ (Fig. 5.4A; Table 5.1), is within the total range of -3 to –12‰ for the Bendigo goldfield (Cox et al., 1995; Gao and Kwak, 1995; Phillips and Hughes, 1996). Similar carbon isotope compositions of carbonates like those in the Central and North Deborah deposits are reported from the Paleoproterozoic Homestake gold mine in South Dakota (-5.6 to –11.2‰; Rye and Rye, 1974), from the Cambrian-Ordovician turbidite-hosted gold deposit of Muruntau in Uzbekistan, and from the Vendian

carbonaceous phyllite-hosted Kumtor in Kyrgyzstan (-5 to –12‰; Drew et al., 1996; Ivanov et al., 2000). This range is also comparable to $\delta^{13}C$ values in the Neoarchean orogenic gold deposits in Australia, Canada, and South Africa, where $\delta^{13}C$ ranges from –11 to +2‰ with a mean of –4‰ (Kerrich, 1987, 1990; Colvine et al., 1988; Golding et al., 1989; de Ronde et al., 1992; McCuaig and Kerrich, 1998).

Carbon in hydrothermal fluids may originate from decarbonation or dissolution of pre-existing carbonates, from magmatic sources, and/or from the oxidation or hydrolysis of reduced carbon in sedimentary or metamorphic rocks. Each of these sources may contribute carbon of differing isotope compositions to hydrothermal fluids (Ohmoto and Rye, 1979). The major carbon reservoirs considered possess distinct carbon isotope compositions: (1) seawater-derived carbonate is characterized by average $\delta^{13}C$ values close to 0 per mil (Ohmoto and Rye, 1979); (2) magmatic and mantle CO_2 mainly shows $\delta^{13}C$ values between –7 and –2‰, with a mean of –5‰ (Deines et al., 1991; Cartigny et al., 1998); (3) reduced carbon in sedimentary or metamorphic rocks has mean $\delta^{13}C$ values of about –25‰; and (4) some reduced carbon that underwent carbon isotope exchange with carbonates in metasedimentary rocks has $\delta^{13}C$ values around –15‰ (Schidlowski et al., 1983; Hoefs, 1987).

The $\delta^{13}C$ values of carbonates in orogenic gold deposits from the Neoarchean to Phanerozoic, including the Bendigo goldfield, have a total range of –11 to +2‰, with the majority < -3‰; Burrows et al., 1986; Kerrich, 1987, 1990; Groves et al., 1988; Golding et al., 1989), ruling out dissolution and/or decarbonation of marine carbonates as this source would lead to $\delta^{13}C \cong 0‰$ for dissolution (Ohmoto and Rye, 1979; Golding et al., 1989), or $\delta^{13}C$ enriched by about 3-5‰ for decarbonation (Burrows et al., 1986; Valley,

1986). The range of $\delta^{13}C$ values of –9 to –5‰ is difficult to interpret uniquely with regard to the carbon source, given that magmatic, sedimentary, and metamorphic rocks are all characterized by average $\delta^{13}C$ values of about –5‰ (Ohmoto and Rye, 1979). However, the total range of $\delta^{13}C$ carbonate in all orogenic gold deposits is between –11 and +2‰. Consequently, both magmatic and mantle degassing models fail to fully account for these deposits, where $\delta^{13}C$ carbonate is beyond their respective ranges (Kerrich, 1987; McCuaig and Kerrich, 1998). In addition, the $\delta^{15}N$ values rule out mantle fluids (Jia and Kerrich, 1999, 2000), and calculated $\delta^{18}O_{H2O}$ in conjunction with the low salinities are unlike magmatic fluids (cf. Kerrich, 1987).

The restricted, uniform and negative carbon isotope compositions of carbonates in the Central and North Deborah mines (< -5 to –9‰) would suggest that the most likely source for carbonic species in the ore fluid is a uniform mixture of isotopically depleted reduced carbon, in the form of graphite, in the sedimentary rocks (turbidites), and carbonate in sedimentary rocks and seawater-altered volcanic rocks. Ohmoto and Rye (1979) point out that reduced organic materials may have generated carbonic species in the ore-forming fluid through oxidation or hydrolysis. The most likely reaction is represented by Ohmoto and Rye (1979) as:

$$2C + 2H_2O = CO_2 + CH_4 \qquad 5.3$$

CO_2 produced at temperatures between 350° and 600°C would have $\delta^{13}C$ values between 3 and 12‰ enriched relative to that of graphite (Ohmoto and Rye, 1979). $\delta^{13}C$ of graphite from graphitic slates within the Bendigo goldfield range between –12.3 and –16.4‰ (Gao and Kwak, 1995).

Similar conclusions that depleted carbon isotope compositions of carbonates in orogenic gold deposits result from intensive reaction of hydrothermal fluid generated by metamorphic devolatilization in the deeper crust with ^{13}C-depleted reduced carbon within sedimentary rocks have been drawn by Kontak and Kerrich (1995) for the Beaver Dam deposit, Nova Scotia, and by Oberthür et al. (1996) for the Ashanti gold belt of Ghana.

5.6.4 Carbonate retrograde exchange

$\delta^{18}O_{quartz}$ values are incompatible with most $\delta^{18}O_{carbonate}$ values, indicative of variable degrees of isotopic disequilibrium. Accordingly, carbonates have undergone variable degrees of retrograde isotope exchange with secondary fluids, whereas quartz is isotopically uniform and robust. These features are also characteristic of carbonates from many other orogenic lode gold deposits (Kerrich, 1987, 1990). Kerrich (1990) interpreted the dispersion of $\delta^{18}O$ values in carbonates to reflect varying degrees of reequilibration at temperatures below the ambient thermal conditions of quartz-carbonate precipitation during later mineral-fluid interaction.

5.6.5 Nitrogen and N isotopes

The isotopic composition of nitrogen has large variations in geological samples (Clayton, 1981; Javoy, 1997; Chapter 3), which makes this isotope system a potentially important tracer for the origin of terrestrial silicates and volatiles.

The N concentrations of muscovites in the Central and North Deborah mines are between 652 and 895 ppm, where $\delta^{15}N$ values range from 2.9 to 4.5‰ (Table 5.1). These values are not consistent with either mantle-derived fluids given the very low N content

and $\delta^{15}N$-depleted character, or magmatic hydrothermal fluids evolved from crystallizing granitoids. It is also unlikely that N in hydrothermal muscovite of the quartz veins is inherited from meteoric surface water. Owens (1987) suggests that global nitrogen isotopic values of meteoric water are 4.4 ± 2.0‰ (n = 263), but nitrogen contents of meteoric water are very low (< 2 μmole; Homes et al., 1998), whereas N_2 has been observed and measured in fluid inclusions (Table 3.10 of Chapter 3; Bottrell et al., 1988). Furthermore, convection of meteoric water occurs at hydrostatic fluid pressure whereas structural analysis of the veins indicates their precipitation during hydraulic fracturing by fluids at lithostatic fluid pressure. Accordingly, deeply convecting meteoric water can be ruled out. Therefore, the results are consistent with ore fluids derived from metamorphic dehydration reactions in sedimentary rocks during metamorphism.

Similar N concentrations and $\delta^{15}N$ values like those in the Central and North Deborah deposits are reported from the southern Mother lode, California with N contents of 733-851 ppm and $\delta^{15}N$ values between 2.6 to 3.8‰ (Chapter 6; Jia and Kerrich, 2000). These results are distinct from those of predominantly volcanic-plutonic terrane-hosted Neoarchean gold deposits in Canada and Australia, which are characterized by lower N concentrations of 20 to 200 ppm but higher $\delta^{15}N$ values of 10 to 24‰ (Fig. 5.6; Jia and Kerrich, 1999).

5.7 Implications

The majority of orogenic gold deposits form in response to high crustal heat flow during late-stage compression and metamorphism in subduction-accretion complexes. Orogenic gold deposits in other settings, such as the granitoid associated deposits of east Asia, also involve enhanced crustal heat flow, perhaps induced by plume impingement

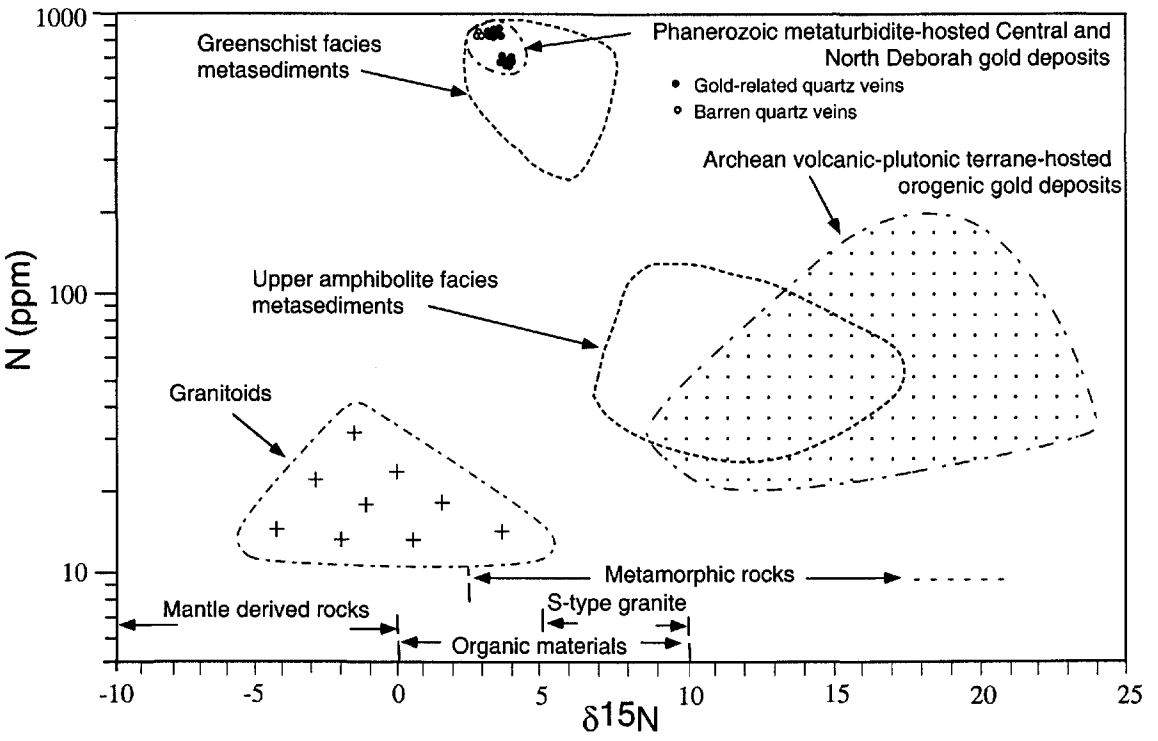

Fig. 5.6. The N content and δ15N values of mica separates from the Central and North Deborah gold deposits in the Bendigo goldfield compared to those of Archean volcanic-plutonic terrane-hosted counterparts in Canada and Western Australia, and spatially related granitoids in the Superior Province. Fields for rock reservoirs: Organic meterials from Peters et al. (1978) and Dubessy and Ramboz (1986), and Williams et al. (1995); Metamorphic rocks from Heandel et al. (1986) and Bebout and Fogel (1992); S-type granites from Boyd et al. (1993); Mantle derived rocks from Javoy et al. (1984), Javoy and Pineau (1991), Boyd et al. (1987, 1992), Marty and Pineau (1991), Boyd and Pillinger (1994), and Cartigny et al. (1998).

or delamination (Kerrich et al., 2000). There is a secular trend in the lithological inventory of subduction-accretion complexes, from volcanic-plutonic dominated Neoarchean, the so-called greenstone hosted gold deposits; to volcanic-sedimentary in the Proterozoic, for example, the Homestake and Birimain gold provinces; to turbidite dominated terranes with minor volcanic and plutonic units in the Phanerozoic.

These observations can be reconciled with the decreasing intensity of plume magmatism through time and plume temperature (Fyfe, 1978; Campbell et al., 1989). Isley and Abbott (1999) have demonstrated a correlation of 99% between plume breakouts in ocean basins forming ocean plateaus and iron formations, between 3.8 and 1.6 Ga. Ocean plateaus will displace marine water onto continents, decreasing continental foreboard, and in turn diminishing the supply of siliciclastic sediments to continental margins, including subduction-accretion complexes. Consequently, deep water Archean volcanic-plutonic subduction-accretion complexes include iron-formation but a low turbidite budget and low organic C content, with the converse true for Phanerozoic complexes like the Victoria slate belt.

In contrast, shallow water siliciclastic rocks are characterized by greater $\delta^{18}O$, more abundant and δD-depleted hydrocarbon compounds, and more abundant and isotopically depleted carbonaceous and nitrogen compounds (Hoefs, 1987). In summary, the secular trends in the isotopic composition of the ore-forming fluids for orogenic gold deposits may be accounted for in part by the relative proportion of siliciclastic rocks in subduction-accretion complexes (Figs. 5. 6 and 5.7). Additional factors controlling the difference of $\delta^{15}N$ between Archean and Phanerozoic gold deposits are discussed in Chapter 6.

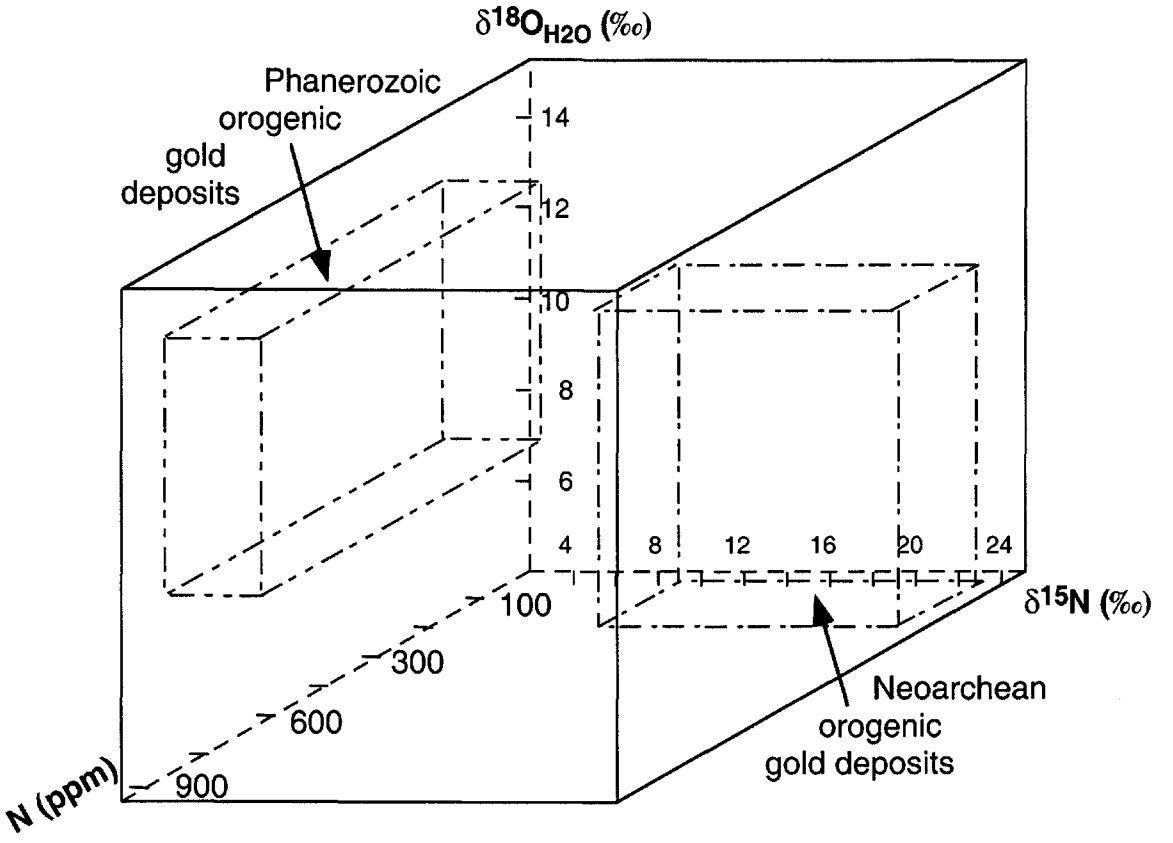

Fig. 5.7. Three demensional plot of fields for $\delta^{18}O_{H2O}$ (‰), $\delta^{15}N$ (‰), and N content of hydrothermal muscovites from the Central and North Deborah deposits in the Bendigo goldfield (data from sample Nos. CD11-21, CD11-13, CD2-18, CD11-3, CD9-18, and CD9-6). Compared with Neoarchean orogenic gold deposits of Canada and Western Australia (data from Jia and Kerrich, 1999, 2000) and Phanerozoic counterparts (data from Jia and Kerrich, 2000, and unpublished data)

5.8 Conclusions

Detailed studies of the stable isotope systematics (H, O, S, C, and N) of hydrothermal quartz vein systems from the metaturbidite-hosted Central and North Deborah mines in the Bendigo goldfield lead to the following interpretations:

(1) Nitrogen contents and $\delta^{15}N$ values of hydrothermal muscovite are consistent with fluids derived from progressive metamorphic dehydration reactions of the regional sedimentary-rich rock sequence.

(2) Coexisting quartz and muscovite in gold-bearing veins are uniform at 15.9 to 17.2‰ and 11.6 to 12.8‰, respectively; they imply uniform ambient temperatures of precipitation for the ore deposits. Quartz-muscovite and sphalerite-galena pairs yield isotopic temperatures of between 250° and 375°C, consistent with those from fluid inclusion studies of Jia et al. (2000).

(3) Uniformity of $\delta^{18}O_{quartz}$ values signifies uniform temperature and $\delta^{18}O$ of ore fluid through the 3 auriferous and 2 barren stages.

(4) The $\delta^{18}O$ values of ore-forming fluid are calculated at 8 (assuming 325°C) to 11‰ (assuming 375°C), and δD –17 to –37‰, indicative of a metamorphic origin of the ore-forming fluid.

(5) Carbonate $\delta^{13}C$ values (-5.5 to –9.0‰, with a mean of –6.5‰) may indicate that the most likely source for carbonic species in the ore fluid is a uniform mixture of isotopically depleted reduced carbon in the form of graphite in the sedimentary rocks, and carbonate in sedimentary rocks and seawater altered volcanic rocks.

(6) Gold-related sulfide $\delta^{34}S$ values (-7 to +8‰, with a median of +2.5‰) may reflect variable exchange of ore fluids with synsedimentary-diagenetic sulfides present in wall rocks during transport of ore fluid to the site of deposition.

Collectively, the stable isotope data, in conjunction with previous detailed studies of fluid inclusions provide a basis for constraining potential source reservoirs for the vein-forming fluids in the Central and North Deborah mines of the Bendigo goldfield. These are considered to be consistent with a metamorphic origin, involving derivation of the vein-forming fluids from mid-crustal levels by metamorphic dehydration reactions at the greenschist to amphibolite transition (Kerrich and Fryer, 1979; Powell et al., 1991). A dilute, aqueous carbonic and N-bearing composition (C-O-H-N) is common to metamorphic fluids (Casquet, 1986; Bottrell et al., 1988; Ortega et al., 1991).

Chapter Six

δD, $\delta^{15}N$, AND Se/S SYSTEMATICS OF SELECTED NORTH AMERICAN CORDILLERAN GOLD QUARTZ VEIN SYSTEMS

6.1 Introduction

The widespread distribution of Au-bearing quartz-carbonate vein systems is well documented in accreted terranes of the western North American Cordillera. These vein systems are structurally controlled by major fault zones, and often reactivated terrane-bounding sutures, which have formed in orogens built during accretion and subduction of allochthonous terranes along the continental margin of western North America. Mineralization ages range from about 189 Ma to 50 Ma, though not all are well established (Fig. 6.1; Böhlke and Kistler, 1986; Leitch et al, 1991; Goldfarb et al., 1997). This duration covers much of the evolution of the Cordilleran orogen.

Vein hosting lithologies vary widely and include ultramafic, mafic to felsic volcanic rocks, and a variety of sedimentary rocks (Table 6.1). The most common types of host rocks are ophiolite slices, and clastic units, largely siltstone and graywacke. Nearly all the units hosting the vein systems have been metamorphosed at lower to upper greenschist grade. The veins are dominated by quartz with lesser amounts of Ca-Fe-Mg carbonate, muscovite, chlorite, albite, and scheelite. Pyrite is the dominant sulfide with varying amounts of arsenopyrite and other sulfide minerals. In the wall rocks adjoining the veins, hydrothermal alteration patterns are similar to Archean counterparts (McCuaig and Kerrich, 1998). The most common type of hydrothermal alteration in these vein systems is extensive additions of quartz, carbonate, muscovite, and sulfide minerals. Alteration mineral assemblages appear to be controlled largely by the host rocks; for

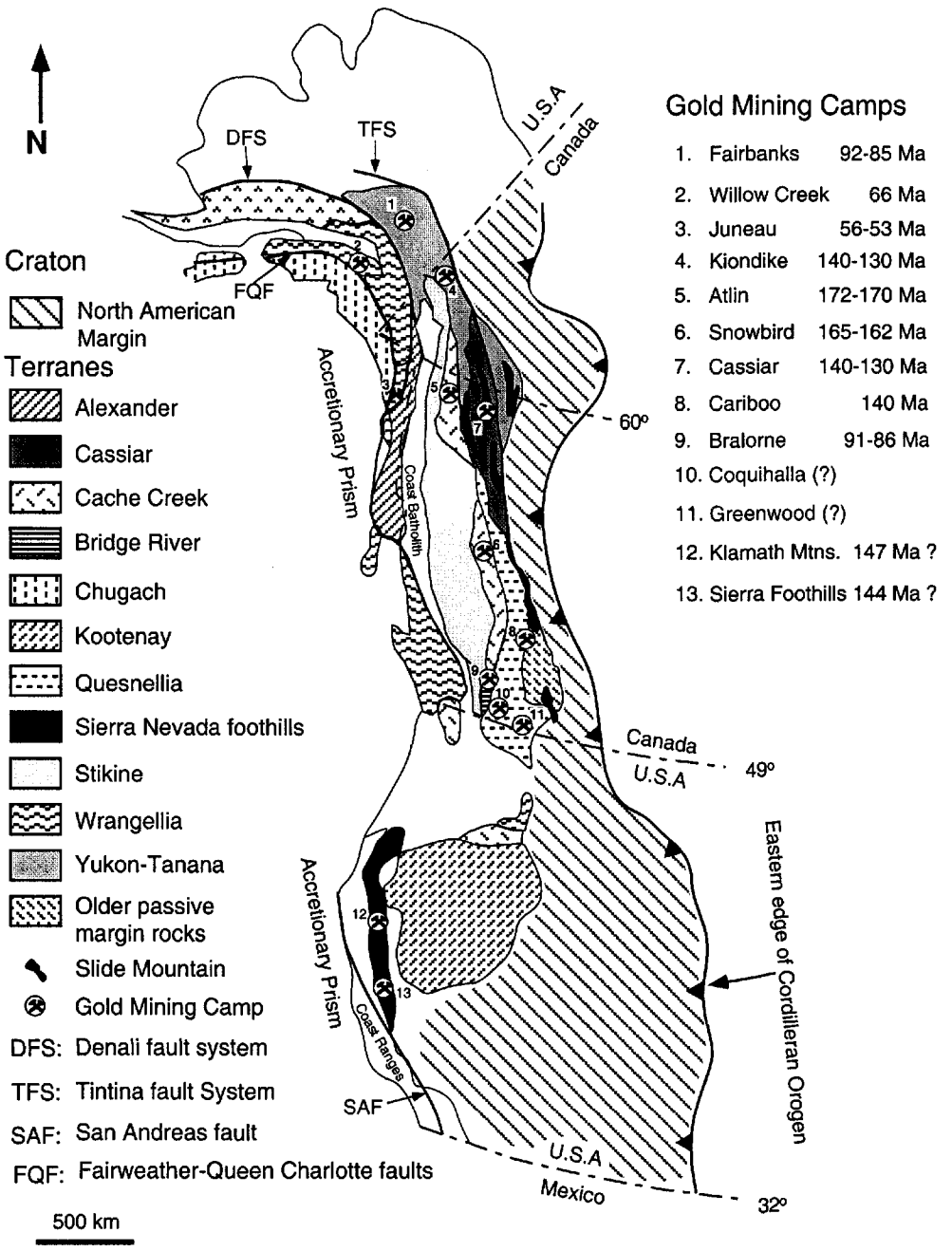

Fig. 6.1. Distributions of synorogenic gold deposits in the western North American Cordillera. Selected accreted superterranes generalized from Coney (1989), Monger (1993, 1999), Wheeler and McFeely (1991). Ages of veining indicated in Table 6.1.

Table 6.1. Summary of the characteristics for quartz-carbonate vein systems sampled in the western North American Cordillera

District Camp	Vein systems	Vein location Lat. (N)	 Long. (w)	Vein mineral assemblage	Tectonostratigraphic terrane	Host rocks, Age Lithology	Vein formation (Ma)	Granitoids (Ma)	References
East-central Alaska									
Fairbanks	Christina	65° 04'	147° 21'	qtz-mus-sul-carb	Yukon-Tanana	E. Pz quartzite and L. Pz schist, mid-Cre diorite	92 - 85	95 - 90	1
South-central Alaska									
Willow Creek	Fern Mine	61° 39'	149° 15'	qtz-mus-sul-carb	Peninsular (Wrangellia composite terrane)	L. Pz schist; L. Cre tonalite	66	79 - 66	1
West-central Yukon Teritory									
Klondike district	Sheba	63° 53'	138° 56'	qtz-mus-chl-sul-carb	Yukon-Tanana	mid-Pz - E. Mz metasedimentary and igneous rocks	140 - 130	?	2
Northernmost British Columbia									
Atlin	(1) Goldstar	59° 34'	133° 42'	qtz-carb-mus-sul	Cache Creek	L. Pz - E. Mz metasedimentary, mafic and ultramafic rocks	172-170	mid-Jur Fouth of July batholith	3, 4
	(2) Anna	59° 33'	133° 37'						
	(3) Surprise	59° 31'	133° 28'						
	(4) Mckee Creek	59° 27'	133° 33'						
Northern British Columbia									
Cassiar	(1) Boomerang veins	59° 16'	129° 41'	qtz-carb-mus-sul	Sylvester (part of the Slide Mtn)	Dev. - E. Tri metasedimentary, volcanic, and ultramafic rocks	140-130	mid-Cre (Cassiar batholith) ca. 100	5 - 7
	(2) Sky	59° 12'	129° 41'						
	(3) Pete	59° 09'	129° 40'						
Central British Columbia									
Stuart Lake belt	Snowbird	54° 27'	124° 30'	qtz-carb-mus-sul	Cache Creek	L. Pz - E. Mz metasedimentary, volcanic, and ultramafic rocks	165-162	mid-Jur 165-162	4, 8
Southwestern British Columbia									
Bridge River	(1) Bralorne mine	50° 46'	122° 49'	qtz-carb-mus-sul	(1) Bridge River	L. Pz - E. Mz	91-86	early Late Cre (albitite dyke)	9, 10
	(2) Pioneer	50° 45'	122° 46'		(2) Cadwaller	(1) Bralorne diorite (2) Cadwaller greenstone		91-86	
Southernmost British Columbia									
Greenwood	(1) Imperial	49° 07'	118° 59'	qtz-carb-mus-sul	Quesnellia	Pz - Mz meta-ultramafic, mafic and sedimentar rocks	(?)	Jur - Cre (Nelson pluton)	11
	(2) Riverside	49° 06'	118° 58'						
Southern California									
Mother Lode	(1) Carson	37° 58'	120° 25"	qtz-carb-mus-sul	Sierra Nevada foothills metamorphic complex	Pz - Mz metasedimentary, volcanic and ultramfic rocks	147-144	Mz - pre-Cre	12 - 14
	(2) Coulterville	37° 43'	120° 12'				125-110 (?)		

Abbrevaiations: L = late, E = early, Pz = Paleozoic, Mz = Mesozoic, Dev = Devonian, Tri = Triassic, Jur = Jurassic, Cre = Cretaceous
: qtz = quartz, carb = carbonate, mus = muscovite, sul = sulfide, BC = British Columbia

References: 1 = Goldfarb et al. (1997); 2 = Rushton et al. (1993); 3 = Ash et al. (1996); 4 = Ash (2001); 5 = Sketchley et al. (1986); 6 = Anderson and Hodgson (1989); 7 = Driver et al. (2000); 8 = Madu et al. (1990); 9 = Leitch et al. (1989); 10 = Leitch et al. (1991); 11 = Church (1997); 12 = Bohlke and Kistler (1986); 13 = Landefeld (1988); 14 = Elder and Cashman (1992)

example, muscovite is associated with felsic igneous or clastic sedimentary rocks, whereas Cr-bearing mica is associated with mafic or ultramafic rocks. These hydrothermal muscovites in and adjacent to the quartz-carbonate vein systems are ideal for analyzing their nitrogen concentrations and nitrogen isotopic compositions to constrain the $\delta^{15}N$ of the ore-forming fluid, and in turn N isotope composition of the source reservoirs, as well as δD. Reconnaissance N-isotope studies on hydrothermal micas from Archean and Paleozoic orogenic lode gold deposits have proven the feasibility of this new approach for mineral deposits research (Jia and Kerrich, 1999, 2000a, b; Jia et al., 2001).

In this study, 100 new analyses of N concentrations and isotopes are reported for hydrothermal muscovites separated from Au-bearing quartz-carbonate veins from the western North American Cordillera: included are the Mother Lode of southern California; the Greenwood, Bridge River, Snowbird, Cassiar, and Atlin camps in British Columbia (BC); the Klondike district in the Yukon; and the Fairbanks and Willow Creek districts of Alaska (Table 6.1). This represents a systematic new nitrogen isotope database of hydrothermal micas in orogenic lode gold deposits, providing new constraints on the origin of the ore-forming fluids.

Pyrite, one of most abundant and ubiquitous sulfides in hydrothermal ore deposits, may have variable contents of trace elements, such as Co, Ni, Cu, Pb, Zn, As, Tl, Au, and Se. Siting of these trace elements in pyrite can be: (1) as inclusions, e.g., Cu, Zn, or Pb sulfides; (2) as nonstoichiometric substitutions in the lattice for As, Tl, and Au; or (3) as the lattice substitution for Fe (Co and Ni) or S (Se and Te) [Huston et al., 1995]. Trace

element characteristics of pyrite have been used as one method for classifying ore deposits.

Selenium contents and Se/S ratios in sulfide minerals have been used to constrain the genesis of sulfide mineralization given large differences in S/Se ratios of most mantle derived magmas and crustal rocks (Brailia et al., 1979; Cabri et al., 1985; Eckstrand and Hulbert; 1987; Phillips et al., 1988; Ripley, 1990). Sulfur and Se behave coherently during anhydrous magmatic processes (Loftus-Hills and Solomon, 1967), such that the Se/S $\times 10^6$ ratios of chondrites, Fe-meteorites, ocean ridge, and intraplate mantle-derived rocks all cluster in the range of 230 to 350 (Eckstrand and Hulbert, 1987). For example, Hertogen et al. (1980), Hamlyn et al. (1985), Morgan (1986) and McDonough and Sun (1995) obtained similar Se/S $\times 10^6$ ratios of 250 to 333, or S/Se between 3000 and 4000, from mid-ocean ridge basalts. Hexavalent Se, however, is less mobile than S^{6+} during hydrous arc magmatism, intracrustal and surficial processes; as a result sedimentary rocks in particular, and the crust in general, possess Se/S $\times 10^6$ ratios much less than that of mantle values (Eckstrand and Hulbert, 1987; McDonough and Sun, 1995).

There are few data on both the S and Se contents of hydrothermal lode gold deposits or their constituent sulfide minerals, although selenides are known to occur sporadically (Boyle, 1979). Bornhorst and Nurmi (1997) measured bulk unoxidized samples from hydrothermal gold deposits in Fennoscandia and North America, and determined a range in abundance of Se from 40 to 140,000 ppb (n=114). The mean abundance of Se is 960 ppb, with a mean Se/S $\times 10^6$ ratio of 74 in mesothermal gold deposits. Therefore, determination of Se contents and Se/S ratios of pyrite from orogenic

lode gold deposits may also shed light on the relative contributions of crust versus mantle source reservoirs to the deposits.

It has not been possible to determine Se by ICP-MS given the isobaric interference of the Ar diamer on ^{80}Se. The new Hexapole ICP-MS method eliminates the Ar diamer. Accordingly, sulfur and Se data are reported for pyrite separates from deposits in three camps from the North American Cordillera, and for purposes of comparison deposits of the Archean Superior Province of Canada, and Norseman, Yilgarn craton. Analytical methods are reported in Appendix I.

The meteoric water model for orogenic gold deposits was based on an apparent covariation of the δD of bulk decrepitated fluid inclusions from gold-quartz veins with the latitudinally controlled variation of present and Tertiary meteoric water (see Nesbitt et al., 1986, 1989; Taylor, 1997 for a review). Accordingly, in this study sampling is designed specifically to span 26° of latitude from California to Alaska to test for latitudinal variations of δD in a subset of robust hydrothermal micas.

6.2. Regional and local geologic settings of gold-bearing quartz vein systems

6.2.1. Geology of the Klondike district, Yukon Territory

The rocks of the Klondike district belong to two distinct terranes: the Yukon-Tanana terrane and the Slide Mountain terrane (Fig. 6.1), which form part of the northern extension of the Omineca belt, one of five tectonic belts making up the Canadian Cordillera (Monger, 1984; Gabrielse and Yorath, 1989). The Yukon-Tanana terrane is an assemblage of mainly middle Paleozoic to early Mesozoic metamorphic and plutonic rocks (Mortenson, 1990). In west central Yukon and eastern Alaska, the Yukon-Tanana terrane is faulted to the northeast against miogeoclinal strata of North America along the

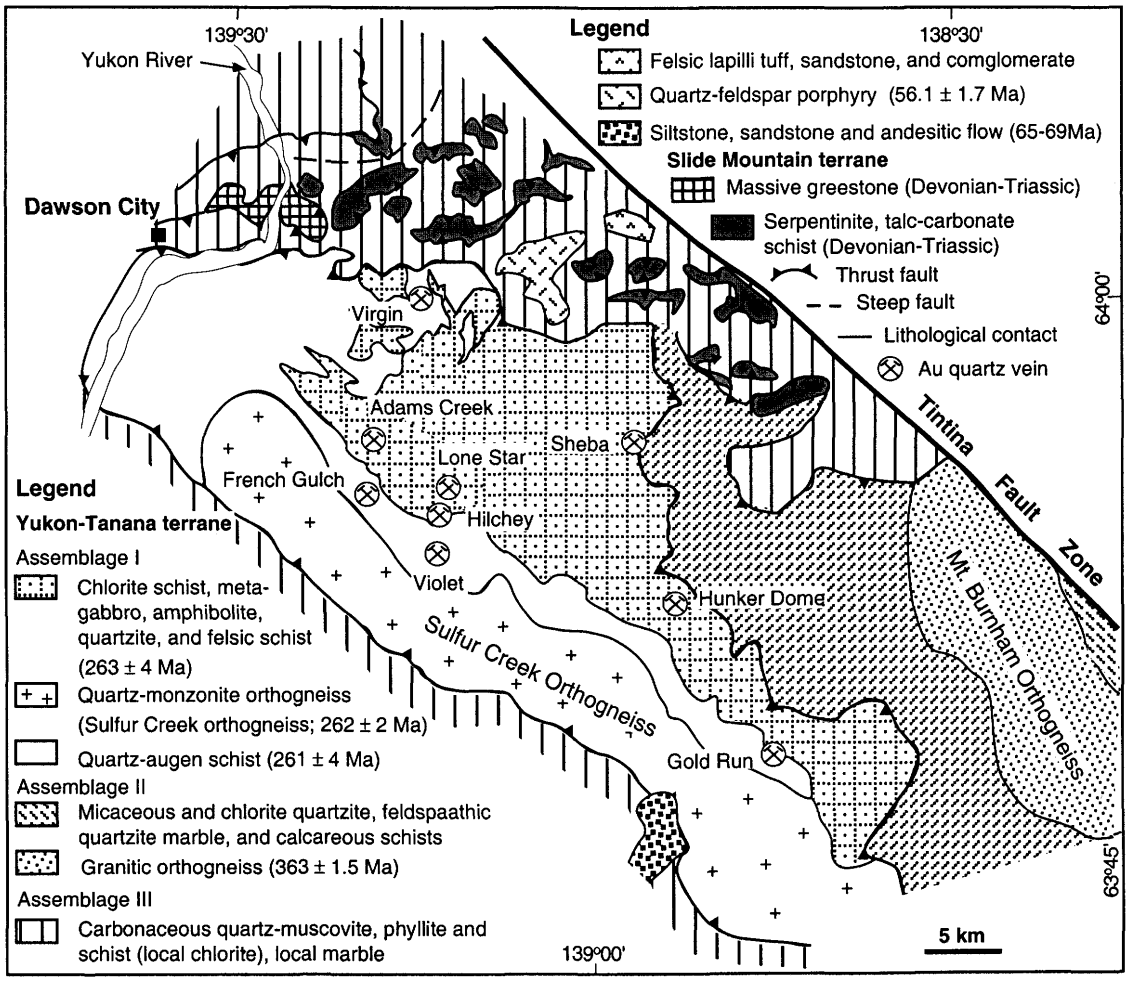

Fig. 6.2. Geology of the Klondike district, with selected Au quartz vein occurrences. Modified from Mortenson (1990) and Rushton et al. (1993).

Tintina fault. The Slide Mountain terrane occurs as a northwest-southeast trending belt of relatively small, isolated allochthons, which extends along the length of the Canadian Cordillera (Fig. 6.1; Hansen, 1990; Wheeler and McFeely, 1991). This terrane consists of greenschist facies to nonmetamorphosed oceanic and arc-related strata, which range from Devonian to Jurassic in age (Gabrielse and Yorath, 1989). However, the relationship between these two terranes is uncertain and the subject of current debate (Rushton et al., 1993).

The geology of the Klondike district has been described in detail by Mortenson (1990). It is composed of three, regional-scale thrust sheets, termed assemblages I to III (Fig. 6.2). The assemblages are composed of interlayered metasedimentary and metavolcanic rocks, which are cut by a variety of deformed and metamorphosed plutons. Small bodies of greenstone and altered ultramafic rocks, thought to be the Slide Mountain terrane, occur discontinuously along the thrust faults. The rocks of assemblage I, the uppermost structurally lithotectonic sequence, are middle Permian in age (261-264 Ma, U-Pb zircon dating), consisting mainly of quartz-actinolite-chlorite schist, quartzite, quartz-muscovite schist, quartz-augen schist, and orthogneiss of quartz monzonite composition; Assemblage II is structurally lower than assemblage I, which consists predominantly of metasedimentary and metaigneous units, including quartzite, marble, and felsic schist, and a late Devonian to early Mississipian granitic orthogneiss (the Mount Burnham orthogneiss, U-Pb zircon age of 363.8 ± 1.5 Ma); and Assemblage III, at the lower structural level, comprises metasedimentary rocks for which no ages are available. Late Cretaceous to early Tertiary intrusive and extrusive rocks and sedimentary rocks are also exposed within the area (Fig. 6.2).

Two distinct types of quartz vein systems have been described from the Klondike region (Mortenson et al., 1992; Rushton et al., 1993). (1) Foliaform veins are lens shaped, parallel to metamorphic foliation, and ubiquitously distributed in metamorphic rocks belonging to all three lithological assemblages. These veins are generally barren of sulfide and Au mineralization. (2) Discordant veins generally crosscut metamorphic foliation, and contain significant Au mineralization. They are massive quartz veins, generally 2 to 3 m thick and up to hundreds of meters long, mainly hosted in assemblage I, although there a few occurrences of Au quartz veins in assemblage II in the southeast portion of this district (see Fig. 6.2).

Veins sampled at the Sheba deposit, Dawson city, include quartz, carbonate, muscovite, and sulfide (mainly pyrite with minor arsenopyrite, chalcopyrite and sphalerite), which is similar to other vein systems such as the Mitchel and Hunker occurrences (Rushton et al., 1993). Gold quartz vein mineralization at the Sheba was Early Cretaceous (140 ± 2.0, and 134 ± 1.5 Ma) from K-Ar dating on hydrothermal muscovite (Hunt and Roddick, 1992). Similar Early Cretaceous vein formation ages have been reported for other mining camps in the Canadian Cordillera such as at Cassiar, northern BC where muscovite yields a K-Ar age of 131 ± 5 Ma (Shetcheley et al., 1986), and at the Cariboo gold quartz mine, central BC with a K-Ar age of 141 ± 5 Ma on muscovite (Alldrick, 1983).

6.2.2. Geology of the Atlin Camp

The Atlin gold district is situated near the northwestern margin of the northern Cache Creek terrane in northwestern British Columbia, within the Intermontane Belt (Fig. 6.1). This terrane consists of allochthonous remnants of a late Paleozoic to early Mesozoic Tethyan oceanic rocks (Monger, 1975, Monger et al., 1982). The island arc

terranes of both Quesnellia and Stikinia presently border the northern Cache Creek terrane along the Teslin and Nahlin faults to the east and west respectively. Mid-Jurassic emplacement of the oceanic Cache Creek rocks westward over Stikinia is well constrained in northern British Columbia both by biostratigraphic evidence (Gabrielse, 1991) and the age of cross-cutting plutons (Mihalynuk et al., 1992). Relationships of the Cache Creek terrane with Quesnellia arc rocks to the east is less well constrained due to the effects of post-collisional, pre-late Cretaceous dextral strike-slip faulting (Gabrielse, 1991).

The Cache Creek terrane is a composite oceanic terrane that comprises two distinctive lithotectonic elements. An upper Triassic to early Jurassic subduction-related accretionary complex (Monger et al., 1982; Monger, 1984; Gabrielse and Yorath, 1989; Coney, 1989), and dismembered ophiolitic assemblages emplaced by obduction of oceanic lithosphere, possibly by collision during final closure of the ancient ocean basin. These ophiolitic assemblages comprise a sequence of strongly disrupted sedimentary, crustal and mantle (alpine-type ultramafic) lithologies of oceanic origin, all of which are components of a typical ophiolite suite (Monger, 1977). Also included are reefoidal limestones of equivocal origin, but suggested by Monger (1977) to have formed on an ocean island or seamount. This interpretation is supported by recent investigations of Cache Creek rocks in the Stuart Lake area of central British Columbia which indicate that massive Permian limestones are associated with basaltic rocks of ocean island affinity (Ash and MacDonald, 1993).

The Atlin gold camp is located on the eastern shore of Atlin Lake. There are two principal lithotectonic elements (Fig. 6.3). A lower composite unit termed the Atlin accretionary complex, which is characterized by a structurally and lithologically diverse

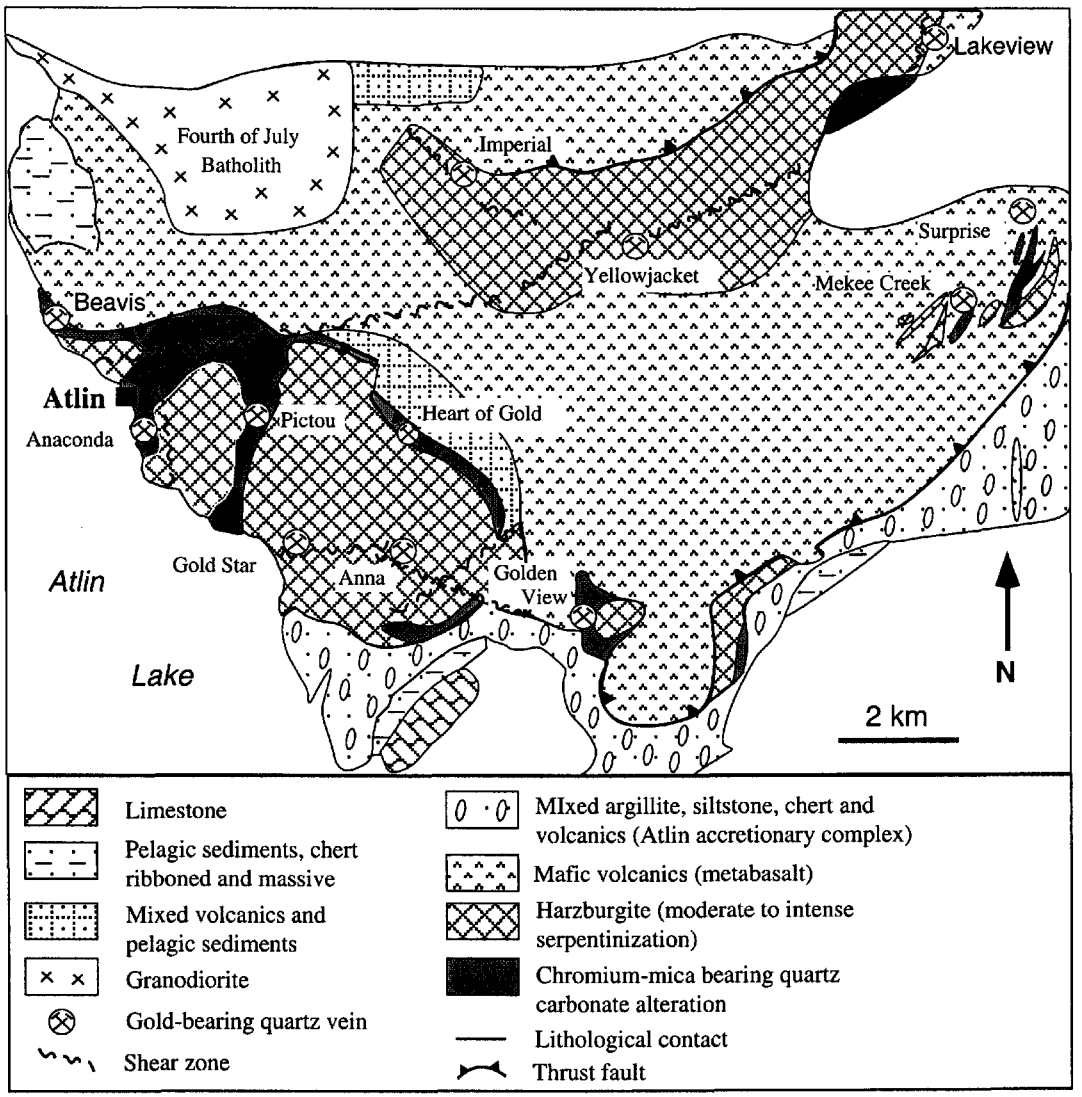

Fig. 6.3. Geological map of the Atlin area. Modified from Ash (2001).

sequence of steeply to moderately dipping, tectonically imbricated slices of pelagic metasedimentary rocks, with lesser amounts of metabasalt, limestone and wackes. The lower accretionary complex is tectonically overlain along the Monarch Mountain thrust by a series of imbricated units of dominantly metamorphosed oceanic crustal and upper mantle lithologies that collectively comprise the Atlin ophiolitic assemblage. Oceanic associations are represented by metamorphosed basalt, gabbro and ultramafic rocks. Mantle lithologies are dominated by variably altered harzburgite (alpine-type peridotite). Both these lithotectonic elements are intruded by the Mid-Jurassic calcalkaline Fourth of July batholith and related dikes, and younger Late-Cretaceous dikes (Fig. 6.3; Mihalynuk et al., 1992).

Gold-bearing quartz vein mineralization throughout the Atlin camp is typically associated with carbonatized ultramafic or mafic lithologies (Fig. 6.3). Ages of hydrothermal Cr-muscovite associated with the gold mineralization suggest an interval of veining between 171 and 167 Ma (Ash, 2001; ^{40}Ar-^{39}Ar dating on Cr-muscovite).

6.2.3. Geology of the Cassiar Camp

This orogenic gold district, located in the Cassiar Mountains of far northern British Columbia, spans two distinct but inter-related terranes, the pericratonic Cassiar terrane and the Slide Mountain terrane. Cassiar vein gold deposits are hosted by the Sylvester allochthonous sequence in part of the Slide Mountain terrane. The former comprises platformal to continental-slope, deep-water strata that range from late Proterozoic to early Permian in age. These units have been correlated along the ancient North American continental margin. The latter is represented by the Sylvester allochthon, a large complex eugeosynclinal klippe (see Fig. 6.1; Monger, 1999).

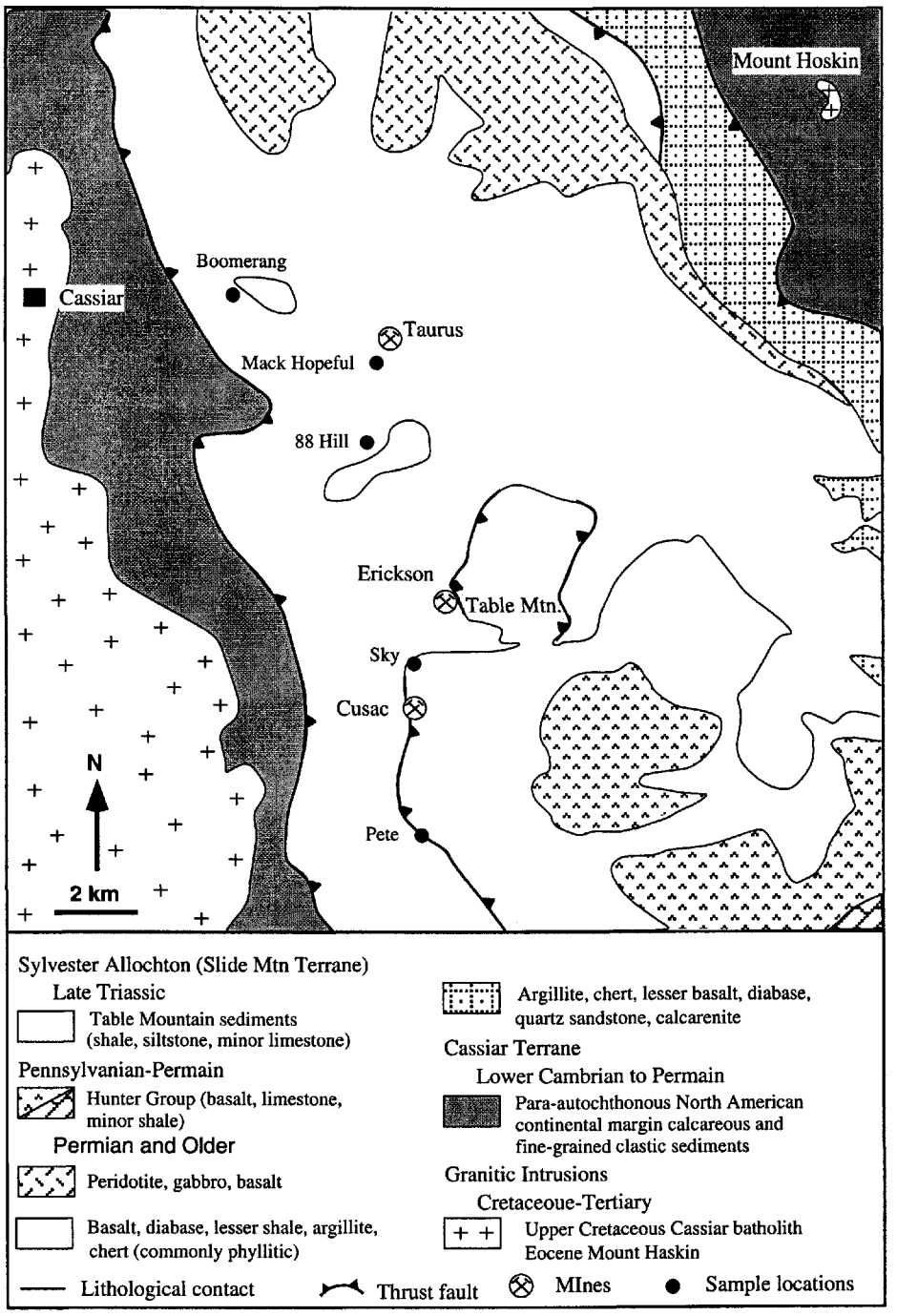

Fig. 6.4. Generalized geology of the Cassiar area, with location of mines and samples. Modified from Nelson and Bradford (1993) and Ash et al. (1996).

The Sylvester allochthon comprises three structurally stacked divisions, each of which represents a separate late Paleozoic tectonic and depositional environment (Nelson and Bradford, 1993). Division I, structurally the lowest, is dominated by pelagic and hemipelagic sediments with a minor basaltic component; it represents a deep-water sedimentary basin. The following Division II includes interleaved basalt-diabase-sedimentary sequences and ultramafic-gabbro slivers that together constitute a late Paleozoic ophiolite suite. The structurally highest Division III, contains a varied volcanic suite of arc-tholeite to calcalkaline affinity, intermediate plutons, and interbedded limestones, cherts, and tuffs. The Cassiar batholith intrudes stratified units of the Cassiar terrane to the west of the Sylvester allochthon (Fig. 6.4). The batholith has been considered to be a single intrusive mass about 100 Ma in age, based mainly on radiometric dating done by the Geological Survey of Canada cited in Nelson and Bradford (1993) and Driver et al. (2000).

Gold mineralization developed in a north-south corridor, about 100 km^2 in size extending from the Cusac veins on the south to the Taurus veins in the north (Fig. 6.4). It comprises a set of east-northeast-trending veins and vein swarms. The veins contain mainly quartz and carbonate with white mica or Cr-bearing muscovite and sulfide minerals. The synaccretionary gold-quartz veins have ages of 130 to 140 Ma (K-Ar dating; Sketchley et al., 1986).

6.2.4. Geology of the Stuart Lake area

The study area covers late Paleozoic to early Mesozoic oceanic rocks of the Cache Creek terrane in central British Columbia (Fig. 6.1), which forms a NNW-trending belt, 450 km long by 60 km wide, termed the Stuart Lake belt. This belt comprises tectonically intercalated units of undifferentiated pelagic sediments, limestone and

subordinate oceanic metavolcanic and plutonic ultramafic rocks (Fig. 6.5). Cache Creek oceanic rocks are intruded throughout by middle Jurassic and later felsic plutonic rocks (Armstrong, 1949; Ash and MacDonald, 1993). The largest intrusive body, the Shass Mountain pluton, is an elongate northwest-trending, middle Jurassic tonalite (Fig. 6.5; Ash and MacDonald, 1993).

The Snowbird gold quartz-carbonate vein system is located 16 km west of Fort St. James, near the southwest end of the Stuart Lake belt (Fig. 6.5). It is hosted by the Sowchea shear zone (Armstrong, 1949), a prominent northwest-trending fault zone dipping from 40° to 50° to the northeast. The fault zone is up to several tens of metres wide and 1,200 m long, characterized by intense carbonate alteration, brecciation, and shearing (Fig. 6.6A). Ore-shoots are hosted by three quartz-carbonate-muscovite–sulfide veins; the Main, Pegleg and Argillite veins (Fig. 6.6B; Madu et al., 1990). Both the Main and Pegleg veins are structurally controlled by the Sowchea fault zone. Argillite veins follow a high-angle cross-fault perpendicular to the Sowchea shear zone. Ar-Ar isotopic analysis of Cr-bearing muscovite from the Main veins by laser step heating methods indicate that the age of gold mineralization is middle Jurassic, between 160 and 165 Ma (Ash, 2001).

6.2.5. Geology of the Bridge River mining camp

The Bridge River gold camp is located along the western edge of the Intermontane Superterrane of the Canadian Cordillera in southwestern British Columbia (Fig. 6.1). It has produced some 130 tonnes (4 million oz.) of Au and 40 tonnes (1.2 million oz.) of Ag over its seventy-year history (Leitch et al., 1991). The geology of the Bridge River area is structurally complex and includes two faulted and fault-bounded units known as

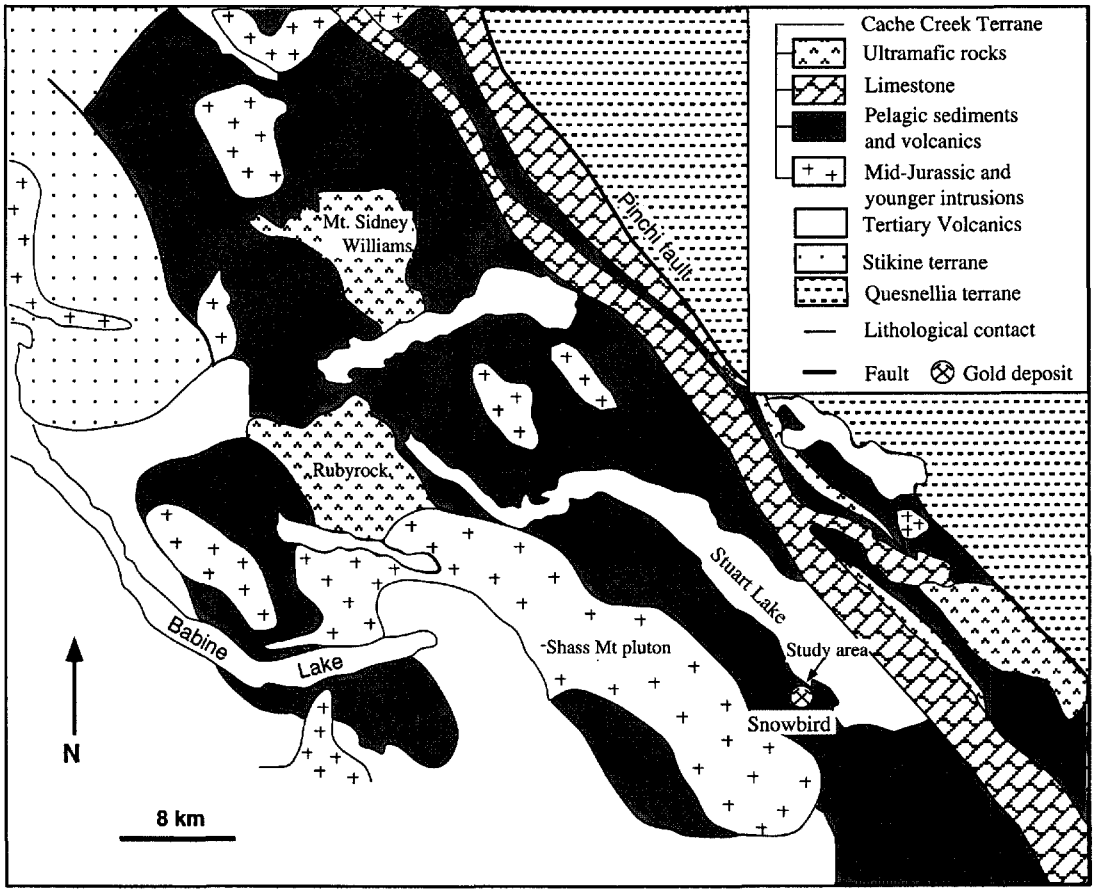

Fig. 6.5. Geological map of southern Stuart Lake belt. Modified from Ash and MacDonald (1993).

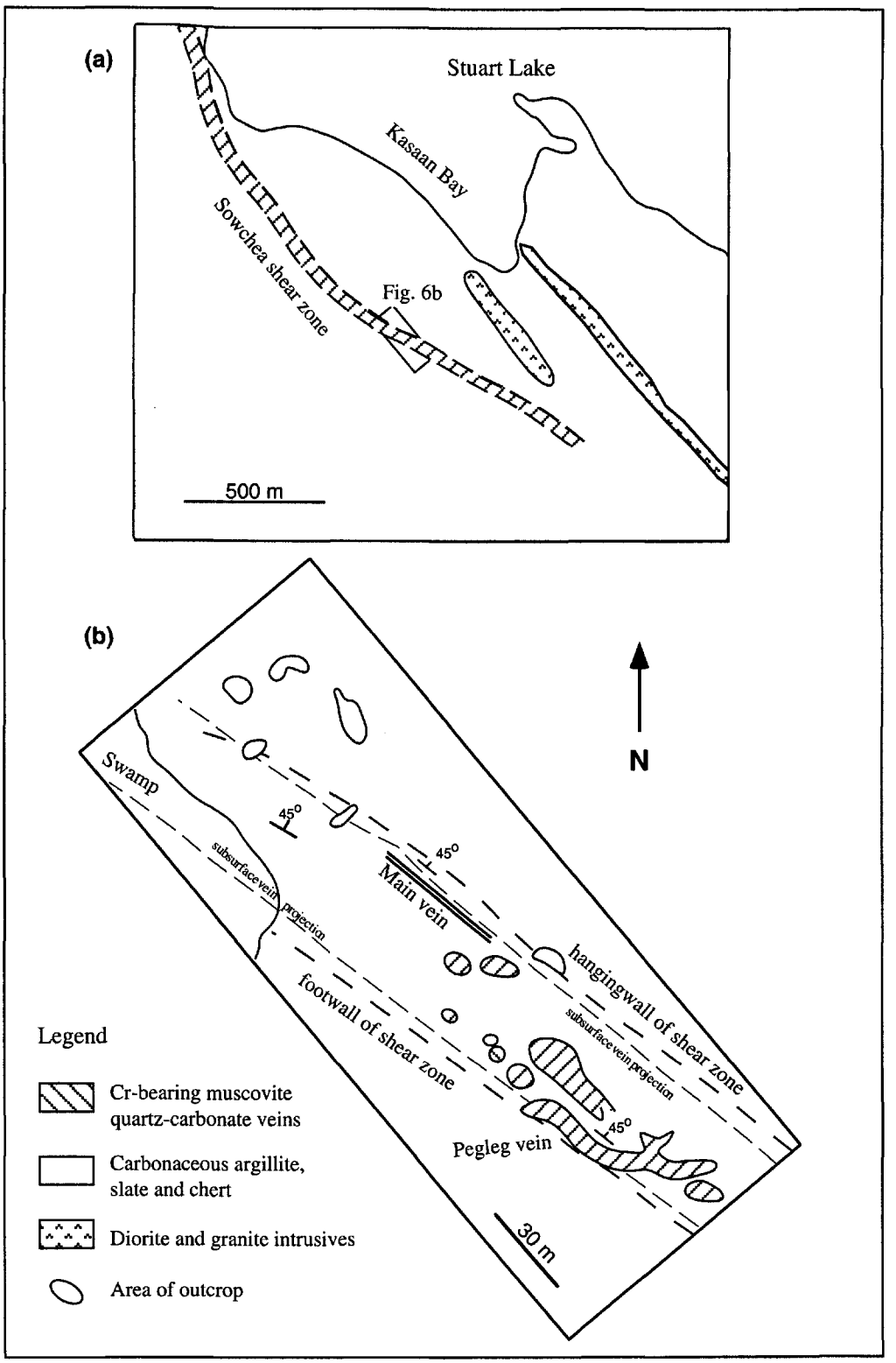

Fig. 6.6. (a). Local geology around the Snowbird property and the location and orientation of the Sowchea shear zone (Armstrong, 1949). (b). Enlargement shows rock outcrop and orientation of the mineralized quartz veins at the property (from Madu et al., 1990).

the Cadwallader and Bridge River complexes (Fig. 6.7). The former has been interpreted as an island arc assemblage belonging to the Stikinia terrane (Rusmore, 1987), whereas the latter contains an oceanic composite lithotectonic assemblage equivalent to the Cache Creek terrane (Fig. 6.1; Potter, 1986). They were likely accreted to North America in the Jurassic (Price et al., 1985).

The Bridge River complex is composed of late Paleozoic to early Jurassic oceanic volcanic and sedimentary rock assemblages (Church et al., 1995). It consists of ribbon cherts, argillites, minor limestone, and basaltic flows, sills and dykes. The Cadwallader group is dominated by a thick sequence of mafic and sedimentary rocks. The basaltic rocks and associated feeder intrusions in the lower part of the Cadwallader group belong to the Pioneer Formation. They are stratigraphically overlain by turbidites of the upper Triassic Hurley Formation (Rosmore, 1987; Church, 1995). Intrusions in the Bralorne district are distributed as small stocks occurring mostly along NW trending faults, hosted by both the Bridge River complex and Cadwallader group, although the contacts are typically tectonic (Fig. 6.7).

There are two main vein types in the Bridge River mining camp; "shear" veins and "extension" veins, which are both structurally controlled by faults (Fig. 6.8A; Leitch, 1990). The main shear veins have been traced continuously for up to 1500 m along a strike of roughly 110° azimuth, and for 1800 m down a dip of about 70° north (see Fig. 6.8B). They are moderately to strongly ribboned veins that average 1 to 2 m in width (Leitch et al., 1991), although they pinch to a few centimeters, or swell to as much as 7 m. Ore shoots with the ribboned veins occupy less than 20 percent of the veins. The extension veins strike roughly 070° azimuth and dip about 75° north. They are smaller

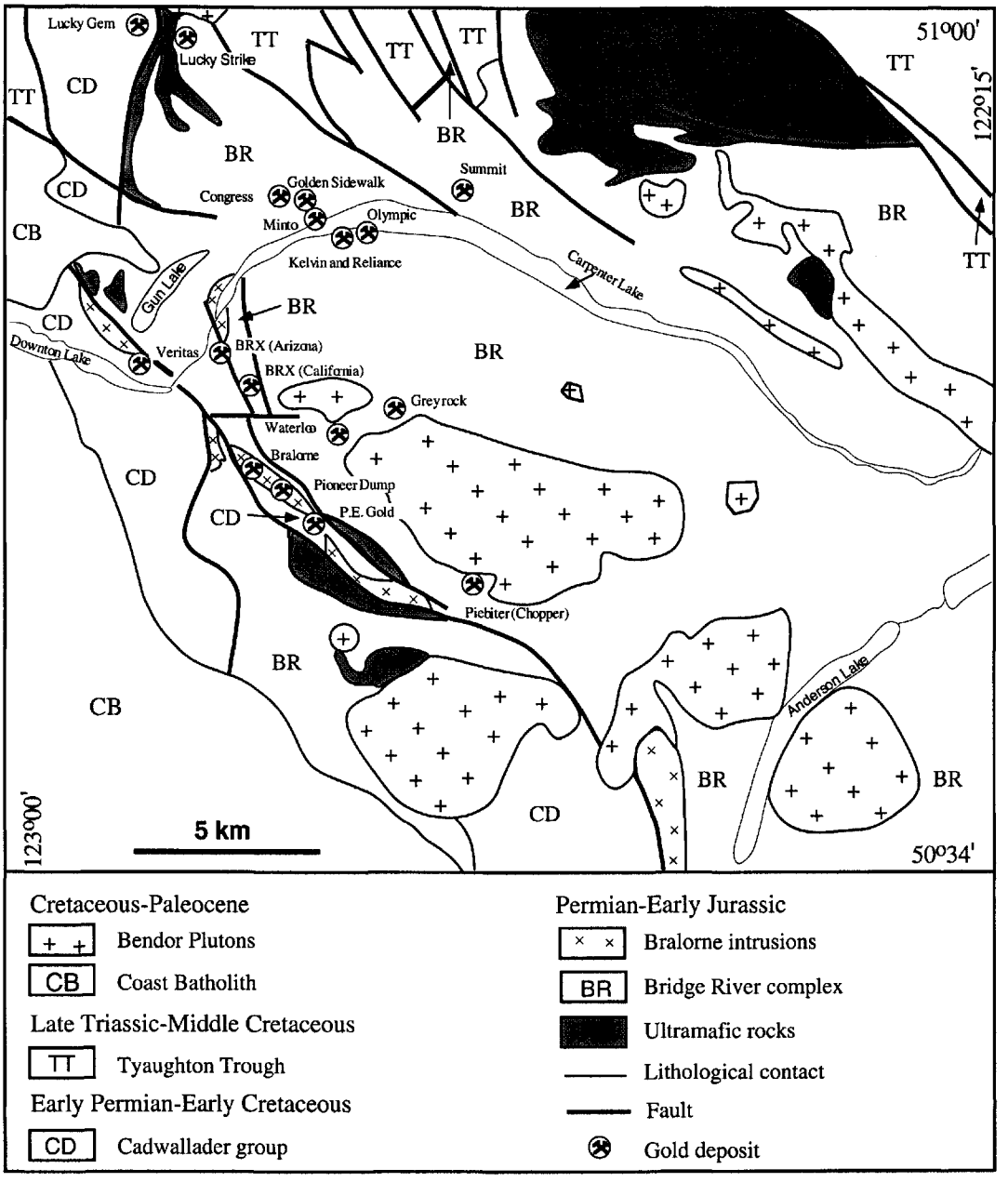

Fig. 6.7. Generalized geological map of the Bridge River district, southwestern British Columbia. Modified from Leitch et al. (1991) and Church (1995). Selected gold deposits are also shown.

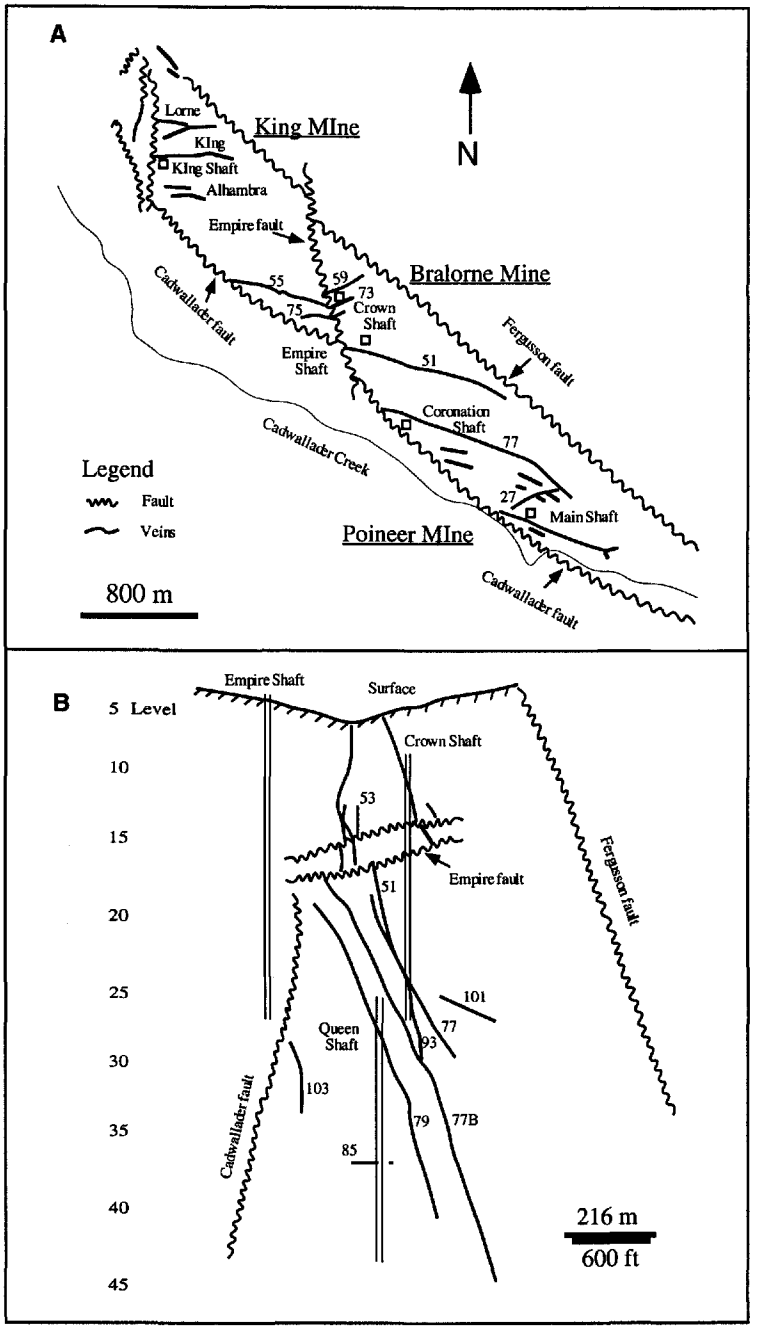

Figs. 6.8. A. Plan view of the main vein systems in the Bralorne-Pioneer deposit (numbers represent vein numbers). The 51 and 55 veins are believed to be offset portions of the same vein across the Empire fault (Leitch, 1990). 7B. Sketch of the major veins in the Bralorne section of the mine (looking to the northwest). The depth extent of the explored system is almost 200 m (Leitch, 1990).

structures than the shear veins, with smaller ore shoot that are occasionally of very rich but often highly variable tenor (Leitch, 1990). Quartz-carbonate-muscovite-chlorite envelopes, up to several metres wide are extensive around the veins, containing disseminated pyrite with lesser chalcopyrite, arsenopyrite, sphalerite and galena.

The timing of mineralization in the Bralorne area is constrained to about the same time as metamorphism by evidence from the alteration of several dyke suites (Leitch and Godwin, 1988). U-Pb zircon and K-Ar whole-rock dating of these dykes indicates that peak conditions of metamorphism and mineralization were early Late Cretaceous (90 Ma).

6.2.6. Geology of the Greenwood mining camp

The Greenwood gold camp is located in southern British Columbia, within the Quesnel terrane in the eastern part of the Intermontane Belt of the Canadian Cordillera (Fig. 6.1). In the Greenwood area Paleozoic and Early Mesozoic units of Quesnellia record a complex deformation history. Middle and late Paleozoic and early Mesozoic sedimentary and volcanic sequences with subordinate plutonic rocks (Church, 1997; Fyles, 1990) were overthrust onto the margin of Precambrian North America. Accretion-related deformation generated extensive folding and faulting, imbricate thrusting, and stacking of various lithologies. Fyles (1990) recognized a series of north-dipping thrust slices of Paleozoic and early Mesozoic rocks with a superimposed east-directed middle Jurassic movement.

Post-accretionary late Cretaceous and Tertiary units in the Greenwood area include a wide variety of granitoid intrusions and a thick continental succession of Eocene volcanic and sedimentary suites. All the units were faulted during Tertiary extension into a series of horsts and graben (Wingate and Irving, 1994; Dostal et al., 2001). Tertiary

extensional faults control the present distribution and configuration of Tertiary and older units (Fyles, 1990).

Paleozoic assemblages in this region have been lithologically divided into the Knob Hill and the Attwood groups (Little, 1983), with Greenwood gabbroic rocks (Church, 1997). The late Paleozoic Knob Hill group consists mainly of deep ocean sedimentary rocks (cherts and argillites), oceanic volcanic rocks (tholeiitic basalts) and serpentinites, and rare thin lenses of limestone. The Attwood group comprises greywackes, chert pebble conglomerates, limestones, laminated argillites, with minor volcanic rocks (island-arc tholeiites). The Greenwood gabbro is compositionally comparable to oceanic plutonic rocks (Dostal et al., 2001). The relationship between the Knob Hill and Attwood groups is unclear, as all of their contacts in the Greenwood area are tectonic. They are unconformably overlain by the middle Triassic Brooklyn Formation, represented largely by limestones, clastic sediments and pyroclastic flows (Dostal et al., 2001).

There are a number of orogenic Au-bearing quartz vein systems in this area. Compared with other vein gold deposits in British Columbia, most of them have not had significant gold production, the maximum being 81,602 oz from the Camp McKinney mine (L. Caron, 1999; personal communication). These gold quartz veins are hosted in the Knob Hill or Attwood group metasedimentary and volcanic rocks, and composed dominantly of quartz, carbonate, muscovite, and pyrite with minor other sulfide minerals. The age(s) of mineralization in this area are poorly constrained.

6.2.7. Geology of the Mother Lode gold province

The Mother lode of California consists of a series of gold deposits distributed in a narrow belt that extends for 200 km along the western foothills of the Sierra Nevada (Figs. 6.1 and 6.9). The western Sierra Nevada foothills are an accretionary complex of

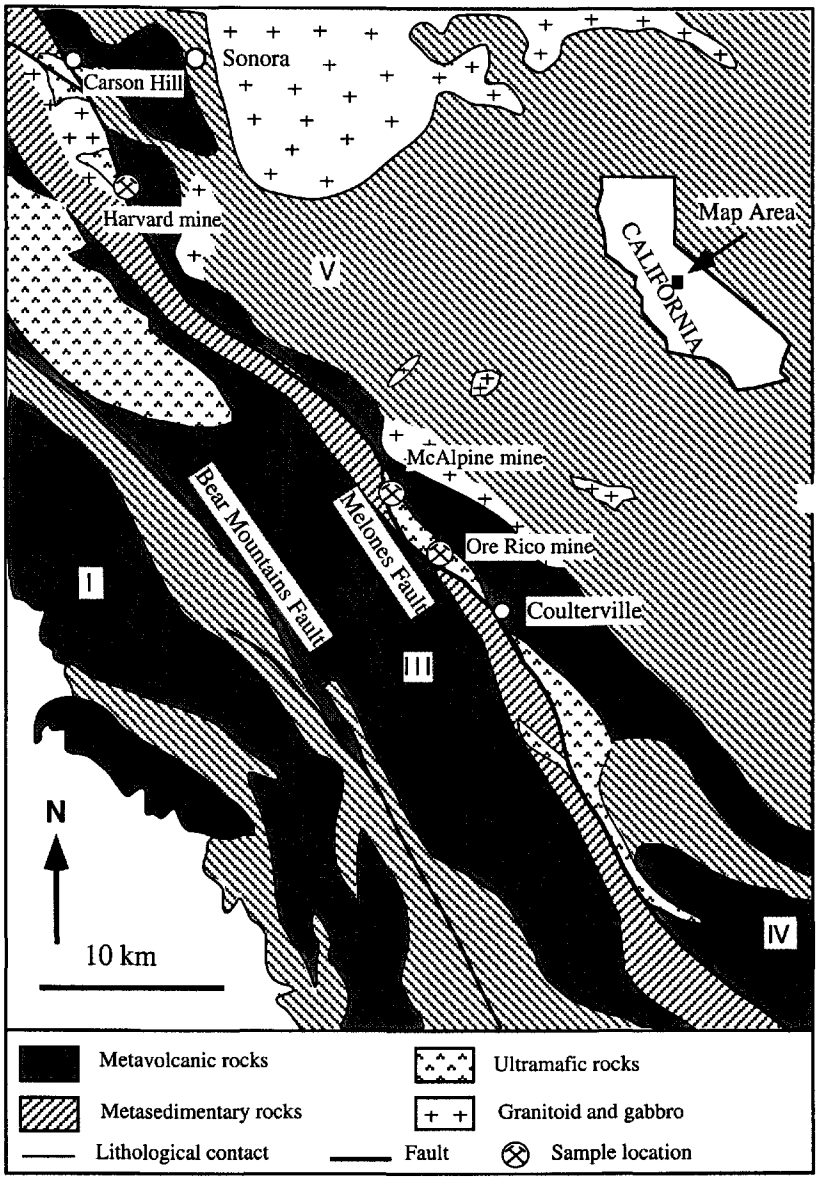

Fig. 6.9. Simplified geologic map of part of the south-central Mother Lode region, showing structural blocks in the western foothills metamorphic belt of the Sierra Nevada and sample locations. Modified from Kistler et al. (1983).

folded sedimentary and volcanic rocks of Paleozoic and Mesozoic age, termed the Foothills Metamorphic complex (Fig. 6.9; Kistler and Dodge, 1983; Böhlke and Kistler, 1986). There are at least six different structural blocks separated by steeply east-dipping faults of the foothills fault system (Bateman and Clark, 1974). Three of the four blocks crop out in the southern Mother Lode region. Blocks I, III, and IV consist largely of metamorphosed marine volcanic rocks and associated graywacke, slate, and conglomerate. Block V, which has been assigned to the Calaveras Formation, consists mainly of highly deformed slate, chert, and lesser amounts of carbonate and quartzite.

Serpentinized ultramafic rocks crop out generally as elongate fault-bounded bodies between the structural blocks. Many of these bodies are currently thought to be remnants of dismembered ophiolite sequences (Kistler and Dodge, 1983). Mineralized veins in the northern Mother Lode occur in basalt, phyllite, and ultramafic rocks. In the Coulterville area sampled in this study, however, gold-bearing veins are associated principally with northwest-trending, elongate serpentinite masses (Fig. 6.9). Cr-bearing muscovite, locally termed mariposite, quartz, and carbonate formed as alteration of the serpentinite involving introduction of CO_2, Si, and K. Introduction of gold was contemporaneous with development of mariposite (Evans and Bowen, 1977).

Most studies have concluded that the Mother lode deposits formed after the pervasive Nevada regional compressional event of about 144 Ma. Böhlke and Kistler (1986) indicate that mariposite formed in the vicinity of the Melones fault zone throughout much of its north-south extent in early Cretaceous time at about 108 to 127 Ma. Alternatively, Landefeld (1988) suggested that geochronologic data indicating Cretaceous mineralization ages are misleading, but rather that mineralization was earlier

than 127 Ma, about mid-Jurassic, between the early and main stages of the Sierra Nevada batholith (Elder and Cashman, 1992; Goldfarb et al., 1998).

6.3. Sample population

Samples used for analyses were from nine regions in the western North American Cordillera. These include east-central Alaska (Christina, in Fairbanks); south-central Alaska (Fern Mine, in Willow Creek); west-central Yukon Territory (Sheba, in the Klondike district); northernmost British Columbia (Goldstar, Anna, Surprise, and Mckee Creek, Atlin camp); northern British Columbia (Pete and Boomerang, at Cassiar); central British Columbia (Snowbird, in Stuart Lake); southwestern British Columbia (Bralorne and Pioneer, in Bridge River), southernmost British Columbia (Imperial and Riverside, in Greenwood), and southern California (Carson and Coulterville, Mother Lode). Samples were collected by the author of this thesis, excepting for characterized samples from the Christina and Fern mine provided by R. Goldfarb, and samples from the Bridge River, Staurt Lake, and Atlin by C. Ash. Analytical methods are reported in Appendix I.

6.4. Results

6.4.1. N and N-isotopic compositions of muscovite

The nitrogen concentrations and $\delta^{15}N$ values of hydrothermal micas from sixteen Au-bearing quartz vein systems in nine mining camps of the western North American Cordillera are strikingly uniform. There is a narrow range within each vein system, where $\delta^{15}N$ typically varies by less than $\pm$ 0.3‰, and overlapping of $\delta^{15}N$ within deposits of a mining camp, and among most mining districts (Table 6.2; Fig. 6.10). This is well illustrated in the results from the Christina and Fern mine vein systems of Alaska, which have mean $\delta^{15}N$ values of 5.8‰ and 5.5‰, and N contents of ranging

Table 6.2. N contents and $\delta^{15}N$ of mica separates from quartz-carbonate vein systems in the western North American Cordillera

Location Vein system	Sample No.	Analyzed Mineral	N content (ppm)	$\delta^{15}N$ (‰) mean ± 1σ
Fairbanks, east-central Alaska				5.8 ± 0.4
Christina	Chr-1	Muscovite	394	5.9
	Chr-2	Muscovite	390	5.4
	Chr-3	Muscovite	401	6.1
Willow Creek, south-central Alaska				5.5 ± 0.3
Fern mine	Fern-1	Muscovite	274	5.8
	Fern-2	Muscovite	260	5.5
	Fern-3	Muscovite	256	5.1
Klondike, Yukon				1.7 ± 0.1
Sheba mine	SH-1-1	Muscovite	275	1.6
	SH-1-2	Muscovite	270	1.6
	SH-2-1	Muscovite	280	1.8
	SH-2-2	Muscovite	280	1.7
	SH-3-1	Muscovite	270	1.7
	SH-3-2	Muscovite	260	1.7
Atlin Camp, northernmost British Columbia				4.5 ± 0.9
Mckee Creek	CAS89.4.1A	Cr-muscovite	1946	4.6
	CAS89.4.1B	Cr-muscovite	1929	4.8
	CAS89.4.1C	Cr-muscovite	1963	4.6
	CAS89.4.1D	Cr-muscovite	1926	4.4
	CAS89.4.1-1	Cr-muscovite	1965	4.9
	CAS89.4.1-2	Cr-muscovite	1947	4.7
	CAS89.4.1-3	Cr-muscovite	1981	4.9
	CAS89.4.1-4	Cr-muscovite	1947	4.8
Surprise	CAS89.14.2.3-1	Cr-muscovite	786	5.8
	CAS89.14.2.3-2	Cr-muscovite	768	5.7
	CAS89.14.2.3-3	Cr-muscovite	767	5.3
	CAS89.14.2.3-5	Cr-muscovite	799	5.6
	CAS89.14.2.3-6	Cr-muscovite	787	5.7
	CAS89.14.2.3-7	Cr-muscovite	786	5.3
Goldstar	CAS89.05.02	Cr-muscovite	330	3.3
	CAS89.05.03	Cr-muscovite	322	3.2
	CAS89.05.04	Cr-muscovite	326	3.0
	CAS89.05.05	Cr-muscovite	338	4.2
	CAS89.05.06	Cr-muscovite	329	3.3
	CAS89.05.07	Cr-muscovite	333	3.4
Anna	CAS89.01.01	Cr-muscovite	848	4.3
	CAS89.01.02	Cr-muscovite	827	4.1
Cassiar Camp, northern British Columbina				2.0 ± 0.2
Pete	PETE3-2-1	Cr-muscovite	1616	1.9
	PETE3-2-2	Cr-muscovite	1666	1.8
	PETE3-2-3	Cr-muscovite	1660	1.8
	PETE3-1-1	Cr-muscovite	2325	2.2
	PETE3-1-2	Cr-muscovite	2664	1.7
	PETE3-1-3	Cr-muscovite	2542	2.1
	PETE3-1-4	Cr-muscovite	2566	2.2
	PETE3-3-2	Cr-muscovite	1635	1.9
	PETE3-3-3	Cr-muscovite	1692	1.7
Boomerang	BV-1	Muscovite	743	2.1
	BV-2	Muscovite	740	2.0
	BV-3	Muscovite	745	1.9
	BV-4	Muscovite	741	2.0
	BV-5	Muscovite	750	2.1
	BV-6	Muscovite	744	2.2

Table 6.2. (continued)

Location Vein system	Sample No.	Analyzed Mineral	N content (ppm)	$\delta^{15}N$ (‰) mean ± 1σ
Stuart Lake, central British Columbia				1.7 ± 0.1
Snowbird	CAS89.41.1-1	Cr-muscovite	3466	1.8
	CAS89.41.1-3	Cr-muscovite	3434	1.6
	CAS89.41.1-4	Cr-muscovite	3497	1.7
	CAS89.41.1-6	Cr-muscovite	3472	1.7
Bridge River Camp, southwestern British Columbia				2.9 ± 0.9
Bralorne mine	CAS91.61-1	Cr-muscovite	3336	2.0
	CAS91.61-2	Cr-muscovite	3303	2.0
	CAS91.61-3	Cr-muscovite	3345	2.1
	CAS91.61-5	Cr-muscovite	3368	2.0
	CAS91.61-6	Cr-muscovite	3341	2.3
	CAS91.61-7	Cr-muscovite	3368	2.5
	CAS91.62-1	Cr-muscovite	3255	2.4
	CAS91.62-3	Cr-muscovite	3310	2.2
	CAS91.62-4	Cr-muscovite	3276	2.2
	CAS91.62-6	Cr-muscovite	3331	2.4
	CAS91.64B	Cr-muscovite	2573	2.7
	CAS91.64C	Cr-muscovite	2593	2.8
	CAS91.64D	Cr-muscovite	2579	3.0
	CAS91.64-1	Cr-muscovite	2473	3.1
	CAS91.64-2	Cr-muscovite	2592	2.8
	CAS91.64-3	Cr-muscovite	2609	2.3
	CAS91.64-4	Cr-muscovite	2597	2.9
Pioneer	CAS91.66-1	Cr-muscovite	930	4.3
	CAS91.66-2	Cr-muscovite	963	4.6
	CAS91.66-3	Cr-muscovite	960	4.7
	CAS91.66-5	Cr-muscovite	977	4.7
	CAS91.66-6	Cr-muscovite	971	4.2
Greenwood, southen British Columbia				3.2 ± 0.6
Imperial	CAS91.40A1	Cr-muscovite	129	2.7
	CAS91.40A2	Cr-muscovite	131	3.0
	CAS91.40A3	Cr-muscovite	124	2.6
	CAS91.40A4	Cr-muscovite	131	2.8
	CAS91.40A5	Cr-muscovite	131	2.2
Riverside	RS-1	Cr-muscovite	148	3.8
	RS-2	Cr-muscovite	132	3.7
	RS-3	Cr-muscovite	132	3.5
	RS-4	Cr-muscovite	128	4.0
Mother Lode, southern California				2.7 ± 0.4
Carson Hill	CH21	Cr-muscovite	850	3.0
	CH22	Cr-muscovite	844	3.2
	CH23	Cr-muscovite	834	2.7
	CH24	Cr-muscovite	837	2.8
	CH25	Cr-muscovite	835	2.6
	CH26	Cr-muscovite	851	2.6
	CH27	Cr-muscovite	832	2.3
Coulterville	CT41	Cr-muscovite	740	3.4
	CT42	Cr-muscovite	733	3.5
	CT43	Cr-muscovite	734	2.8
	CT44	Cr-muscovite	733	2.3
	CT45	Cr-muscovite	738	2.0
	CT46	Cr-muscovite	729	2.0
	CT47	Cr-muscovite	748	2.8
	CT48	Cr-muscovite	750	2.5
	CT49	Cr-muscovite	745	2.3

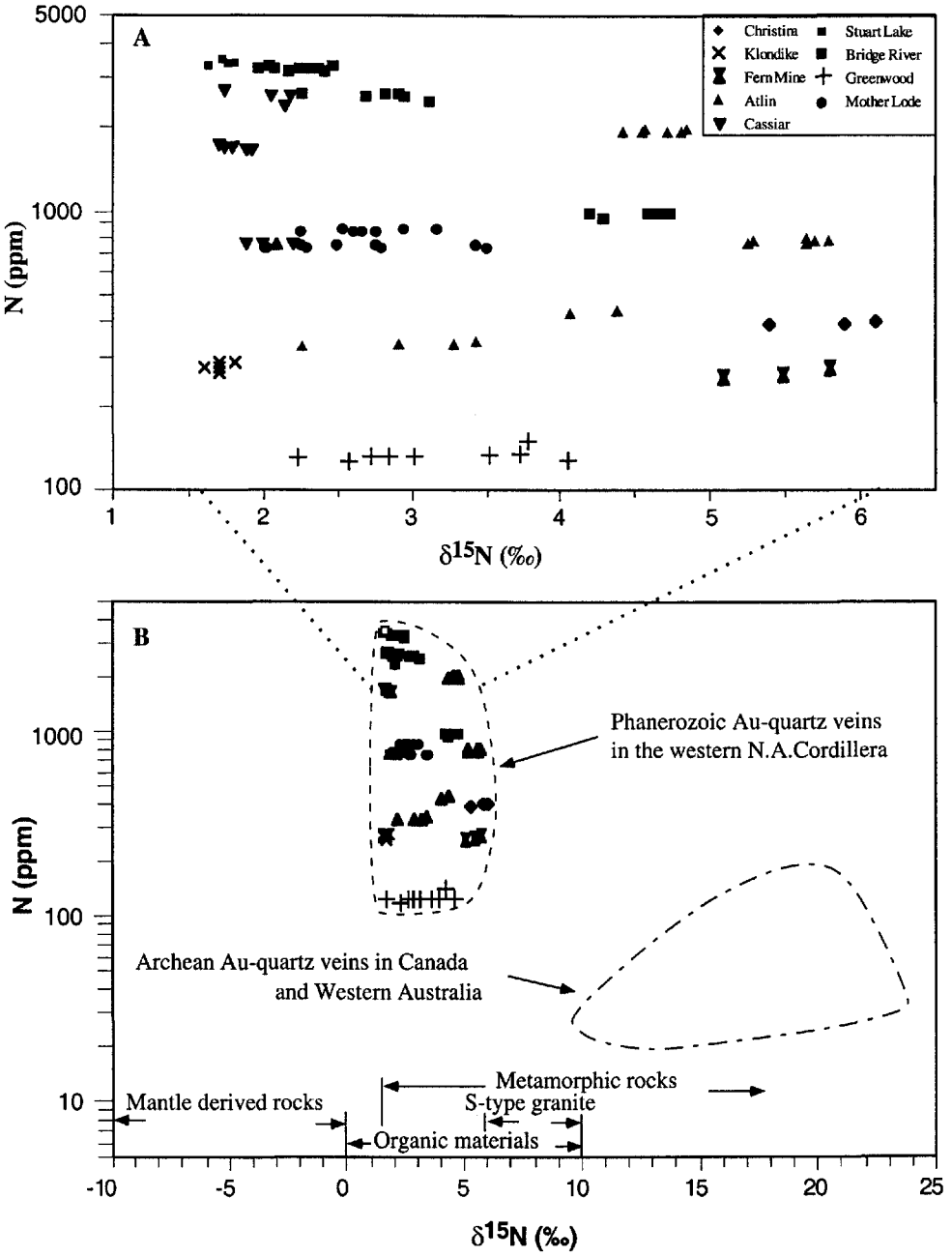

Fig. 6. 10. A. The N content and $\delta^{15}N$ values of hydrothermal muscovite separates from the western North American Cordillera quartz vein systems. B. Comparison to those of Archean volcanic-plutonic terrane-hosted counterparts in Canada and Western Australia (Jia and Kerrich, 1999, 2000). Fields for rock reservoirs: Organic meterials from Peters et al. (1978), Williams et al. (1995), and Ader et al. (1998); Metamorphic rocks from Heandel et al. (1986) and Bebout and Fogel (1992); granites from Boyd et al. (1993); Mantle derived rocks from Javoy et al. (1984), Javoy and Pineau (1991), Boyd et al. (1987, 1992), Marty (1995), Marty and Pineau (1991), Boyd and Pillinger (1994), and Cartigny et al. (1998).

from 390 to 401 ppm and 256 to 274 ppm, respectively. In the Sheba vein, Klondike district of the Yukon, six muscovite separates from quartz veins have a range of $\delta^{15}N$ values between 1.6 and 1.8‰, and N contents 260 and 280 ppm.

In the Cassiar mining camp of northern BC where samples from two vein systems (Pete vein with Cr-bearing mica and Boomerang vein with white mica) possess mean $\delta^{15}N$ values of 1.9 ± 0.2‰ (1σ; n = 9) to 2.1 ± 0.1‰ (1σ; n = 6), respectively, over about 16 km in distance. Similarly, in the Atlin mining district quartz vein systems at the Mckee Creek, Surprise, Goldstar, and Anna deposits have mean $\delta^{15}N$ values ranging from 3.3 to 5.7‰ (n = 22) over about 180 km^2. For the Bridge River, Greenwood, and Mother Lode district, the mean $\delta^{15}N$ values are 2.9 ± 0.9‰ (1σ; n = 22), 3.2 ± 0.6‰ (1σ; n = 9), and 2.7 ± 0.4‰ (1σ; n = 16), respectively. At the regional scale, from the Mother Lode in California to Fairbanks, Alaska, the total range of $\delta^{15}N$ is 1.6 to 6.1‰ with a mean of 3.0‰, and nitrogen contents span 130 to 3500 ppm with a mean of 1535 ppm (Table 6.2; Fig. 6.10).

6.4.2. Oxygen and hydrogen isotopic compositions of silicates

The total range of $\delta^{18}O$ values for vein quartz samples in this study is 14.6 to 22.2‰. There is also uniformity in the $\delta^{18}O$ values in given individual mining camps (Table 6.3). A narrow range of $\delta^{18}O$ values in the Carson and Coulterville camps from the Mother Lode is between 16.5 and 18.6‰. Similar intradistrict isotopic homogeneity of vein quartz is noted in the Bridge River, Cassiar and Atlin districts, where $\delta^{18}O$ values of vein quartz range from 17.8 to 18.1‰, 16.9 to 17.1‰, and 21.4 to 22.2‰ respectively. In the Sheba deposit, Klondike district $\delta^{18}O$ values are also uniform ranging from 14.6 to 15.1‰ (Table 6.3).

Table 6.3. Oxygen and hydrogen isotope data from gold-bearing quartz veins. * represents duplicates.

Vein location	Sample no.	$\delta^{18}O$ (‰) Quartz	δD (‰) Muscovite
Klondike	SH-1	15.1	-161
	SH-2	14.9	-168
	SH-3	14.6	-172
Atlin	CAS89.14.2.3	21.7	-110
	CAS89.05	21.4	-66
	CAS89.01	22.2	-112
Cassiar	BV-1	17.1	-95
	BV-4	16.9	-98
Bridge River	CAS91.66	17.8	-60
	CAS91.66*	18.1	
Mother Lode	CH1	18.6	
	CH2	16.5	-65
	CH2*	16.9	-62
	CT4	17.6	-65

The majority of muscovites are in a range of δD values from –60 to –110‰ (Table 6.3). Two samples, collected from the Carson and Coulterville areas in the southern Mother Lode (Lat. 37° N), both yield δD values of –65‰ (Table 6.3). The Bridge River camp in southern British Columbia (Lat. 50° N) possesses a δD value of –60‰. Samples from the Boomerang vein in the Cassiar camp of northern British Columbia (Lat. 59° N) yield δD values of –95‰. In the Atlin district, three samples from different vein locations spread over 180 km^2 yield δD values ranging from –66 to –112‰. Three samples from Sheba in the Klondike area (Lat. 63° N) are outliers, with δD values ranging from -161 to –172‰.

6.4.3 Se/S systematics in hydrothermal pyrite

Measured Se and S contents and calculated Se/S ratios for individual hydrothermal pyrite minerals in these orogenic gold deposits are listed in Table 6.4 and plotted in Figure 6.11. Analytical methods are reported in Appendix I. Selenium values overlap, within narrow ranges of 10.3 to 15.2 ppm in the Mother Lode, 10.8 for the Bridge River, and 12.5 to 17.7 in the Greenwood district, corresponding Se/S $\times 10^6$ ratios being 20 to 30, 21, and 25 to 34 respectively (Table 6.4).

6.5. Discussion

6.5.1. N and N-isotope characteristics

The N and N-isotope results for hydrothermal micas from the gold-bearing vein systems of the western North American Cordillera are not consistent with either mantle-derived fluids, or magmatic hydrothermal fluids evolved from crystallizing granitoids. Mantle nitrogen concentrations and isotope composition have previously been determined from oceanic basalts and diamonds (Table 3.9, Chapter 3; Javoy et al., 1984; Javoy and Pineau, 1991; Boyd et al., 1987, 1992; Marty, 1995; Marty and Humbert, 1997). Their results show that nitrogen contents are very low (<1-2 ppm), and that δ^{15}N-values are negative (-8.7 up to –1.7‰) with a mean of –6 to –5‰ (Chapter 2).

The characteristics of the hydrothermal micas are distinct from mantle volatiles both in terms of more enriched δ^{15}N values and high N contents (Table 6.2 and Fig. 6.10). A mantle source for Archean orogenic gold deposits can also be ruled out on the basis of radiogenic Sr and Pb isotope compositions (McCuaig and Kerrich, 1998).

Boyd et al. (1993) studied granites in southwestern England that had δ^{15}N values between 8.4 and 10.2‰ (two outliers of 5.1 and 7.0‰). Granitic rocks, worldwide, have

Table 6.4. S and Se contents in hydrothermal pyrites from Cordilleran Au deposits and counterparts in the Superior Province of Canada, and Norseman, West Australia, and in Ni-Cu sulfide ores from Sudbury, Ontario and Boliden, Sweden.

District	Sample no.	Se (ppm)	S (%)	Se/S × 10^6
Orogenic lode gold deposits				
Greenwood, southern British Columbia				
City of Pairs	CP	12.5	50.68	25
Golden Drop	GD	17.2	51.51	33
Golden Drop	GD#	17.7	51.51	34
Bridge River, southwestern British Columbia				
Bralorne	91.64	10.8	51.03	21
Mother Lode, southern California				
Carson Hill	CH2	10.3	51.02	20
Carson Hill	CH2#	12.8	51.00	25
Coulterville	CT4	15.2	51.11	30
Superior Province of Canada				
Hollinger	HG-1	6.6	51.81	13
Hollinger	HG-3	4.7	51.23	9
Macassa	MA-I	3.4	50.31	7
Macassa	MA-II	1.7	51.35	3
Mayflower	MF-I	3.7	50.65	7
Mayflower	MF-2	5.3	51.04	10
Williams	WL	3.6	51.63	7
Williams	WL#	2.4	51.63	5
David Bell	DB	8.3	51.72	16
Macleod	MAC	0.9	51.80	2
Dudee-Parkhill	DP	6.2	51.57	12
Sigma	S	2.6	51.05	5
Goldhawk	GK	6.6	51.31	13
Dome	D	6.6	51.54	13
Norseman, Western Australia				
Norseman	NR10	6.8	51.24	13
	NR9/220	10.1	51.75	20
	02-1	8.6	49.61	17
	02-3	6.9	51.00	14
Ni-Cu sulfide ores				
Sudbury, Ontario		72, 77, 75	29.38	245, 262, 255
Boliden, Sweden		92, 93, 96	34.05	270, 273, 282
Mantle-derived materials				
Mantle-derived rocks[1]				230 to 350
Mid-ocean ridge basalt[2]				250 to 333

represents duplicates

[1] Eckstrand and Hulbert (1987); [2] Morgan (1986) and McDonough and Sun (1995)

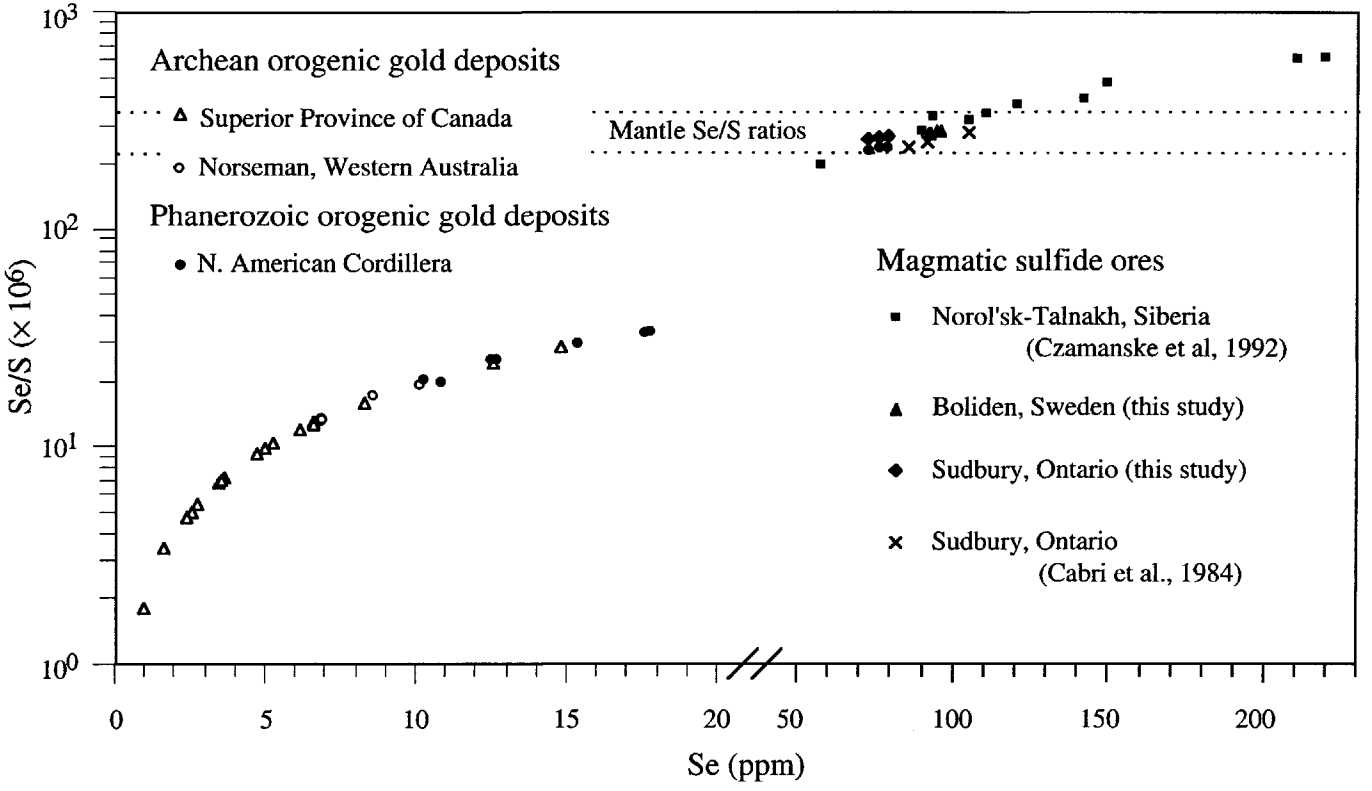

Fig. 6.11. Se/S ($\times 10^6$) ratios of pyrites from orogenic lode gold deposits compared to those of tsulfides in mantle-derived magmas. Sources: Se/S ($\times 10^6$) ratios from magmatic sulfide ore deposits of Noril'sk-Talnakh of Siberia, R ussia; Boliden of Sweden; and Sudbury in Ontario of Canada are close to chondritic values (approximately 200 to 600, with most between 230 and 350; Eckstrand and Hulbert, 1987; McDonough and Sun, 1995).

low nitrogen contents of 21 to 27 ppm (Chapter 2; Wlotzka, 1972; Hall, 1999). Collectively, nitrogen isotope compositions of hydrothermal muscovites from the North American Cordillera are depleted relative to granitic rocks, and their N contents are high.

The meteoric water model is difficult to rule out based on the N-isotopic composition of the hydrothermal micas of these gold-bearing quartz vein systems, given global nitrogen isotopic values of meteoric water of 4.4 ± 2.0‰ (n = 263; Owens, 1987), which overlaps with these gold deposits. However, N-contents of meteoric water are very low < 2 μmole (Homes et al., 1998), whereas N_2 has been observed and measured in fluid inclusions from orogenic gold deposits (Table 3.10 of Chapter 3; Casquet, 1986; Bottrell et al., 1988; Ortega et al., 1991). Furthermore, vein geometry requires hydraulic fracturing under conditions:

$$P_{fluid} > P_{lithostatic} + T \qquad 6.1$$

and metamorphic fluids are generated under conditions:

$$P_{fluid} \geq P_{lithostatic} \qquad 6.2$$

Where T is the tensile strength (Fyfe et al., 1978; Jia et al, 2000).

Accordingly, deeply convecting meteoric water at hydrostatic pressure can be ruled out. Other geological and geochemical evidence such as the δD characteristics of primary fluid inclusions and other isotope systems (O, Sr, and Pb) of these quartz vein systems are also inconsistent with the meteoric water model (McCuaig and Kerrich, 1998).

Nitrogen contents and $\delta^{15}N$ values of gold deposits in the western North American Cordillera are consistent with those reported for metasedimentary rocks in the Catalina

Schist subduction zone complex of California, where nitrogen contents are 60 to 2100 ppm and $\delta^{15}N$ values range from 1.6 to 6.0‰ (n = 123; Bebout and Fogel, 1992; Bebout, 1997), concordant with average Phanerozoic crust (Haendle et al., 1986; Williams et al., 1995; Kao and Liu, 2000). They are also comparable to data for the turbidite-hosted Paleozoic quartz-carbonate vein systems of the Bendigo-Ballarat region in the Tasman orogen of southeastern Australia, where N = 652-895 ppm and $\delta^{15}N$ is +2.8 to +4.5‰ (Chapter 5; Jia et al., 2001).

Archean and Phanerozoic orogenic gold vein systems have similar characteristics and typically are hypothesized to be products of the same type of hydrodynamic regime (e.g Kerrich and Wyman, 1990; Groves et al., 1998). However, the results from the western North American Cordillera veins are distinct from their Late Archean counterparts in Canada and Western Australia, which are characterized by relatively low N concentrations of 20 to 200 ppm but higher $\delta^{15}N$ values of 10 to 24‰ (Table 4.3 in Chapter 4; Jia and Kerrich, 1999, 2000).

There are two interpretations of these differences between Archean and Phanerozoic orogenic gold deposits. One is that Archean subduction complexes were volcanic-plutonic dominated terranes containing limited volumes of sedimentary rocks and associated organic material (Jia et al., 2001). In this model the Archean hydrothermal micas plot in the lower right hand sector of the progressive metamorphism trend of Haendel et al. (1986) from low $\delta^{15}N$ but high N content in low grade metamorphic rocks to low N content but elevated $\delta^{15}N$ in high grade rocks (Fig. 5.6 of Chapter 5; Jia et al., 2001). Phanerozoic subduction-accretion complexes, in

contrast, are characterized by siliciclastic turbidite-plutonic terranes. In these terranes lithologies would be dominated by high N, low $\delta^{15}N$ metasedimentary rocks.

Alternatively, it is proposed here based on the new N data for Archean and Phanerozoic sedimentary rocks that there are secular variations of crustal N contents and $\delta^{15}N$ values through geological time. These variations result from progressive sequestering of atmospheric N and its cycling in the atmosphere-crust-mantle systems, where Archean crust had a high median $\delta^{15}N$ value of +16‰ and 30 ppm N (total N mass of 0.6 $\times 10^{18}$ kg), whereas the Phanerozoic is characterized by low $\delta^{15}N$ values with a median of +3‰ and about 100 ppm N (total N mass of 2.1 $\times$ 10^{18} kg) (Jia and Kerrich, 2001). In this interpretation the trend from ^{15}N enriched Archean to ^{15}N depleted Phanerozoic hydrothermal micas reflects the ore fluids sampling the bulk crustal reservoir.

Haendel et al. (1986) showed that N contents of metamorphic rocks decrease, while $\delta^{15}N$ values trend to increase, with increasing metamorphic grade. The composite trend, however, involves different metamorphic lithologies and ages; high N contents and low $\delta^{15}N$ values were from Phanerozoic phyllites, whereas low N contents and higher $\delta^{15}N$ were from Precambrian gneiss. There are a number of studies on the N-isotopic fractionations during metamorphism by both direct measurements and experiments, which clearly indicate that N content decreases from low to high grade metamorphism, but N-isotopic composition does not change significantly with metamorphic grade (up to 600°C; Wada et al., 1975; Delwiche and Steyn, 1970; Heaton, 1986; Williams et al., 1995; Ader et al., 1998). Studies by Jia and Kerrich (2000) on hydrothermal micas in Archean orogenic gold deposits also show that N contents would decrease, but its

isotopic composition does not change significantly with increasing temperature of formation (Figs. 4.3 and 4.4 in Chapter 4). Accordingly, the 'metamorphic trend' of Haendel et al. (1986) [Chapter 2] can be reinterpreted in terms of secular evolution of crustal N and $\delta^{15}N$.

6.5.2. Origin of the ore-forming fluid

The $\delta^{18}O$ and δD values of ore fluids in equilibrium with vein quartz and muscovite were calculated using mineral-water fractionation equations of Matsuhisa et al. (1979) and Suzuoki and Epstein (1976), assuming vein formation at 300°C. Fluid inclusion studies show that vein-forming fluids from the Mother Lode goldfield, California; the Bralorne mine, Snowbird, and Cassiar in British Columbia; and the Klondike district, Yukon Territory, generally have low salinity (1 to 6 wt% NaCl equiv), with varying mole fractions of CO_2 ranging from 5 to 15 percent. These veins formed at temperatures between 220° and 400°C, under pressures of 70 to 300 MPa, with emplacement depths estimated from about 3 to 12 km (Böhlke and Kistler, 1986; Weir and Kerrick, 1987; Madu et al., 1990; Leitch et al., 1991; Nelson et al., 1993; Rushton et al., 1993; Goldfarb et al., 1989, 1991b, 1997).

The calculated $\delta^{18}O_{H20}$ and δD_{H20} for the Carson and Coulterville mines in the southern Mother Lode are between 9 to 12‰ and –20 to –15‰ respectively, which fall within the ranges of $\delta^{18}O_{H20}$ = 8 to 14‰ and δD_{H20} = –50 to –10‰ reported in other studies (Table 6.5; Kistler and Silberman, 1983; Böhlke and Kistler, 1986). In the Bridge River district, British Columbia's largest gold camp, isotopic composition of ore fluids is estimated to be about 11 to 12‰ $\delta^{18}O$, and –15‰ δD. These results are consistent with those of Maheux (1989) who show that the calculated $\delta^{18}O$ and δD

Tabe 6.5. Oxygen and hydrogen isotope compositions of quartz-carbonate veins in the western North American Cordillera, and counterparts worldwide.

Gold Province		$\delta^{18}O_{quartz}$ (‰)[a]			$\delta^{18}O_{ore\ fluid}$ (‰)[b]	$\delta D_{ore\ fluid}$ (‰)[b]	References
District	Vein location	range	mean ± 1σ	T (°C)	range	range	
Cordillera							
Juneau gold belt	Juneau	15.2 to 20.8		225 ~ 375	7 to 13	-35 to -15	2
Klondike, Yukon Territory	Sheba	14.6 to 15.1	14.9 ± 0.25 (3)		7 to 8	-130 to -120	1
		14.7 to 15.1	15.0 ± 0.2 (4)	323 ± 18	8.9 ± 0.6		3
Atlin, northernmost BC	Superise, Goldstar, and Anna	21.4 to 22.2	21.7 ± 0.4 (3)		13 to 16	-65 to -20	1
Cassiar, northern BC	Boomerang	16.9 to 17.1			10 to 11	-55 to -50	1
	Vollaug and others	14.3 to 19.2	16.9 ± 1.3 (18)	250 ~ 300			4
Stuart Lake, central BC	Snowbird	21.0 to 24.2	22.7 ± 1.2 (8)	210 ~ 260	12 to 15		5
Bridge River, southern BC	Pioneer	17.8 to 18.1			11 to 12	-15	1
	Bralorne and Pineer	17.1 to 19.4	18.4 ± 0.8 (22)	230 ~ 350	10 to 13	-38 ± 18	6, 7
Mother Lode, California	Carson and Coultervile	16.5 to 18.6	17.6 ± 0.8 (5)		9 to 12	-20 to -15	1
	Oro Rico and McAlpine	15.0 to 17.5	17.1 ± 0.3 (24)	300	6 to 11		8
Alleghany, California	Oriental	17.3 to 19.4		250 ~ 325	8 to 15	-50 to -10	9
Tasman Orogenic Belt							
Bendigo, Australia	Central and North Deborah	14.4 to 17.2	16.3 ± 0.7 (20)	350 ± 25	8 to 11	-37 to -17	10
Hill End gold field, Australia	Hill End gold field	15.2 to 17.1	16.3 ± 0.5 (20)	420	8 to 12	-49 to -36	11
Birimian Greenstone Belt							
Ashanti, West Africa	Ashanti gold belt	12.8 to 15.6	14.9 ± 0.7 (14)	400 ± 50	9 to 12	-53 to -37	12
Superior Province of Canada							
Abitibi Belt	Hollinger-McIntype, Dome	12.5 to 15.0		220 ~ 450	6 to 11	-80 to -20	13
Yilgarn craton, W. Australia							
Norseman-Wiluna Belt	Kalgoorlie and Norseman	114.3 to 13.4		220 ~ 500	5 to 9	-40 to -10	14

Note: a, data are reported as mean one standard deviation, followed by number of determinations in brackets; b, the $\delta^{18}O$ values for vein-forming fluid were calculated from quartz-water equilibrium eqations of Matsuhisa et al. (1979), and from muscovite-water fractionation factors of Suzuoki and Epstein (1976) using fluid incluision homogenization temperature T = 300°C.

References: 1 = this study; 2 = Goldfarb et al. (1991b); 3 = Rushton et al. (1993); 4 = Nesbitt et al. (1989); 5 = Madu et al. (1990); 6 = Leitch et al. (1991); 7 = Maheux (1989); 8 = Weir and Kerrick (1987); 9 = Bohlke and Kistler (1986); 10 = Jia et al. (2001); 11 = Lu et al. (1996); 12 = Oberthur et al. (1996); 13 = Kerrich (1987); 14 = Golding et al. (1989).

values of hydrothermal fluids in equilibrium with quartz and sericites from many of the deposits in the Bridge River district were 10 to 13‰ and –38 ± 18‰, respectively (Table 6.5). The estimated $\delta^{18}O$ and δD values of ore fluids are 10 to 11‰ and -55 ± 5‰ in the Cassiar, and 13 to 16‰ and –65 to –20‰ in the Atlin districts. Muscovite separates from the Sheba vein in the Klondike district have δD values of –170 to –160‰ and thus probably formed from a fluid of about –120 to –130‰, a composition depleted relative to those of the other studied vein micas.

The narrow range of 15 to 22‰ for vein quartz in different mining districts, spanning over 26° latitude in the western North American Cordillera, is typical for vein quartz from orogenic lode gold deposits of all ages from Archean to Cenozoic ($\delta^{18}O$ = 12 to 18‰; Böhlke and Kistler, 1986; Curti, 1987; Kerrich, 1987; Golding et al., 1989; Goldfarb et al., 1991b; de Ronde et al., 1992; Oberthür et al., 1996). This distinct uniformity of $\delta^{18}O$ values of quartz for individual orogenic gold deposits has been interpreted as a corresponding isotopic homogeneity of the hydrothermal ore fluids, and uniform ambient temperatures of ore formation. In contrast, epithermal gold deposits are characterized by a range of $\delta^{18}O$ quartz values that result from variable temperatures and water/rock ratios (Taylor, 1997).

Collectively, the isotopic composition of the ore forming fluid for the Mother Lode, Bridge River, Cassiar and Atlin gold districts cluster between 8 and 14‰ $\delta^{18}O$ and –65 and –10‰ δD, with vein precipitation at 300°C. The calculated ranges of $\delta^{18}O$ and δD are consistent with estimates for other gold-bearing vein systems elsewhere within the western North American Cordillera; they are consistent with metamorphic fluids. Some overlap the magmatic field but others extend to higher $\delta^{18}O$ (Table 6.5 and

Fig. 6.12). These results are also similar to $\delta^{18}O_{H2O}$ values of 8 to 12‰ for other metasedimentary rocks hosted gold deposits worldwide (Table 6.5; Lu et al., 1996; Oberthür et al., 1996; Jia et al., 2001). This range overlaps with, but tends to higher overall fluid $\delta^{18}O$ values of 6 to 11‰ obtained for Neoarchean orogenic gold deposits (Table 6.5; Kerrich, 1987; Golding et al., 1989; de Ronde et al., 1992; McCuaig and Kerrich, 1998). Together, the calculated $\delta^{18}O$ and δD values are not consistent with magmatic hydrothermal fluids.

In addition to the isotopic arguments, geochronologic constraints appear to rule out a direct magmatic source for the mineralizing fluids. In the Cassiar mining camp there is no defined magmatic episode coeval with vein mineralization, nor a spatial association between felsic intrusions and gold quartz veins in any of the mined vein systems. The age of gold veining was 130 Ma by conventional K-Ar methods (Panteleyev, 1985), and a number of recent Ar-Ar isotopic age determinations on hydrothermal sericites throughout the camp yield similar results (134 Ma; Ash, 2001). However, the Cassiar batholith has been considered to be a single intrusive mass about 100 Ma in age, based mainly on radiometric dating done by the Geological Survey of Canada and Driver et al. (2000).

In the Klondike district, although volcanic activity and plutonism were widespread across the Yukon-Tanana terrane between the Jurassic and the Tertiary, there was a period of quiescence across most of the Cordillera between 150 to 125 Ma (Armstrong, 1988). K-Ar dates reported for hydrothermal muscovites from the Sheba vein (ca. 140-135 Ma; Rushton et al., 1993) fall within this magmatic gap and thus appear to preclude a magmatic fluid source. Some gold quartz vein camps are spatially or temporally

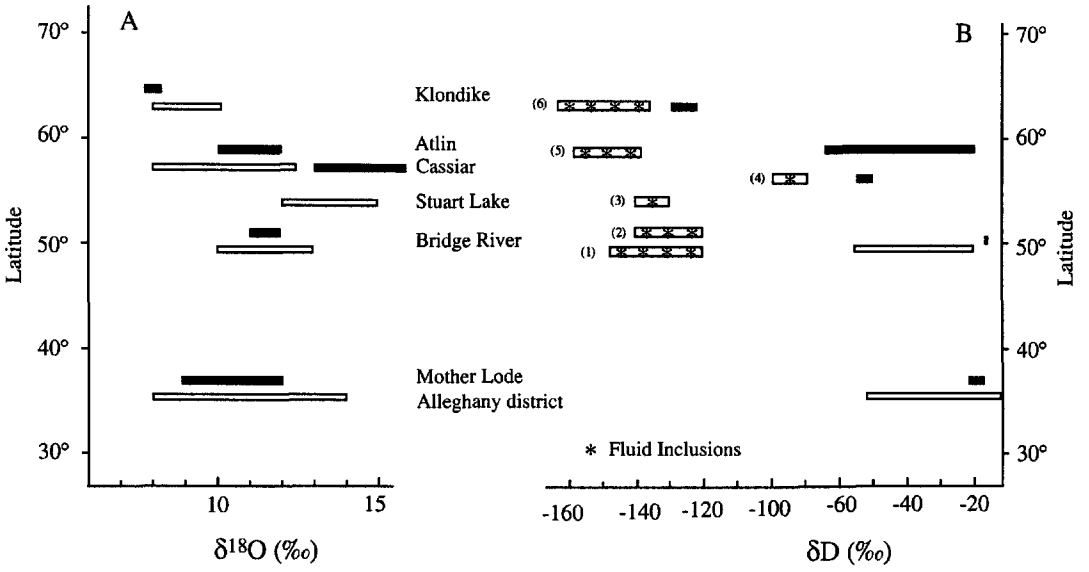

Fig. 6.12. Ranges of calculated $\delta^{18}O$ (A) and δD (B) values of ore fluids plotted with latitude (data source from Table 6). Note: closed bars represent this study, open bars represent previous studies from Böhlke and Kistler (1986), Maheux (1989), Nesbitt et al. (1989), Madu et al. (1990), Goldfarb et al. (1991), Leitch et al. (1991), and Rushton et al. (1993). All data from silicates, excepting ⊠ bulk decrepitation of fluid inclusions with star symbols: (1) Fairview and Oro Fino (Zhang et al., 1989), (2) Ridge River (Nesbitt et al., 1989), (3) Staurt Lake (Madu et al., 1990), (4) Juneau (Goldfarb et al., 1991), (5) Cassiar (Nesbitt et al., 1989), (6) Klondike (Rushton et al., 1993).

associated with intrusions, but here their association is interpreted to reflect only rheological control of igneous bodies on structural development.

Nesbitt et al. (1986, 1989) proposed a model of deep circulation of meteoric water along transcurrent faults under conditions of low water/rock ratios for Cordilleran lode gold deposits. This model is based primarily on the observations that δD_{H2O} values obtained by decrepitating bulk fluid inclusions from some vein quartz were depleted (< -100‰) and apparently latitudinally dependent. However, the calculated δD_{H2O} values of ore fluids based on robust silicates from the Mother Lode, southern California, to the Atlin and Cassiar camps in northern British Columbia are neither depleted (-65 to –10‰), nor show any latitudinal control, but rather are consistent with metamorphic fluid sources (Table 6.5; Fig 6.12). It is likely that low δD values from bulk extraction of fluid inclusions in some deposits (Nesbitt et al., 1986, 1989) reflect dominantly secondary inclusions formed in the presence of meteoric water during uplift of the deposits (Goldfarb et al., 1991; McCuaig and Kerrich, 1998).

Furthermore, given paleometeoric water with δD –140‰ in northern British Columbia, $\delta^{18}O$ would have been –19‰. Consequently, $\delta^{18}O$ in the meteoric ore fluid would shift by more than 27‰ from –19‰ to observed values of +8‰ by fluid-rock interaction at low water/rock ratios (< 0.1) at 300°C within sedimentary-dominant sequences of the Cordilleran gold districts. Given these conditions, much of the descending water will rehydrate metamorphic minerals within the uplifting and cooling metamorphic terrane. The only way to avoid such a scenario is to assume that meteoric fluids were strongly channelled during downward flow, then pervasively interacted with rock with shifting isotope compositions, and finally were channelled back into narrow

structural conduits during upward flow. It is difficult, however, to imagine conditions which could consistently lead to such a mechanism of fluid flow (Goldfarb et al., 1993).

More significantly, it seems unlikely that all orogenic gold vein-forming fluids in the Cordillera, as well as those from elsewhere in the world could be shifted from variably ^{18}O-depleted meteoric water values depending on latitude to all having a $\delta^{18}O$ of +8 to 10‰ (Kerrich, 1989). If the ore fluids are not derived from deep crustal metamorphic processes, we expect at least some variation in $\delta^{18}O$ trending toward original, depleted isotopic values as seen in epithermal gold deposits (Field and Fifarek, 1985; Taylor, 1997). Yet, this is not observed.

An additional complexity for the meteoric water model is the actual latitude at the time the deposits formed, given the allochthonous character of the host terranes. These Cordilleran gold provinces from the Mother Lode in southern California, through deposits in the Canadian Cordillera, to Juneau Alaska are of Jurassic to Cenozoic ages (147 Ma-53Ma). From paleomagnetic and geologic data these allochthonous terranes have translated along the western margin of North America before or after the deposits formed. The studies show that at 100 to 90 Ma, the Interior domain comprising much of interior British Columbia, central Yukon, and eastern and central Alaska was situated at the latitude of northern California. The Coast domain including southeastern Alaska, much of the Coast Ranges and islands of British Columbia, and the Coast Cascade Mountains of Washington was situated at a latitude similar to northern Mexico. Subsequently, both domains moved northward about 3000 km, reaching their present locations before 45 Ma (Fig. 2.3. Chapter 2; Irving et al., 1995, 1996; Wynne et al., 1995; Ward et al., 1997).

An additional premise of the meteoric water model is that there exists a genetic relationship between orogenic lode Au deposits and Sb and Hg deposits in the Canadian Cordillera; for example, mercury (Hg) mineralization at the Pinchi Lake mine being a shallower level expression of deeper gold mineralization at the Snowbird mine (Nesbitt et al., 1989). However, the distance between the two mines is more than 25 km, and the age of veining at the Snowbird gold prospect is well constrained as mid-Jurassic (160 to 163 Ma; Ash, 2001). This predates the age of mercury mineralization at the Pinchi Lake mine, which is at the earliest, post-Cretaceous, as this mineralizing event overprints sedimentary rocks of that age (Patterson, 1977). According to Ash (2001) the Hg mineralization is possibly Eocene. This age and spatial relationships suggest that mercury mineralization along the Pinchi Fault is unrelated to the much older gold vein mineralization at Snowbird.

Anomalous δD values of -160 to –170‰ for muscovite from the Sheba vein in the Klondike district is depleted compared to those from other vein systems in the western North American Cordillera. However, as pointed out by Taylor et al. (1991), hydrothermal micas associated with gold veins in British Columbia and the Yukon Territory are characterized by both isotopically depleted and enriched values. Optical study on these depleted micas clearly shows recrystallization. Accordingly, depleted δD values in the Sheba vein are best interpreted as reflecting isotopic exchange during regional uplift between originally δD-enriched micas and meteoric water.

6.5.3. Se/S systematics: crust versus mantle source discrimination

On the basis of the Se and Se/S results for hydrothermal pyrite from these orogenic vein gold deposits, it is concluded that Se in pyrite is unlikely to have been derived from

mantle-derived fluids given very distinct Se content and Se/S ratio between the deposits and mantle pyrite. Mantle-derived Se/S ratios have previously been determined from mid-ocean ridge basalts (MORBs) (Hertogen et al., 1980; Hamlyn et al., 1985; Morgan, 1986), from olivine gabbro, troctolite (Eckstrand and Humbert, 1987), and from sulfide ore deposits of Noril'sk-Talnakh of Siberia, Russia, Boliden in Sweden, and Sudbury, Ontario (Table 6.5 and Fig. 6.11; Eckstrand and Humbert, 1987; Cabri et al., 1984; Paktune et al., 1990; Czamanske et al., 1992). Ratios of Se/S $\times$ 10^6 are close to chondritic values, approximately 200 to 600, with most between 230 and 350.

Six of Ni-Cu sulfide ore minerals from the Sudbury and the Boliden deposits were analyzed together with the pyrites to evaluate the new Hexapole ICP-MS method. These magmatic sulfides in mantle-derived rocks are characterized by systematically higher Se contents ranging from 72 to 77 ppm and 92 to 96 ppm, respectively. The ratios of Se/S $\times$ 10^6 range from 245 to 262 and 270 to 282, respectively. The results are consistent with other studies of Se contents in pentlandite, chalcopyrite, and pyrrhotite from the Sudbury deposit, which have mean Se contents of 85, 102, and 92 ppm, and mean values of Se/S $\times$ 10^6 of 233, 253, and 292, respectively (Fig. 6.11; Cabri et al. (1984).

Selenium contents and Se/S ratios from orogenic gold deposits are much lower, between 10.3 and 17.7 ppm Se, and 20 and 34 for Se/S ratios respectively (Table 6.4). The results are consistent with Se derived dominantly from crustal rocks. Selenium contents and calculated Se/S rations of hydrothermal pyrite in the western North American Cordillera are consistent with counterparts in the Superior Province of Canada, and Norseman, Western Australia, having 0.9 to 10.1 ppm Se, corresponding to Se/S $\times$ 10^6 ratios of 3 to 20 (Table 6.4). These new results are also consistent with

previous reconnaissance studies. For examples, the Archean-hosted mesothermal lode gold deposits are notable for having lower Se contents (median of 320 ppb) and lower Se/S $\times 10^6$ ratios (median value of 28.7; Bornhorst and Nurmi, 1997). At the Canadian Arrow mine, Ontario, where Au mineralization is hosted in part by a tronjemitic stock and lamprophyre dykes (McNeill and Kerrich, 1986), Se/S $\times 10^6$ ratios are much lower, between 10 and 20. Se contents are 1 to 5 ppm in pyrites from Kalgoorlie, corresponding to Se/S $\times 10^6$ ratios of 2 to 10 (King and Kerrich, 1987).

Coexisting sulfides may influence Se/S ratios of pyrite. Yamamoto et al. (1984) suggest that there is no systematic difference in Se/S ratios among coexisting sulfide minerals based on studies on fractionation of Se among pyrite, pyrrohotite, and chalcopyrite from the Besshi deposits, Japan. Therefore, Se/S ratios in pyrite are compatible to other sulfide minerals. The Se/S results of hydrothermal pyrites in orogenic gold deposits are also consistent with the results of sulfur isotopic studies where $\delta^{34}S$ of hydrothermal pyrite is typically from –1 to 8‰, (for a review see McCuaig and Kerrich, 1998) and indicative of sulfur being derived from variable proportions of crustal metaigneous and metasedimentary rocks.

Huston et al. (1995) suggest that, based on the conditions of pyrite deposition and thermodynamic data for FeS_2, $FeSe_2$, and aqueous S and Se species in volcanogenic hydrothermal fluid systems, variations in Se contents of pyrite could be caused by fractionation of Se with temperature, changes in redox conditions, or mixing of hydrothermal fluids with seawater. However, the relationships between Se contents in pyrite and temperature are still controversial, and the effect of redox on Se content is only significant under oxidized ($\sum SO_4 > \sum H_2S$) conditions. Huston et al. (1995) indicate

that Se levels in pyrite decrease with increasing temperature under constant m_{H2Se}/m_{H2S} ratio of 10^{-4} and temperatures between 50° and 300°C, whereas Tischendorf and Ungethum (1964) concluded the opposite. Temperatures for orogenic gold deposits are higher, between 200° and 500°C, and Se contents in pyrite are not sensitive to redox because most ore-forming fluids are reduced, below the H_2S/SO_4 redox boundary. Previous geochemical studies on orogenic gold deposits have ruled out a seawater fluid source (Roberts, 1987; Böhlke and Irwin, 1992).

In Se versus Se/S coordinates, the population of data plots on a mixing trend from crustal to near mantle sources (Fig. 6.11). The Cordilleran subduction-accretion terranes are dominated by arc related volcanic and plutonic rocks, siliciclastic sedimentary rocks, and locally basalt sequences representing tectonic slice of ocean plateau. Archean volcanic-plutonic greenstone belts have two principal volcanic associations: komatiite-basalt sequences representing fragments of intraoceanic plateaus derived from mantle plumes, and bimodal arc-basalt-dacite sequences paired with trench turbidites, collectively intruded by subduction-related tonalite batholiths. For both the Archean and Phanerozoic subduction-accretion terranes, the anhydrous ocean plateau sequences would likely have mantle Se/S ratios, whereas arc-related volcanic-plutonic units, and sedimentary rocks would have crustal or intermediate values. Consequently, the crust-mantle mixing trend can be interpreted in terms of S and Se contributions from mantle derived and crustal lithologies in the crust, rather than between mantle and crustal fluids, consistent with nitrogen data where N contents and $\delta^{15}N$ both rule out any significant mantle nitrogen.

6.6. **Conclusions**

Detailed studies of the stable isotope systematics (H, N, and O) and Se/S ratios of hydrothermal quartz vein systems from different mining districts in the western North American Cordillera, spanning more than 30° latitude, lead to the following interpretations:

(1) Nitrogen contents and $\delta^{15}N$ values of hydrothermal micas are between 130 and 3500 ppm and 1.7 and 5.5‰ which rule out a mantle hypothesis (low N contents of 1 to 2 ppm and $\delta^{15}N$ = -5‰), or granitic fluids (N contents of 21 to 27 ppm and $\delta^{15}N$ = 6 to 10‰), but is consistent with fluids derived from metamorphic dehydration reactions of the Phanerozoic subduction- accretion complexes, with $\delta^{15}N$ values of 1 to 6‰.

(2) Vein quartz $\delta^{18}O$ values are between 14.6 and 22.2‰, but for individual vein systems are strikingly uniform, varying less than ±1‰ from average values. They imply uniform ambient temperatures of precipitation for the ore deposits.

(3) The $\delta^{18}O$ values of gold-bearing vein-forming fluid are calculated between 8 and 16‰ (assuming 300°C) and δD –10 to –65‰, indicative of a deep crustal source for the ore-forming fluids, most likely of metamorphic origin.

(4) The δD values of ore fluids do not show any latitudinal control, which strongly discounts the meteoric water model for the Cordillera orogenic lode gold deposits. The low δD range of –120 to –130‰ for the Sheba vein in Klondike district reflects post-crystallization reequilibration between the mica and circulating meteoric waters.

(5) Hydrothermal pyrites have Se abundances from 0.9 to 15.2 ppm (n = 28), corresponding to Se/S $\times 10^6$ ratios of 2 to 34, which also are distinct from mantle-derived rocks all clustering in the range of 230 to 350, but are consistent with ore-forming fluids derived from metamorphic dehydration of the crustal rocks.

Collectively, the stable isotope data, in combination with Se/S systematics of hydrothermal pyrite provide a basis for constraining potential source reservoirs for the vein-forming fluids in the western North American Cordillera. These are considered to be consistent with a metamorphic origin, involving derivation of the vein-forming fluids from mid-crustal levels by metamorphic dehydration reactions at the greenschist to amphibolite transition (cf. Kerrich and Fryer, 1979; Powell et al., 1991). A dilute, aqueous carbonic and N-bearing composition (C-O-H-N) is common to metamorphic fluids (Casquet, 1986; Bottrell et al., 1988; Ortega et al., 1991).

Chapter Seven

SECULAR VARIATION OF CRUSTAL N CONTENTS AND $\delta^{15}N$ IN THE TERRESTRIAL RESERVOIRS

7.1 Introduction

The origin and evolution of N in Earth's major reservoirs of atmosphere, crust, and mantle is controversial (Brown, 1952; Sano and Pillinger, 1990). According to some authors, the mantle acquired a $\delta^{15}N$ of –25‰ corresponding to enstatite chondrite (Javoy et al., 1984; Kung and Clayton, 1978), and the secondary atmosphere from late accretion of volatile-rich C1 carbonaceous chondrites was +30 to +43‰ (Javoy and Pineau, 1983; Kerridge, 1985). In some models exchange with the mantle shifts the atmosphere down to the present-day value of 0‰ (Javoy et al., 1984; Boyd et al., 1987; Javoy, 1997; Cartigny et al., 1998), whereas others propose a uniform atmosphere of 0‰ from 4.3 Ga (Sano and Pillinger, 1990; Beaumont and Robert, 1999), and a much lower $\delta^{15}N$ of –30‰ for both the early atmosphere and mantle evolving to the present-day atmosphere of 0‰ and upper mantle value of –5‰ (Tolstikin and Marty, 1998).

The $\delta^{15}N$ of some diamonds, likely sourced in the lower mantle, and enstatite chondrites are both –25‰; the isotopic match endorses early accretion of all or part of the silicate earth from this class of chondritic meteorite (Javoy et al., 1984, Kung and Clayton, 1978). The initial atmosphere is thought to have been 'blown off' by some combination of heating by meteorite bombardment, forming of a magma ocean (Drake, 2000), and intense solar 'wind' during the T-tauri stage of the early sun (Ahrens, 1990). The present atmosphere and hydrosphere were acquired from late accretion of a 'veneer'

of volatile-rich C1 carbonaceous chondrites having $\delta^{15}N$ of +30 to +42‰ (Javoy and Pineau, 1983; Kerridge, 1985), and possibly comets formed in the vicinity of Jupiter (Delsemme, 2001). Subsequently, depleted upper mantle shifted from –25 to –5‰, as recorded in the majority of diamonds and mid-ocean ridge basalts (MORB) (Boyd et al., 1987, 1992; Cartigny et al., 1997, 1998), whereas the atmosphere shifted from +30 to +43‰ down to the present value of 0‰. However, the mechanisms by which shifts in these reservoirs occurred is not well constrained.

This chapter documents a secular trend of N content and $\delta^{15}N$ in the Earth's continental crust reservoir. The secular trends are interpreted in terms of early growth of continental crust that sequestered atmospheric nitrogen, and its recycling into the mantle, providing a mechanism for the observed N-isotope shifts in both the atmosphere and mantle reservoirs.

7.2 Sampling and methodology

Nitrogen comprises 78% of the Earth's atmosphere, and is a principal element of living biomass (2.5‰) and sedimentary hydrocarbons (average C/N weight ratio of 5.1 to 14.8 with depth from 0 to 325 cm; Berner, 1971; Hopkins et al., 1998; Owens and Watts, 1998; Jaffe, 2000). Nitrogen as NH_4^+ substitutes for potassium in many common rock-forming minerals in the crust such as micas and K-feldspar (Honma and Itihara, 1981), is a significant component of crustal metamorphic fluids (Bottrell et al., 1988), and is present in trace quantities of 2-36 ppm in mantle volatiles (Chapter 3; Javoy, 1997; Marty, 1995; Cartigny et al., 1998).

There are abundant data for Phanerozoic crustal rocks, but sparse data for Precambrian counterparts. Two approaches have been adopted to estimate the N content

and $\delta^{15}N$ of Precambrian crustal rocks. First, direct analysis of sedimentary rocks or low-grade metasedimentary rocks. Second, indirect analysis of bulk crust from hydrothermal K-micas in giant shear zone-hosted quartz-carbonate-mica vein systems. These structurally hosted vein systems are present in subduction-accretion style orogenic belts of Archean to Cenozoic age, and locally are rich in gold. The structures extend along strike for up to 300 km and some have been seismically imaged to the MOHO (Kerrich and Ludden, 2000). For the 2.7 Ga Canadian Abitibi greenstone belt veins, it is estimated that 6000 km^3 hydrothermal fluid advected up to the structures from metamorphic dehydration of 150,000 km^3 of mid- to lower crust. Consequently, the NH_4^+ bearing K-micas provide proxy samples of bulk crust.

In this study sedimentary rocks were analyzed from well-documented 2.7 Ga black shales in the Hoyle Pond area of the Abitibi belt, Canada, and 2.2 Ga carbonaceous schist in the Ashanti belt of Ghana, West Africa. These sedimentary rocks have undergone sub-greenschist to greenschist facies metamorphism (Table 7.1). Quartz vein mica separate samples were from the 2.2 Ga Ashanti greenstone belt of Ghana, West Africa, 1.8 Ga Trans-Hudson orogen in Saskatchewan and Manitoba, and Mesozoic western Qilian belt of the North China craton. Other nitrogen isotope data for vein micas of Archean to Phanerozoic hydrothermal systems are from Chapters 4, 5, and 6.

7.3 New measurements and compilations of data

Previous studies show that Phanerozoic sedimentary rocks have N contents ranging from 100 to 2800 ppm, with a mean of 660 ppm (n = 256), and a mean $\delta^{15}N$ of +3.5‰ (n = 159; Haendel et al., 1986; Bebout and Fogel, 1992; Williams et al., 1995; Ader et al., 1998). Precambrian metasedimentary rocks show relatively lower N concentrations but

Table 7.1. Nitrogen contents and isotopic compositions of sediments and hydrothermal vein systems

Era	Age	Sediments†				Ref.§	Hydrothermal vein micas				Ref.§
Sample location	(Ma)	N (ppm)	n	$\delta^{15}N_{AIR}$ (‰)	n		N (ppm)	n	$\delta^{15}N_{AIR}$ (‰)	n	
Archean											
Superior Province, Canada	2700	32 ± 13	9	14.5 ± 1.8	8	1, 2	95 ± 72	44	16.3 ± 3.0	44	1, 3
Norseman, Western Australia	2700						32 ± 20	13	17.2 ± 4.1	13	1
Hoyle Pond area, Canada	2700	157 ± 67		16.0 ± 1.7	10	4					
Proterozoic											
Ashanti, Ghana, West Africa	2200	377 ± 67		10.8 ± 1.1	11	4	1650 ± 250	9	10.2 ± 1.5	9	4
Trans-Hudson orogen, Canada	1800						112 ± 6	8	7.2 ± 0.6	8	4
Phanerozoic											
Bendigo-Ballarat Zone, Australia	450 to 420						733 ± 103	20	3.5 ± 0.4	20	5
Bramsche Massif, Germany	320 to 290			3.2 ± 0.4	8	6					
Pennsylvania, U.S.A	320 to 290			4.6 ± 0.4	10	6					
Western Qilian, N. China craton	210 to 220						1260 ± 760	8	4.0 ± 2.0	8	4
North American Cordillera	180 to 90						1535 ± 1080	22	3.0 ± 1.2	85	4
Catalina Schist, California	145 to 65	540 ± 270	27	3.0 ± 1.2	46	7					
Sandstone, Louisiana	145 to 65	1600 ± 100	64	3.1 ± 1.4	51	8					
Taiwan, China	Tertiary	800 ± 100	5	3.9 ± 0.1	5	9					

Note: Isotope data represent mean $\delta^{15}N$ values ± 1 standard deviation; AIR- Atmospheric N_2 stardard.

†Nitrogen abundances represents bulk sediments; $\delta^{15}N$ values represent organic matter of sediments

§References: 1 = Jia and Kerrich (2000); 2 = Honma (1996); 3 = Jia and Kerrich (1999); 4 = This study ; 5 = Jia et al. (2001); 6 = Ader et al. (1998); 7 = Bebout and Fogel; (1992); 8 = Williams et al. (1995); 9 = Kao and Liu (2000).

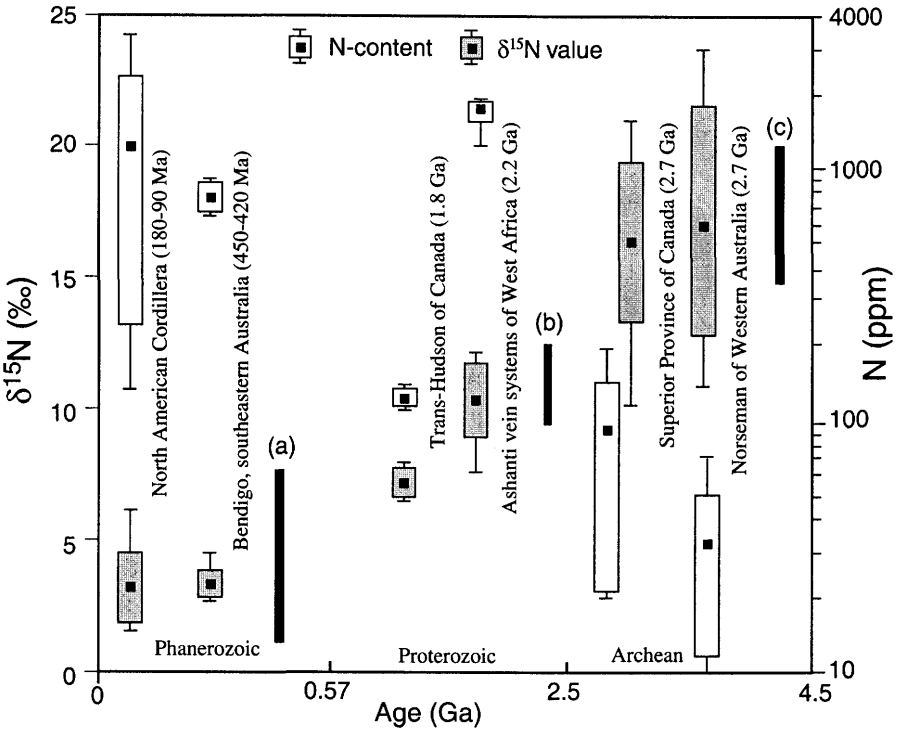

Fig. 7.1. Variations of N concentrations and nitrogen isotopic compositions of quartz-carbonate- mica veins systems in orogenic belts of Archean to Phanerozoic age. Open and shaded box whisker symbols represent the ranges, mean values with (1σ) of N contents and $\delta^{15}N$ values, respectively. Data sources: North American Cordillera from this study; the Bendigo district of southeastern Australia from (Jia et al., 2001), the Proterozoic Trans-Hudson orogen, Canada (Table 7.1); the Archean Superior Province of Canada and Western Australia from (Jia and Kerrich, 1999, 2000). Black bars represent nitrogen isotope compositions of metasedimentary rocks of: (a) Phanerozoic (Haendel et al., 1986; Bebout and Fogel, 1992; Williams et al., 1995); (b) Proterozoic Ashanti belt of Ghana, West Africa; and (c) Archean Superior Province of Canada (data in Table 7.1).

higher $\delta^{15}N$ values. The 2.2 Ga carbonaceous schists in West Africa have 290 ± 130 ppm N and $\delta^{15}N$ values of 9.7 ± 1.0‰, and 2.7 Ga sedimentary rocks in the Abitibi belt of Canada have 32 ± 13 ppm N and $\delta^{15}N$ values of 15.4 ± 1.9‰, which are similar to other data for Archean sedimentary rocks of the Superior Province (Table 7.1). Collectively, other Archean metasedimentary rocks, from central Greenland, S. Africa, and Kenya have N contents ranging from 16 to 100 ppm (mean 30 ppm; n = 58), but there are no data for $\delta^{15}N$ in these rocks (Honma, 1996).

Results of indirect measurement of bulk crust N content and $\delta^{15}N$ values using hydrothermal micas show similar trends to direct measurements of crustal sedimentary rocks. Phanerozoic micas have mean values of N = 1535 ppm and $\delta^{15}N$ = 3.0 ± 1.2‰ (n = 100) from the western North American Cordillera, 1260 ppm and 4.0 ± 2.0‰, from the western Qilian of North China craton, and 773 ppm and 3.5 ± 0.4‰ from the Bendigo region in the Tasman orogen of southeastern Australia (Fig. 7.1 and Table 7.1). Micas from the 2.2 Ga quartz veins in the Birimian greenstone belt of Ghana have 1650 ppm N and 10.2‰ for $\delta^{15}N$, micas from the 1.8 Ga quartz veins in the Trans-Hudson orogen in Saskatchewan have 112 ppm N and 7.2‰ for $\delta^{15}N$, and Archean counterparts from Western Australia and Canada have 32 ppm and 95 ppm N, and 17.2‰ and 16.3‰ $\delta^{15}N$, respectively (Fig. 7.1 and Table 7.1).

7.4 Discussion

The $\delta^{15}N$ values of depleted upper mantle, represented by most diamonds and mid ocean ridge basalts (MORB), are uniform at –6 ± 1‰ (Javoy et al., 1984; Boyd et al., 1987, Marty and Humbert, 1997). The diamonds are thought to form from upper mantle carbonate melts reacting with continental lithospheric mantle (CLM), and to be Archean

in age (Richardson, et al., 1984). Accordingly, the upper mantle $\delta^{15}N$ may have been uniform at about –6‰ for ≥ 2.7 Ga. The present atmosphere-hydrosphere system has a $\delta^{15}N$ = 0‰, and the present continental crust is estimated to be +3 to +6‰. Clearly, the atmosphere - hydrosphere system and continental crust cannot have evolved directly from primary mantle having $\delta^{15}N$ of –25‰ of enstatite chondrites given an isotopic imbalance between the internal (mantle) and the external reservoirs (atmosphere + crust).

The nitrogen isotope characteristics of these reservoirs have been accounted for in a two stage model: early accretion of the bulk of the silicate earth from enstatite chondrites having $\delta^{15}N$ of –25‰, and late accretion of a 'veneer' of C1 carbonaceous chondrite type material having $\delta^{15}N$ of 30 to 42‰ (Javoy and Pineau, 1983). It has been suggested, without specifying a process, that recycling of the ^{15}N enriched 'veneer' into the upper mantle shifts its $\delta^{15}N$ from –25‰ to about –5‰ (Javoy, 1997; Cartigny et al., 1998).

The secular trends of N content and $\delta^{15}N$ identified in Earth's crustal reservoir in this study allows a specific mechanism to be identified for shifting atmospheric $\delta^{15}N$ down and depleted mantle up. The early atmosphere is estimated to have been 2 to 5 times its present mass (Delsemme, 1998; Javoy, 1997; Drake, 2000). Atmospheric CO_2 has been sequestered to form marine carbonate formations, and hydrocarbons that are incorporated into sedimentary rocks (Tajika and Matsui, 1990; Delsemme, 1998). Similarly, Cartigny et al. (1998) postulated that atmospheric nitrogen was also sequestered and stored in sedimentary rocks during the early history of the Earth because of the increased solubility of nitrogen under reducing conditions.

At present, atmospheric nitrogen is sequestered by biological nitrogen fixation to form organic nitrogen compounds, which have $\delta^{15}N$ values of -5.0 ± 0.4‰ for chlorin in

sapropels (n = 7; Sachs and Repeta, 1999), and –4.0 ± 0.9‰ for plants (n = 14; Kao and Liu, 2000), given negative fractionations between atmosphere and microorganisms. Organic nitrogen compounds decomposed during diagenesis are stored in sedimentary rocks as kerogen having $\delta^{15}N$ values of 3.6 ± 0.5‰ (n = 22; Ader et al., 1998; Williams et al., 1995), with a corresponding flux of ^{15}N depleted nitrogen back to the atmosphere. Phanerozoic sedimentary rocks and bulk crust having $\delta^{15}N$ values of +3.0 to +3.5‰ are virtually indistinguishable from the isotopic composition of the kerogen, which implies that the source of NH_4^+ incorporated in sedimentary K-silicates is from organic matter, consistent with insignificant nitrogen isotope fractionation between kerogen and nitrogen fixed as NH_4^+ in minerals (Delwiche and Steyn, 1970; Williams et al., 1995; Ader et al., 1998).

Models for growth of the continental crust range from early growth with rapid recycling of continental and oceanic crust into the mantle, to progressive growth and minimal recycling of continental crust (see Windley, 1995 for a review). Recent data on the Nb/U and Nb/Th systematics of basalts erupted from Archean mantle plumes, and reinterpretation of radiogenic isotope data, support early growth and recycling of continental crust (Sylvester et al., 1997; Kerrich et al., 1999; Albarede, 2001). If the initial mass of continental crust having $\delta^{15}N$ of about +30 to +42‰ had formed by ~4.3 Ga, with continuous growth balanced by recycling into the mantle, then mass balance shows that by 2.7 Ga this would induce a 20‰ negative shift in both crustal rocks and atmosphere from +30 to +43‰ to +10 to 23‰, which matches the measured $\delta^{15}N$ values from Archean metasedimentary rocks and crustal hydrothermal systems (Fig. 7.1; Jia and Kerrich, 1999, 2000). Crustal recycling would induce a corresponding positive shift of

the depleted upper mantle from –25‰ to –6 ± 1‰ as obtained for most Archean diamonds (Richardson et al., 1984, 1993; Cartigny et al., 1998), consistent with an early growth model.

High $\delta^{15}N$ values of 16.5 ± 3.3‰ for Archean sedimentary rocks and vein micas, but low $\delta^{15}N$ values of 3.0 ± 1.2‰ in Phanerozoic counterparts, cannot be accounted for N-isotopic fractionations during metamorphic dehydration (see Chapter 6). This study does not show any trend of increasing $\delta^{15}N$ with metamorphic grade (Chapter 4; Jia and Kerrich, 1999, 2000). Pinti et al (2001) report N-isotope data in 3.8 to 2.8 Ga metasediments from the Isukasia greenstone belt of Western Greenland and the Pilbara craton, NW Australia, using step heating; they also show low N contents and high $\delta^{15}N$ values of 10 to 20‰. Negative $\delta^{15}N$ values obtained at low temperature may reflect contamination.

A model for the initial atmospheric $\delta^{15}N$ close to 0‰ (Sano and Pillinger, 1990; Beaumont and Robert, 1999) may be ruled out given the secular evolution of nitrogen isotopic composition for crustal rocks from Archean to the Phanerozoic. Tolstikhin and Marty (1998) suggested that both atmospheric and mantle nitrogen isotopic compositions start with enstatite chondrite $\delta^{15}N$ of –30‰ at end of Earth accretion. However, the Earth's early atmosphere was lost (Drake, 2000; Delsemme, 2001). The results suggest a more limited flux of nitrogen from the atmosphere to the mantle via crust during the Proterozoic and Phanerozoic, since most of the mantle shift from –25 to –5‰ was established by the Archean, and given that most Archean diamonds and recent MORB have similar $\delta^{15}N$ (Cartigny et al., 1998; 2001).

The N-isotope evolution of the Earth's atmosphere, continental crust, and mantle have been numerically modeled using present day masses, concentrations, and isotopic values, estimates of these for end-accretion, measurements on Archean diamonds, the new data for Archean, and Proterozoic crust, and compilations for Phanerozoic crust (Table 7.2; Fig. 7.2). Archean continents are assumed to be the mass of the present continental crust, but the recycling rate is set at 3 times the present given decay of radioactive heat production (Stacey, 1992). The model confirms the qualitative arguments for shifts of $\delta^{15}N$ in Earth's atmosphere, crust, and mantle.

The endmember model in which the initial mantle $\delta^{15}N$ was –25‰, as recorded in rare diamonds, corresponding to ^{15}N depleted enstatite chondrites, can be refined from new Cr isotope data. The bulk silicate earth has a $^{53}Cr/^{52}Cr$ ratio in ε unit (1ε unit = one part in 10^4) defined to be 0 ε, intermediate between enstatite chondrites of ~ +0.17 ε and carbonaceous chondrites with ~ -0.43 ε (Lugmair and Shukolyukov, 1998; Shukolyukov and Lugmair, 1998). Consequently, the bulk initial mantle ($\delta^{15}N^{i}_{mantle}$) might have been constrained under conditions:

$$\delta^{15}N^{i}_{mantle} \times M^{N}_{total} = \delta^{15}N_{EH} \times M^{N}_{EH} + \delta^{15}N_{C1} \times M^{N}_{C1} \quad 7.1$$

$$M^{N}_{total} = M^{N}_{EH} + M^{N}_{C1} \quad 7.2$$

$$M^{N}_{EH} = M_{EH} \times C_{EH} \quad 7.3$$

$$M^{N}_{C1} = M_{C1} \times C_{C1} \quad 7.4$$

Where $\delta^{15}N_{EH}$ and $\delta^{15}N_{C1}$ represent depleted ^{15}N enstatite chondrites of –43‰ and C1 carbonaceous chondrites with +42‰ respectively (Table 3.8 in chapter 3; Kung and Clayton, 1978; Javoy and Pineau, 1983; Kerridge, 1985); M_{EH} and M_{C1}, and C_{EH} and

Table 7.2. Calculated results for N mass and its isotope compositions in the atmosphere, continental crust, and mantle

$\delta^{15}N$ Mass	Atmosphere (A)	Continental Crust (B)	Upper mantle (C)
Initial	+30 to +42‰	+42‰	-25 to -30‰
mass	13.3×10^{18} kg	0	28.5×10^{18} kg
Archean	13 to 21‰	16 to 24‰*	-5‰*
mass	5.4×10^{18} kg	0.6×10^{18} kg	38.0×10^{18} kg
Present	0‰	+4‰*	-5‰*
mass	3.8×10^{18} kg	2.1×10^{18} kg	38.0×10^{18} kg

All values assumed, excepting measured values* (see text for references).

Note: (A) Atmospheric $\delta^{15}N$ starts with a C1 carbonaceous chondrite value of +42‰ (Javoy and Pineau, 1983; Kerridge, 1985), through +13 to 21‰ in the Archean, to its present-day value of 0‰. N mass starts 3.5 times the present (Javoy, 1997), through 5.4×10^{18} kg by the Archean, to its present mass.

(B) Continental $\delta^{15}N$ starts with a C1 carbonaceous chondrite value of +42‰, shifting to +16 to 24‰ by the with Archean, to the present value of +3.5‰. Crustal N mass starts at 0 to about 0.6×10^{18} kg in the Archean, then to the present mass of 2.1×10^{18} kg.

(C) Upper mantle $\delta^{15}N$ stars with an enstatite chondrite value of -25‰ (Kerridge and Clayton, 1978; Javoy et al., 1984) shifting to -5‰ in the Archean and maintaining this value to the present. N mass starts at 7.5 times the present atmospheric N (Javoy, 1997). changing to ten times present atmospheric N in the Archean, then maintained approximately uniform. Lower mantle is assumed to remain uniform (Richards et al., 1984; Cartigny et al., 1998; Moreira et al., 2001).

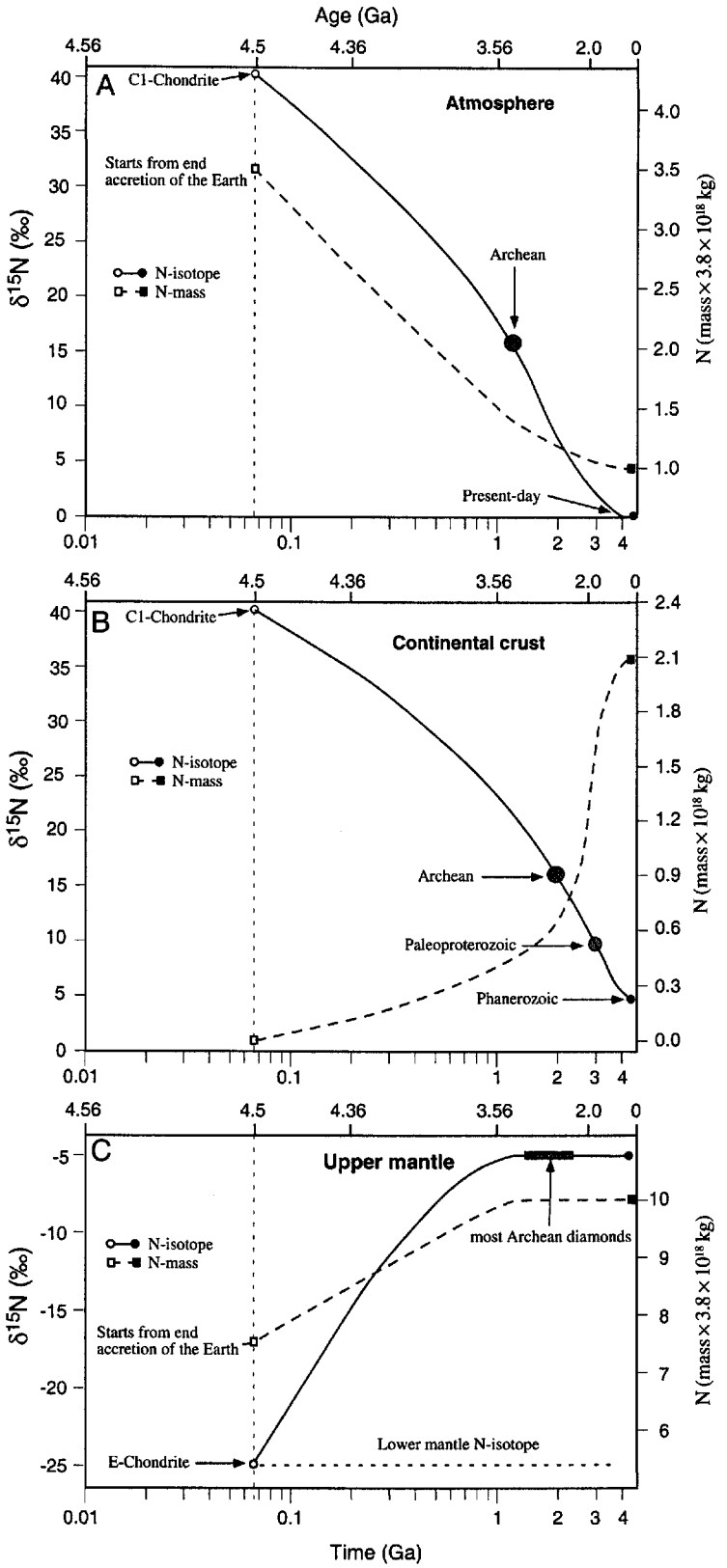

Fig. 7.2. Nitrogen and $\delta^{15}N$ evolutionary trends for the atmosphere (A), continental crust (B), and mantle (C) reservoirs (see Table 7.2 for detail).

C_{CI} represent the mass and N concentrations of N in enstatite and carbonaceous chondrites respectively. Assuming the total N mass of initial mantle was 1:

$$M_{EH} \times C_{EH} + M_{CI} \times C_{CI} = 1 \qquad 7.5$$

Consequently, the N mass proportions of enstatite chondrites and carbonaceous chondrites are 72% and 28% in the initial mantle based on the Cr-isotope data (Lugmair and Shukolyukov, 1998; Shukolyukov and Lugmair, 1998). Assuming conditions above, the calculated bulk initial mantle had a nitrogen isotopic composition of –20‰ to -5‰, which approaches the relatively ^{15}N depleted enstatite chondrites recorded in some diamonds (Cartigny et al., 1998).

7.5 Summary

New measurements and compilations of N concentrations and $\delta^{15}N$ values in sedimentary rocks and crustal hydrothermal systems show systematic trends over 2.7 billion years from the Archean ($\delta^{15}N$ = 15.4 ± 1.9‰; 16.5 ± 3.3‰); through Paleoproterozoic ($\delta^{15}N$ = 9.7 ± 1.0‰; 9.5 ± 2.4‰); to the Phanerozoic ($\delta^{15}N$ = 3.5 ± 1.0‰; 3.0 ± 1.2‰). Crustal N content has increased in parallel from 84 ± 67 ppm, through 103 ± 91 ppm, to 810 ± 1106 ppm. If the initial mantle $\delta^{15}N$ was –25‰, whereas the initial atmosphere was +30 to +43‰, then shifts of $\delta^{15}N$ in these reservoirs to their present values of –5‰ (upper mantle) and 0‰ (atmosphere) can be accounted for by early growth of the continents, sequestering of atmospheric N_2 into sediments, and recycling into the mantle.

Chapter Eight

CONCLUDING STATEMENT

The detailed findings of this study are summarized at the end of individual chapters. Several of the principal features, however, are reiterated and discussed collectively in this chapter.

Orogenic gold deposits constitute a distinctive class of epigenetic precious metal deposit; their origin, however, remains controversial after many decades of research. Several contrasting genetic models have been proposed including mantle, granitoid, meteoric water, and metamorphic-derived ore-forming fluids based on several lines of geochemical evidence. Nitrogen isotope systematics of hydrothermal micas and Se/S systematics of hydrothermal pyrites from lode gold deposits provide less ambiguous signatures of the ore-forming fluid source reservoir(s) than other geochemical systems. New data on N-isotopic compositions of robust hydrothermal K-silicates in orogenic gold deposits from Archean to Phanerozoic rule out magmatic, mantle, or meteoric water ore fluids. Se/S systematics indicate crustal not mantle sources.

The origin and evolution of N in the Earth's major reservoirs of atmosphere, crust, and mantle is controversial. The initial mantle acquired a $\delta^{15}N$ of –25 to –30‰ based on rare diamonds that correspond to ^{15}N-rich enstatite chondrite, or a mixture of ^{15}N-depleted enstatite chondrites with ^{15}N-enriched C1 chondrites. The final atmosphere from late accretion of volatile-rich C1 carbonaceous chondrite was +30 to +42‰. In some models the shift of mantle from about ≥ –25‰ to the present-day value of –5‰ represented by most diamonds and MORBs, compensates the shift of atmosphere from

+42‰ to 0‰. In other models, both the atmosphere and mantle nitrogen isotope compositions start with enstatite chondrite $\delta^{15}N$ of –30‰ at the end of Earth accretion; atmospheric and crustal nitrogen was outgassed from the mantle. Yet other models propose a uniform atmosphere of 0‰ from 4.3 Ga. However, for the first model, the mechanisms by which shifts in these reservoirs occurred is not well constrained, and the other hypotheses are not consistent with the isotopic imbalance that exists between the internal (upper mantle, -6 ± 1‰) and the external (atmosphere 0‰, crust from +1 to > +20‰) reservoirs.

From limited N-isotope data crustal sedimentary rocks and crustal hydrothermal systems show systematic trends over 2.7 billion years from higher $\delta^{15}N$ and lower N contents in the Archean to lower $\delta^{15}N$ and higher N contents in the Phanerozoic. These results may provide a specific mechanism for shifting atmospheric $\delta^{15}N$ down from +30 to +43‰ to ~ +16‰ between end-accretion and the Archean by sequestering atmospheric N in crustal rocks and recycling into the mantle, and for shifting upper mantle $\delta^{15}N$ up from ≥ –25‰ to –5‰. These new results also bear on the long standing questions of: (1) how the mass of the early atmosphere was reduced from three to five times to its present value, as only H can escape to space; and (2) recycling of atmospheric gases into the mantle. The results may provide new constraints on the controversial issues of when the continents grow, and whether or not crust recycling into the mantle has been significant. Provisional results come down clearly on the side of very early growth of continents and fast recycling in the Archean. Albarede (2001) has recently argued that many commonly used isotopic systems, including Sm-Nd, Rb-Sr, Lu-Hf, and several of the U-Pb isotopes, have attained secular equilibrium in the

Earth and do not record a memory of the early differentiation of the crust, and also that their systematics require the presence at depth in the mantle of an additional reservoir containing early recycled crust. The results may also provide some new evidence on the evolution of early atmospheric O_2.

Further study is needed, by systematic sampling and analysis, to better establish an understanding of N cycling in the atmosphere-hydrosphere-crust-mantle systems in the Earth's history from Archean to the Recent, expanding the limited existing database of N-isotope systematics of crustal hydrothermal systems conducted in this Ph.D. program. Three independent approaches could be adopted in future research to evaluate secular variations of $\delta^{15}N$: (1) N-isotope systematics of sedimentary rocks and sedimentary organic matter, (2) K-silicates in crustal hydrothermal systems as a proxy of bulk crust, and (3) seawater K-altered rocks in the footwall of VMS deposits as a monitor of marine $\delta^{15}N$. Collectively, these would provide new constraints on modeling N cycling in the Earth's major reservoirs through geological time.

References

Abraham, A.P.G., Davis, D.W., Kamo, S.L., Spooner, E.T.C., 1994, Geochronology constraints on late Archean magmatism, deformation and gold-quartz vein mineralization in the northwestern Anialik River greenstone belt and igneous complex, Slave Province, N.W.T.: Canadian Journal of Earth Sciences, v. 31, p. 1365-1383.

Abzalov, M.Z., 1999, Gold deposits of the Russian North East (The Northern Circum Pacific): Metallogenic overview: PACRIM'99, The Austrlasian Institute of Mining and Metallury, Carlton, Victoria, Austrlai, p. 701-714.

Adams, C.J., Barley, M.E., Fletcher, I.R., and Pickard, A.L., 1998, Evidence from U-Pb zircon and $^{40}Ar/^{39}Ar$ muscovite detrital mineral ages in metasanstones for movement of Torlesse suspect terrane around the eastern margin of Gondwanaland: Terra Nova, v. 10, p. 183-194.

Ader, M., Boudou, J.P., Javoy, M., 1998, Isotope study on organic nitrogen of Westphalian anthrzcites from the Western Middle field of Pennsylvanian (U.S.A.) and from the Bramsche Massif (ermany): Organic Geochemistry, v. 29, p. 315-323.

Ahrens, L.H., 1964, Si-Mg fractionation in chondrites: Geochimica et Cosmochimica Acta, v. 28, p. 411-423.

Ahrens, T.J., 1990, Earth accretion, *in* Newson H.E., and Jones J.H., eds., Origin of the Earth: New York, Oxford University Press, p. 211-227.

Albarede, F., 2001, Radiogenic ingroth in systems with multiple reservoirs: applications to the differentiation of the mantle-crust system: Earth and Planetary Science Letters, v. 189, p. 59-73.

Albino, G.V., Jahal, S., and Christensen, K., 1995, Neoproterozoic mesothermal gold mineralization at Sukhaybarat East mine, Sardi Arabia: Trans. Inst. Min. Metall. V. 104, p. B157-B210.

Andersen, T., Austrheim, H., Burke, E.A.J., and Elvevold, S., 1993, N_2 and CO_2 in deep crustal fluids: evidence from the Caledonides of Norway: Chemical Geology, v. 108, p. 113-132.

Anderson, P.G., and Hodgson, C.J., 1989, The structure and geological development of the Erickson gold mine, Cassiar district, British Columbia, with implications for the origin of Mother-Lode type gold deposits: Canadian Jouranl of Earth Sciences, v. 26, p. 2645-2660.

Andrews, A.J., and Wallaca, H., 1983, Alteration, metamorphism and structural patterns associated with Archean gold deposits – preliminary observations in the Red Lake area, in Colvine, A.C., ed., The Geology of Gold on Ontario: Ontario Geological Survey Miscellaneous Paper 110, 278p.

Anhaeusser, C.R., 1986, Archean gold minerlaization in the Barberton Mountain Land, in Anhaeusser, C.R., and Maske, S., edds., Deposits of Southern Africa: Geological Society of South Africa, Johannesburg, South Africa, p. 113-154.

Ansdell, K.M., Kyser, T.K., 1992, Mesothermal gold mineralization in a Proterozoic greenstone belt: Western Flin Flon domain, Saskatchewan, Canada: Economic Geology, v. 87, p. 1496-1524.

Armstrong, R.A., 1988, Mesozoic and early Cenozoic magmatic evolution of the Canadian Cordillera: Geological Society of America Special Paper 218, p. 55-92.

Arne, D.C., Bierlein, F.P., McNaughton, N.J., Wilson, C.J.L., and Morand, V.J., 1988, Absolute timing of gold mineralization in central Victoria: New constraints from SHRIMP II analysis of zircon grains from felsic intrusive rocks: Ore Geology Reviews, v. 13, p. 251-273.

Arribas, A., J., Cunningham, C.G., Rytuba, J.J., Rre, R.O., Kelly, W.C., Podwysocki, M.P., Mckee, E.H., and Tosdal, R.M., 1995, Geology, geochemistry, fluid inclusions, and isotope geochemistry of the Rodalquilar gold Alunite deposit, Spain: Economic Geology, v. 90, p. 795-822.

Ash, C.H., 2001, Ophiolite related gold quartz veins in the North American Cordillera: B.C. Ministry of Energy and Mines, Energy and Minerals Division, Geological Survey Branch, Bulletin 108, 139p.

Ash, C.H., Reynolds, P.H., MacDold, R.W.J., 1996, Mesothermal gold-quartz vein deposits in British Columbia oceanic terranes, New Minerla Deposits Models of the Cordillera: British Columbia Ministry of Employment and Investment, Energy and Minerals Devision, Geological Survey Branch, Short Course Notes, Vancouver, p. O1-O32.

Ashley, P.M., 1997, Silica-carbonate alteration zones and gold mineralization in the Great Serpentinite Belt, New England orogen, New South Wales. In: Ashley, P.M., Flood, P.G., eds., Tectonics and Metallogenesis of the New England Orogen: Geol. Soc. Aust. Spec. Publ. V. 19. P. 212-225.

Auclair, G., Fouquest, G., and Bohn, M., 1987, Distribution of selenium in high-temperature hydrothermal sulfide deposits at 13° north, east Pacific Rise: Canadian Mineralogist, v. 25, p. 577-587.

Bain, J.H.C., Mackenzie, D.E., Black, L.P., Wellman, P., Bultitude, R.J., Hutton, L.J., Rienks, I.P., Draper, J., and Whitnall, I.W., 1998, The Tasman orogenic system in North Queensland: key elements: Abstracts, Geological Society of Australia, Sydney, N.S.W., Austalia, v. 49, p. 15.

Balakrishnan, S., Hanson, G.N., and Rajamani, V., 1990, Pb and Nd isotope constraints on the origin of high Mg and tholeiitic amphibolites, Kolar Schist Belt, South India: Contributions to Mineralogy and Petrology, v. 107, p. 279-292.

Balakrishnan, S., Rajamani, V., and Hanson, G.N., 1999, U-Pb ages for zircon and titanite from the Ramagiri area, southern India: evidence for accretionary origin of the eastern Dharwar craton during the late Archean: Journal of Geology, v. 107, p. 69-86.

Barker, A.J., and Fodter, R.P., 1993, Metamorphic fluids and mineral deposits: Mineralogical Magazine, v. 57, p. 363-364.

Barley, M.E., and Groves, D.I., 1992, Supercontinent cycles and the distribution of metal deposits through time: Geology, v. 20, p. 291-294.

Barnes, S.J., and Francis, D., 1995, The distribution of platinum- group elements, Nickle, Copper, and Gold in the Muskox layered intrusion, Northwest Territories, Canada: Economic Geology, v. 90, p. 135-154.

Barnicoat, A.C., Henderson, I.H.C., Knipe, R.J., Yardley, B.W.D., Napier, R.W., Fox, N.P.C., Kenyon, A.K., Muntingh, D.J., Stryom, D., Winkler, K.S., Lawrence, S.R, and Cornford, C., 1997, Hydrothermal gold mineralization in the Witwatersrand basin: Nature, v. 386, p. 820-924.

Bayley, R.W., Proctor, P.D., and Condie, K.C., 1973, Geology of the South Pass area, Fremont County, Wyoming: U.S. Geol. Surv. Prof. Pap. 793, 39p.

Bebout, G.E., 1997, Nitrogen isotope tracers of high-temperature fluid-rock interactions: Case study of the Catalina Schist, California: Earth and Planetary Science Letters, v. 151, p. 77-90.

Bebout, G.E., and Fogel, M.L., 1992, Nitrogen-isotope compositions of metaseimentary rocks in the Catalina Schist, Calfornia: Implications for metamorphic devolatilization history: Geochimica et cosmochimica Acta, v. 56, p. 2839-2849.

Berner, R., 1971, Principles of Chemical Sedimentology. Mcgraw-Hill Book Company, New York, p. 86-137.

Berhe, S.M., 1997, The Arabian-Nubian Shield, in Greenstone Belts, de Wit, M.J., and Ashwal, L.D., eds., Oxford Monographs on Geology and Geophysics, Oxford University Press, Oxford, United Kingdom, p. 761-771.

Bethke, P.M., and Barton, JR. P.B., 1971, Distribution of some minor elements between coexisting sulfide minerals: Economic Geology, v. 66, p. 140-163.

Bierlein, F.P., Arne, D.C., McKnight, S., Lu, J., Reeves, S., Besanko, J., Marek, J., and Cooke, D., 2000, Wall-rock petrology and geochemistry in alteration halos associated with mesothermal gold mineralization, central Victoria, Australia: Econimic Geology, v. 95, p. 283-312.

Bierlein, F.P., Fuller, T., Arne, D.C., and Keays, R.R., 1998, Wall rock alteration associated with turbidite-hosted gold deposits – examples from central Victoria, Australia: Ore Geology Reviews, v. 13, p. 345-380.

Bierlein, F.P., McKnight, S., Arne, D.C., and Foster, D.A., 1999, Timing of gold mineralization in the Ballarat gold field, central Victoria: Constraints from $^{40}Ar/^{39}Ar$ results: Australian Journal of Earth Sciences, v. 46, p. 301-309.

Bigeleisen, J., Pearlman, M.L., and Prosser, H.C., 1952, Conversion of hydrogenic materials to hydrogen for isotope analysis: Analytical Chemistry, v. 24, p. 1356-1357.

Billstrom, K., and Weihed, P., 1996, Age and provenance of host rocks and ores in the Paleoproterozoic Skellefte district, northern Sweden: Economic Geology, v. 91, p. 1054-1072.

Blenkinsop, T.G., and Frei, R., 1996, Archean and Proterozoic mineralization and tectonics at the Renco Mine (Northern marginal zone, Limpopo belt, Zimbabwe): Economic Geology, v.91, p. 1225-1238.

Bloem, E.J.M., Dalstra, H.J., Groves, D.I., and Ridley, J.R., 1994, Metamorphic and structural setting of Archean amphibolite-hosted gold deposits near Southern Cross, Sothern Cross Province, Yilgarn Block, Western Australia: Ore Geology Review, v. 9, p. 193-203.

Boer, R.H., Meyer, F.M., Robb, L.J., Graney, J.R., Vennemann, T.W., and Kesler, S.E., 1995, Mesothermal-type minerlaization in the Sabie-Pilgrim's Rest gold field, South Africa: Economic Geology, v. 90, p. 860-876.

Böhlke, J.K., 1999, Mother Lode gold: Geological Society of America Special Paper 338, p. 55-67.

Böhlke, J.K., and Irwin, J.J., 1992, Laser microprobe analyses of Cl, Br, I, and K in fluid inclusion: Implications for sources of salinity in some ancient hydrothermal fluids: Geochimica et Cosmochimica Acta, v. 56, p. 203-225.

Böhlke, J.K., and Kistler, R.W., 1986, Rb-Sr, K-Ar, and stable evidence for the ages and sources of fluid components of gold-bearing quartz veins in the Northern Sierra Nevada Foothlls metamorphic belt, California: Economic Geology, v, 81, p. 296-322.

Borg, G., 1994, The Geita gold deposit in NW Tanzania-Geology, ore petrology, geochemistry and timing of events, Metallogensis of Selected Gold Deposits in Africa: Geologisches Jahrbuch Reihe, D, Heft 100, Hannover, p. 545-595.

Bornhorst, T.J., and Nurmi, P.A., 1997, Selenium: A common trace element in hydrothermal gold deposits: Geological Society of America, Abstracts with Programs 29, p49.

Bortnikov, N.S., Gamuanin, G.N., Alpatov, V.A., Naumov, V.B., Nosik, L.P., and Mironova, O.F., 1998, Mineralogy, geochemistry and origin of the Nezdaninsk gold deposi (Sakha-Yakutia, Russia): Geol. Ore Deposits, v. 40, p. 121-138.

Bos, A., Duit, W., Eerden, M.J., and Jansen, J.B.H., 1988, Nitrogen storage in biotite: An experimental study of the ammonium and potassium partitioning between 1M-phlogopite and Vapour at 2 kb: Geochimica et cosmochimica Acta, v. 52, p. 1275-1283.

Bottrell, S.H., and Miller, M.F., 1990, The geochemistry behaviour of nitrogen compounds during the formation of balck shale hosted quartz-vein gold deposits, north Wales: Applied Geochemistry, v. 5 p. 289-296.

Bottrell, S.H., Carr, L.P., and Dubessy, J., 1988, A nitrogen-rich metamorphic fluid and coexisting minerals in slates from North Wales: Mineralogical Magazine, v. 52, p. 451-457.

Bouchot, V., and Feybesse, J.L., 1996, Paleoproterozoic gold mineralization of the Eteke Archean greenstone belt (Gabon): its relation to the Eburnean orogen: Precambrian Research, v. 77, p. 143-159.

Boyd, S. R., 2001, Ammonium as a biomarker in Precambrian metasediments: Precambrian Research, v. 108 p. 159-173.

Boyd, S.R., and Philippot, P., 1998, Precambrian ammonium biogeochemistry: a study of the Moine metasediments, Scotland: Chemical Geology, v. 144, p. 257-268.

Boyd, S.R., and Pillinger, C.T., 1994, A preliminary study of $^{15}N/^{14}N$ in octahedral growth form diamonds: Chemical Geology, v.116, p. 43-59.

Boyd, S.R., Hall, A., and Pillinger, C.T., 1993, The measurement of (15N in crustal rocks by static vacuum mass spectrometry: Application to the origin of the ammonium in the Cornubian batholith, southwest England: Geochimica et Cosmochimica Acta, v. 57, p. 1339-1347.

Boyd, S.R., Mattey, D.P., Pillinger, C.T., Milledge, H.J., Mendelssohn, M., and Seal, M., 1987, Multiple growth events during diamond genesis: an integrated study of carbon and nitrogen isotopes and nitrogen aggregation state in coated stone: Earth and Planetary Science Letters, v. 86, p. 341-353.

Boyd, S.R., Pillinger, C.T., Milledge, H.J., Mendelssohn, M., and Seal, M., 1992, C and N isotopic composition and the infrared absorption spectra of coated diamonds: evidence for the regional uniformity of CO_2-H_2O rich fluids in lithospheric mantle: Earth and Planetary Science Letters, v. 109, p. 633-644.

Boyle, R.W., 1979, The geochemistry of gold and its deposits: Geological Survey of Canada Bulletin, v. 280, p. 584.

Bralia, A., Sabatini, G., and Troja, F., 1979, A revalution of the Co/Ni ratios in pyrite as geochemical tool in ore genesis problems: Mineralium Deposita, v. 14, p. 353-374.

Brauhart, C.W., Groves, D.I., and Morant, P., 1998, Regional alteration systems associated with volcanogenic massive sulfide mineralization at Panorma, Pibara, Western Australia: Economic Geology, v. 93, p. 292-302.

Brown, P.E., and Hagemann, S.G., 1995, MacFlinCor and its application to fluids in Archean lode-gold deposits: Geochimica et Cosmochimica Acta, v. 59, p. 3943-3952.

Brown, P.G. et al., 2000, The fall, recovery, orbit, and composition of the Tagish Lake meteorite: a new type of carbonaceous chondrite: Science, v. 290, p. 320-325.

Burrows, D.R., and Spooner, E.T.C., 1987, Generation of a magmatic H_2O-CO_2 fluid enriched in Mo, Au, and W within an Archean sodic granitic stock, Mink Lake, northwestern Ontario: Economic Geology, v. 82, p. 1931-1957.

Burrows, D.R., and Spooner, E.T.C., 1989, Relationships between Archean gold quartz vein-shear zone mineralization and igneous intrusions in the Val d'Or and Timmins areas, Abitibi Subprovince, Canada: Economic Geology Mono.6. p. 424-444.

Burrows, D.R., Spooner, E.T.C., Wood, P.C., and Jemielita, R.A., 1993, Structural controls on formation of the Hollinger-McIntyre Au quartz vein system in the Hollinger shear zone, Timmins, Southern Abitibi greenstone belt, Ontario: Economic Geology, v. 88, p. 1643-1663.

Burrows, D.R., Wood, P.C., and Spooner, E.T.C., 1986, Carbon isotope evidence for a magmatic origin for Archean gold-quartz vein ore deposits: Nature, v. 321, p. 851-854.

Cabri, L.J., Campbell, J.L., Laflamme, J.H.G., Leigh, R.G., Maxwell, J.A., and Scott, J.D., 1985, Proton-microprobe analysis of trace elements in sulfides from some massvie ñsulfide deposits: Canadian Mineralogist, v. 23, p. 133-148.

Caddey, S.W., Bachman, R.L., Campbell, T.J., Reid, R.R., and Otto, R.P., 1991, The Homestake gold mine, an Early Proterozoic iron-formation-hosted gold deposit, Lawrence County, southDakota: U.S. Geol. Surv. Bull. 1857-J, 67p.

Cameron, E.M., 1988, Archean gold: Relation to granulite formation and redox zoning in the crust: Geology, v. 16, p. 109-112.

Campbell, I.H., Compston, D.M., Richards, J.P., Johnson, J.P., and Kent, A.J.R., 1998, Review of the application of isotopic studies to the genesis of Cu-Au minerlaization at Olympic Dam and Au mineralization at Porgera, the Tannant Creek district and Yilgarn craton: Australian Journal of Earth Scinces, v. 45, p. 201-218.

Campbell, I.H., Griffiths, R.W., and Hill, R.I., 1989, Melting in an Archean mantle plume: heads it's basalts, tails it's komatiites: Nature, v. 339, p. 697-699.

Cartigny, P., Boyd, S.R., Harris, W.J., and Javoy, M., 1997, Nitrogen isotopes in peridotitic diamonds from Fuxian, China: the mantle signature, Terra Nova, v. 9, p. 175-179.

Cartigny, P., Harris, J.W., and Javoy, M., 1998, Eclogitic diamond formation at Jwaneng: No room for a recycled component: Science, v. 280, p. 1421-1424.

Cartigny, P., Harris, J.W., and Javoy, M., 2001, Diamonds genesis, mantle fractionations and mantle nitrogen content: a study of δ^{13}C-N concentrations in diamonds: Earth and Planetary Science Letters, v. 185, p. 85-98.

Cartigny, P., Harris, J.W., Phillips, D., Girard, M., and Javoy, M., 1998, Subduction-related diamonds? – The evidence for a mantle-derived origin from coupled δ^{13}C - δ^{15}N determinations: Chemical Geology, v. 147, p. 147-159.

Cartwright, I., 1994, The two-dimensional pattern of metamorphic fluid flow at Mary Kathlean, Australia: fluid focusing, transverse dispersion, and implications for modeling fluid flow: American Mineralogist, v. 79, p. 526-535.

Cas, R.A.F., and VanderBerg, A.H.M., 1988, Ordovician, in Douglas, J.G., and Ferguson, J.A., eds., Geology of Victoria, Geological Association of Australia special publication 45, p. 63-102.

Casquet, C., 1986, C-O-H-N fluids in quartz segregations from a major dutile shear zone: the Berzosa fault, Spanish Central System: Journal of metamorphic Geology, v. 4, p. 117-130.

Cassidy, K.F., and Bennett, J.M., 1993, Gold mineralization at the Lady Bountiful MIne, Western Austrslia: an exmaple of a granitoid-hosted Archean lode gold deposit: Mineralium Deposita, v. 28, p. 388-408.

Chadwick, B., Vasudev, V.N., and Hegde, G.V., 2000, The Dharwar craton, southern India, interpreted as the result of Late Archean oblique convergence: Precambrian Research, v. 99, p. 91-111.

Chamberlain, C.M., Herrington, R.J., and Wikinson, J.J., 2000, A two-stage model for mineralization at Bulyanhulu, Sukumaland greenstone belt, Tanzania: Gold in 2000, Extended Abstract Volume, Lake Tahoe, Nevada, p. 25-30.

Chauvet, A., Faure, M., Dossin, I., and Charvet, J., 1994, A three-stage structural evilution of the Quadrilatero Ferrfero: consequences for the Neoproterozoic age and the formation of gold concentrations of the Ouro Preto area, Minas Gerais, Brazil: Precambrian Research, v. 68, p. 139-167.

Church, B.N., 1997, Age of mineralization, City of Paris, Greenwood area (82E/2E): B.C. Ministry of Energy, Mines and Petroleum Resources, Geological Fieldwork 1996, paper 1997-1, p. 211-213.

Clayton, R.N., 1981, Isotopic variations in primitive meteorites: Philosophical transactions of the Royal Society of London, v. 303, p. 339-349.

Clayton, R.N., and Mayeda, T.K., 1963, The use of bromine pentafluoride in the extraction of oxygen from oxides and silicates for isotopic analysis: Geochimica et Cosmochimica Acta, v. 27, p. 43-52.

Colvine, A.C., 1989, An empirical model for the formation of Archean gold deposits: products of final cratonization of the Superior Province, Canada: Economic Geology Mongraph 6, p. 37-53.

Colvine, A.C., Andrews, A.J., Cherry, M.E., Durocher, M.E., Fyon, A.J., Lavigne, M.J., Macdonald, A.J., Marmont, S., Poulsen, K.H., Springer, J.S., and Troop, D.G., 1984, An integrated model for the origin of Archean lode gold deposits: Ontario Geolocal Survey, Open File Report 5524, 98p.

Colvine, A.C., Fyon, J.A., Heather, Marmont, S., Smith, P.M., and Troop, D.G., 1988, Archean lode gold deposits in Ontario: Ontario Geological Survey Miscellaneous Paper 139, 136p.

Compton, J., Williams, L.B., and Ferrell JR, R.E., 1992, Mineralization of organogenic ammonium in the Monterey Formatin, Santa Maria and San Joaquin basins, California, USA: Geochimica et Cosmochimica Acta, v. 56, P. 1979-1991.

Coney, J.P., 1989, Structural aspects of suspect terranes and accretionary tectonics in western North America: Journal of Structural Geology, v. 11, p. 107-125.

Cooper, D.C., and Bradley, A.D., 1990, The ammonium content of granites in the English Lake: Geological Magazine, v. 127, p. 579-586.

Cooper, J.A., and Ding, P.Q., 1997, Zircon ages constrain the timing of deformation events in the Granites-Tanami region, northwest Australia: Australian Journal of Earth Sciences, v. 44, p. 777-788.

Cooper, R.A., and Tulloch, A.J., 1992, Early Paleozoic terranes in New Zealand and their relationship to the Lachlan flod belt: Tectonophysics, v. 214, p. 129-144.

Coutinho, M.G.N., and Alderton, D.H.M., 1998, Character and genesis of Proterozoic shear zone-hosted gold deposits in Borborema Province, northeast Brazil: Institution of Mining and Metallurgy, Transactions, Section B: Applied Earth Scince, v. 107, p. 109-119.

Cowan, D.S., Brandon, M.T., and Garver, J.I., 1997, Geologic tests of hypotheses for large coastwise displacements – A critique illustrated by the Baja British Columbia Controversy: American Journal of Science, v. 297, p. 117-178.

Cox, P.A., 1995, The Elements on Earth: Inorganic Chemistry in the Environment, Part II, Oxford, University Press, Oxford, p. 197-209.

Cox, S.F., Ceplecha, J., Wall, V.J., Etheridge, M.A., Cas, R.A.F., Hammond, R., and Willman, C., 1983, Lower Ordovician Bendigo trough sequence, Castlemaine area, Victoria: deformational style and implications for the evolution of the Lachlan Fold Belt: Geological Society of Australia Abstract 9, p. 41-42.

Cox, S.F., Etheridge, M.A., Cas, R.A.F., and Clifford, B.A., 1991b, Deformational style of the Castlemaine area, Ballarat-Bendigo Zone: implications for the evolution of crustal structure in central Victoria: Australian Journal of Earth Sciences, v. 38, p. 151-170.

Cox, S.F., Sun, S-S., Etheridge, M.A., Wall, V.J., and Potter, T.F., 1995, Structural and geochemistry controla on the development of turbidite-hosted gold quartz vein deposits, Wattle Gully Mine, Central Victoria, Australia: Economic Geology, v. 90, p. 1722-1746.

Cox, S.F., Wall, V.J., Etheridge, M.A., and Potter, T.F., 1991a, Deformational and metamorphic processes in the formation of mesothermal vein-hosted gold deposits-examples from the Lachlan fold belt in central Victoria, Australia: Ore Geology Review, v. 6, p. 391-423.

Cranfield, L.C., Shorten, G., Scott, M., and Barker, R.M., 1997, Geology and mineralization of the Gympie Province. In: Ashley, P.M., Flood, P.G., eds., Tectonics and Metallogenesis of the New England Orogen: Geological Society of Australia, Special Publication, Springwood, NSW, Australia, v. 19, p 128-147.

Craw, D., 2000, Fluid flow at fault intersections in an active oblique collision zone, southern Alps, New Zealand: Journal of Geochemical Exploration, v. 69-70, p. 523-526.

Craw, D., Windle, S.J., and Angus. P.V., 1999, Gold mineralization without quartz veins in a ductile-brittle shear zone, Macraes Mine, Otago Schist, New Zealand: Mineralium Deposita, v. 34, p. 382-394.

Crawford, A.J., 1988, Cambrian, *in* Douglas, J.G., and Ferguson, J.A., eds., Geology of Victoria, 2nd ed., Victorian Division of the Geological Society of Australia, Melbourne, p. 37-62.

Curti, E., 1987, Leas and oxygen isotope evidence for the origin of the Monte Rosa gold lode deposits (Western Alps, Italy): A comparison with Archean lode deposits: Economic Geology, v. 82, p. 2115-2140.

Curtis, S.F., Pattrick, R.A.D., Jenkin, G.R.T., Fallick, A.E., Boycee, A.J., and Treagus, J.E., 1993, Fluid inclusion and stable isotope study of the fault-related mineralization in Tyndrum area, Scotland: Trans. Inst. Min. Metall. V. 102, p. B39-B47.

Czamanske, G.K., Kunilov, V.E., Zientek, M.L., Cabri, L.J., Likhachev, A.P., Calk, L.C., and Oscarson, R.L., 1992, A proton-microprobe study of magmatic sulfide ores from the Noril'sk-Talnakh district, Siberia: Canadian Mineralogist, v. 30, p. 249-287.

Dahl, P.S., Holm, D.K., Gardner, E.T., Hubacher, F.A., and Foland, K.A., 1999, New constraints on the timing of Early Proterozoic tectonism in the Black Hill (south Dakota), with implications for docking of the Wyoming province with Laurentia: Geological Society of American Bulletin, v. 111, p. 1335-1349.

Dalpe, C., Baker, D.R., and Sutton, 1995, Synchrotron X-ray-fluorescence and laser-ablation ICP-MS microprobes: Useful instruments for analysis of experimental run-products: Canadian Mineralogist, v. 33, p.481-498.

Darbyshire, D.P.F., Pitfield, P.E.J., and Campbell, 1996, Late Archean and Early Proterozoic gold-tungsten mineralization in the Zimbabwe Archean craton: Rb-Sr and Sm-Nd isotope constraints: Geology, v. 24, p. 19-22.

Darimont, A., Burke, E., and Touret, J., 1988, Nitrogen-rich metamorphic fluids in Devonian metasediments from Bastogene, Belgium. Bull. Mineral. v. 111, p. 321-330.

Dauphas, N., and Marty, B., 1999, Heavy nitrogen in carbonatites of the Kola eninsulaL A possible signature of the deep mantle: Science, v. 286, p. 2488-2490.

de Ronde, C.E.J., and de Wit, M.J., 1994, The tectonothermal evolution of the the Barberton greenstone belt, south Africa: 490 million years of crustal evolution: Tectonics, v. 13, pp. 983-1005.

de Ronde, C.E.J., Faure, K., Bray, C.J., and Whitford, D.J., 2000, Round Hill shear zone-hosted gold deposits, Macraes Flat, Otago, New Zealand: Evidence of a magmatic ore fluid: Economic Geology, v. 95, p. 1025-1048.

de Ronde, C.E.J., Spooner, E.T.C., de Wit, M.J., and Bray, C.J., 1992, Shear zone-related Au quartz vein deposits in the Barberton greenstone belt, South Africa: Field and petrological characteristics, fluid properties, and light stable isotope geochemistry: Economic Geology, v. 88, p. 366-402.

de Ronde, C.EJ., Kamo, S.L., Davis, D.W., de Wit, M.J., and Spooner, E.T.C., 1991, Field, geochemical, and U-Pb isotopic constraints from hypabyssal felsic intrusion within the Barberton greenstone belt, South Africa: implications for tectonics and the timing of gold mineralization: Precambrian Research, v. 49, pp. 261-280.

Dee, S.J., and Roberts, S., 1993, Late-kinematic gold mineralization during regional uplift and the role of nitrogen: An example from the La Codosera area, W.Spain: Mineralogical Magazine, v. 57, p. 437-450.

Deines, P., Harris, J.W., and Gurney, J.J., 1991, The carbon isotopic composition and nitrogen content of lithospheric and asthenospheric diamonds from the Jagersfontein and Koffieontein kimberlites, South Africa: Geochimica et Cosmochimica Acta, v. 53, p. 2615-2626.

Deines, P., Harris, J.W., and Gurney, J.J., 1993, Depth-related carbon isotope and nitrogen concentration variability in the mantle below the Orapa kimberlite, Botswana, Arfica: Geochimica et Cosmochimica Acta, v. 57, p. 2781-2796.

Delsemme, A., 1998, Our Cosmic Origins from the Big Bang to the Emergence of Life and Intelligence: Cambridge University Press, Cambridge, United Kingdom, p. 155-193.

Delwiche, C., and Steyn, P.L., 1970, Nitrogen isotope fractionations insoils and microbial reactions: Environmental Science & Technology, v. 4, p. 929-935.

Drake, M., 2000, Accretion and primary differentiation of the Earth: A personal journey: Geochimica et Cosmochimica Acta, v. 64, p. 2363-2370.

Drew, L.J., Berger, B.R., and Kurbanov, N.K., 1996, Geology and structural evolution of the Muruntau gold deposit, Kyzylkum desert, Uzbekistan: Ore Geology Reviews, v. 11, p. 175-196.

Drew, L.J., Berger, B.R., and Kurbanov, N.K., 1998, Gelogy and structural evolution of the Muruntau gold deposits, Kyzylkum Desert, Uzbekistan: Global Tectonics and Metallogeny 6, p. 177-180.

Driver, L.A., Creaser, R.A, Chacko, T., and Erdmer, P., 2000, Petrogenesis of the Cretaceous Cassiar batholith, Yukon0British Columbia, Canada: Implications for magmatism in the North American Cordilleran Interior: GSA Bulletin, v. 112, p. 1119-1133.

Drummond, M.S., Defant, M.J., and Kepezhinskas, P.K., 1996, Petrogenesis of slab-derived trondhjemite-tonalite-dacite/adakites: Trans. Royal Soc.Edinburgh Sci. v. 87, p. 205-215.

Dubessy, J., and Ramboz, C., 1986, The history of organic nitrogen from early diagenesis to amphibolite facies: mineralogical, chemical, mechanical and isotope implications: Abstract Progam International Symposium On water-rock Interaction Vth, p. 170-174.

Dufresne, A., 1960, Selenium and tellurium in meteorites: Geochimica et Cosmochimica Acta, v. 20, p. 141-148.

Duit, W., Jansen, J.B.H., Breemen, A.V., and Bos, A., 1986, Ammonmium micas in metamorphic rocks as exemplified by Dome de Líagout (France): American Journal of Science, v.286, p. 703-732.

Durocher, M.E., and Hugon, H., 1983, Structural geology and hydrothermal alteration in the Flat Lake-Howwey Bay deformation zone, Red Lake area, in White, O.L., Barlow, R.B., and Colvine, A.C., eds., Summary if Field Work, 1983: Ontario Geological Survey, Miscellaneous Paper 116, 313p.

Eckstrand, O.R., and Humbert, L.J., 1987, Selenium and the source of sulfur in magmatic nickel and platinum deposits: Geological Association of Canada-Mineralogical Association of Canada, Program with Absract, v. 12, p. 40.

Eckstrand, O.R., Grinenko, L.N., Krouse, H.R., Paktunc, A.D., Schwann, P.L., and Scoates, R.F.J., 1989, Preliminary data on sulfur isotopes and Se/S ratios, and the

source of sulphur in magmatic sulphides from the Fox River Sill, Molson Dykes and Thompson nickel deposits, northern Manitoba: in Current Research, Part C, Geological Survey of Canada, Paper 89-1C, p. 235-242.

Ehrlich, H.L., Geomicrobiology. Marcel Dekker Inc., New York, p. 262-275.

Eilu, P., 1999, FINGOLD – a public database on gold deposits in Finland: Geological Survey of Finland, Report Investigations, v. 146, 224p.

Elder, D., and Cashman, S.M., 1992, Tectonic control and fluid evolution in the Quartz Hill, California, lode gold deposits: Economic Geology, v. 87, p. 1795-1812.

Elevevold, S., and Andersen, T., 1993, Fluid evolution during metamorphism at increaing pressure: carbon -and nitrogen-bearing fluid inclusions in granulites from Oksfjord, north Norwegian Caledonides: Contributions to Mineralogy and Petrology, v. 114, p. 236-246.

Epstein, S., Graf, D.L., and Degens, E.T., 1963, Oxygen isotope studies on the origin of dolomites, *in* Craig, H., Miller, S.L., and Wasserburg, G.J., eds., Isotope and Chemistry, North-Holland Publishing Company, Amsterdam, p. 169-180.

Exley, R.A., Boyd, S.R., Mattey, D.P., and Pillinger, C.T., 1986/87, Nitrogen isotope geochemistry of basaltic glasses: Implications for mantle degassing and structure?: Earth and Planetary Science Letters, v. 81, p. 163-174.

Fedorowich, J., Stauffer, M., and Kerrich, R., 1991, Structural setting and fluid characteristics of the Proterozoic Tartan Lake gold deposit, Trans-Hudson orogen, northern Manitoba: Economic Geology, v. 86, p. 1434-1467.

Ferguson, S.A., Buffam, B.S.W., Carter, O.F., Griffis, A.T., Holmes, T.C., Hurst, M.E., Jones, W.A., Lane, H.C., and Langley, C.S., 1968 Geology and ore deposits of Tisdale Township, District of Cochrane: Ontario Department of Mines, Geological Report 58, 177p.

Fergusson C.L., Gray, D.R., and Cas, R.A.F., 1986, Overthrust terranes in the Lachlan Fold Belt, southeastern Australia: Geology, v. 14, p. 519-522.

Ferkous, K., and Monie, P., 1997, Petrostructural data and 40Ar/39Ar laser probe dating of the Pan-African shearing and related gold-mineralization in the East In Ouzzal district (Western Hoggar, Algeria). In Papunen, H., ed., Research and Exploration – Where Do They Meet? Balkema, Rotterdam, p. 185-189.

Field, C.W., and Fifarek, R.H., 1985, Light stable isotope systematics in the epithermal environment: Reviews in Economic Geology, v. 2, p. 99-128.

Fornarii, M., Herail, G., 1991, Lower Paleozoic gold occurrences in the 'Eastern Cordillera' of southern Peru and northern Bolivia: a genetic model. In: Ladeira, E.A., ed., Brazil Gold'91, Balkema, Rotterdam, p. 135-142.

Fortes, P.T.F.O., Cheilletz, Z., Giuliani, G., and Féraud, G., 1997, Brasiliano age (500 ± 5 Ma) for the Mina III gold deposit, Crixás greenstone belt, central Brazil: International Geology Review, v. 39, p. 449-460.

Foster, D.A., 1997, Gold mineralization in Europe – characteristics and tectonic setting: Miner. Ind. 24-31.

Foster, D.A., Gray, D.R., Kwak, T.A.P., and Bucher, M., 1998, Chronology and tectonic framework of turbidite-hosted gold deposits in the Western Lachlan Fold Belt, Victoria, $^{40}Ar/^{39}Ar$ results: Ore Geology Reviews, v. 13, p.229-250.

Foster, R.P., and Piper, D.P., 1993, Archean lode-gold deposits in Africa: Crustal setting, metallogenesis and cratonization: Ore Geology Reviews, v.8, p.303-347.

Franchi, I.A., Wright, I.P., and Pillinger, C.T., 1993, Constraints on the formation conditions of iron meteorites based on concentrations and isotopic compositions of nitrogen: Geochimica et Cosmochimica Acta, v. 57, p. 3105-3121.

Fryer, B.J., Jackson, S.E., and Longerich, H.P., 1995, The design, operation and role of the laser-ablation microprobe coupled with an inductively coupled plasma-mass spectrometer (LAM-ICP-MS) in the earth sciences: Canadian Mineralogist, v. 33, p. 303-312.

Fyfe, W.S, Price, N.J., and Thompson, A.B., 1978, Fluids in the earth crust: Amsterdam, Elsevier, 383p.

Fyfe, W.S., 1978, The evolution of the earth's crust: modern plate tectonics to ancient hot spot tectonics?: Chemical Geology, v. 23, p. 89-114.

Fyon, J.A., Schwarcz, H.P., and Crocket, H.J., 1984, Carbonatization and gold mineralization in the Timmins area Abitibi greenstone belt: genetic links with Archean mantle-CO2-degassing and lower crust granulitizaon: Geological Association of Canada Program wit Abstracts, v. 9, p. 65.

Fyon, J.A., Troop, D.G., Marmon, S., and Macdonald, A.J., 1989, Introduction of gold into Archean crust, Superior Province, Ontario--coupling between mantle-initiated magmatism and lower crustal thermal maturation: Economic Geology Mono.6. p. 479-490.

Galloway, J.N., Schlesinger, W.H., Levy II, H., Michaels, A., and Schnoor, J.L., 1995, Nitrogen fixation: Anthropogenic enhancement-environmental response: Global Biogeochemical Cyclies, v. 9, p. 235-252.

Gao, Z.L., and Kwak, T.A.P., 1995, Turbidite-hosted gold deposits in the Bendigo-Ballarat and Melbourne zones, Australia. I. Geology, mineralization, stable isotopes, and implications for exploration: International Geology Reviews, v. 37, p. 910-944.

Garba, I., 1996, Tourmalinization related to late Proterozoic-early Paleozoic lode gold mineralization in the Bin Yauri area, Nigeria: Minerlaium Deposita, v. 31, p. 201-209.

Gartz, V.H., and Frimmel, H.E., 1999, Complex metamorphism of an Archean placer in the Witwatersrand Basin, South Africa: The Ventersdrop contact reef – A hydrothermal aquifer? Economic Geology, v. 94, p. 689-706.

Gebre-Mariam, M., Groves, D.I., McNaughton, N.J., Mikucki, E.J., and Vearncombe, J.R., 1993, Archean Au- Ag mineralization at Racetrack, near Kalgoorlie, Western

Australia: a high crustal-level expression of the Archean composite lode-gold system: Mineral. Deposita, v. 28, p. 3 75-387.

Ghazi, A.M., Vanko, D.A., Roedder, E., and Seeley, R.C., 1993, Determination of rare earth elements in fluid inclusions by inductively coupled plasma-mass spectrometry (ICP-MS): Geochimica et Cosmochimica Acta, v. 57, p. 4513-4516.

Ghazi, A.M., Vanko, D.A., Ruiz, J., McCandless, T., and Roedder, E., 1994, Trace and rare element analysis in single fluid inclusions: An application of laser ablation ICP-MS: EOS 75 (44), p. 695.

Gibbons, W., Doig, R., Gordon, T., Murphy, B., Reynolds, P., and White, J.C., 1998, Mylonite to megabreccia: tracking fault events within a transcurrent boundary in Nova Scotia, Canada: Geology, v. 24, p. 411-414.

Glassley, W.E., Bridgwater, D., and Konnerup-Madsen, J., 1984, Nitrogen in fluids effecting retrogression of granulite facies gneisses: a debatable mantle conection: Earth and Planetary Science Letters, v. 70, p. 417-425.

Goldfarb, R.J., Groves, D.I., and Gardoll, S., 2001, Orogenic gold and geologic time: A global synthesis: Ore Geology Reviews, v. 18, p. 1-75.

Goldfarb, R.J., Hart, C., Miller, M., Miller, L., Farmer, G.L., and Groves, D.I., 2000, The Tintina Gold Belt – a global perspective. The Tintina Gold Belt: Concept, Exploration, and Discoveries: British Columbia and Yukon Chamber of Mines. Vancouver, p 5-34.

Goldfarb, R.J., Leach, D.L., Miller, M.L., and Pickthorn, W.J., 1986, Geology, metamorphic setting, and genetic constraints of epigenetic lode-gold mineralization within the Cretaceous Valdez Group, south-central Alaska. In: Keppie, J.D., Boyle, R.W., and Haynes, S.J., eds., Turbidite-Husted Gold Deposits: Geological Association of Canada Special Paper, v. 32, p. 87-105.

Goldfarb, R.J., Leach, D.L., Rose, S.C., and Landis, G.P., 1989, Fluid inclusion geochemistry of gold-bearing quartz veins of the Juneau gold belt, southeastern Alaska: Implications for orer genesis: Economic Geology Monograph 6, p. 363-375.

Goldfarb, R.J., Miller, L.D., Leach, D.L., and Snee, L.W., 1997, Gold deposits in metamorphic rocks in Alaska: Economic Geology Monograph 9, p. 151-190.

Goldfarb, R.J., Newnerry, R.J., Pickthorn, W.J., and Gent, C.A., 1991b, Oxygen, hydrogen, and dulfur isotope dtudies in the Juneau gold belt, Southeastern Alaska: constraints on the origin of hydrothermal fluids: Economic Geology, v. 86, p. 66-80.

Goldfarb, R.J., Phillips, G.N., and Nokleberg, W.J., 1998, Tectonic settings of synorogenic gold deposits of the Pacific Rim: Ore Geology Reviews, v. 13, p. 185-218.

Goldfarb, R.J., Snee, L.W., and Pickthorn, W.J., 1993, Orogenesis, high-T thermal events, and gold vein formation within metamorphic rocks of the Alaskan Cordillera: Mineralogical Magazine, v. 57, p. 375-394.

Goldfarb, R.J., Snee, L.W., Miller, L.D., and Newberry, R.J., 1991a, Rapid dewatering of the crust deduced from ages of mesothermal gold deposits: Nature, v. 354, p. 296-298.

Golding, S.D., McNaughton, N.J., Barley, M.E., Groves, D.I., Ho, S.E., Rock, N.M.S., and Turner, J.V., 1989, Archean carbon and oxygen reservoirs: their significance for fluid sources and circulation paths for Archean mesothermal gold deposits of the Norseman-Wiluna Belt, Western Australia: Economic Geology Monograph 6, P. 376-388.

Goodfellow, W.D., and Peter, J.M., 1999, Reply: Sulphur isotope composition of the Brunswick no. 12 massive sulphide deposit, Bathurst Mining Camp, New Brunswick: implications for ambient environment, sulphur source, and ore genesis: Canadian Journal of Earth Science, v. 36, p. 127-134.

Goryachev, N.A., and Edwards, A.C., 1999, Gold metallogeny of North East Asia: PACRIM'99. The Australasian Institute of Mining and Metallury, Carlton, Victoria, Australia, p. 287-302.

Graney, J.R., and Kesler, S.E., 1995, Factors affecting gas analysis of inclusion fluid by quadrupole mass apectrmetry: Geochimica et Cosmochimica Acta, v. 59, p. 3977-3986.

Gray, D.R., 1988, Structure and tectonics, in Douglas, J.G., and Ferguous J.A. eds., Geology of Victoria, Geological Society of Australia, Victoria Division, Melbourne, p. 1-36.

Gray, D.R., and William, C.E., 1991, Deformation in the Ballarat slate belt, central Victoria, and implications for the crustal structure across southeast Australia: Australian Journal of Earth Science, v. 38, p. 171-201.

Greenland, L., 1967, The abundances of selenium, tellurium, silver, palladium, cadmium, and zinc in chondritic meteorites: Geochimica et Cosmochimica Acta, v. 31, p. 849-860.

Gregory, R.T., Gray, D.R., and Durney, D.W., 1988, Regional oxygen isotope distributions in quartz veins from the Lachlan fold belt, Australia: a new tectonostratigraphic mapping tool: EOS, Transactions, American Geophysical Union, v. 69, p. 1434.

Groves, D.I., 1993, The crustal continuum model for late-Archaean lode-gold deposits of the Yilgarn Block, Western Australia: Mineralium Deposita, v. 28, p. 366-374.

Groves, D.I., and Phillips, G.N., 1987, The genesis and tectonic controls on Archean lode gold deposits of the Western Australian ahield: a metamorphic-replacement model: Ore Geology Reviews, v. 2, p. 287-322.

Groves, D.I., Barley, M.E., and Ho, S.E., 1989, Nature, genesis, and tectonic setting of mesothermal gold mineralization in the Yilgarn Block, Western Australia: Economic Geology Monograph 6, P. 71-85.

Groves, D.I., Goldfarb, R.J., Grebre-Mariam, M., and Robert, F., 1998, Orogenic gold deposits: A proposed classification in the context of their crustal sidtribution and relationship to other gold deposit types: Ore Geology Reviews, v. 13, p. 7-27.

Groves, D.I., Golding, S.D., Rock, N.M.S., Barley, M.E., and McNaughton, N.J., 1988, Archean carbon reservoirs and their relevance to the fluid source for gold deposits: Nature, v. 331, p. 254-257.

Groves, D.I., Phillips, N., Ho, S.E., Houstoun, S.M., and Standing, C.A., 1987, Craton-scale distribution of Archean greenstone gold deposits: Predictive capacity of the metamorphic model: Economic Geology, v. 82, p. 2045-2058.

Guen, M.L., Lescuyer, J.L., and Marcoux, E., 1992, Lead-isotope evidence for a Hercynain origin of the Salsigne gold deposit (Southern Massif Central, France): Mineralium Deposita, v. 27, p. 129-136.

Guha, J., Lu, H., Dube, B., Robert, F., and Gagnon, M., 1991, Fluid charateristics of vein and altered wall rock in Archean mesothermal gold deposits: Economic Geology, v. 86, p. 667-684.

Guidotti, C.V., and Sassi, F.P., 1998, Petrogenetic significance of Na-K white mica mineralogy: Recent advances for metamorphic rocks: European Journal of Mineralogy, v. 10, p. 815-854.

Guilhaumou, N., Dhamelincourt, P., Touray, J.C., and Touret, j., 1981, Etude des inclusions fluids du systeme N_2-CO_2 de dolomites et de quartz de Tunisie septentrionale. Donnees de la micrcryoscopie et de I'analyse a la microsonde a effet Raman: Geochimica et Cosmochimica Acta, v. 45, p. 657-673.

Gulson, B.L., Mizon, K.J., and Atkinson, B.T., 1993, Source and timing of gold and other mineralization in the Red Lake area, northwestern Ontario, based on lead-isotope investigations: Canadian Journal of Earth Sciences, v. 30, p. 2366-2379.

Haeberlin, Y., Moritz, R., Cosca, M., Chiaradia, M., and Fontbote, L., 1999, The Pataz gold province: a Peruvian record of a major crustal-scale hydrothermal event during the Variscan: Journal of Conference Abstracts 4, p.479.

Haendel, D., Muhle, K., Nitzsche, H.M., Stiehl, G., and Wand, U., 1986, Isotopic variations of the fixed nitrogen in metamorphic rocks: Geochimica et Cosmochimica Acta, v.50, p.749-758.

Haeussler, P.J., Bradley, D., Goldfarb, R.J., Snee, L.W., and Taylor, C.D., 1995, Link between ridge subduction and gold mineralization in southerm Alaska: Geology, v. 23, p. 995-998.

Hall, A., 1987, The ammonium content of Caledonian granites: Journal of the Geological Society, London, v. 144, p. 671-674.

Hall, A., 1988, The distribution of ammonium in granites from Southwest England: Journal of the Geological Society, London, v. 145, p. 37-41.

Hall, A., 1989, Ammonium in spilitized basalts of southwest England and its implications for the recycling of nitrogen: Geochemical Journal, v. 23, p. 19-23.

Hall, A., 1999, Ammonium in granites and its petrogenetic significance: Earth-Science Reviews, v. 45, p. 145-165.

Hall, A., and Liverton, T., 1992, Trace ammonium in granites of the southern Yukon and its petrogenetic significance: Yukon Geology, v. 3, p. 45-51.

Hall, A., and Neiva, A.M.R., 1990, Distribution of the ammonium ion in pegmatites, aplites and their minerals from central northern Portugal: Mineralogical Magzine, v. 54, p. 455-461.

Hall, A., and Stamatakis, M.G., 1992, Ammonium in zeolitized tuffs of the Karlovassi Basin, Samos, Greece: Canadian Mineralogist, v. 30, p. 423-430.

Hall, A., Bencini, A., and Poli, G., 1991, Magmatic and hydrothermal ammonium in granites of the Tuscan magmatic province, Italy: Geochimica et Cosmochimica Acta, v. 55, p. 3657-3664.

Hall, A., Stamatakis, M.G., and Walsh, N.J., 1994, Ammonium enrichment associated with diagenetic alteration in Tertiary pyroclastic rocks from Greece: Chemical Geology, v. 118, p. 173-183.

Hallam, M., and Eugster, H.P., 1976, Ammonium silicate stability relations: Contributions to Mineralogy and Petrology, v. 57, p. 227-244.

Hamilton, J.V., and Hodgson, C.J., 1986, Mineralization and structure of the Kolar gold field, India. In: MacDonald, A.J., ed., Gold'86: An International Symposium on the Geology of Gold Deposits, Toronto, p. 270-283.

Hamlyn, P.R., Keays, R.R., Cameron, W.E., Crawford, A.J., and Waldron, H.M., 1985, Precious metals in magnesian low-Ti lavas: implications for melaogenesis and sulfur saturation in primary magmas: Geochimica et Cosmochimica Acta, v. 49, p. 1797-1811.

Hanschmann, G., 1981, Berechnung von isotopieeffekten auf quantenchemischer grundlage am beispiel stickstoffhaltiger molekule: Zfl-Mitt., v. 41, p. 19-31.

Hart, C., Goldfarb, R.J., Qiu, Y., Snee, L.W., Miller, L.D., Miller, M.L., and Nie, F.-J., 2002, Gold deposits of the northern margin of the North China craton: Mineralium Deposita, v. 36, in press.

Hattori, K, 1993, Diverse metal sources of Archean gold deposits: Evidence from in situ lead-isotope analysis of individual grains of galena and altaite in the Ross and Kirkland Lake deposits, Abitibi Greenstone belt, Canada: Contributions to Mineralogy and Petrology, v. 113, p. 185-195.

Hayashi, K., and Ohmoto, H., 1991, Solubility of gold in NaCl- and H_2S-bearing aqueous solutions at 250-350 C: Geochimica et Cosmochimica Acta, v. 55, p. 2111-2126.

Haynes, S.J., 1987, Classification of quartz veins in turbidite-hosted gold deposits, greenschist facies, eastern Nova Scotia: CIM Bulletin, p. 37-51.

Heather, K.B., and Aria, Z.G., 1987, Geological setting of gold mineralization in the Goudreau-Lochalsh area, district of Algoma, in Barlow, R.B., Cherry, M.E., Colvine,

A.C., Dressler, B.O., and White, O.L., eds., Summary of Field Work and Other Actities: Ontario Geological Survey, Miscellanceous Paper 137, p. 155-162.

Heaton, T.H.E., 1986, Isotopic study of nitrogen pollution in the hydrosphere and atmosphere: A review: Chemical Geology, v. 59, p. 87-102.

Herrington, H.H., 1995, Late Archean structure and gold mineralization in the Kadoma region of the Midlands greenstone belt, Zimbabwe. In: Coward, M.P., Reis, A.C., eds., Early Precambrian Preocesses: Geological Society of London Special Publication, v. 95, p. 173-191.

Hertogen, J., Janssens, M.J., and Palme, H., 1980, Trace elements in ocean ridge basalt glasses: implications for fractionation during mantle evolution and petrogenesis: Geochimica et Cosmochimica Acta, v. 44, p. 2125-2143.

Hinde, S., 1989, Central Deborah: Perth, University of Western Australia, University Extension Publication 13, p. 28-31.

Hirner, A.V., Graf, W., Treibs, R., Melzer, A.N., and Hahn-Weinheimer, P., 1984, Stable sulfur and nitrogen isotopic compositions of crude oil fractions from Southern Germany: Geochimica et Cosmochimica Acta, v. 48, p. 2179-2186.

Ho, S.E., Groves, D.I., McNaughton, N.J., Mikucki, E.J., 1992, The source of ore fluids and solutes in Archean lode gold deposits of Western Australia: Journal of Volcanology and Geothermal Research, v. 50, p. 173-196.

Hobbie, E.A., Macko, S.A., and Shugart, H.H., 1998, Patterns in N dynamics and N isotopes during primary succession in Glacier Bay, Alaska: Chemical Geology, v. 152, p. 3-11.

Hodgson, C.J., 1983, The structure and geological development of the Porcupone camp – A re-evaluation, in Colvine, A.C., ed., The Geology of Gold in Ontario: Ontario Geological Survey, Miscellaneous Paper 110, p. 211-225.

Hodgson, C.J., 1989, The structure of shear-related, vein-type gold deposits: a review: Ore Geology Review, v. 4, p.231-273.

Hodgson, C.J., and MacGreehan, P.J., 1982, A review of the Geological characteristics of 'gold-only' deposits in the Superior Province of the Canadian Shield, in Hodder, R.W., and Petruk, W., eds., Geology of Canadian Gold Deposits: Canadian Institute of Mining Special Vol. 24, p. 211-229.

Hodgson, C.J., Love, D.A., and Hamilton, J.V., 1993, Giant mesothermal gold deposits, in Whiting, B.H., Hodgson, C.J., Mason, R. Ed., Giant Ore Deposits: Society of Economic Geology Special Publication 2, p. 157-211.

Hoefs, J., 1987, Stable isotope feochemistry: New York, Springer-Verlag, 241p.

Hoering, T.C., 1955, Variations in nitrogen-15 in naturally occurring substances: Science, v. 122, p. 1233-1234.

Home, S.R., Mclelan, J., Sigman, D.M., Fry, B., and Peterson, B.J., 1998, Measuring $^{15}N\text{-}NH_4^+$ in marine, estuarine, and fresh water: An adaptation of the ammonia

diffusion methods for samples with low ammonium concentrations: Marine Chemistry, v. 60, p. 235-243.

Honma, H., 1996, Hammonium contents in the 3800 Ma Isua supracrustal rocks, central West Greeland: Geochimica et Cosmochimica Acta, v. 60, p. 2173-2178.

Honma, H., and Itihara, Y., 1981, Distribution of ammonium in minerals of metamorphic and granite rocks: Geochimica et Cosmochimica Acta, v. 45, p. 983-988.

Hopkins, D.W., Wbeatley, R.E., and Robinson, D., 1998, Stable isotope studies of soil nitrogen, *in* Griffiths, H., ed., Stable Isotopes – integration of biological, ecological and geochemical processes: BIOS Scientific Publishers Ltd., U.K., p. 75-88.

Hoppe, P., Amari, S., Zinner, E., and Lewis, R.S., 1995, Isotopic compositions of C, N, O, Mg, and Si, trace element abundances, and morphologies of single circumstellar graphite grains in four density fractions from the Murchism meteorite: Geochimica et Cosmochimica Acta, v. 59, p. 4029-4056.

Howard III, J.H., 1977, Geochemistry of selenium: formation of ferroselite and selenium behavior in the vicinity of oxidizing sulfide and uranium deposits: Geochimica et Cosmochimica Acta, v. 41, p. 1665-1678.

Hrdy, F., and Kyser, F., 1995, Origin, timing, and fluid charateristics of an auriferous event: The proterozoic Jasper lode gold deposit, Saskatchewan, Canada: Economic Geology, v.90, p. 1918-1933.

Huot, D. Sattran, V., and Zida, P., 1987, Gold in Birrimian green stone belts of Burkina Faso, West Africa: Eeconomic Geology, v. 82, p. 2033-2044.

Huston, D.L., Sie, S.H., Suter, G.F., Cooke, D.R., and Both, R.A., 1995, Trace elements in sulfide minerals from eastern Australian volcanic-hosted massive sulfide deposits: Part I, Proton microprobe analyses of pyrite, Chalcopyrite, and sphalerite, and Part II. Selenium levels in pyrite: composition with $\delta^{34}S$ values and implications for the source of surfur in volcanogenic hydrothermal systems: Economic Geology, v. 90, p. 1167-1196.

Huston, D.L., Taylor, T., Fabray, J., and Patterson, D.J., 1992, A comparison of the geology and mineralization of the Balcooma and Dry River South volcanic-hosted massive sulfide deposits, northern Queensland: Eeonomic Gelogy, v. 87, p. 785-811.

Hutchinson, R.W., 1975, Lode gold deposits; the case for volcanogenic derivation: 5th Money Session and Gold Technical Session, Pacific Northwest Metals and Minerals Conference, Oregon Dept. Geol., Miner. Ind. Publ., p. 64-105.

Hutchinson, R.W., 1987, Metallogeny of Precabrian gold deposits: Space and time relationships: Economic Geology, v. 82, p. 1993-2007.

Ibrahim, M.S., and Kyser, T.K., 1991, Fluid inclusion and isotope systematics of the high-temperature Proterozoic Star Lake lode gold deposits, northern Sasatchewan, Canada: Economic Geology, v. 8, p. 1468-1490.

Iewis, R.S., Anders, E., Wright, I.P., Norris, S.J., and Pillinger, C.T., 1983, Isotopically anomalous nitrogen in primitive meteorites: Nature, v. 305, p. 767-771.

Injerd, W.D., and Kaplan, I.P., 1974, Nitrogen isotope distribution in meteorites: Meteoritis, v. 9, p. 352-353.

Irving, E., Thorkelson, D.J., Wheadon, P.M., and Enkin, R.J., 1995, Paleomagnetism of the Spences Bridge Group and northward displacement of the Intermontene Belt, British Columbia: A second look: Journal of Geophysical Research, v. 100, p. 6057-6071.

Irving, E., Wynne, P.J., Thorkeson, D.J., and Schiarizza, P., 1996, Large (1000 to 4000 km) northward movements of tectonic domains in the northern Cordillera, 83 to 45 Ma: Journal of Geophysical Research, v. 101, p. 17,901-17,916.

Isley, A.E., and Abbott, D.H., 1999, Plume-related mafic volcanism and the deposition of banded iron formation: Journal of Geophysical Research, v. 104, p. 15,461-15,477.

Itihara, Y., and Honma, H., 1979, Ammonium in biotite from metamorphic and granitic rocks of Japan: Geochimica et Cosmochimica Acta, v. 43, p. 503-509.

Itihara, Y., and Suwa, K., 1985. Ammonium contents of biotites from Precambrian rocks in Finland: The significance of NH_4^+ as a possible chemical fossil: Geochimica et cosmochimica Acta, v. 49. 145-151.

Itihara, Y., and Tainosho, Y., 1989, Ammonium and insoluble nitrogen in precambriam rocks from the Gawler craton, Australia: Inference of life activity: Journal of the Geological Society of Japan, v. 95, p. 439-445.

Itihara, Y., Suwa, K., and Hoshino, M., 1986, Organic matter in the Kavirondian sedimentary rocks of Archean period in Kenya: Geochemical Journal, v. 20, p. 201-207.

Ivanov, S.M., Ansdell, K.M., and Melrose, D.L., 2000, Ore texture and stable isotope constraints on ore deposition mechanisms at the Kumtor lode gold deposit, in Bucci, L.A., and Mair, J.L., eds., Gold in 2000: Extended Abstract Volume, p. 47-52.

Jackson, S.L., and Cruden, A.R., 1995, Formation of Abitibi greenstone belt by arc-trench migration: Geology, v. 23, p. 471-474.

Jacobson, M.C., Charlson, R.J., Rodhe, H., and Orians, G.H., 2000, Earth System Science from Biogeochemical Cycles to Global Change: International Geophysics Series, v. 72, 527p.

Jaffe, D.A., 2000, The nitrogen cyclie, in Jacobson, M.C., Charlson, R.J., Rodhe, H., and Orians, G.H., eds., Earth System Science: International Geophysics Series, v. 72, P. 321-342, Academic Press, San Diego.

Jarvis, K.E., and Williams, J.G., 1993, Laser ablation inductively coupled plasma mass spectrometry (LA-ICP-MS): A rapid technique for the direct, quantitative determination of major, trace and rare-earth elements in geological samples: Chemical Geology, v. 106, p. 251-262.

Javoy, M., 1995, The integral enstatite chondrite model of the earth: Geophysical Research Letters, v. 22, p. 2219-2222.

Javoy, M., 1997, The major volatile elements of the Earth: Their origin, behavior, and fate: Geophysical Research Letters, v. 24, p. 177-180.

Javoy, M., 1998, The birth of the Earth's atmosphere: the behaviour and fate od its major elements: Chemical Geology, v. 147, p. 11-25.

Javoy, M., and Pineau, F., 1983, Stable isotope constraints on a model Earth from a study of mantle nitrogen: Meteoritics, v. 18, p. 320-321.

Javoy, M., and Pineau, F., 1991, The volatiles record of a "popping" rock from the Mid Atlantic Ridge at 14° N: chemical and isotopic composition of gas trapped in the vesicles: Earth and Planetary Science Letters, v. 107, p. 598-611.

Javoy, M., and Pineau, F., and Delorme, H., 1986, Carbon and nitrogen isotopes in the mantle: Chemical Geology, v. 57, p. 41-62.

Javoy, M., Pineau, F., and Allègre, C.J., 1982, Carbon geodynamic cycle: Nature, v. 300, p. 171-173.

Javoy, M., Pineau, F., Demaiffe, D., 1984, Nitrogen and carbon isotopic composition in the diamonds of Mbuji Mayi (Zaïre): Earth and Planetary Scicence Letters, v. 68, p. 399-412.

Jensen, L.S., 1980, Archean gold mineralization in the Kirkland Lake – Larder Lake area, in Roberts, R.G., ed., Genesis of Archean, Volcanic Hosted Gold Deposits: Ontario Geological Survey, Open File Report 5293, p. 280-302.

Jia, Y., 2002, ^{15}N-enriched nitrogen in the Archean Atmosphere-crust-mantle systems: GAC-MAC Annual Meeting, Saskatoon, May 27-29, 2002.

Jia, Y., and Kerrich, 2000, Nitrogen and carbon isotope data for quartz veins in the southern Mother Lode gold province, California: Constraints on the origin of the hydrothermal fluids: GSA Annual Meeting, Abstracts with programs, p. A84.

Jia, Y., and Kerrich, R. 2001, Nitrogen recycling in the atmosphere-crust-mantle systems: Evidence from secular variation of crustal N abundances and $\delta^{15}N$ values, Archean to Present: EOS, Transactions, American Geophysucal Union, v. 82, p. F695.

Jia, Y., and Kerrich, R., 1999, Nitrogen isotope evidence for a metamorphic origin of mesothermal lode gold deposits: GAC-MAC Annual Meeting, Abstract Volume 24, p. 57-58.

Jia, Y., and Kerrich, R., 1999, Nitrogen isotope systematics of mesothermal lode gold deposits: Metamorphic, granitic, meteoric water, or mantle origin? Geology, v. 27, p. 1051-1054.

Jia, Y., and Kerrich, R., 2000, Giant quartz vein systems in accretionary orogenic belts: The evidence for a metamorphic fluid origin from $\delta^{15}N$ and $\delta^{13}C$ studies: Earth and Planetary Science Letters, v. 184, pp. 211-224.

Jia, Y., and Kerrich, R., 2001, Secular variation of crustal N content and $\delta^{15}N$ through time from Archean to Recent: Geology (submitted).

Jia, Y., Kerrich, R., and Goldfarb, R.J., 2001, Metamorphic Origin of Ore-Forming fluids for Orogenic Gold Quartz Vein Systems in the North American Cordillera: Constraints from δD, $\delta^{15}N$, $\delta^{18}O$ and Se/S: Economic Geology (submitted).

Jia, Y., Li, X., and Kerrich, R., 2000, A fluid inclusion study of Au-bearing quartz vein systems in the Central and North Deborah Deposits of the Bendigo gold field, central Victoria, Australia: Economic Geology, v. 95, pp. 467-496.

Jia, Y., Li, X., and Kerrich, R., 2001, Stable isotope (O, H, S, C, and N) systematics of quartz vein systems in the turbidite hosted Central and North Deborah gold deposits of the Bendigo goldfield, central Victoria, Australia: Constraints on the origin of ore-forming fluids: Economic Geology, v. 96, p. 705-721.

Jonasson, I.R., and Sangster, D.F., 1983, A preliminary report on the gold content of sulfide separates from some Canadian base-metal deposits: in Current Research, Part B, Geological Survey of Canada, Paper 83-1B, p. 47-52.

Junge, F., Seltmann, R., and Stiehl, G., 1989, Nitrogen isotope characteristics of breccias, granitoids and greisens from eastern Erzgebirge tin ore deposits (Sadisdorf: Altenberg), G.D.R: Proc. 5th Working Meeting Isotopes in Nature, Leipzig, p. 321-332.

Juster, T.C., Brown, P.E., and Bailey, S.W., 1987, NH_4^+-bearing illite in very low grade metamorphic rocks associated with coal, northeastern Pennsylvania: Armerican Mineralogist, v. 72, p. 555-565.

Kaltoft, K., Schlatter, D.M., and Kludt, L., 2000, Gold occurrences and lead isotopes in Ketilidian mobile belt, south Greenland: Trans. Inst. Min. Metall. V. 109, pp. B23-B33.

Kao, S.J., and Liu, K.K., 2000, Stable carbon and nitrogen isotope systematics in a human-disturbed watershed (Lanyang-His) in Taiwan and the estimation of biogenic particulate organic carbon and nitrogen fluxes: Global Biogeochemical Cycles, v. 14, p. 189-198.

Kent, A.J.R., and Hagemann, S.G., 1996, Constraints on the timimg of lode-gold mineralization in the Wiluna greenstone belt, Yilgarn craton, Western Australia: Australian Journal of Earth Science, v. 43, p. 573-588.

Kent, A.J.R., and McDougall, I., 1995, Constraints on the timing of gold mineralization in the Kalgoorilie goldfield, Western Australia, from 40Ar/39Ar and U-Pb dating: Evidence for multiple mineralization episodes: Economic Geology, v. 90, p. 845-859.

Kent, A.J.R., Cassidy, K.F., and Fanning, C.M., 1996, Archean gold mineralization syschronous with the final stages of cratonization, Yilgarn craton, Western Australia: Geology, v. 24, p.879-882.

Kerrich, R., 1987, The stable isotope geochemistry of Au-Ag vein deposits in metamorphic rocks: Mineralogical Association of Canada Short Course Handbook, v. 13, p. 287-336.

Kerrich, R., 1989, Geodynamic setting and hydraulic regimes: shear zone hosted mesothermal gold deposits, in Bursnall, J.T. ed., Mineralization and Shear Zones: Geological Association of Canada Short Course Notes 6, p. 89-128.

Kerrich, R., 1990, Carbon isotope systematics of Archean Au-Ag vein deposits in the Superior Province: Canadian Journal of Earth Sciences, v. 27, p. 40-56.

Kerrich, R., 1994, Dating Archean auriferous quartz vein deposits in the Abitibi greenstone belt, Canada: $^{40}Ar/^{39}Ar$ evidence for a 70-100 m.y.-time gap between plutonism-metamorphism and mineralization. A discussion: Economic Geology, v. 89, p. 679-686.

Kerrich, R., and Allison, I., 1978, Flow mechanism in rocks: microscopic and mesocopic structures, and their relation to physical conditions of deformation in the crust: Geoscience of Canada, v. 5, p. 110-118.

Kerrich, R., and Cassidy, K.F., 1994, Temporal relationships of lode-gold mineralization to accretion, magmatism, metamorphism and deformation, Archean to present: A review: Ore Geology Review, v. 9, p.263-310.

Kerrich, R., and Fryer, B.J., 1979, Archean precious-metal hydrothermal systems, Dome mine, Abitibi greenstone belt. II REE and oxygen isotope relations: Canadian Journal of Earth Sciences, v. 16, p. 440-458.

Kerrich, R., and Watson, G.P., 1984, The Macssa Mine Archean lode gold deposits, Kirkland Lake, Ontario: Geology, patterns of alteration, and hydrothermal regimes: Economic Geology, v. 79, p. 1104-1130.

Kerrich, R., and Wyman, D., 1990, Geodynamic setting of mesothermal gold deposits: an association with accretionary tectonic regimes: Geology, v. 18, p. 882-885.

Kerrich, R., Goldfarb, R. J., Groves, D. I. Garwin, S., and Jia, Y., 2000, The characteristics, origins, and geodynamic settings of supergiant gold metallogenic provinces: Science in China, v. 43, pp. 1-68.

Kerrich, R., and Ludden, J., 2000, The role of fluids during formation and evolution of the Southern Superior Province lithosphere: A review: Canadian Journal of Earth Sciences, v.37, p. 135-165.

Kerrich, R., Wyman, D., Hollings, P., and Polat, A., 1999, Variability of Nb/U and Th/La in 3.0 to 2.7 Ga Superior Province ocean plateau basalts: implications for the timing of continental growth and lithosphere recycling: Earth and Planetary Science Letters: v. 168, p. 101-115.

Kerrick, D.M., and Caldeira, K., 1998, Metamorphic CO_2 degassing from orogenic belts: Chemical Geology, v. 145, p. 213-232.

Kerridge, J.F., 1982, Nitrogen isotope systematics in meteorites: Meteoritics, v. 17, p. 235-236.

Kerridge, J.F., 1985,Carbon, hydrogen and nitrogen in carbonaceous chondrites: Abundances and isotopic compositions in bulk samples: Geochimica et Cosmochimica Acta, v. 49, p. 1707-1714.

Khan, A.A., and Baur, W.H., 1972, Salt hydrates: VIII. The crystal structures of sodium ammonium orthochromate dehydrate and magnesium diammonium bis (hydrogen orthophosphate) tetrahydrate and a discussion of the ammonium ion: Acta Crystallgr. B28, p. 683-693.

Khiltova, V.Y., and Pleskach, G.P., 1997, Yenisey fold belt. In: Rundqvist, D.V., Gillen, C., eds., Precambrian Ore Deposits of the East European and Siberian Craton: Elsevier, Amsterdam, pp. 289-316.

King, J., and Helmstaedt, H., 1997, The Slave Province, North-West Territory, Canada. In: de Wit, M., Ashwal, L.D., eds., Greenstone Belts: Clarendon Press, Oxford, pp. 459-479.

King, R.W., and Kerrich, R., 1987, S/Se and trace element systematics of auriferous pyrite in Abitibi mesothermal Au deposits: Geological Society of Canada-Mineralogical Society of Canada, Abstract, v. 14, p. 3.

Kishida, A., and Kerrich, R., 1987, Hydrothermal alteration zoning and gold concentration at the Kerr-Addison Archean lode gold deposit, Kirkland Lake, Ontario: Economic Geology, v. 82, p. 649-690.

Kisters, A.F.M., Kolb, J., and Meyer, F.M., 1998, Gold mineralization in high-grade metamorphic shear zones of the Renco mine, southern Zimbabwe: Economic Geology, v. 93, pp. 598-601.

Kistler, R.W., and Silberman, M.L., 1983, Isotopic studies of mariposite-bearing rocks from the south-central Mother Lode, Calfornia: California Geology, Sept. 1983, p. 201-203.

Kistlers, A.F.M., Meyer, F.M., Seravkin, I.B., Znamensky, S.E., Kosarev, A.M., and Ertl, R.G.W., 1999, The geologic setting of lode-gold deposits in the central southern Urals: a review: Geol. Rundsch. V. 87, p. 603-616.

Knight, J.T., Groves, D.I., and Ridley, J.R., 1993, The Coolgardie goldfield, Western Australia: district-scale controls on an Archean gold camp in an amphibolite facies terrane: Mineral. Deposita, v. 28, p. 436-456.

Kolb, J., Kisters, A.M.F., Hoernes, S., and Meyer, F.M., 2000, The origin of fluids and nature of fluid-rock interaction in mid-crust auriferous mylonites of the Renco mine, southern Zimbabwe: Mineralium Deposita, v. 35, p. 109-125.

Konstantinov, M., Dankovtsev, R., Simkin, G., and Cherksov, S., 1999, Deep structure of the north Enisei gold district (Russia) and setting of ore deposits: Geol. Ore Deposits, v. 41, p. 425-436.

Kontak, D.J., and Kerrich, R., 1995, Geological and geochemical studies of a metaturbidite-hosted lode gold deposit: The Beaver Dam deposit, Nova Scotia: II. isotopic studies: Economic Geology, v. 90, p. 885-901.

Kontak, D.J., Smith, P.K., Peynolds, P., and Taylor, K., 1990, Geological and 40Ar/39Ar geochronological constraints on the timing of quartz vein formation in Meguma Group lode-gold deposits, Nova Scotia: Atlantic Geology, v. 26, p. 201-227.

Koval, V.B., Koptyukh, Y.M., Yaroshchuk, M.A., Fomin, Y.A., and Lapusta, V.F., 1997, Gold ore deposits of the Ukrainian Shield (Ukraine): Geol. Ore Deposits, v. 39, p. 294-310.

Kreulen, R., and Schuling, R.D., 1982, N_2-CH_4-CO_2 fluid during formation of the Dome de líAgout, France: Geochimica et Cosmochimica Acta, v. 46, p. 193-203.

Kreulen, R., Breemen, A.V., and Duit, W., 1986, Nitrogen and carbon isotopes in metamorphic fluids from the Dome de I'Agout, France, in: Geochronology, Cosmochronolgy and Isotope Geology, 5th International Conference, p. 191.

Krivolutskaya, N.A., 1997, Paragenetic associations of minerals and formation conditions of the Klyuchevsk gold deposit (East Transbaikal region): Russian Geol. Ore Deposits, v. 39, p. 294-310.

Krogstad, E.J., Balakrishnan, S., Mukhopadhyay, D.K., Rajamani, V., and Hanson, G.N., 1989, Plate tectonics 2.5 billion years age: Evidence at Kolar, South India: Science, v. 243, p. 1337-1340.

Kuhns, S., Ogola, J., and Sango, P., 1990, Regional setting and nature of gold minerlaization in Tanzania and southwest Kenya: Precambrian Research, v. 46, pp. 71-82.

Kung, C.C., and Clayton, R.N., 1978, Nitrogen abundances and isotopic compositions in stony meteorites: Earth and Planetary Science Letters, v. 38, p. 421-435.

Kushev, V.G., and Kornilov, M.F., 1997, The Ukrainian Shield, in Greenstone Belts, de Wit, M.J., and Ashwal, L.D., eds., Oxford Monographs on Geology and Geophysics, Oxford University Press, Oxford, United Kingdom, p. 726-729.

Kyser, T.K., and O'Neil, J.R., 1984, Hydrogen isotope systematics of submarine basalts: Geochimica et Cosmochimica Acta, v. 48, p. 2123-2133.

Lambert, I.B., Phillips, G.N., and Groves, D.I., 1984, Sulfur isotope compositions and genesis of Archean gold mineralization, Australia and Zimbabwe, *in* Foster, R.P., ed., Gold'82: Rotterdam, Balkema, p. 373-387.

Landefeld, L.A., 1988, The geology of the Mother Lode gold belt, Sierra Nevada Foothills metamorphic belt, California: Bicentennial Gold 88, Extended Abstracts, Oral Programme. Geological Society of Australia, Melbourne, p. 167-172.

Lapointe, B., and Chown, E.H., 1993, Gold-bearing iron-formation in a granulite terrane of the Canadian Shield: a possible deep-level expression of an Archean gold-mineralization system: Mineral. Deposita, v. 28, p. 191-197.

Larin, A.M., Rytsk, Y.Y., Sokolov, Y.M., 1997, Baikal-Patom fold belt. In: Rundqvist, D.V., Gillen, C.,eds., Precambrian Ore Deposits of the East European and Siberian Cratons: Elsevier, Amsterdam, p. 317-362.

Lattanzi, P.F., Curti, E., and Bastogi, M., 1989, Fluid inclusion studies on the gold deposits of the Upper Anzasca Valley, Northwestern Alps, Italy: Economic Geology, v. 84, p. 1382-1397.

Lattanzi, P., Rye, D.M., and Rice, J.M., 1980, Behavior of 13C and 18O in carbonates during contact metamorphism at Marysville, Montana: implications for isotope systemaics in impure dolomitic limestone: American Journal of Science, v. 280, p. 890-906.

Lavigne, M.J., 1983, Gold deposits of the Geraldton area, in Wood, J., White, O.L., Barloe, R.B., and Colvine, A.C., eds., Summary of Field Work, 1983: Ontario Geological Survey, Miscellaneous Paper 116, 313p.

Lavigne, M.J., and Crocket, J.H., 1983, Geology of the East South C Ore Zone, Dickenson mine, in Milne, V.G., ed., Geoscience Research Grant Program, Summary of Research, 1986-87: Ontario Geological Survey, Miscellanceous Paper 136, p. 27-34.

LeAnderson, P.J., Yoldash, M., Johnson, P.R., and Offield, T.W., 1995, Structure, vein paragenesis, and alteration in the Al Wajh gold district, Saudi Arabia: Economic Geology, v. 90, p. 2262-2273.

Leitch, C.H.B., Dawson, K.M., and Godwin, C.I., 1989, Early late Cretaceous, Early Tertiary gold mineralization: A galena lead isotope study of the Bridge River mining camp, southwestern British Columbia: Economic Geology, v. 84, p. 2226-2236.

Leitch, C.H.B., Godwin, C.I., Brown, T.H., and Taylor, B.E., 1991, Geochemistry of mineralizing fluids in the Bralorne-Pioneer mesothermal gold vein deposits, British Columbia, Canada: Eeonomic Geology, v. 86, p. 318-353.

Lenoir, J.L., Liegeois, J.P., Thenunissen, K., and Klerkx, J., 1994, The Paleoproterozoic Ubendian shear belt in Tanzania: geoochronology and structure: Journal of African Earth Sciences, v. 19, p. 169-184.

Lewis, R.S., Anders, E., Wright, I.P., Norris, S.J., and Pillinger, C.T., 1983, Isotopically anomalous nitrogen in primitive meteorites: Nature, v. 305, p. 767-771.

Li, X., 1998, Genesis of the Bendigo gold deposits, central Victoria, Australia – geology, hydrothermal alteration, fluid inclusion, stable isotope and geochronology studies: unpublished PhD thesis, Latrobe University, Australia, P. 176-199.

Li, X., Kwak, T.A.P., and Brown, R., 1998, Wall rock alteration in the Bendigo gold ore field, Victoria, Australia; Uses in exploration: Ore Geology Reviews, v. 13, p. 381-406.

Lobato, L.M., Noce, C.M., Ribeiro-Rodrigues, L.C., Zucchetti, M., Baltazar, O.F., de Silva, L.C., and Pinto, C.P., 2001, The Archean Rio das Velhas greenstone belt in the Quadrlatero Ferrfero region, Mines Gerais, Brazil: Part II. Description of selected gold deposits: Mineralium Deposita, v. 36, in press.

Loftus-Hills, G., and Solomon, M., 1967, Cobalt, nickel and seleniumin sulfides as indicators of ore genesis: Mineralium Deposita, v. 2, p. 228-242.

Loucks, R.R., and Mavrogenes, J.A., 1999, Gold solubility in supercritical hydrothermal brines measured in synthetic fluid inclusions: Science, v. 284, p. 2159-2163.

Lu, A., and Seccombe, P.K., 1993, Fluid evolution in a slate-belt gold deposit-- A fluid inclusion study of the Hill End goldfield, NSW, Australia: Mineralium Deposita, v. 28, p. 310-323.

Lu, J., Seccombe, P.K., Foster, D., and Andrew, A.S., 1996, Timing of mineralization and source of fluids in a slate-belt auriferous vein system, Hill End goldfield, NSW, Australia – evidence from 40Ar.39Ar dating and 0- and H-isotopes: Lithos, v. 38, p. 147-165.

Lugmair, G.W., and Shukolyukov, A., 1998, Geochimica et Cosmochimca Acta, v. 62, p. 2863-

MacDonald, A.J., 1983, The Iron formation – gold association: evidence from Geraldton area, in Colvine, A.C., ed., The Geology of Gold in Ontario: Ontario Geological Survey, Miscellaneous Paper 110, p. 75-83.

MacRae, N.D., and Nesbitt, 1985/86, Grant 269 compositional charateristics of pyrite in Barren and gold mineralized veins: in Milne, V.G. ed., Geoscience Research Grant Program Summary of Research, 1986, p.219-225.

Madden-McGuire, D.J., Silberman, M.L., and Church, S.E., 1989, Geologic relationship, K-Ar ages and isotopic data from the Willow Creek gold mining district, southern Alaska: Economic Geology Monograph, v. 6, p. 242-251.

Madu, B.E., Nesbitt, B.E., and Muehlenbachs, K., 1990, A mesothermal gold-stibnite-quartz vein occurrence in the Canadian Cordillera: ECONOMIC GEOLOGY, v. 85, p. 1260-1268.

Maheux, P.J., 1989, A fluid inclusion and light stable isotope study of antimony-associated gold mineralization in the Bridge River district, British Columbia, Canada: Unpub. M.S. thesis, Univ. Alberta, 160p.

Manac'h, G., Lécuyer, C., and Juteau, T., 1999, Afluid inclusion and stable isotope study of hydrothermal circulation in a transform zone: Western Blanco Depression, northeast Pacific: Journal of Geophysical Research, v. 104, p. 12941-12969. Marty, B., 1995, Nitrogen content of the mantle inferred from N_2-Ar correlation in oceanic basalts: Nature, v. 377, p. 326-329.

Mao, J., Qiu, Y., Goldfarb,R.J., Zhang, Z., Xu, W., and Deng, J., 2002, Gold deposits in the Xiaoqinling-Xiong'ershan region, Qinling Mountains, central China: Mineralium Deposita, v. 36, in press.

Marignac, C., and Cuney, M., 1999, Ore Deposits of the french massif central: insight into the metallogenesis of the Variscan collision belt: Mineralium Deposita, v. 34, p. 472- 504.

Marshall, D., Meisser, N., and Taylor, R.P., 1998, Fluid inclusion, stable isotope, and Ar-Ar evidence for the age and origin of gold-bearing quartz veins at Mont Chemin, Awizerland: Mineralogy and Petrology, v. 62, p. 147-165.

Marty, B., 1995, Nitrogen content of the mantle inferred from N_2-Ar correlation in oceanic basalts: Nature, v. 377, p. 326-329.

Marty, B., and Humbert, F., 1997, Nitrogen and argon isotopes in oceanic basalts: Earth and Planetary Science Letters, v. 152, p. 101-112.

Marty, B., and Zimmermann, L., 1999, Volatiles (He, C, N, Ar) in mid-ocean ridge basalts: Assesment of shallow-level fractionation and characterization of source composition: Geochimica et Cosmochimica Acta, v. 63, p. 3619-3633.

Marty, B., Lenoble, M., and Vassard, N., 1995, Nitrogen, helium and argon in basalt: a static mass psectrometry study: Chemical Geology, v. 120, p. 183-195.

Mason, B., 1963, The carbonaceous chondrites: Space Science Review, v. 1, p. 621-646.

Matsuhisa, Y., Goldsmith, J.R., and Clayton, R.N., 1979, Oxygen isotope fractionation in the system quartz-albite-anorthite-water: Geochimica et Cosmochimica Acta, v. 43, p. 1131-1140.

Matthai, S.K., Henley, R.W., and Heinrich, C.A., 1995, Gold precipitation by fluid mixing in bedding-parallel fractures near carbonaceous slates at the Cosmopolitan Howley gold deposit, Northern Australia: Economic Geology, v. 90, p. 2123-2142.

Mawer, C.K., 1987, Mechanics of formation of gold-bearing quartz veins, Nova Scotia, Canada: Tectonophysics, v. 135, p. 99-119.

Mayewski, P.A., Lyons, W.B., Spencer, M.J., Twickler, M., Dansgaard, W., Koci, B., Davidson, C.I., and Honrath, R.E., 1986, Sulfate and nitrate concentrations from a South Greeland ice core: Science, v. 232, p. 975-977.

Mayne, K.L., 1957, Natural variations in the nitrogen isotope abundance ratios in igneous rocks: Geochimica et Cosmochimica Acta, v. 12, p. 185-189.

McArdle, P., 1989, Geological setting of gold mineralization in the Republic of Ireand: Trans. Inst. Min. Metall., v. 98, p. B7-B12.

McCoy, d., Newberry, R.J., Layer, P., Dimarchi, J.J., Bakke, A., Masterman, J.S., and Minehand, D.L., 1997, Plutonic-related gold deposits of interior Alaska: Economic Geology Monograph, v. 9, p. 191-241.

McCuaig, T.C., Kerrich, R., 1998, P-T-t-deformation-fluid charateristics of lode gold deposits: evidence from alteration systematics: Ore Geology Reviews, v. 12, p. 381-453.

McCuaig, T.C., Kerrich, R., Groves, D.I., and Archer, N., 1993, The nature and dimensions of reginal and local gold-related hydrothermal alteration in the tholeiitic metabasalts in the Norseman goldfields: the missing link in a crustal continuum of gold deposits? Mineralium Deposita, v. 28, p. 420-435.

McCuaig, T.C., Kerrich, R., Groves, D.I., and Archer, N., 1993, The nature and dimensions of regional and local gold-related hydrothermal alteration in tholeiitic metabasalts in the Norseman goldfelds: the missing link in a crustal coninuum of gold deposits: Mineralium Deposita, v. 28, p. 420-435.

McDonough, W.F., and Sun, S.S., 1995, The composition of the Earth: Chemical Geology, v. 120, p. 223-253.

Mckeag, S.A., and Craw, D., 1989, Contrasting fluids in gold-bearing quartz vein systems formed progressively in a rising metamorphic belt – Otago Schist, New Zealand: Economic Geology, v. 84, p. 22-33.

McKeag, S.A., and Craw, D., 1989, Contrasting fluids in gold-bearing quartz vein systems formed progressively in a rising metamorphic belt: Otago Schist, New Zealand: Economic Geology, v. 84, p. 22-33.

McNeil, A.M., and Kerrich, R., 1986, Archean lamprophyric dykes and gold mineralization, Matheson, Ontario: the conjunction of LIL-enriched mafic magmas,

deepcrustal structures and Au concentration: Canadian Journal of Earth Sciences, v. 23, p. 324-342.

Mikucki, E.J., and Ridley, J.R., 1993, The hydrothermal fluid of Archean lode-gold deposits at different metamorphic grades: composional constraints from ore and wallrock alteration assemblages: Mineralium Deposita, v. 28, p. 469-481.

Milledge, H.J., Mendelessohn, M.J., Seal, M., Rouse, J.E., Swart, P.K., and Pillinger, C.P.T., 1983, Carbon isotope variation in spectral type II diamonds: Nature, v. 303, p. 791-792.

Miller, L.D., Goldfarb, R.J., Gehrels, G.E., and Snee, L.W., 1994, Genetic links among fluid cycling, vein formation, regional deformation, and plutonism in the Juneau gold belt, southeastern Alaska: Geology, v. 22, p. 203-206.

Miller, L.D., Goldfarb, R.J., Hart, C.J.R., Nie, F.J., Miller, M.L., Yang, Y., and Liu, Y., 1998, North China gold – a product of multiple orogens: Society of Economic Geology Newsletter, v. 33 p. 6-12.

Miller, L.D., Goldfarb, R.J., Snee, L.W., Gent, C.A., and Kirkham, R.A., 1995, Structural geology, age, and mechanisms of gold vein formation at the Kensington and Jualin deposits, Berners Bay District, Southeast Alaska: Economic Geology, v.90, p. 343-368.

Milovskiy, A.V., and Volynets, V.F, 1966, Nitrogen in metamorphic rocks: Geochemistry International, v. 3, p. 752-758.

Mironoc, G., and Zhmodik, S.M., 1999, Gold deposits of the Urikkitoi metallogenic zone (Eastern Sayan, Russia): Geol. Ore Deposits, v. 41, p. 46-60.

Mironov, A.G., and Zhmodik, S.M., 1999, Gold deposits of the Urik-Kitoyskiy metallogenic zone, eastern Sayan, Russia: Geologiya Rudnykh Mestorozhdeniy, v. 41, p. 54-69.

Mishra, B., and Panigrahi, M.K., 1999, Fluid evolution in the Kolar gold field: evidence from fluid inclusion studies: Mineralium Deposita, v. 34, p. 173-181.

Moine, B., Guillot, C., and Gibert, F., 1994, Control of the composition of nitrogen-rich fluids originating from reaction with graphite and ammonium-bearing biotite: Geochimica et cosmochimica Acta, v. 58, p. 5503-5523.

Monger, J.W.H., 1993, Canadian Cordillera tectonics: from geosynclines to crustal collage: Canadian Journal of Earth Sciences, v. 30, p. 209-231,

Monger, J.W.H., 1999, Review of the geology and tectonics of the Canadian Cordillera: notes for a short course sponsored by the British Columbia Geological Survey Branch, 72p.

Morand, V.J., Ramsay, W.R.H., Hughes, M., And Stanley, J.M., 1995. The Southern Avoca Fault Zone: site of a newly identified "greenstone" belt in western Victoria: Australian Journal of Earth Science, v. 42, p.133-143.

Moravek, P., 1996a, Gold in metallogeny of the Central and Western European units of the Peri-Alpine Vriscan belt: Global Tectonic Metallogeny, v. 5, p. 145-163.

Moravek, P., 1996b, Gold deposits in Bohemia: Czech Geological Surevy, Prague, 96p.

Moreira, M., Breddam, K., Curtice, J., and Kurz, M.D., 2001, Solar neon in the Icelandic mantle: new evidence for an undegassed lowermantle: Earth and Planetary Science Letters, v. 185, p. 15-23.

Moreira, M., Kunz, J., and Allègre, C.J., 1998, Rare gas systematics on popping rock estimates of isotopic and elemental compositions in the upper mantle: Science, v. 279, p. 1178-1181.

Morgan, J.W., 1986, Ultramafic xenoliths: Clues to Earth's late accretionary history: Journal of Geophysical Research, v. 91, p. 12,375-12,387.

Morrison, C.A., Lambert, D.D., Morrison, R.J.S., Ahlers, W.W., and NIcholls, I.A., 1995, Laser ablation-inductively coupled plasma-mass spectrometry: An investigation of elemental responses and matrix effects in the analysis of geostandard materals: Chemical Geology, v. 119, p. 13-29.

Mueller, A.G., De Laeter, J.R., and Groves, D.I., 1991, Strotium isotope systematics of hydrothermal minerals from epigenetic Archean gold deposits in the Yilgarn Block, Western Australia: Economic Geology, v. 86, p. 780-809.

Muir, R.J., Ireland, T.R., Weaver, S.D., and Bradshaw, J.D., 1996, Ion microprobe dating of Paleozoic granitoids: Devonian magmatism in New Zealand and correlations with Australia and Antarctica: Chemical Geology, v. 127 p. 191-210.

Muller, P.J., 1977, C/N ratios in Pacific deep-sea sediments: Effect of inorganic ammonium and organic nitrogen compounds sorbed by clays: Geochimica et cosmochimica Acta, v. 41, p. 765-776.

Mumin, A.H., Fleet, M.E., and Longstffe, F.J., 1996, Evolution of hydrothermal fluids in the Ashanti gold belt, Ghana: Stable isotope geochemistry of carbonates, graphites, and quartz: Economic Geology, v. 91, p. 135-148.

Murakami, T., Utsunomiya, S., Imazu, Y., and Prasad, 2001, Direct evidence of late Archean to early Proterozoic anoxic atmosphere from a product of 2.5 Ga old weathering: Earth and Planetary Science Letters, v. 184, p. 523-528.

Murphy, P.J., and Roberts, S., 1997, Evolution of a metamorphic fluid and its role in lode gold mineralization in the Central Iberian Zone: Mineralium Deposita, v. 32, p. 59-474.

Murty, S.V.S., and Marti, K., 1994, Nitrogen isotope signatures in Cape York: Implications for formation of Group III A irons: Geochimica et Cosmochimica Acta, v. 58, p. 1841-1848.

Muzuka, A.N.N., Macko, S.A., and Pedersen, T.F., 1991, Stable carbon and nitrogen isotope compositions of organic matter from sites 724 and 725, Oman Margin, *in* Prell, W.L., and Niitsuma, N., eds., Proceeding ODP: Science Results, v. 117, p. 571-586

Myers, J.S., Shaw, R.D., and Taylor, I.M., 1996, Tectonic evolution of Proterozoic Australia: Tectonics, v. 15, p. 1431-1446.

Naganna, C., 1987, Gold mineralization in the Hutti mining area, Karnataka, India: Economic Geology, v. 82, p. 2008-2016.

Neall, F.B., and Phillips, G.N., 1987, Fluid-wall rock interaction in an Archean hydrothermal gold deposit: A thermodynammic model for the Hunt Mine, Kambalda: Economic Geology, v. 82, p. 169-1694.

Nedelhoffer, K.J., and Fry, B., 1981, Controls on natural ^{15}N and ^{13}C abundances in forest soil organic matter: Soil Science Society American Journal, v. 52, p. 1633-1640.

Neimark, L.A., Rytsk, E.Y., Ovchinnikova, G.V., Sergeeva, N.A., Gorokhovskii, B.M., and Skopintsev, V.G., 1995, Lead isotopes in gold deposits of the East Sayan (Russia): Geol. Ore Deposits, v. 37, p. 201-212.

Nesbitt, B.E., 1988, Gold deposit continuum: a genetic model for lode Au mineralization in the continental crust: Geology, v. 16, p. 1044-1048.

Nesbitt, B.E., Muehlenbachs, K., and Murowchick, J.B., 1989, Genetic implications of stable isotope charateristics of mesothermal Au deposits and related Sb and Hg deposits in the Canadian Cordillera: Economic Geology, v. 84, p. 1489-1506.

Nesbitt, B.E., Murowchick, J.B., and Muehlenbachs, K., 1986, Dual origin of lode gold deposits in the Canadian Cordillera: Geology, v. 14, p. 506-509.

Neumaye, P., Groves, D.I., Ridley, J.R., and Koning, C.D., 1993, Syn-amphibolite facies Archean lode gold mineralization in the Mt. York District, Pilbara Block, Western Australia: Mineralium Deposita, v. 28, p. 457-468.

Neumayr, P., Hagemann, S.G., and Couture, J.F., 2000, Structural setting, textures, and timing of hydrothermal vein systems in the Val d'Or camp, Abitibi, Canada: implications for the evolution of transcrustal, second- and third-order fault zones and gold mineralization: Canadian Journal of Earth Sciences, v. 37, p. 95-114.

Neumayr, P., Ridley, J.R., and Groves, D.I., 1995, Physicochemical conditions of fluid-wall rock interaction at amphibolite-facies conditions in two Archean hydrothermal gold deposits in the Mt. York district, Pilbara craton, Western Australia: Canadian Journal of Earth Sciences, v. 32, p. 993-1016.

Neumayr, P., Ridley, J.R., McNaughton, N.J., Kinny, P.D., Barley, M.E., and Groves, D.I., 1998, Timing of gold mineralization in the Mt. York district, Pilgangoora greenstone belt, and implications for the tectonic and metamorphic evolution of an area linking the western and eastern Pilbara craton: Precambrian Research, v. 88, p. 249-265.

Newberry, R.J., 2000, Mineral deposits and associated Mesozoic and Tertiary igneous rocks within interior Alaska and adjacent Yukon portions of the 'Tinina Gold Belt': a progress report. The Tinina Gold Belt: Concept, Exploration, and Discoveries: British Columbia and Yukon Chamber of Mines, Vancouver, p. 59-88.

Nokleberg, W.J., Bundtzen, T.K., Dawson, K.M., Eremin, R.A., Koch, R.D., Ratkin, V.V., et al., 1996, Significant metalliferous lode deposits and placer distrcts for the

Russian Far East, Alaska, and the Canadian Cordillera: U.S. Geological Survey Open-File Report, v. 96-513A, 385p.

Nokleberg, W.J., Bundtzen, T.K., Grybeck, D., Koch, R.D., Eremin, R.A., Rozenblum, I.S., et al., 1993, Metallogenesis of mainland Alaska and the Russian Northeast: Mineral deposits maps, models, and tables, metallogenic belt maps and interpretation, and references cited: U.S. Geological Survey, Open-File Report, v. 93-339, 222p.

Norcross, C.E., Davis, D.W., Spooner, E.T.C., and Rust, A., 2000, U-Pb and Pb-Pb age constraints on Paleoproterozoic magmatism, deformation and gold mineralization in the Omai area, Guyana Shield: Precambrian Research, v. 102, p. 69-86.

Norman, D.I., and Musgrave, J.A., 1994, N_2-Ar-He compositions in fluid inclusions: Indicators of fluid source: Geochimica et Cosmochimica Acta, v. 58, p. 1119-1131.

Norris, T.L., and Schaeffer, O.A., 1982, Total nitrogen content of deep sea basalts: Geochimica et Cosmochimica Acta, v. 46, p. 371-379.

O'Neil, J.R., 1986, Theoretical and experimental aspects of isotope fractionations: Reviews in Mineralogy, v. 16, p. 1-40.

O'Neil, J.R., and Taylor, H.P., 1969, Oxygen isotope equilibrium between muscovite and water: Journal of Geophysical Research, v. 74, p. 6012-6022.

Oberthür, T., Blenkinsop, T.G., Hein, U.F., Hoppner, M., Hohndorf, A., and Weiser, T.W., 2000, Gold mineralization in the Mazowe area, Harare-Bindura-Shamva greenston belt, Zimbabwe-Genetic relationships deduce from mineralogical, fluid inclusion and stable isotope studies, and the Sm-Nd isotopic composition of scheelites: Mineralium Deposita, v. 35, p. 138-156.

Oberthür, T., Vetter, U., Davis, D.W., and Amanor, J.A., 1998, Age constraints on gold mineralization and Paleoproterozoic crustal evolution in the Ashanti belt of southern Ghana: Precambrian Research, v. 89, p. 129-143.

Oberthür, T.U., Mumm, A.S., Vetter, U., Simon, K., and Amanor, J.A., 1996, Gold mineralization in the Ashanti belt of Ghana: genetic constraints of the stable isotope geochemistry: Economic Geology, v. 289-302.

Ohmoto, H., 1986, Stable isotope geochemistry of ore deposits: Reviews in Mineralogy, v. 16, p. 491-560.

Ohmoto, H., and Goldhaber, M.B., 1997, Sulfur and carbon isotopes, *in* Barnes, H.L., ed., Geochemistry of Hydrotheraml Ore Deposits: Wiley Interscience, New York, p. 435-486.

Ohmoto, H., and Rye, R.O., 1979, Isotopes of sulfur and carbon, in Barnes, H.L., ed., Geochemistry of Hydrothermal Ore Deposits: Wiley Interscience, New York, p. 509-567.

Olivo, G.R., Gauthier, M., Gariepy, C., and Carignan, J., 1996, Transamazonian tectonism and Au-Pd mineralization at the Caue mine, Itabira district, Brazil: Pb isotopic evidence: Journal of South American Earth Sciences, v. 9, p. 273-279.

Ortega, L., Vindel, E., and Beny, C., 1991, C-O-H-N fluid inclusions associated with gold-stibnite mineralization in low-grade metamorphic rocks, Mari Rosa mine, Cacers, Spain: Mineralogical Magazine, v. 55, p. 235-247.

Ostrom, N.E., Knoke, K.E., Hedin, L.O., Robertson, G.P., and Smucker, A.J.M., 1998, Temporal trends in nitrogen isotope values of nitrate leaching from an agricultural soil: Chemical Geology, v. 146, p. 219-227.

Owens, N.J.P., 1987, Natural variations in ^{15}N in the marine environment: Advance on Maraine Biology, v. 24, p. 389-451.

Owens, N.J.P., and Watts, L.J., 1998, 15N and the assimilation of nitrogen by marine phytoplankton: the past, present and future? *in* Griffiths, H., ed., Stable Isotopes – integration of biological, ecological and geochemical processes: BIOS Scientific Publishers Ltd., U.K., p. 257-283.

Ozima, M., 1989, Gases in diamonds: Annual review of Earth and Planetary Science, v. 17, p. 361-384.

Paktunc, A.D., Hulbert, L.J., and Harris, D.C., 1990, Partitioning of the platinum-group and other trace elements in sulfides from the Bushveld Complex and Canadian occurrences of nickel-copper sulfides: Canadian Mineralogist, v. 28, p. 475-488.

Pan, Y., and Fleet, M.E., 1995, The late Archean Hemlo gold deposit, Ontario, Canada: a review and synthesis: Ore Geology Reviews, v. 9, p. 455-488.

Panteleyev, A., 1985, Cassiar map area (104P/4,5): Geology in British Columbia 1977-1981, B.C. Ministry of Energy, Mines and Petroleum Resources, p. 188-190.

Parfenov, L.M., 1995, Tectonics and regional metallogeny of the Verkhoyansk-Kolyma region. In: Bundtzen, T.K., Fonseca, A.L., and Mann, R., eds., The Geology and Mineral Deposits of the Russian Far East: Alaska Miners Association, Anchorage, Alaska, p. 61-84.

Paterson, C.J., 1986, Controls on gold and tungsten mineralization in metamorphic-hydrothermal systems, Otago, New Zealand. In: Keppie, J.D., Boyle, R.W., Haynes, S.J., eds., Turbidite-Hosted Gold Deposits: Geological Association of Canada Special Paper, v. 32, p. 25-39.

Paterson, I.A., 1977, Geology and evolution of the Pinchi fault zone at the Pinchi Lake, central British Columbia: Canadian Journal of Earth Sciences, v. 14, p. 1324-1342.

Perkins, C., and Kennedy, A.K., 1998, Permo-Carboniferous gold epoch of Northeast Queensland: Australian Journal of Earth Sciences, v. 45, p. 185-200.

Perkins, W.T., Pearce, N.J.G., and Jeffries, T.E., 1995, Laser ablation inductively coupled plasma mass spectrometry: A new technique for determination of trace and ultra-trace elements in silicates: Geochimica et Cosmochimca Acta, v. 57, p.475-482.

Peters, K.E., Sweeney, R.E., and Kaplan, I.R, 1978, Correlation of carbon and nitrogen stable ratios in sedimentary organic matter: Limnology and Oceanography, v. 23. p. 598-604.

Peters, S.C., 1993, Polygenetic melange in the Hodgkinson goldfield, northern Tasman orogenic zone: Australian Journal of Earth Sciences, v. 40, p. 115-129.

Peters, S.G., Golding, S., and Dowling, K., 1990, Melange-and sediment-hosted gold-bearing quartz veins, Hodgkinson goldfield, Queensland, Australia: Economic Geology, v. 15, p. 312-327.

Pettke, T., and Diamond, L.W., 1997, Oligocene glod quartz veins at Brusson, NW Alps: Sr isotopes tracce the source of ore-bearing fluid to over a 10-Km depth: Economic Geology, v. 92, p.389-406.

Pettke, T., Diamond, L.W., Villa, I.M., 1999. Mesothermal gold veins and metamorphic devolatilization in the northwestern Alps: the temporal link: Geology, v. 27, p. 641-644.

Phillips G.N., and Hughes M.J., 1996, The geology and gold deposits of the Victorian gold province: Ore Geology Reviews, v. 11, p. 255-302.

Phillips, G,N., and Groves, D.I., 1983, The nature of Archean gold-bearing fluids as deduced from gold deposits of Western Australia: Journal of the Geological Society of Australia, v. 30, p. 25-39.

Phillips, G.N., 1993, Metamorphic fluids and gold: Minerological Magazine, v. 57, p. 365-374.

Phillips, G.N., and Groves, D.I., 1983, The nature of Archean gold-bearing fluids as deduced from gold deposits of Western Australia: Journal of the Geological Society of Australia, v. 30, p. 25-39.

Phillips, G.N., and Myers, R.E., 1989, The Witwatersrand gold field: Part II. An origin for Witwatersrand gold during metamorphism and associated alteration: Economic Geology Monography 6, p. 597-607.

Phillips, G.N., and Powell, R., 1993, Link bewteen gold provinces: Economic Geology, v. 88, p 1084-1098.

Phillips, G.N., and Zhou, T., 1999, Gold-only deposits and Archean granites: SEG Newsletter, No. 37, April '99, p. 8-14.

Phillips, G.N., Groves, D.I., Amaro, D., Hallbauer, D.K., and Fotios, M.G., 1988, Morphology and trace-element compositions of pyrites from Kalgoorlie gold deposits: senstive indicators of syndeformational fluid regimes and depositional processes: Geology Department & University Extension, The University of West Australia, Publication 12, p. 217-226.

Phillips, G.N., Groves, D.I., and Martyn, J.E., 1984, An epigenetic origin for Archean banded iron-formation-hosted gold deposits: Economic Geology, v. 79, p. 162-171.

Phillips, G.N., Myers, R.E., and Palmer, J.A., 1987, Problems with the placer model for Witwatersrand gold: Geology, v. 15, p. 1027-1030.

Pickthorn, .J., Goldfarb, R.J., and Leach, D.L., 1987, Dual origins of lode gold deposits in the Canadian Cordillera: Comment: Geology, v. 15, p. 471-472.

Pinna, P., Cocherite, A., Jezequell, P., and Kayogoma, E., 1999, The Archean evolution of the Tanzanian craton (2.03-2.53 Ga): Journal of African Earth Science, v. 28, p. 62-63.

Pizzarello, S. et al., 2001, The organic content of the Tagish Lake meteorite: Science, v. 293, p. 2236-2239.

Polat, A., and Kerrich, R., 1999, Formation of an Archean tectonic melange in the Schreiber-Hemlo greenstone belt, Superior Prvince, Canada: implications for Archean subduction-accretion process: Tectonics, v. 18, p. 733-755,

Poujol, M., Robb, L.J., and Respaut, J.P., 1999, U-Pb and Pb-Pb isotope studies realting to the origin of gold mineralization in the Evander Goldfield, Witwatersrand Basin, South Africa: Precambrian Research, v. 95, p. 167-185.

Poujol. M., and Anhaeusser, C.R., 2001, The Johannesburg Dome, South Africa; new single zircon U-Pb isotopic evidence for early Archean granite-greenstone development within the central Kaapvaal craton: Precambrian Research, v. 108, p. 139-157.

Poulson, S.R., Chamberlain, C.P., and Friedland, A.J., 1995, Nitrogen isotope variation of tree rings as a potential indicator of environmental change: Chemical Geology, v. 125, p. 307-315.

Powell, R., Will, T.M., and Phillips, G.N., 1991, Metamorphism in Archean greenstone belts: calculated fluid compositions and implications for gold mineralization: Journal of Metamorphic Geology, v. 9, p. 141-150.

Powell, W.G., Carmichael, D.M., and Hodgson, C.J., 1995, Conditions and timimg of metamorphism in the southern Abitibi greenstone belt, Quebec: Canadian Journal of Earth Science, v. 32, p. 323-328.

Powell, W.G., Pattison, D.R.M., and Johnston, P., 1999, Metamorphic history of the Hemlo gold deposit from Al2SiO5 mineral assembladges, with implications for the timimg of mineralization: Canadian Journal of Earth Science, v. 36, p. 33-46.

Prombo, C.A., and Clayton, R.N., 1993, Nitrogen isotopic compositions of iron meteorites: Geochimica et Cosmochimica Acta, v. 57. p. 3749-3761.

Puchkov, V.N., 1997, Tectonics of the Urals – model concepts: Geotectonics, v. 31, p. 294-312.

Pyke, D.R., 1982, Geology of the Timmins area, district of Cochrane: Ontario Geological Survey Report, 219p.

Qiu, Y., and McNaughton, N.J., 1999, Source of Pb in orogenic lode-gold mineralization: Pb isotope constraints from deep crustal rocks from the southwestern Archean Yilgarn craton, Australia: Mineralium Deposita, v. 34, p. 366-381.

Quinn, P.K., Charlson, R.J., and Bates, T.S., 1988, Similtaneous observations of ammonia in the atmosphere and ocean: Nature, v. 335, p. 336-338.

Radhakrishna, B.P., and Curtis, L.C., 1994, How much gold is there at Hutti?: Journal of the Geological Society of India, v. 44, p. 359-366.

Ramsay, W.R.H., Bierlein, F.P., Arne, D.C., and VandenBerg, A.H.M., 1998, Turbidite-hosted gold deposits of central Victoria, Australia; their regional setting, mineralizing styles: Ore Geology Reviews, v. 13, p. 131-151.

Rapela, C.W., Pankhurst, R.J., Casquet, C., Baldo, E., Saavedra, J., and Galindo, C., 1998, Early evolution of the Proto-Andean margin of South America: Geology, v. 26, p. 707-710.

Rau, G.H., Arthur, M.A., and Dean, W.E., 1987, $^{15}N/^{14}N$ variations in Cretaceous Atlantic sedimentary sequences: Implication for past changes in marine nitrogen biogeochemistry: Earth and Plantary Science Letters, v. 82, p. 269-276.

Richards, J.R., and Singleton, O.P., 1981, Paleozoic Victoria, Australia: Igneous rocks, ages, and their interpretation: Geological Society of Australia Journal, v. 28, p. 395-421.

Richet, P., Bottinga, Y., and Javoy, M., 1977, A review of hydrogen, carbon, nitrogen, oxygen, sulfur, and chlorine stable isotope fractionation among gaseous molecules: Annual Reviews on Earth and Planetary Science, v. 5, p. 65-110.

Ridley, J., 1993, The relations between mean rock stress and fluid flow in the crust: With reference to vein-and lode-style gold deposits: Ore Geology Review, v. 8, p. 23-37.

Ridley, J., Miikucki, E.J., and Groves, D.I., 1996, Archean lode-gold deposits: Fluid flow and chemical evolution in vertically extensive hydrothermal systems: Ore Geology Reviews, v. 10, p. 279-293.

Rigby, D., and Batts, B.D., 1986, The isotopic composition of nitrogen in Australian coals and oil shales: Chemical Geology, v. 58, p. 273-282.

Ripley, E.M., 1990, Se/S ratios of the Virginia formation and Cu-Ni sulfide mineralization in the Babbitt area, Duluth Complex, Minnesota: Economic Geology, v. 85, p. 1935-1940.

Robert, F., 1990, Dating old gold deposits: Nature, v. 346, p. 792-793.

Robert, F., 1996, Quartz-carbonate vein gold. In: Eckstrand, O.R., Sinclair, W.D., Thorpe, R.I., eds., Geology of Canadian Mineral Deposit Types: The Geology og North America Geological Society of America, Boulder, CO, p. 350-366.

Robert, F., and Brown, A.C., 1986, Archean gold-bearing veins at the Sigms Mine, Abitibigreestone belt, Quebec: Part I. Geologic relations and formation of the vein system: Economic Geology, v. 81, p. 578-592.

Robert, F., and Epstein, S., 1982, The concentration and isotopic composition of hydrogen, carbon and nitrogen in carbonaceoous chondrites: Geochimica et Cosmochimica Acta, v. 44, p. 81-95.

Robert, F., and Kelly, W.C., 1987, Ore-forming fluids in Archean gold-bearing quartz veins at the Sigma Mine, Abitibi greenstone belt, Quebec, Canada: Economic Geology, v. 82, p. 1464-1482.

Robert, F., Poulsen, K.H., and Dubé, B., 1997, Gold deposits and their geological classification, *in* Gubins, A.G., ed., Proceedings of Exploration'97: Fourth Decennial International Conference on Mineral Exploration, GEO F/X. p. 209-220.

Roberts, F.I., 1982, Trace element chemistry of pyrite: a useful guide to the occurrence of sulfide base metal mineralization: Journal of Geochemical Exploration, v. 17, p. 49-62.

Rock, N.M.S., and Groves, D.I., 1988, Do lamprophyres carry gold as well as Diamonds?: Nature, v. 332, p. 253-255.

Rock, N.M.S., Groves, D.I., Perring, C.S., and Golding, S.D., 1989, Gold, lamprophyres, and porphyries: What does their association mean?: Economic Geology Monograph 6, p. 609-625.

Rose, A.W., 1967, Trace elements in sulfide minerals from the Central district, New Mexico and the Bingham district, Utah: Geochimica et Cosmochimica Acta, v. 31, p. 547-585.

Rowins, S.M., Groves, D.I., McNaughton, N.J., Palmer, M.R., and Eldrige, C.S., 1997, A reinterpretation of the role of granitoids in the genesis of Neoproterozoic gold mineralizatoin in the Telfer dome, Western Australia: Economic Geology, v. 92, p. 133-160.

Rushton, R.W., Nesbitt, B.E., Muehlenbachs, K., and Mortensen, J.K., 1993, A fluid inclusion and stable isotope study of Au quartz veins in the Klondikke District, Yukon Territory, Canada: A section through a mesothermal vein system: Economic Geology, v.88, p. 647-678.

Rumble, D.III., 1982, Stable isotope fractionation during metamorphic devolatilization reactions: Reviews in Mineralogy, v. 10, p. 327-353.

Ryall, W.R., 1977, Anomalous trace elements in pyrite in the vicinity of mineralized zones at Woodlawn, N.SW., Australia: Journal of Geochemical Exploration, v. 8, p. 73-83.

Rye, D.M., and Rye, R.O., 1974, Homestake gold mine, South Dakota: I. Stable isotope studies: Economic Geology, v. 69, p. 293-317.

Rytsk, E.Y., Neimark, L.A., and Amellin, Y.V., 1998, Paleozoic granitoids in the northern part of the Baikalian orogenic area: age and past geodynamic settings: Geotectonics, v. 32, p. 379-393.

Saager, R., Oberthur, T., and Tomschi, H.P., 1987, Geochemistry and mineralogy of banded iron-formation-hosted gold mineralization in the Gwanda greenstone belt, Zimbabwe: Economic Geology, v. 82, p. 2017-2032.

Sachs, J.P., and Rapeta, D.J., 1999, Ologotrophy and nitrogen fixation during eastern Mediterranean sapropel event: Science, v. 286, p. 2485-2488.

Sachs, J.P., Repeta, D.J., and Goericke, R., 1999, Nitrogen and carbon isotopic ratios of chorophyll from marine phytoplankton: Geochimica et Cosmochimica Acta, v. 63, p. 1431-1441.

Sadofshy, SJ., and Bebout, G.E., 2000, Ammonium partitioning and nitrogen-isotope fractionation among coexisting micas during high-temperature fluid-rock interactions: Examples from the New England Appalachians: Geochimica et Cosmochimica Acta, v. 64, p. 2835-2849.

Safonov, Y.G., 1997, Hydrothermal gold deposits – distribution, geological/genetic types, and productivity of ore-forming systems: Geol. Ore Deposits, v. 39, p. 20-32.

Sakai, H., Marais, D.M., Ueda, A., and Moore, J.G., 1984, Concentrations and isotope ratios of carbon, nitrogen and sulfur in ocean-floor basalts: Geochimica et Cosmochimica Acta, v. 48, p. 2433-2441.

Samson, I.M., Bas, B., and Holm, P.E., 1997, Hydrothermal evolution of auriferous shear zones, Wawa, Ontario: Economic Geology, v. 92, p.325-342.

Sandiford, M., and Keays, R.R., 1986, Structure and tectonic constraints on the origin of gold deposits in the Ballarat slate belt, Victoria, *in* Keppie, J. D., Boyle, R. W., and Haynes S. J. eds., Turbidite-hosted Gold Deposits, Geological Association of Canada Special Paper 32, p. 15-24.

Santos, D.O.S., Groves, D.I., Hartmann, L.A., Moura, M.A., McNaughton, N.J., 2001, Gold deposits of the Tapajos and Alta Floresta domains, Tapajos – Parima orogenic belt, Amazon craton, Brazil: Mineralium Deposits, v. 36, in press.

Santos, J.O.S., 1999, New understanding of the Amazon craton gold province, New Developments in Economic Geology: Central for Teaching and Research in Strategic Mineral Deposits, University of Western Australia, Nedlands, Western Australia.

Scalan, R.S., 1959, The isotopic composition, concentration and chemical state of the nitrogen in igneous rocks: unpublished Ph.D. thesis, University of Arkansas. "University Microfilms" Ann Arbor. Michigan Microfilm No. 59-1379.

Sccombe, P.K., 1977, Surfur isotope and trace metal composition of stratiform sulfides as an ore guide in the Canadian Shield: Journal of Geochemical Exploration, v. 8, p. 117-137.

Schidowski, M., Hayes, J.M., and Kaplan, I.R., 1983, Isotopic inferences of ancient biochemistry: carbon, sulfur, hydrogen and nitrogen, *in* Schopf, J.W. ed., Earth's Earliest Biosphere: Princeton, NJ, Princeton University Press, p. 149-186.

Schmidt-Mumm, A., Oberthur, T., and Blenkinsop, T.G., 1994, The Redwing gold mine, Mutare greenstone belt, Zimbabwe: a fluid-dynamic metallogenetic model. (Abstrcts) In: Schmidt-Mumm, A., ed., Abstracts Volume, Conference on Metallogenesis of Gold in Africa. Hannover, Germany, p. 71-72.

Schmus, W.R.Van., and Wood, J.A., 1967, A chemical-petrologic classification for the chondritic meteorites: Geochimica et Cosmochimica Acta, v. 31, p. 747-765.

Schramm, D.N., and Clayton, R.N., 1978, Did a supernova trigger the formation of the solar system?: Scientific American, v. 239, p. 124-139.

Seccombe, P.K., Lu, J., Andrew, A.S., Gulson, B.L., and Mizon, K.J., 1993, Nature and evolution of metamorphic fluids associated with turbidite-hosted gold deposits: Hill End goldfield, NSW, Australia: Minerological Magazine, v. 57, p. 423-436.

Seitz, J.C., Blencoe, J.G., Joyce, D.B., and Bodnar, R.J., 1994, Volumetric properties of CO_2-CH_4-N_2 fluids at 200 °C and 1000 bars: A comparison of equations of state and experimental data: Geochimica et Cosmochimica Acta, v. 58, p. 1065-1071.

Sharpe, E.N., and MacGeehan, P.J., 1990, Bendigo Goldfield: Australian Institute of Mining and Metallurgy Monograph 5, 1287-1296.

Shearer, G., and Kohl, D.H., 1993, Natural abundance of ^{15}N: Fractional contribution of two sources to a commsink and use of isotope discrimination, in Knowles, R., and Blackburn, T.H., eds., Nitrogen Isotope Techniques: Academic Press. Chapter 4, p. 89-124.

Shelto, K.L., So, C.S., and Chang, J.S., 1988, Gold-rich mesothermal vein deposits of the Repulic of Korea: Geochemical studies of the Jungwon gold area: Economic Geology, v. 83, p. 1221-1237.

Shelton, K.L., So, C.S., Haeussler, G.T., Lee, K.Y., and Chi, S.J., 1990, Geochemical studies of the Tongyong gold-sliver deposits, Republic of Korea: evidence of meteoric water dominace in a Te-bearing epithermal system: Economic Geology, v. 85, p.1114-1132.

Shepherd, T.J., and Chenery, S.R., 1995, Laser ablation ICP-MS elemental analysis of individual fluid inclusions: An evaluation study: Geochimica et Cosmochimca Acta, v. 59, p. 3997-4007.

Shikazono, N., 1978, Selenium content of acanthite and the chemical enviroments of Japanese vein-type deposits: Economic Geology, v. 73, p. 524-533.

Shukolyukov, A., and Lugmair, G.W., 1998, Isotopic evidence for the cretaceous-Tertiary impactor and its type: Science, v. 282, p. 927-929.

Sibson, R.H., Robert, F., and Poulsen, H., 1988, High angle faults, fluid pressure cycling and mesothermal gold-quartz deposits: Geology, v. 16, p. 551-555.

Sketchley, D.A., Sinclair, A.J., and Godwin, C.I., 1986, Early Cretaceous gold-silver mineralization in the Sylvester allochthon, near Cassiar, north central British Columbia: Canadian Journal of Earth Sciences, v. 23, p. 1455-1458.

Skirrow, R.G., Camacho, A., Layons, P., Pieters, P.E., Sims, J.P., Stuart-Smith, P.G., and Miro, R., 2000, Metallogeny of the southern Sierras Pampeanas, Argentina: geological, 40Ar./39Ar dating and stable isotope evidence for Devonian Au, Ag-Pb-Zn and W ore formation: Ore Geology Reviews, 17, p. 39-81.

Slack, J.F., Palmer, M.R., Stevens, B.P., and Barnes, R.G., 1993, Origin and significance of tourmaline-rich rocks in the Broken Hill District, Australia: Economic Geology, v. 88, p. 505-541.

Smith, D.S., 1997, Hydrothermal alteration at the mineral Hill mine, Jardine, Montana: Alower amphibolite facies Archean lode gold deposits of probabale synmetamorphic origin-A repley: Economic Geology, v.92, p. 378-379.

Smith, J.W., and Kaplan, I.P., 1970, Endogenous carbon in carbonaceous meteorites: Science, v. 167, p. 1367-1370.

Solomon, M., 1999, Discussion: Sulphur isotope composition of the Brunswick no. 12 massive sulphide deposit, Bathurst Mining Camp, New Brunswick: implications for ambient environment, sulphur source, and ore genesis: Canadian Journal of Earth Science, v. 36, p. 121-125.

Spiridonov, E.M., 1995, Inversion plutongenic gold quartz formation in the Caledonides of North Kazakhstan: Geologiya Rudnykh Mestorozhdeniy, v. 37, p. 179-207.

Stahl, W.J., 1977, Carbon and nitrogen isotopes in hydrocarbon research and exploration: Chemical Geology, v. 20, p. 121-149.

Stein, H.J., and Cathles, H.M., 1997, A special issue on thre the timing and duration of hydrothermal events: Economic Geology, v. 92, p. 763-765

Stein, H.J., Markey, R.J., Morgan, J.W., Hannah, J.L., Zak, K., and Zacharias, J., 1997, Re-Os dating of gold deposits using accessory molybdenite at the Kasperske Hory and Petrackova Hora mines, Czech Republic: Journal of the Czech Geological Society, v. 42, p. 26.

Stepanov, V.A., 1998, Telmagmatic gold deposits: Rudy I Metally, v. 1998, p. 65-69.

Stevenson, F.J., 1962, Chemical state of the nitrogen in rocks: Geochimica et Cosmochimica Acta, v. 26, p. 797-809.

Stiehl, G., and Lehmann, M., 1980, Isotopenvariationen des stickstoffs humoser und bituminöser natürlicher organischer substanze: Geochimica et Cosmochimica Acta, v. 44, p. 1737-1746.

Stowell, H.H., Lesher, C.M., Green, N.L., Sha, P., Guthrie, G.M., and Krishna, S., 1996, Metamorphic and gold mineralization in the Blue Ridge, southernmost Appalachians: Economic Geology, v. 91, p. 1115-1144.

Stuart, F.M., Burnard, P.G., Taylor, R.P., and Turner, G., 1995, Resolving mantle and crustal contributiona to ancient hydrothermal fluid: He-Ar isotopes in fluid inclusions from Dae Hwa W-Mo mineralization, South Korea: Geochimica et Cosmochimica Acta, v. 59, p. 4663-4673.

Sucha, V., Elsass, F., Eberl, D.D., Kuchta, L.,Madejova, J., Gates, W.P., and Komadel, P., 1998, Hydrothermal synthesis of ammonium illite: American Mineralogist, v. 83, p. 58-67.

Sugisaki, R., 1987, Behavior and origin of helium, neon, argon, and nitrogen from active faults: Journal of Geophysical Research, v. 92, p. 12523-12530.

Sundblad, K. Weihed, P., Billstrom, K., Markkula, H., makela, M., 1993, Source of metal and age constraints for epigenetic gold deposits in the Skellefte and Pohjanmaa d

Sutton-Pratt, A., 1996, Gold mining in Africa: Transaction. Institution of Mining and Metallury (Sect. B), p. 105.

Suzuoki, T., and Eostein, S., 1976, Hydrogen isotope fractionation between OH-bearing minerals and water: Geochimica et Cosmochimica Acta, v. 40, p. 1229-1240.

Tainosho, Y., and Itihara, Y., 1988, The difference in NH_4^+ content of biotites between I-type and S-type granitic rocks in Australia: Journal of Geological Society of Japan, v. 94, p. 749-756.

Tajika, E., and Matsui, T., 1990, The evolution of the terrestrial environment, *in* Newson H.E., and Jones J.H., eds., Origin of the Earth: New York, Oxford University Press, p. 347-370.

Tarney, J., and Jones, C.E., 1994, Trace element geochemistry of orogenic igneous rocks and crustal growth models: Journal of Geological Society, London, v. 151, p. 855-868.

Taylor, B.E., Robert, F., Ball, M., and Leitch, C.H.B., 1991, Mesozoic 'Mother Lode type' gold deposits in North America – Primary vs secondary (meteoric) fluids: Geological Society of America, Abstracts with Program, v. 23, A174.

Taylor, H.P., 1997, Oxygen and hydrogen isotope relationships in hydrothermal mineral deposits, *in* Barnes, H.L., ed., Geochemistry of Hydrothermal Ore Deposits: New York, John Wiley, p. 229-288.

Templeton, A.S., Craw, D., Koons, P.O., and Chamberlain, C.P., 1999, Near-surafce expression of a young mesothermal gol mineralizing system, Sealy Range, Southern Alps, New Zealand: Mineralium Deposita, v. 34, p. 163-172.

Thienmens, M.H., and Calyton, R.N., 1981, Nitrogen isotopes in the Allende meteorite: Earth and Planetary Science Letters, v. 55, p. 363-369.

Thomas, D.E., 1953, Mineralization and its relationship to the structure of Victoria, *in* Edwards, A.B., ed., Geology of Australian Ore Deposits: Melbourne, Victoria, Australian Institute of Mining and Metallurgy, p. 1042-1053.

Thompson, J.E., 1938, The Crow River area: Ontario Department of Mines, Annual Report, v. 47, p. 37-49.

Tischendorf, G., and Ungethum, H., 1964, Uber die Bbildungsbedingungen von Clausthalit and Benerkungen zur Selenverteilung im Galenit in Abhangigkeit vom Redoxpotential und vom Ph-Wert: Chemie der Erde, v. 23, p. 279-311 (in German).

Tolstikhin, I.N., and Marty, B., 1998, The evolution of terrestrial volatiles: a view from helium, neon, argon and nitrogen isotope modeling: Chemical Geology, v. 147, p. 27-52.

Valeriano, C.M., de Almeida, J.C.H., and Simoes, L.S.A., 1995, evolution of the Brazilian Belt external domain in the southwesern Minas Gerais: records of pre-Brazilian age tectonics: Revista Brasileria de Geociencias, v. 25, p. 221-234.

Valley, J.W., 1986, Stable isotope geochemistry of metamorphic rocks: Reviews in Mineralogy, v. 16, p. 445-489.

VandenBerg, A.H.M., 1978, The fold system in Victoria: Tectonophysics, v. 48, p. 267-279.

VandenBerg, A.H.M., Garratt, M.J., Schleiger, N.W., and Spencer, J.D., 1976, Silurian-middle Devonian: Geological Society of Australia, Special Publication 5, p. 45-76.

Vasudev, V.N., Chadwick, B., Nutman, A.P., and Hegde, G.V., 2000, Rapid development of the late Archean Hutti schist belt, northern Karnataka: implications of new field data and SHRIMP U/Pb zircon ages: Journal of the Geological Society of India, v. 55, p. 529-540.

Vedder, W., 1965, Ammonium in muscovite: Geochimica et cosmochimica Acta, v. 29, p. 221-228.

Vinyu, M.L., Frei, R., and Jelsma, H.A., 1996, Timing between granitoid emplacement and associated gold mineralization: Examples from the ca. 2.7 Ga Harare-Shamva greenstone belt, northern Zimbabwe: Canadian Journal of Earth Science, v.33, p. 981-992.

Wada, E., Kadonaga, T., and Matsuo, S., 1975, ^{15}N abundance in nitrogen of naturally occurring substances and global assessment of denitrification from isotopic viewpoint: Geochemical Journal, v. 9, p. 139-148.

Waite, M.E., Ge, S., and Spetzler, H., 1999, A new conceptual model for fluid flow in discrete fractures: An experimental and numerical study: Journal of Geophysical Research, v. 104, p. 13049-13059.

Walsh, J.F., Kesler, S.E., Duff, D., and Cloke, P.L., 1988, Fluid inclusion geochemistry of high-grade, vein-hosted gold ore at the Pamour Mine, Porcupine Camp, Ontario: Economic Geology, v. 83, p. 1347-1367.

Wang, L.G., McNaughton, N.J., and Groves, D.I., 1993, An overview of the relationship bewteen granitoid intrusions and gold mineralization in the Archean Murchison Province, Western Australia: Mineral. Deposita, v. 28, p. 482-494.

Waples, D.W., and Sloan, J.R., 1980, Carbon and nitrogen diagenesis in deep sea sediments: Geochimica et cosmochimica Acta, v. 44, p. 1463-1470.

Ward, P.D., Hurtado, J.M., Kirschvink, J.L., and Verosub, K.L., 1997, Measurements of the Cretaceous paleolatitude of Vancouver island: Consistent with the Baja-British Columbia hypothesis: Science, v. 277, p. 1642-1645.

Weir, R.H.Jr., and Kerrick, D.M., 1987, Mineralogic, fluid inclusion, and stable isotope studies of several gold mines in the Mother Lode, Tuolumne and Mariposa counties, California: Economic Geology, 82, p. 328-344.

Wellman, R.P., Cook, F.D., and Krouse, H.R., 1968, Nitrogen-15 microbiological alteration of abundance: Science, v. 161, p. 269-270.

Wheeler, J.O., and McFeely, P., 1991, Tectonic assemblage map of the Canadian Cordillera and adjacent parts of the United States of America: Geological Survey of Canada, Map 1712A, scale 1:2 000 000.

Whiting, R.G., and Bowen, K.G., 1976, Geology of Victoria, Chapter 12: Economic Geology, gold: Geological Society of Australia Special Publication 5, p. 434-451.

Whittaker, E.J.W., and Muntus, R., 1970, Ionic radii for use in geochemistry: Geochimica et Cosmochimica Acta, v. 34, p. 945-956.

Wikinson, J.J., Jenkin, G.R.T., Fallick, A.E., and Foster, R.P., Oxygen and hydrogen isotopic evolution of Variscan crustal fluids, south Cornwall, U.K.: Chemical Geology, v. 123, p. 239-254.

Williams, L.B., Ferrel, R.E., Hutcheon, I., Bakel, A.J., Walsh, M.M., and Krouse, H.R., 1995, Nitrogen isotope geochemistry of organic matter and minerals during diagenesis and hydrocarbon migration: Geochimica et Cosmochimica Acta, v. 54, p. 765-799.

Williams, L.B., Ferrell, R.E., Chinn, E.W., and Sassen, R., 1989, Fixed-ammonium in clays associated with crude oils: Applied Geochemistry, v. 4, p. 605-616.

Williams, L.B., Wilcoxon, B.R., Ferrell, R.E., and Sassen, R., 1992, Diagenesis of ammonium during hydrocabon maturation and migrationm Wilcox Group, Iouisiana, U.S.A.: Applied Geochemistry, v. 7, p. 123-134.

Witt, W.K., 1991, Reginal metamorphic controls on alteration associated with gold mineralization in the Eastern Goldfields province, Western Australia: I mplications for the timing and origin of Archean lode-gold deposits: Geology, v. 19, p. 982-985.

Witt, W.K., Hickman, A.H., Townsend, D., and Preston, W.A., 1998, Mineral potential of the Archean Pilbara and Yilgarn cratons, Western Australia: AGSO Journal of Australian Geology and Geophysics, v. 17, p. 201-221.

Wlotzka, F., 1961, Untersuchungen zur geochemie des stickstoffs: Geochimica et Cosmochimca Acta, v. 24, p. 106-154.

Wlotzka, F., 1972, Nitrogen, *in* Wedepohl, K.H., ed., Handbook of Geochemisrty II, New York, Springer-Verlag, p. 7B-1-7O-3.

Wynne, P/J., Irving, E., Maxson, J.A., and Kleinspehn, 1995, Paleomagnetsm of the Upper Cretaceous strata of Mount Tatlow: Evidence for 3000 km of displacement of the eastern Coast Belt, British Columbia: Journal of Geophysical Research, v. 100, p. 6073-6091.

Yakubchuk, A.S., and Edwards, A.C., 1999, Auriferous Paleozoic accretionary terranes within the Mongolia-Okhotsk suture zone, Russia Far East: Australasian Institute of Mining and Metallurgy, v. 4-99, p. 347-358.

Yamamoto, M., 1976, Relationship between Se/S and sulfur isotope ratios of hydrothermal sulfide minerals: Mineralium Deposita, v. 11, p. 197-209.

Yamamoto, M., Kase, K., and Tsutsumi, M., 1984, Fractionation of sulfur isotopes and selenium between coexisting sulfide minerals from the Besshi deposits, central Shikoku, Japan: Mineralium Deposita, v. 19, p. 237-242.

Yao, Y., Morteani, G., and Trumbull, R.B., 1999, Fluid inclusion microthermametry and the P-T evolution of gold-bearing hydrothermal fluids in the Niuxinshan gold deposit, eastern Hebei, NE China: Mineralium Deposita, v. 34, p. 348-365.

Yardley, B.W.D., Banks, D.A., Bottrell, S.H., and Diamond, L.W., 1993, Post-metamorphic gold-quartz veins from N.W. Italy: The composition and origin of the ore fluid: Minerological Magazine, v. 57, p. 407-422.

Yarmolyuk, V., Kovalenko, V.I., Kotov, A.B., and Salnikova, E.B., 1997, The Angara - Vitim Batholith: on the problem of batholith geodynamics in the central Asia fold belt: Geotectonics, v. 31, p. 359-373.

Zhang, D., and Clayton, R.N., 1988, Nitrogen abundances and isotopic composition in MORB and subduction zone rocks: Eos Transactions American Geophysical Union 69, p. 510-511.

Zhang, X., Nesbitt, B.E., and Muehlenbachs, K., 1989, Gold mineralization in the Okanagan Valley, Southern British Columbia: Fluid inclusion and stable isotope studies: Economic Geology, v. 84, p. 410-424.

Zorin, Y.A., 1999, Geodynamics of the western part of the Mongolia-Okhatsk collisional belt, Trans-Baikal region (Russia) and Mongolia: Tectonphysics, v. 306, p. 33-56.

Appendix I. Sample Preparation and Analytical Methodologies

I-1 Sample Preparation

Mica-rich samples for N, $\delta^{15}N$, $\delta^{18}O$, $\delta^{13}C$, δD, and Se/S analyses were selected from the sequence of vein quartz systems of different mines in the Superior Province of Canada, Norseman-Wiluna greenstone belt of western Australia, Victorian goldfields, southeastern Australia, North American Cordillera, and north margin of the China craton. The mineralization ages of these lode gold deposits span from late Archean to Phanerozoic. Selected samples were carefully examined in thin section for grain size, texture, and mineralogy. Any specimens in which there is mineralogical or textural evidence of disequlibrium were rejected. The subpopulation was reduced by sawing to suitable pieces of size, then crushed using jaw machine into <15 mm size for further separation. The detailed procedures are as follows:

(1) Hand-picked mica-rich crushed samples were ground in a TEMA mill crusher for about 10 seconds, sieved into different grain size fractions (60/100/170/230/270/325 meshe), washed in water to remove fines, and dried. (2) Using a binocular microscope the size fractions with non-intergrown grains were selected for separation. (3) A hand magnet was used to remove strongly magnetic minerals, such as magnetite. (4) A Frantz isodynamic magnetic separator was used to separate relatively more magnetic minerals (e.g., micas, ± chlorite, ± tourmaline, ± actinolite, dolomite), from relatively weak magnetic minerals (e.g., quartz, calcite, pyrite). (5) Re-using Frantz and fine-turning amperage, forward slope, and side tilt on the Franz to separate micas from carbonates, chlorite, tourmaline, and actinolite. Heavy liquid (Methylene iodide) of density of 3.3

was used on the non-magnetic fraction to separate heavy minerals including pyrite from quartz and calcite. Pure quartz was separated from calcite by dissolving in 1:1 hydrochloric acid for several days and rinsing with distilled water. Finally, the concentrationswere checked under binocular microscope for pure mica, quartz, and pyrite separates, and all samples were examined by X-Ray Diffraction (XRD) in order to ensure that the sample purities were more than 98%. Samples were beaeched with dichloromethane-ethanol (9:1) to remove any possible organic material.

I.2 Analytical Methodologies

I.2.1. N and $\delta^{15}N$ of micas

Nitrogen contents and nitrogen isotope ratios of mica separates were analyzed using the techniques described by Jia and Kerrich (1999, 2000). Each pure muscovite sample was finely ground to less than 250 mesh, and loaded into a tin capsule in a clean room. By heating samples up to ca.1200°C for about 10 minutes, structural nitrogen is completely released (Bebout and Fogel, 1992; Boyd et al., 1993) and oxidized by passing the combustion products through a bed of chromium trioxide at 1000°C using a helium carrier gas, then passed through a second furnace containing copper at 600°C where excess oxygen was absorbed and nitrogen oxides were reduced to elemental nitrogen. Nitrogen gas is then bled into a mass-spectrometer where the nitrogen isotopes are ionized then separated in a magnetic field. Analyses were conducted using a Continuous Flow- Isotope Ratio mass spectrometer (CF-IRMS) at the Soil Science Laboratory, University of Saskatchewan (Fig. A1).

Analytical reproducibilities on unknown are ca. $\pm$ 0.3‰ (or generally $\leq$ 0.3‰ for $n \geq 3$) for $\delta^{15}N$. The long-term reproducibility for international nitrogen isotope

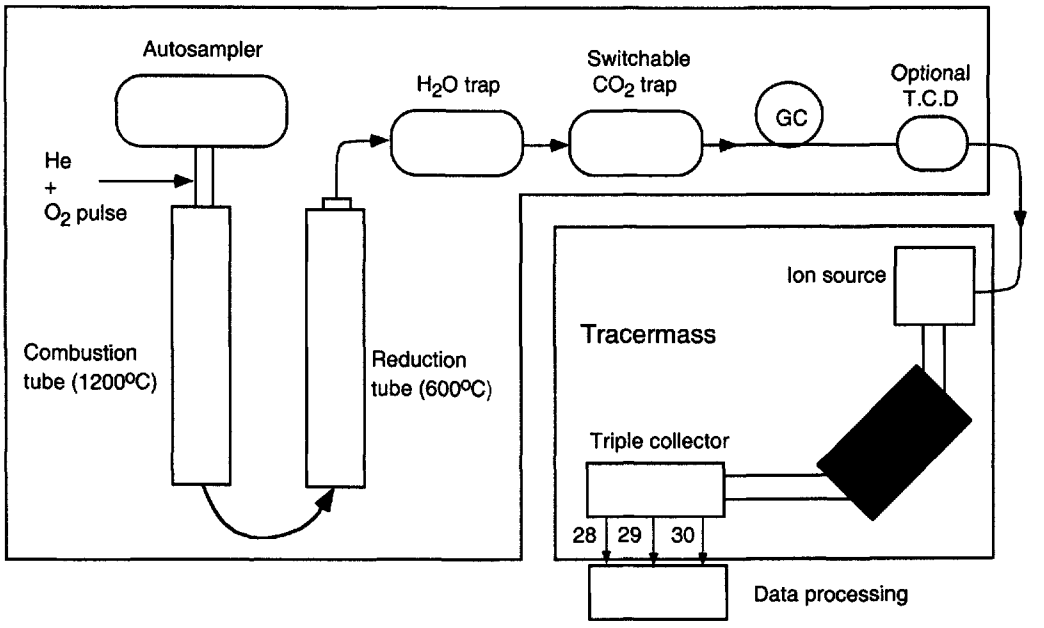

Fig. A1. Schematics of the continuous flow isotope ratio mass spectrometer

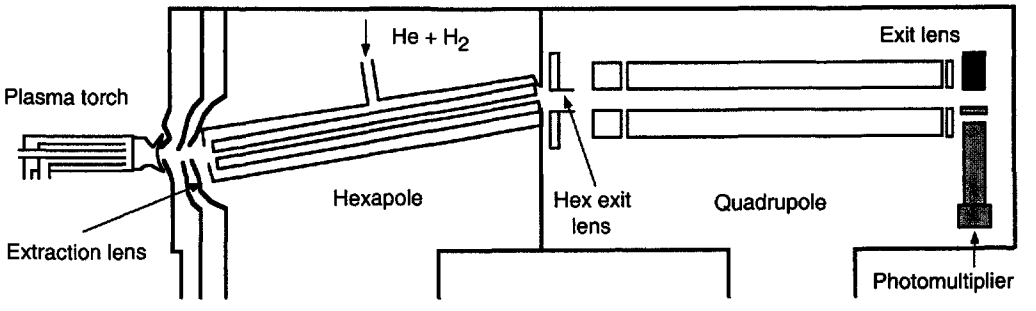

Fig. A2. Schematics of instrument configuration of the Hexapole ICP-MS

standard materials are: IAEA-N1, 0.54 ± 0.07‰ (n = 15, accepted value 0.53‰); IAEA-N2, 20.34 ± 0.08‰ (n = 10, accepted value 20.41‰); and for the internal laboratory standard material: BLN.SOIL, 5.15 ± 0.21‰ (n = 20, accepted value 5.15‰). Reproducibilities are influenced by the sample matrix. Ten replicate analyses of the muscovite mineral separate sample CD11-21-1 yielded a mean $\delta^{15}N$ value of 3.43 (1σ = 0.06‰). Nitrogen contents were obtained from each sample based on system calibration using known standards. Isotopic compositions are given in the standard δ-notation. The standard is atmospheric N_2 defined to be $\delta^{15}N_{std}$=0 ‰.

I.2.2. $\delta^{13}C$ and $\delta^{18}O$ of carbonates

Whole rock sample powders were reacted with 100% H_3PO_4 for 2 hours at 25°C to select calcite CO_2. The sample was pumped on for 2 hours, and then reacted at 50°C for 24 hours to obtain dolomite CO_2 (Epstein et al., 1963). Analyses were conducted using a Finnigan Mat Delta mass spectrometer for carbon and oxygen isotopes on whole-rock powder samples, at the Isotope Laboratory, Department of Geological Sciences, University of Saskatchewan.

The $\delta^{13}C$ and $\delta^{18}O$ values of NBS-19 (standard) limestone are 1.9‰ and 28.6‰, respectively. Analytical reproducibilities are ± 0.20‰ and ± 0.19‰ for $\delta^{13}C$ and $\delta^{18}O$ on carbonates, respectively. Isotope data are reported in standard δ-notation relative to the Peedee Belemnite limestone (PDB) standard for carbon and the Vienna SMOW standard for oxygen.

I.2.3. $\delta^{18}O$ and δD analyses

Oxygen isotope ratios were determined using conventional procedures at the University of Saskatchewan. Silicates (quartz and mica separates) were reacted with

bromine pentaflouride (BrF_3) in nickel bombs at 550°C, followed by quantitative conversion to CO_2 (Clayton and Mayeda, 1963). For hydrogen isotope analysis, muscovite separates were loaded into a molybdenum bucket and fused using an RF heater. The resulting gases are passed through a getter heater to 450°C and frozen down with liquid nitrogen. The trap is then exchanged for a dry ice slush trap to freeze down the water so other gases can be pumped away. Residual water is reacted with zinc pellets for 15mins at 450°C to produce hydrogen. Isotope standards for O and H are the Vienna SMOW. Analyses were conducted using a Finnigan Mat Delta mass spectrometer for oxygen isotopes on quartz at the Isotope Laboratory, Department of Geological Sciences, University of Saskatchewan, and a MM602E mass spectrometer at Queens University for hydrogen isotopes on muscovite.

Using these techniques, the $\delta^{18}O$ value of NBS-28 quartz is 9.6‰, and the δD value of NBS-30 biotite is -65‰, respectively. Analytical reproducibilities are ± 0.18‰ for $\delta^{18}O$ on silicates and ± 2.0‰ for δD on micas, respectively. Isotope data are reported in standard δ-notation relative to the Vienna SMOW standard for oxygen and hydrogen

I.2.4. Se and S analyses

For selenium analysis, about 100 mg of each cleaned pyrite separate was placed in pre-cleaned Teflon® vessels with a loosely fitted Teflon® lid, using 2.5 ml 16N HNO_3 at 60°C for one week until samples were completely dissolved, then transferred to a 100 g bottle and diluted gravimetrically a 1000 fold with DDW. Sulfur concentrations of pyrite were determined using a JEOL 8600 Superprobe microprobe analyzer (EMP).

Given the Ar-diamer interference on ^{80}Se, a new analytical technique was developed using a Micromass Hexapole Inductively coupled plasma-mass spectrometer (ICP-MS), at the Department of Geological Sciences, University of Saskatchewan. The Hexapole collision cell, which is bled with He and H_2, greatly reduces the Ar diamer interference on ^{80}Se, resulting in superior Se detection limits of 0.5 to 5 ppt. Indium was used as an internal standard to correct matrix effects and instrumental drift, and pure Se standard for external calibration. The precision of Se analysis was estimated to be better than 5% relative standard deviation (Fig. A2). The precision of S analysis was between 0.2 to 0.3 percent relative standard derivations.

I.3 Data report

There are insufficient data on any single rock type or mineral separate to establish the statistical distribution of data. Accordingly, ranges and averages are reported, with averages and standars derviations for groups of samples.

Appendix II.

Table A4.1. Representative compositions of mica in quartz veins, the Superior Province, Canada

Mining camp	Kirkland Lake		Porcupine				
Sample Name	Kerr-Addison I	Kerr-Addison II	Dome	Goldhawk	Hollinger I	Hollinger II	Beaumont
Mineral	Muscovite	Muscovite	Muscovite	Muscovite	Muscovite	Muscovite	Muscovite
Points	4	4	6	5	3	4	3
SiO_2	48.93	47.92	48.39	48.94	48.05	47.64	47.76
TiO_2	0.17	0.25	0.30	0.15	0.27	0.45	0.20
Al_2O_3	31.12	31.00	33.47	31.97	34.83	33.94	29.69
Cr_2O_3	1.94	1.66	0.02	1.73	0.00	0.04	3.16
FeO	0.44	1.04	0.89	0.46	0.89	0.82	0.60
MgO	1.77	1.95	1.34	1.65	1.35	1.26	1.84
MnO	0.02	0.04	0.03	0.01	0.00	0.01	0.00
CaO	0.01	0.02	0.04	0.06	0.00	0.01	0.04
Na_2O	0.31	0.34	0.03	0.27	0.24	0.28	0.33
K_2O	**10.70**	**11.30**	**11.20**	**10.87**	**11.36**	**11.30**	**11.04**
Cl	0.02	0.00	0.04	0.05	0.00	0.02	0.00
F	0.00	0.00	0.00	0.00	0.00	0.00	0.01
Total	**95.43**	**95.94**	**95.85**	**96.15**	**96.99**	**95.76**	**94.87**
FeO/(FeO+MgO)	0.20	0.35	0.40	0.22	0.40	0.39	0.24
$Al_2O_3/(Cao+Na_2O+K_2O)$	2.82	2.66	2.97	2.86	3.00	2.93	2.60
			Number of cations based on 22 oxygen				
Si	6.502	6.386	6.392	6.455	6.281	6.312	6.459
^{IV}Al	1.499	1.614	1.608	1.545	1.719	1.688	1.541
Total	8.000	8.000	8.000	8.000	8.000	8.000	8.000
^{VI}Al	3.373	3.231	3.601	3.427	3.646	3.610	3.189
Ti	0.017	0.028	0.030	0.015	0.026	0.045	0.020
Cr	0.204	0.198	0.003	0.180	0.000	0.004	0.338
Fe	0.049	0.127	0.098	0.051	0.098	0.091	0.067
Mg	0.351	0.419	0.265	0.324	0.262	0.250	0.371
Mn	0.002	0.009	0.003	0.002	0.000	0.001	0.000
Total	3.996	4.011	3.999	3.997	4.033	4.000	3.986
Ca	0.002	0.004	0.006	0.008	0.000	0.002	0.005
Na	0.081	0.094	0.068	0.069	0.061	0.071	0.087
K	1.814	2.005	1.866	1.830	1.894	1.909	1.904
Total	1.897	2.103	1.939	1.906	1.955	1.982	1.997
Cl	0.004	0.000	0.008	0.011	0.001	0.004	0.001
F	0.000	0.000	0.000	0.000	0.000	0.000	0.000

Table A4.1. (continued)

Mining camp	Hemlo		Geraldton		Pickle Lake	Red Lake	
Sample Name	Williams	David Bell	Hardrock	Macleod	Pickle-Crow	Cochenour	Mackenzie
Mineral	Muscovite	Muscovite	Muscovite	Muscovite	Biotite	Muscovite	Biotite
Point	3	2	3		3	5	3
SiO_2	48.65	45.13	47.90	47.14	36.50	47.22	35.95
TiO_2	0.41	1.67	0.12	0.25	2.11	0.46	1.87
Al_2O_3	34.34	31.05	34.65	29.17	17.29	32.21	17.13
Cr_2O_3	0.02	0.06	1.88	0.02	0.09	0.01	0.14
FeO	0.85	0.54	0.27	3.40	18.76	2.48	21.06
MgO	1.27	2.17	0.70	2.00	10.11	1.69	9.01
MnO	0.01	0.05	0.03	0.00	0.12	0.01	0.11
CaO	0.03	0.04	0.01	0.10	0.02	0.01	0.09
Na_2O	0.27	0.41	1.10	0.23	0.11	0.26	0.20
K_2O	**11.03**	**9.94**	**9.39**	**11.00**	**9.51**	**9.87**	**9.13**
Cl	0.00	0.01	0.00	0.00	0.01	0.01	0.12
F	0.00	0.00	0.00	0.02	0.00	0.00	0.58
Total	**97.08**	**91.06**	**96.05**	**93.38**	**94.61**	**95.76**	**95.38**
FeO/(FeO+MgO)	0.40	0.20	0.28	0.63	0.65	0.59	0.70
$Al_2O_3/(Cao+Na_2O+K_2O)$	3.03	2.99	3.30	2.58	1.80	3.18	1.82
			Number of cations based on 22 oxygen				
Si	6.349	6.275	6.279	6.452	5.581	6.327	5.553
^{IV}Al	1.651	1.725	1.721	1.549	2.419	1.673	2.447
Total	8.000	8.000	8.000	8.000	8.000	8.000	8.000
^{VI}Al	3.630	3.363	3.632	3.144	0.697	3.410	0.673
Ti	0.040	0.174	0.012	0.018	0.242	0.047	0.218
Cr	0.002	0.006	0.195	0.383	0.011	0.001	0.017
Fe	0.093	0.063	0.030	0.041	2.399	0.279	2.721
Mg	0.204	0.449	0.136	0.381	2.303	0.338	2.074
Mn	0.001	0.006	0.003	0.001	0.015	0.001	0.014
Total	3.969	4.062	4.008	3.967	5.668	4.076	5.717
Ca	0.005	0.006	0.002	0.015	0.002	0.001	0.014
Na	0.068	0.110	0.279	0.103	0.033	0.067	0.059
K	1.837	1.762	1.570	1.920	1.854	1.948	1.800
Total	1.909	1.878	1.852	2.037	1.890	2.016	1.874
Cl	0.001	0.002	0.000	0.003	0.002	0.003	0.032
F	0.000	0.000	0.000	0.000	0.000	0.000	0.282

Table A4.2. Representative compositions of biotite in quartz veins, Norseman district, Western Australia

Sample No.	Princess Royal	NR7	Mararoa	NR10	RT9/220	VHW
Point	4	4	4	4	2	2
SiO_2	36.60	37.78	37.54	36.36	36.71	37.22
TiO_2	1.34	1.39	1.00	1.79	1.87	1.22
Al_2O_3	17.17	17.32	19.00	16.48	16.07	17.93
Cr_2O_3	0.08	0.07	0.07	0.11	0.03	0.06
FeO	17.00	14.17	10.43	18.46	17.68	11.86
MgO	13.35	14.78	17.25	12.36	12.65	17.50
MnO	0.20	0.18	0.17	0.13	0.10	0.12
CaO	0.01	0.00	0.00	0.02	0.01	0.02
Na_2O	0.11	0.05	0.20	0.15	0.07	0.19
K_2O	**9.50**	**10.08**	**9.87**	**8.87**	**9.34**	**9.09**
Cl	0.02	0.02	0.00	0.09	0.05	0.02
F	0.00	0.00	0.00	0.00	0.00	0.00
Total	**95.37**	**95.84**	**95.48**	**94.81**	**94.56**	**95.22**
FeO/(FeO+MgO)	0.56	0.49	0.38	0.60	0.58	0.40
Al_2O_3/(NaCl+K_2O+Cao)	1.79	1.71	1.88	1.82	1.71	1.93
	Number of cations based on 22 oxygen					
Si	5.511	5.583	5.459	5.536	5.592	5.454
^{IV}Al	2.489	2.418	2.541	2.464	2.409	2.547
Total	8.000	8.000	8.000	8.000	8.000	8.000
^{VI}Al	0.557	0.599	0.715	0.495	0.476	0.550
Ti	0.152	0.155	0.109	0.205	0.214	0.135
Cr	0.010	0.009	0.008	0.013	0.004	0.006
Fe	2.141	1.751	1.269	2.350	2.252	1.453
Mg	2.995	3.256	3.739	2.806	2.872	3.824
Mn	0.026	0.022	0.021	0.016	0.014	0.015
total	5.880	5.792	5.861	5.885	5.831	5.982
Ca	0.002	0.000	0.001	0.003	0.001	0.003
Na	0.032	0.015	0.058	0.044	0.019	0.055
K	1.824	1.900	1.819	1.722	1.814	1.697
Total	1.857	1.916	1.877	1.770	1.835	1.755
Cl	0.005	0.005	0.001	0.024	0.012	0.005
F	0.000	0.000	0.000	0.000	0.000	0.000

Apendix III. Location of Archean samples

District	Deposit/ metasedimentary rocks	Source
Superior Province, Canada		
	Deposit	
Porcupine	Hollinger, Dome, Goldhawk, Beaumont, Geraldton, Pickle Lake, and Red Lake	King and Kerrich (1987), King (1990)
	Kirkland Lake	Kishida and Kerrich (1987)
	Hemlo	Pan and Fleet (1995)
	Metasedimentary rocks	
Timmins	Dome Formation, Beaty Formation	Feng and Kerrich (1990)
	Hoyle Pond Black shales	From A. Still (KINROSS Gold Corporation)
Western Australia		
	Deposit	
Norseman	Norseman	McCuaig et al. (1993)